Usage des terres, ruissellement de surface, érosion des sols : analyse multi-échelles de l'impact des plantations de teck dans un agro-écosystème montagneux tropical humide

Layheang Song

THÈSE

En vue de l'obtention du

DOCTORAT DE L'UNIVERSITÉ DE TOULOUSE

Délivré par l'Université Toulouse 3 - Paul Sabatier

Cotutelle internationale: Institut de Technologie du Cambodge

---

Présentée et soutenue par

Layheang SONG

Le 23 novembre 2021

Usage des terres, ruissellement de surface, érosion des sols: analyse multi-échelles de l'impact des plantations de teck dans un agro-écosystème montagneux tropical humide

---

Ecole doctorale : **SDU2E - Sciences de l'Univers, de l'Environnement et de l'Espace**

Spécialité : **Surfaces et interfaces continentales, Hydrologie**

Unité de recherche :
GET - Geosciences Environnement Toulouse

Thèse dirigée par
Laurie BOITHIAS, Chantha OEURNG et Olivier RIBOLZI

Jury

Mme Olga VIGIAK, Rapporteure
M. Luc DESCROIX, Rapporteur
Mme Pinnara KET, Examinatrice
M. Guillaume NORD, Examinateur
M. Christian VALENTIN, Examinateur
Mme Laurie BOITHIAS, Directrice de thèse
M. Chantha OEURNG, Co-directeur de thèse
M. Olivier RIBOLZI, Co-directeur de thèse

[This page intentionally left blank]

Land use, surface runoff, soil erosion: multi-scale impact assessment of teak tree plantation management in a tropical humid mountainous agro-ecosystem

Mots clés
ruissellement de surface, perte en terre, bassin versant agricole, érosion et mesure d'atténuation, export sédimentaire, modélisation de l'érosion hydrique des sols,

Keywords
surface runoff, soil loss, cultivated catchment, erosion and mitigation measure, sediment export, soil erosion model

[This page intentionally left blank]

Table of Contents

Abstract

Soil erosion is yet known as one of the most concerning problems of the environment in the world. Soil erosion is particularly and increasingly driven by anthropogenic activities under the changing climate. In Lao PDR, a tropical country, soil erosion is significantly due to inappropriate land management on the sloping land. The Houay Pano, a cultivated catchment of the northern Lao PDR, is prone to soil erosion, particularly after the conversion from shifting cultivation to teak tree plantation. Land mismanagement by clearing the understory under the teak tree plantation is considered as an underlying cause of higher runoff coefficient (Rc) and soil erosion. Some mitigations such as understory and riparian vegetation are suggested for alleviating soil erosion. However, the mitigation measure of soil erosion and the effect of land use management on surface runoff (SR) and soil loss/sediment yield (Sl) on multiple scales in the teak tree plantation are not fully assessed. In this context, we hypothesize that understory and riparian grass mitigate the soil erosion in the teak tree plantation and that teak tree plantation impacts on SR and Sl driven by dominant processes (inter rill erosion, linear erosion, and deposition) on various spatial scales. Therefore, the objectives set out for this work are: (1) to assess the effect of understory management on SR and Sl in the teak tree plantation on the microplot scale; (2) to assess the ability of riparian grass buffers to mitigate SR and Sl, and to assess their water and sediment trapping efficiencies in the teak tree plantations with no understory on the hillslope scale; and (3) to assess the effect of teak tree plantation on SR and Sl on various spatial scales (microplot, hillslope including micro-catchment, and catchment scales) in a mixed land uses mountainous tropical catchment. In this study, Ban Kokngew village and Houay Pano catchment were selected as experimental study areas during the rainy season. Microplots, Gerlach traps, and weirs were used to estimate SR and Sl on each scale. We followed the TEST model developed for inter rill erosion, which requires a few parameters, to assess Sl on the microplot and upscale it to predict Sl on the hillslope and catchment scale. In a study performed in 2017 in the teak tree plantations of Ban Kokngew on the microplot scale, we showed that Rc and Sl (23%, 381 $Mg \cdot km^{-2}$, respectively) under teak tree with understory were less than those under teak tree with no understory (60% and 5455 $Mg \cdot km^{-2}$, respectively). Hence, soil erosion mitigation by keeping the understory under teak tree plantation reduces Sl by 14 times. In a study performed in 2014 in the teak tree plantations of Houay Pano on both the microplot and the hillslope scales, we showed that leaving the riparian grass buffer of at least 6 m could limit SR and Sl discharging downstream during small storms (24-hour rainfall < 54.8 mm) with the trapping efficiency up to 88%. Lastly, in a study

performed in 2014 in the teak tree plantations of Houay Pano on various scales, we showed that SR and Sl were significantly higher (p-value < 0.05) in the teak-dominated micro-catchment than in the mixed-land-use micro-catchment. SR and Sl decreased from the microplot (122 – 196 mm, 275 – 1065 $Mg \cdot km^{-2}$, respectively) to the micro-catchment (24 – 188 mm, 95 – 3635 $Mg \cdot km^{-2}$, respectively) and catchment scale (33 mm, 236 $Mg \cdot km^{-2}$, respectively), except that Sl in teak tree plantation increased from the microplot (1065 $Mg \cdot km^{-2}$) to the micro-catchment scale (3635 $Mg \cdot km^{-2}$). The findings of this thesis, based on the multi-scale assessment of surface runoff and soil losses, will provide social and scientific communities quantitative results on soil erosion from the plot scale to the catchment scale. This information may help farmers and policymakers to adopt and promote sustainable land management practices.

Résumé

L'érosion des sols est pourtant connue comme l'un des problèmes environnementaux les plus préoccupants au monde. L'érosion des sols est particulièrement et de plus en plus entraînée par les activités anthropiques dans le cadre du changement climatique. En RDP lao, un pays tropical, l'érosion des sols est due de manière significative à une gestion inappropriée des terres sur les terrains en pente. Le Houay Pano, un bassin versant cultivé du nord de la RDP lao, est exposé à l'érosion des sols, en particulier après la conversion de la culture itinérante en plantation de teck. La mauvaise gestion des terres en défrichant le sous couvert végétal sous la plantation de teck est considérée comme une cause sous-jacente du coefficient de ruissellement (Rc) plus élevé et de l'érosion des sols. Certaines mesures d'atténuation telles que le sous couvert végétal et la végétation rivulaire sont suggérées pour atténuer l'érosion des sols. Cependant, la mesure d'atténuation de l'érosion des sols et l'effet de la gestion de l'utilisation des terres sur le ruissellement de surface (SR) et la perte en sols/rendement de sédiments (Sl) à plusieurs échelles dans la plantation de teck ne sont pas entièrement évalués. Dans ce contexte, nous émettons l'hypothèse que le sous couvert végétal et l'herbe rivulaire atténuent l'érosion du sol dans la plantation d'arbres à teck et que les plantations d'arbres à teck ont des impacts sur SR et Sl entraînés par des processus dominants (l'érosion en nappe, l'érosion linéaire et le dépôt de sédiment) sur diverses échelles spatiales. Par conséquent, les objectifs fixés pour ce travail sont : (1) d'évaluer l'effet de la gestion du sous couvert végétal sur le ruissellement de surface et la perte en sols dans la plantation de teck à l'échelle de la micro-parcelle ; (2) d'évaluer la capacité des zones tampons d'herbes rivulaires à atténuer SR et Sl, et d'évaluer leur efficacité de piégeage de l'eau et des sédiments dans les plantations de teck sans sous couvert végétal à l'échelle du versant ; et (3) d'évaluer l'effet de la plantation de teck sur SR et Sl à diverses échelles spatiales (échelles de micro-parcelle, de versant incluant micro-bassin versant, et de bassin versant) dans un bassin versant tropical montagneux à utilisations mixtes de terre. Dans cette étude, le village de Ban Kokngew et le bassin versant d'Houay Pano ont été sélectionnés comme zones d'étude expérimentale pendant la saison des pluies. Des micro-parcelles, des pièges Gerlach et des déversoirs ont été utilisés pour estimer SR et Sl à chaque échelle. Nous avons suivi le modèle TEST développé pour l'érosion en nappe, qui nécessite quelques paramètres, pour évaluer Sl sur la micro-parcelle et le mettre en hautes échelles spatiales pour prédire Sl à l'échelle du versant et du bassin versant. Dans une étude réalisée en 2017 dans les plantations de teck de Ban Kokngew à l'échelle micro-parcelle, nous avons montré que Rc et Sl (23%, 381 $Mg \cdot km^{-2}$, respectivement) sous teck avec sous couvert végétal étaient inférieurs à

ceux sous teck sans sous couvert végétal (60 % et 5455 $Mg \cdot km^{-2}$, respectivement). Par conséquent, l'atténuation de l'érosion des sols par le maintien du sous couvert végétal sous la plantation de teck réduit Sl de 14 fois. Dans une étude réalisée en 2014 dans les plantations de teck de Houay Pano à l'échelle de la micro-parcelle et du versant, nous avons montré que laisser la bande rivulaire enherbée d'au moins 6 m pouvait limiter les rejets de SR et Sl en aval lors de petits orages (24 heures précipitations < 54,8 mm) avec une efficacité de piégeage jusqu'à 88 %. Enfin, dans une étude réalisée en 2014 dans les plantations de teck de Houay Pano à différentes échelles, nous avons montré que SR et Sl étaient significativement plus élevés (p-value < 0,05) dans le micro-bassin dominé par le teck que dans celui dominé par la jachère. SR et Sl ont diminué de la micro-parcelle (122 – 196 mm, 275 – 1065 $Mg \cdot km^{-2}$, respectivement) au micro-bassin (24 – 188 mm, 95 – 3635 $Mg \cdot km^{-2}$, respectivement) et à l'échelle du bassin versant (33 mm, 236 $Mg \cdot km^{-2}$, respectivement), sauf que Sl dans les plantations de teck a augmenté de la micro-parcelle (1065 $Mg \cdot km^{-2}$) à l'échelle du micro-bassin (3635 $Mg \cdot km^{-2}$). Les résultats de cette thèse, basés sur l'évaluation multi-échelle du ruissellement de surface et des pertes en sols, fourniront aux communautés sociales et scientifiques des résultats quantitatifs sur l'érosion des sols de l'échelle de la parcelle à l'échelle du bassin versant. Ces informations peuvent aider les agriculteurs et les décideurs à adopter et à promouvoir des pratiques de gestion durable des terres.

សេចក្តីសង្ខេប

សំណឹកដី នៅតែត្រូវបានចាត់ទុកថាជាបញ្ហាដ៏គួរឱ្យព្រួយបារម្ភចំពោះបរិស្ថាន នៅលើពិភពលោក។ សំណឹកដី បង្កឡើងដោយជាពិសេសនិងកាន់តែកើនឡើង ដោយសារសកម្មភាពមនុស្ស ក្នុងបរិបទនៃការប្រែប្រួលអាកាសធាតុ។ នៅប្រទេសឡាវ ដែលស្ថិតក្នុងតំបន់ត្រូពិច សំណឹកដី បង្កឡើងគួរឱ្យកត់សម្គាល់ដោយសារការគ្រប់គ្រងដីមិនត្រឹមត្រូវ លើដីជម្រាលភ្នំ។ ហួយប៉ាណូ ជាផ្ទៃរងទឹកភ្លៀងដែលត្រូវបានធ្វើការដាំដុះនៅភាគខាងជើងនៃប្រទេសឡាវ ងាយទទួលរងនឹងសំណឹកដី ជាពិសេសបន្ទាប់ពីការផ្លាស់ប្តូរពី ការដាំដុះលក្ខណៈឆ្លាស់ ទៅជាការដាំដើមម៉ៃសាក់។ ការគ្រប់គ្រងដីមិនត្រឹមត្រូវដោយការឈូសឆាយរុក្ខជាតិតូចៗ ក្រោមចម្ការដើមម៉ៃសាក់ ត្រូវបានគេចាត់ទុកថាជាបុព្វហេតុនៃមេគុណរំហូរទឹក(Rc) និងសំណឹកដីខ្ពស់ជាងមុន។ វិធានការកាត់បន្ថយសំណឹកដី ដូចជាដើមរុក្ខជាតិតូចៗ និងរុក្ខជាតិនៅតាមមាត់អូរ ត្រូវបានណែនាំសម្រាប់ការកាត់បន្ថយការសំណឹកដី។ ទោះយ៉ាងណាវិធានការកាត់បន្ថយសំណឹកដី និងផលប៉ះពាល់នៃការគ្រប់គ្រងការប្រើប្រាស់ដីទៅលើរំហូរទឹកលើផ្ទៃដី(SR) និងការបាត់បង់ដីឬទិន្នផលដីល្បាប់(SI) លើកម្រិតពហុមាត្រដ្ឋាននៃទំហំលំហ នៅក្នុងចម្ការដើមម៉ៃសាក់មិនត្រូវបានសិក្សាពេញលេញនៅឡើយទេ។ នៅក្នុងបរិបទនេះ យើងធ្វើសម្មតិកម្មថា រុក្ខជាតិតូចៗ និងស្មៅនៅតាមមាត់អូរ កាត់បន្ថយសំណឹកដី នៅក្នុងចម្ការដើមម៉ៃសាក់ ហើយចម្ការដើមម៉ៃសាក់ មានផលប៉ះពាល់ដល់ SR និង SI ដែលជំរុញដោយដំណើរសំណឹក (សំណឹកinterrill សំណឹកលើនអែរ និងការឆ្លាក់រងនៃដីល្បាប់) លើមាត្រដ្ឋានលំហផ្សេងៗ។ ដូច្នេះគោលបំណងដែលបានកំណត់សម្រាប់និក្ខេបបទនេះគឺ៖ ទី១ ដើម្បីវាយតំលៃពីឥទ្ធិពលនៃការគ្រប់គ្រងរុក្ខជាតិតូចៗ ទៅលើ SR និង SI នៅក្នុងចម្ការដើមម៉ៃសាក់ នៅលើមាត្រដ្ឋានតូច ហើយទី២ ដើម្បីវាយតម្លៃសមត្ថភាពរបស់ស្មៅនៅតាមមាត់អូរ ដើម្បីកាត់បន្ថយ SR និង SI និងវាយតម្លៃប្រសិទ្ធភាពរបស់ស្មៅនោះលើការស្រោចទឹកនិងដីល្បាប់ នៅក្នុងចម្ការដើមម៉ៃសាក់ នៅលើមាត្រដ្ឋានជម្រាលភ្នំ និងទី៣ ដើម្បីវាយតម្លៃពីឥទ្ធិពលនៃចម្ការដើមម៉ៃសាក់ ទៅលើ SRនិង SI លើមាត្រដ្ឋានលំហផ្សេងៗគ្នា (ខ្នាតMicroplot ខ្នាតជម្រាលភ្នំរួមទាំងផ្ទៃរងទឹកភ្លៀងខ្នាតតូច និងផ្ទៃរងទឹកភ្លៀង) នៅក្នុងផ្ទៃរងទឹកភ្លៀងតំបន់ភ្នំត្រូពិច ដែលមានការប្រើប្រាស់ដីលាយឡំគ្នា។ នៅក្នុងការសិក្សានេះ កូមិបានកុកញូ និងផ្ទៃរងទឹកភ្លៀងហួយប៉ាណូ ត្រូវបានជ្រើសរើសជាតំបន់សិក្សាពិសោធន៍ក្នុងរដូវវស្សា។ Microplots ឧបករណ៍Gerlach និងសំណង់បង្ហៀរត្រូវបានប្រើប្រាស់ដើម្បីប៉ាន់ស្មាន SR និង SI នៅលើមាត្រដ្ឋាននីមួយៗ។ យើងបានធ្វើតាមគំរូម៉ូដែល TEST ដែលបង្កើតឡើងសម្រាប់សំណឹកinter-rill ដែលត្រូវការប៉ារ៉ាម៉ែត្រមួយចំនួន ដើម្បីវាយតម្លៃ SI នៅលើខ្នាតMicroplot ហើយបំប្លែងមាត្រដ្ឋាននៃម៉ូដែលឱ្យខ្ពស់ ដើម្បីទស្សន៍ទាយ SI នៅលើមាត្រដ្ឋានជម្រាលភ្នំនិងផ្ទៃរងទឹកភ្លៀង។ នៅក្នុងការសិក្សាមួយនៅឆ្នាំ ២០១៧ នៅចម្ការដើមម៉ៃសាក់នៃកូមិបានកុកញូ លើមាត្រដ្ឋានខ្នាតMicroplot យើងបានបង្ហាញថា Rc និង SI (២៣% និង ៣៨១ $Mg \cdot km^{-2}$ រៀងគ្នា) ក្នុងចម្ការដើមម៉ៃសាក់ដែលមានរុក្ខជាតិតូចៗនៅខាងក្រោម តូចជាងចម្ការដើមម៉ៃសាក់ដែលមិនមានរុក្ខជាតិតូចៗនៅខាងក្រោម (៦០% និង ៥៤៥៥ $Mg \cdot km^{-2}$ រៀងគ្នា)។ ដូច្នេះការកាត់បន្ថយសំណឹកដីដោយការរក្សារុក្ខជាតិតូចៗនៅក្រោមចម្ការដើមម៉ៃសាក់ កាត់បន្ថយ SI បាន១៤ដង។ នៅក្នុងការសិក្សាមួយនៅឆ្នាំ២០១៤ នៅចម្ការដើមម៉ៃសាក់នៃផ្ទៃរងទឹកភ្លៀងហួយប៉ាណូទាំងនៅលើខ្នាតMicroplotនិងជម្រាលភ្នំ យើងបានបង្ហាញថា ការទុកចន្លោះស្មៅនៅមាត់អូរយ៉ាងតិច ៦ម អាចកាត់បន្ថយ SR និងSIនៅផ្នែកខាងក្រោមផ្ទៃរងទឹកភ្លៀង ក្នុងពេលមានភ្លៀងកម្រិតទាប (កម្ពស់ទឹកភ្លៀងក្នុង២៤ម៉ោង<៥៤.៨ មម) ជាមួយនឹងប្រសិទ្ធភាពនៃការស្រោចទឹកនិងដីល្បាប់បានរហូតដល់៨៨%។ ជាចុងក្រោយ នៅក្នុងការសិក្សាមួយនៅឆ្នាំ២០១៤ នៅចម្ការដើមម៉ៃសាក់នៃផ្ទៃរងទឹកភ្លៀងហួយប៉ាណូ លើមាត្រដ្ឋានផ្សេងៗ យើងបានបង្ហាញថា SR និង SI គឺខ្ពស់គួរអោយកត់សម្គាល់ (p-value <0.05) នៅក្នុងផ្ទៃរងទឹកភ្លៀងខ្នាតតូចដែលគ្រប់

គ្រងដោយដើមម៉ៃសាក់ ដែលខ្ពស់ជាងនៅក្នុងផ្ទៃរងទឹកភ្លៀងខ្នាតតូចដែលគ្រប់ដណ្តប់ដោយដីទំនេរ។ SR និង SI បានថយចុះពីខ្នាតMicroplot (១២២-១៩៦ មម និង ២៧៥-១០៦៥ Mg•km^{-2} រៀងគ្នា) ទៅផ្ទៃរងទឹកភ្លៀងខ្នាតតូច (២៤-១៨៨ មម និង ៩៥-៣៦៣៥ Mg•km^{-2} រៀងគ្នា) និងខ្នាតផ្ទៃរងទឹកភ្លៀង (៣៣ មម និង ២៣៦ Mg•km^{-2} រៀងគ្នា) លើកលែងតែ SI នៅក្នុងចម្ការដើមម៉ៃសាក់កើនឡើងពីខ្នាតMicroplot (១០៦៥ Mg•km^{-2}) ទៅខ្នាតផ្ទៃរងទឹកភ្លៀងតូច (៣៦៣៥ Mg•km^{-2})។ ការរកឃើញក្នុងនិក្ខេបបទនេះ ដោយផ្អែកលើការវាយតម្លៃពហុមាត្រដ្ឋាននៃហូរទឹកលើផ្ទៃដី និងការបាត់បង់ដី នឹងផ្តល់ឱ្យសហគមន៍និងសង្គមវិទ្យាសាស្ត្រ នូវលទ្ធផលជាបរិមាណ ស្តីពីសំណឹកដីពីមាត្រដ្ឋានតូច រហូតដល់មាត្រដ្ឋានធំ។ ព័ត៌មាននេះអាចជួយកសិករនិងអ្នកបង្កើតគោលនយោបាយ ក្នុងការអនុម័តនិងលើកកម្ពស់ការអនុវត្តការគ្រប់គ្រងដីប្រកបដោយនិរន្តរភាព។

Acknowledgements

I would like to extend my sincere thanks to the French government and Ministry of Education, Youth and Sports of Cambodia for awarding me a scholarship for this PhD study.

Throughout the writing of this thesis, I have received a great deal of support and assistance.

I would first like to express my deepest gratitude to my supervisor, Dr. BOITHIAS Laurie, whose constructive and professional advice was invaluable in formulating the research question and structuring my thesis. Her insightful feedback pushed me to sharpen my thinking and brought my work to a higher level.

I would like to express the deepest appreciation to my co-supervisor, Dr. RIBOLZI Olivier, for his professional guidance, constructive advice and immense supports in formulating the concept and methodology. His perfection provided me a good experience to pay careful attention at all time to become a professional researcher.

I would like to offer my grateful thanks to my co-supervisor, Dr. OEURNG Chantha for his valuable guidance throughout my studies. You provided me with the experience that I needed to choose the right direction and successfully complete my dissertation.

I would like to sincerely thank the authors from LPTP, IRD, Faculty of Agriculture of Lao PDR, and DALaM for their support and contribution to this research thesis.

I would also like to extend my gratitude to the thesis committees for providing me useful advice for the improvement of thesis.

I would like to acknowledge my working place, the Institute of Technology of Cambodia for letting me pursue this PhD study and my colleagues for their wonderful collaboration.

Special thanks to the secretary and colleagues in Géoscience Environnement Toulouse for their kind support in making a comfortable place during my time in France.

My deepest appreciation goes to my beloved wife and son for letting me be far away from them. I fully understand her hard time for taking care of our son alone. This successful PhD would not have happened without their sacrifice.

In addition, I would like to thank my parents for their emotional support. They are always there for me. My deepest thank to my parents-in-law and all my family and relatives for their emotional and financial supports. Finally, I could not have completed this dissertation without

the support of my friends who provided stimulating discussions as well as happy distractions to rest my mind outside of my research.

Last but not least, I would like to sincerely thank all the committee members for acknowledging my work and for providing comments and suggestions to the improvement of my thesis.

List of figures

List of tables

List of abbreviations

Alg	Algae
Cha	Charcoals
Con	Entering suspended sediment concentration
Ec	Erosion crust
EI30	Erosivity index
Fa	Free aggregates
Fg	Free gravel
Gc	Gravel crust
GNT/G	Grass near teak
Gra	Grass areal percentage
GWT/GT	Grass with teak
I30	Maximum 30-min rainfall intensity
KE	Rainfall kinetic energy
KEo	Rainfall kinetic energy at open space with grass
KEt	Rainfall kinetic energy in teak tree plantation
Mos	Mosses
Ped	Pedestal areal percentage
Pedm	Height of pedestal
PLSR	Partial least square regression
R/Rfa	Rainfall
Rc	Runoff coefficient
Res	Residue areal percentage
Run	Entering surface runoff
Sc	Structural crust
SCTE	Sediment concentration trapping efficiency
Sl/Sla	Soil loss
SR	Surface runoff
SSC	Suspended sediment concentration
STE	Sediment trapping efficiency
Tc	Total crust

Td	Teak with no understory at the downslope
TBG	Teak with broom grass
TEST	Terrace Erosion and Sediment Transport model
THU	Teak without high density of understory
TLU	Teak with low density of understory
Tm	Teak with no understory in the middle slope
TNU/T	Teak with no understory
Tu	Teak with no understory at upslope
TWU	Teak with understory
Und	Understory
UNEP	United Nations Environment Programme
VIP	Variable importance for the projection
Wor	Wormcasts
WTE	Water trapping efficiency

Chapter 1. Introduction

"Drop by drop is the water pot filled. Likewise, the wise man, gathering it little by little, fills himself with good." – *Buddha*

Chapitre 1
Introduction

L'érosion des sols est pourtant connue comme l'un des problèmes les plus préoccupants de l'environnement dans le monde. L'érosion mondiale des sols est particulièrement et de plus en plus due à l'expansion des terres cultivées. La plus forte augmentation devrait se produire en Afrique subsaharienne, en Amérique du Sud et en Asie du Sud-Est, en particulier dans les pays les moins développés avec les taux d'érosion des sols les plus élevés, qui étaient, en 2001, trois fois plus élevés que les pays développés (Borrelli et al., 2017). Les auteurs ont souligné que le niveau élevé d'érosion des sols dans les pays en développement est attribuable à la croissance démographique entraînant une pénurie alimentaire sans tenir compte des mesures de prévention de l'érosion des sols. En outre, l'érosion des sols dans les pays en développement est attribuée à une politique gouvernementale inappropriée, à la pauvreté, au manque d'intervention technologique et institutionnelle (Jayanath and Gamini, 2003). Avec l'augmentation de la population, la demande de produits agricoles augmente également, ce qui conduit à augmenter les surfaces consacrées aux terres de culture. Cette intensité agricole entraîne une grave érosion des sols, surtout lorsqu'il n'y a pas de gestion appropriée de l'utilisation des terres (Ribolzi et al., 2017).

Par conséquent, l'érosion des sols entraîne des graves impacts sur la fertilité des sols et sur les services écosystémiques fournis à l'échelle du bassin versant (Borrelli et al., 2017), qui pourraient être classés à la fois comme des effets sur site et hors site. Les effets sur site incluent la perte en sols, la dégradation des sols et le déclin de la production agricole (Bhat et al., 2019). Les effets hors site comprennent les catastrophes liées à l'eau, l'épuisement des eaux souterraines, la pollution des sources d'eau (charge sédimentaire élevée, bactéries potentiellement pathogènes, etc.) (Ahmad et al., 2020; Gateuille et al., 2014; Ribolzi et al., 2011a) et l'envasement des retenues de barrages (Annandale, 2006; Owens et al., 2005). Tous les effets contribuent aux pertes économiques. 75 milliards de tonnes de sol érodé chaque année sur les terres arables du monde entier auraient contribué à une perte financière estimée à 400 milliards de dollars américains par an (GSP, 2016).

Les problèmes de dégradation des terres sont directement liés aux pratiques d'utilisation des terres, en particulier l'expansion et l'intensification agricoles (Lestrelin, 2010). En Asie du Sud-Est, toutes les terres sont presque dégradées par l'agriculture et la déforestation étant les deux principaux facteurs contributifs (Van Lynden and Oldeman, 1997). En RDP lao, un pays

tropical, l'érosion des sols est importante et due au changement d'utilisation des terres et à une gestion inappropriée des terres sur les terrains en pente (Chaplot et al., 2005b; Ribolzi et al., 2017; Valentin et al., 2008). Une mauvaise gestion des terres agricoles peut entraîner une érosion de surface qui entraîne une dégradation des terres et des taux de sédimentation plus élevés en aval (Cerdà et al., 2018).

Il est généralement reconnu que le reboisement des terres avec des cultures agricoles telles que la plantation d'arbres servirait de forêt naturelle et empêcherait l'érosion du sol (Eldridge et al., 2003). Cependant, certaines recherches ont révélé qu'une mauvaise gestion des terres cultivées, telles que la plantation d'arbres, entraîne une érosion des sols plus élevée. Par exemple, Ribolzi et al. (2017) ont constaté que la conversion de la culture itinérante traditionnelle en plantations de teck a entraîné une forte augmentation des écoulements de surface et de l'érosion des sols. Comme mesures d'atténuation, certaines recherches récentes ont souligné que l'inclusion de la culture sous couvert végétal dans la plantation d'arbres limiterait l'érosion du sol (Lacombe et al., 2018) et laisser l'herbe indigène dans la zone rivulaire éviterait l'érosion des terres en pente immédiatement adjacentes aux cours d'eau (Vigiak et al., 2008). Cependant, ces mesures d'atténuation ne sont pas encore évaluées dans la plantation de teck.

Dans ce contexte, l'objectif général de cette thèse est de tester les options d'atténuation et de fournir des recommandations de pratiques de gestion des terres dans la zone cultivée en teck. Plus précisément, la thèse vise à mieux comprendre les processus entraînant la génération de ruissellement de surface, le détachement du sol et l'exportation de sédiments dans les plantations d'arbres de teck cultivées dans la zone montagneuse du nord de la RDP lao, en utilisant une approche multi-échelle : échelle de parcelle, de versant/micro-bassin versant, et de bassin versant. La thèse est organisée en sept chapitres, dont trois portent sur les expérimentations scientifiques.

Le chapitre 2 est une section décrivant le contexte général de la thèse, passant en revue les mécanismes de génération de ruissellement de surface et de perte en sols, les causes et effets de l'érosion des sols, l'importance de conserver à la fois le sous-étage dans la plantation d'arbres et la zone tampon rivulaire sur le versant cultivé, et les profite de l'agroécosystème en maintenant la culture sous couvert végétal dans la plantation d'arbres. Le chapitre donne un aperçu des pratiques de gestion des terres dans la plantation d'arbres de teck dans le nord de la RDP lao. Enfin, le chapitre passe en revue les approches de modélisation hydrologique et sédimentaire. Sur la base de cet état de l'art, nous avons défini les objectifs spécifiques de la thèse.

Le chapitre 3 décrit les domaines d'étude, les matériels et les méthodes utilisés pour atteindre les objectifs spécifiques énoncés dans le chapitre 2.

Le chapitre 4 est un chapitre scientifique étudiant le rôle du sous-couvert végétal dans la limitation du ruissellement de surface et de la perte en sols dans les plantations de teck à l'échelle de la microparcelle.

Le chapitre 5 est un chapitre scientifique évaluant le ruissellement de surface et la perte en sols, et l'efficacité de piégeage de l'herbe indigène dans la zone tampon rivulaire pour capturer le ruissellement de surface et le sol détaché des hautes terres plantées de teck en utilisant une approche multi-échelle (échelles de microparcelle et de versant).

Le chapitre 6 est un chapitre scientifique qui évalue le comportement hydro-sédimentaire dans le bassin versant dominé par des plantations de jachères et de teck en utilisant une approche multi-échelle, c'est-à-dire les échelles de microparcelle, versant/micro-bassin versant et de bassin versant. Ce chapitre a également comparé le ruissellement de surface et l'exportation de sédiments des micro-bassins à dominance en jachère et en teck.

Le chapitre 7 est une conclusion générale des résultats issus des chapitres scientifiques. Le chapitre surligne les principaux résultats de l'efficacité des pratiques d'atténuation de l'utilisation du sous-couvert végétal et de la zone tampon d'herbes rivulaires, et le comportement hydro-sédimentaire à différentes échelles spatiales caractérisé par leurs processus pertinents et leurs facteurs d'influence. Ce chapitre propose des recommandations pour parvenir à une gestion durable des plantations d'arbres dans le contexte du climat tropical et des terres à forte pente. Sur la base des conclusions de cette thèse, des perspectives de recherches aux futures sont suggérées.

Chapter 1

Introduction

Soil erosion is yet known as one of the most concerning problems of the environment in the world. Global soil erosion is particularly and increasingly driven by cropland expansion. The greatest increase was predicted to occur in Sub-Saharan Africa, South America and Southeast Asia, especially in the least developed countries with the highest soil erosion rates three times higher than developed countries (Borrelli et al., 2017). The authors emphasized that the high level of soil erosion in developing countries is attributable to the population increase. In addition, soil erosion in developing countries is attributed to inappropriate government policy, poverty, lack of technological and institutional intervention (Jayanath and Gamini, 2003). With the population increase, the demand for agricultural products also increases and may cause food shortage and increase land surface area devoted to cultivation. Hence, soil erosion prevention measures may be not seriously considered either. This agricultural intensity leads to severe soil erosion, especially when there is no proper land use management (Ribolzi et al., 2017).

Consequently, soil erosion leads to serious impacts on soil fertility and on the ecosystem services supplied on the catchment scale (Borrelli et al., 2017), which could be categorized as both on-site and off-site effects. The on-site effects include soil loss (Sl), soil degradation and decline of agricultural production (Bhat et al., 2019). The off-site effects include water-related disasters, groundwater depletion, water source pollution (high sediment load, potentially pathogenic bacteria, etc.) (Ahmad et al., 2020; Gateuille et al., 2014; Ribolzi et al., 2011a), and dam reservoir siltation (Annandale, 2006; Owens et al., 2005). All of the effects contribute to economic losses. 75 billion tons of soil eroded every year from arable lands worldwide was reported to contribute to an estimated financial loss of US $400 billion per year (GSP, 2016).

Land degradation issues are directly connected to land use practices, especially agricultural expansion and intensification (Lestrelin, 2010). In Southeast Asia, all land is almost degraded with agriculture and deforestation as the two significant contributory factors (Van Lynden and Oldeman, 1997). In Lao PDR, a tropical country, soil erosion is significant due to land use change and inappropriate land management on the sloping land (Chaplot et al., 2005b; Ribolzi et al., 2017; Valentin et al., 2008). Mismanagement of agricultural land may lead to surface erosion which leads to land degradation, higher sediment rates downstream (Cerdà et al., 2018).

It is generally acknowledged that reforesting the land with agricultural cultivation, such as planting tree would serve as the natural forest and prevent soil from erosion (Eldridge et al.,

2003). However, some research revealed that improper management of cultivation land such as tree plantation causes higher soil erosion. For example, Ribolzi et al. (2017) found that the conversion from traditional shifting cultivation to teak tree plantations led to a dramatic rise in overland flow and soil erosion. As mitigation measures, some recent researches highlighted that including understory in the tree plantation would limit soil erosion (Lacombe et al., 2018) and leaving the native grass in the riparian area would avoid erosion taking place in the sloping land immediately adjacent to streams (Vigiak et al., 2008). However, these mitigation measures are not yet evaluated in the teak tree plantation.

In this context, the general objective of this thesis is to test mitigation options and to provide a recommendation of land management practices in the teak-cultivated area. More specifically, the thesis aims at better understanding the processes driving surface runoff (SR) generation, soil detachment, and sediment exportation in teak tree plantations grown in the mountainous area of northern Lao PDR, by using a multi-scale approach: microplot, hillslope/micro-catchment, and catchment scale. The thesis is organized into seven chapters, three of which focus on scientific experimentations.

Chapter 2 is a section describing the general context of the thesis, reviewing the mechanisms of the generation of SR and of Sl, the causes and effects of soil erosion, the importance of keeping both the understory in the tree plantation and the riparian buffer zones on the cultivated hillslope and agroecosystem benefits from keeping the understory in the tree plantation. The chapter gives an overview of land management practices in the teak tree plantation in the northern Lao PDR. Lastly, the chapter reviews hydrological and sedimentary modelling approaches. Based on this state-of-the-art review, we defined the specific objectives of the thesis.

Chapter 3 describes the study areas, the materials and methods used to achieve the specific objectives stated in Chapter 2.

Chapter 4 is a scientific chapter investigating the role of the understory in limiting SR and Sl in teak tree plantations on the microplot scale.

Chapter 5 is a scientific chapter assessing SR and Sl, and the trapping efficiency of the native grass in the riparian buffer in capturing SR and detached soil from the upland planted with teak trees by using a multi-scale approach (microplot and hillslope scales).

Chapter 6 is a scientific chapter that evaluates the hydro-sedimentary behaviour in the catchment with mixed land uses and dominated teak tree plantation by using a multi-scale approach, i.e., microplot, hillslope/micro-catchment, and catchment scales. This chapter also compared the SR and sediment exportation from mixed-land-use and teak-dominated micro-catchments.

Chapter 7 is a general conclusion of the results stemming from the scientific chapters. The chapter highlights the main findings of the efficiency of mitigation practices using understory and riparian grass buffer and the hydro-sedimentary behaviour on various spatial scales characterized by their relevant processes and influencing factors. This chapter suggests recommendations to achieve sustainable management of tree plantations in the context of tropical climate and steeply sloping land. Based on the conclusions of this thesis, perspectives for future research are suggested.

[This page intentionally left blank]

Chapter 2. General contexts, problem statements and objectives

"The greatest glory in living lies not in never falling, but in rising every time we fall." – *Nelson Mandela*

Chapter 2

General contexts, problem statements and objectives

2.1. GENERAL CONTEXT

Global human population growth amounts to 0.84% per year based on the prediction of the United Nations (2019). Population growth alongside overconsumption is a key driver of environmental concerns, such as land use change, biodiversity loss, and climate change, due to resource-intensive human development that exceeds planetary boundaries (UNEP, 2021). Due to the population growth, the rise in good consumption in general (including food demand and wood consumption to make furniture, etc.) contributes to the extension of land devoted to agricultural purposes.

Oldeman (1994) reported that global land area had faced water erosion, which was twice higher than wind erosion, and Asia is a leading continent facing severe soil erosion. Borrelli et al. (2017) predicted that Asia was preceded by South America and Africa in terms of soil erosion (**Figure 2.1**), and Southeast Asia had the most significant increases in soil erosion. The authors suggested that developing countries experienced high predictions of soil erosion. Soil degradation due to erosion in developing countries is closely linked to personal and national poverty (Oldeman, 1992). Poor farmers with no resources to fall back on may be forced to put immediate needs before the land's long-term health. Under pressure from foreign debt, weak commodity prices and the needs of their urban populations, coupled with domestic policies that are biased against agriculture, governments often fail to give adequate technical support to rural people (Loftas and Ross, 1995). A potential overall increase in global soil erosion is rendered by an accelerative expansion of agricultural lands replacing the natural forest, soil and land mismanagement, unsustainable farming system, extension and intensification of agricultural land which is converted from the natural forest (Bhat et al., 2019; Borrelli et al., 2017; Mohamadi and Kavian, 2015; Prokop and Poręba, 2012; Sartori et al., 2019; Wuepper et al., 2020). Locally, steep slopes and high-relief topography also induce high soil erosion rates. Similarly, regions with generally sparse vegetation cover across the year experience high soil erosion rates. Soil erosion is also exacerbated by the changing climate with more extreme rainfall (Borrelli et al., 2020).

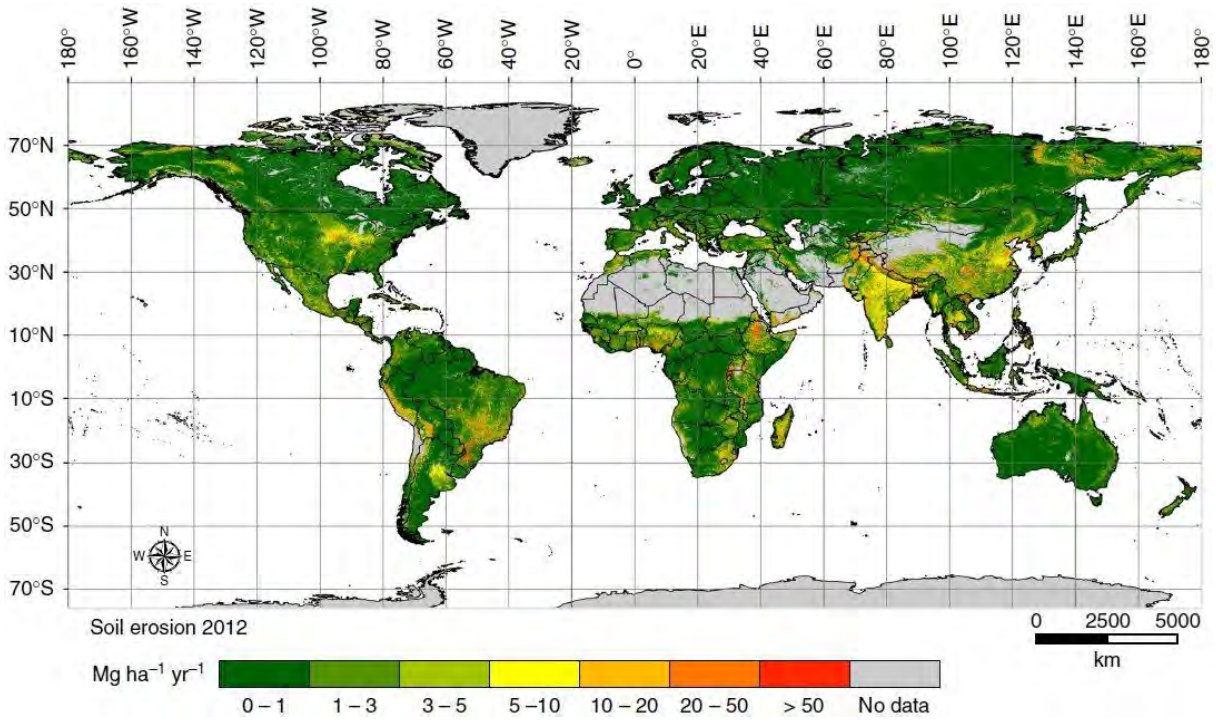

Figure 2.1: A global map of soil erosion in 2012 (source: Borrelli et al. (2017))

Soil erosion has become one of the widespread environmental concerns in the world due to its adverse economic and environmental impacts (Lal, 1998). Soil erosion leads to severe impacts on soil fertility and on the ecosystem services supplied on the catchment scale (Borrelli et al., 2017). Soil erosion causes the annual absolute land productivity losses due to soil fertility depletion, which severely affects the countries in the inter-tropical belt (**Figure 2.2**). Those impacts could be categorized as both on-site and off-site effects, which contribute to the economic loss (Pimentel et al., 1995). On-site effects of increased soil erosion involve soil degradation and decline of agricultural production due to soil and nutrient losses (Bhat et al., 2019; Douglas Jr. et al., 1998; José et al., 2005; J. W. Poesen and Hooke, 1997; Sartori et al., 2019; Valentin and Rajot, 2018).

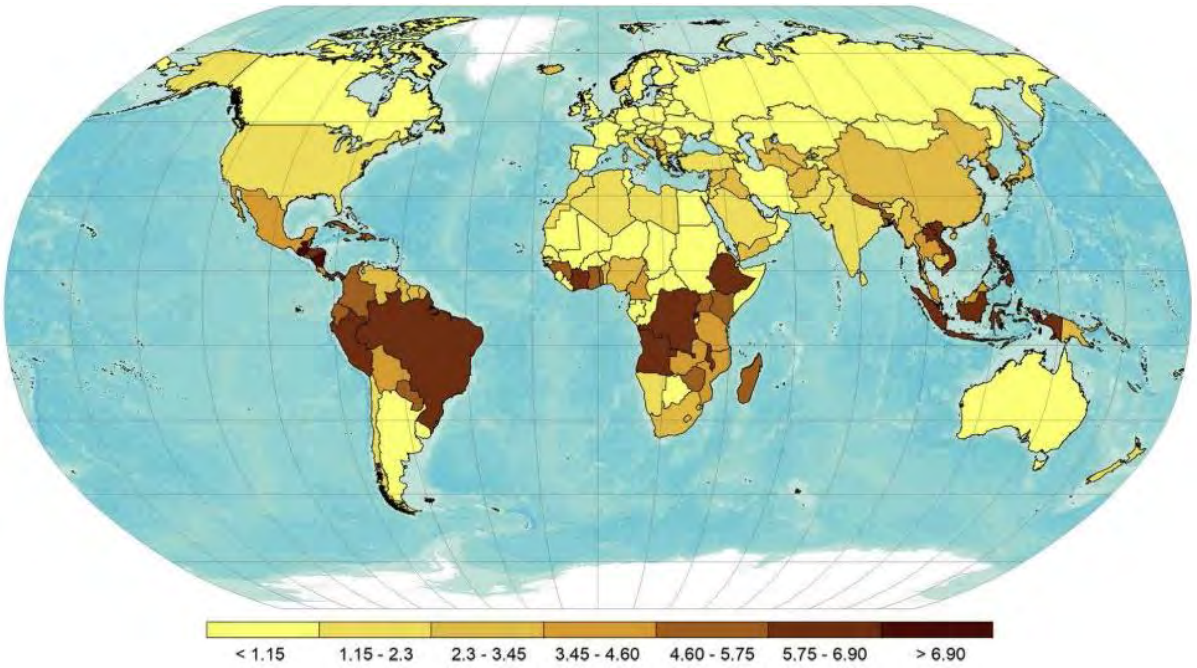

Figure 2.2: Estimated annual absolute land productivity losses (%) from the Global RULS model (Sartori et al., 2019).

Off-site effects include floods, depletion of groundwater recharge, degradation of stream environments, infrastructure (ditch, road, and drainage system), and downstream sedimentation (Ledermann et al., 2010; Mahabaleshwara and Nagabhushan, 2014; Owens et al., 2005; Valentin and Rajot, 2018). Soil erosion contributes to siltation of water ways and reservoirs, and additional costs involved in water treatment (Efthimiou et al., 2016; Lal, 1998; Thothong et al., 2011; Zarris et al., 2011), and loss of other ecosystem services (Boithias et al., 2016b). In addition, the adsorption of organic and inorganic matter on soil particles and suspended sediments plays a leading role in the transport of nutrients (Yuan et al., 2019), radionuclides (Chartin et al., 2013), metals (Turner et al., 2008), pesticides (Domagalski and Kuivila, 1993), and bacterial pathogens (Gateuille et al., 2014; Ribolzi et al., 2011a). Higher contamination of rivers by faecal bacteria is often correlated to higher in-stream suspended sediment concentration and causes health issues such as diarrheal diseases (Boithias et al., 2016a; Kim et al., 2018), which is a vital issue of tropical countries (Rochelle-Newall et al., 2015; Rochelle-Newall et al., 2016). Soil degradation fuels climate change by releasing soil carbon into the atmosphere (Harrabin, 2019). Even though a lot of negative impacts of soil erosion have been observed on-site and off-site, soil erosion brings some benefits to livelihood and biodiversity downstream. Nutrients washed off by on-site erosion processes can be distributed to the downslope area via overland flow and to downstream areas (floodplains and deltas) via rivers, which essentially support agriculture and ecosystem downstream (Fondriest Environmental,

2014; WMO, 2006). Most of the effects lead to high economic and ecological costs (Ribaudo, 1986; Sartori et al., 2019).

In the mountainous region of northern Lao PDR, agricultural practices such as shifting cultivation and teak tree plantations are known to increase SR, soil erosion, and in-stream suspended sediment concentrations compared to the natural forest (Patin et al., 2012; Valentin et al., 2008). In particular, commercial perennial monocultures, such as teak tree plantations, lead to a drastic SR increase (Lacombe et al., 2016) and exacerbate Sl along hillslopes and in the river network (Lacombe et al., 2018; Ribolzi et al., 2017). In teak tree plantations, such as the old teak trees (high timbers with broad leaves) growing in the Houay Pano catchment (an experimental and tropical catchment located in northern Lao PDR (Boithias et al., 2021; Valentin et al., 2008)), SR and soil erosion are likely related to the recurrent understory and leaf litter suppression by burning at the end of the dry season, leaving the soil bare and exposed to the kinetic energy of the raindrops (Patin et al., 2018). Land use, understory cover, and soil surface condition are the main drivers influencing water infiltration into the soil (Chaplot et al., 2007; Ribolzi et al., 2011b).

Erosion can, however, be reduced along with the load of sediment reaching the river network, and eroded land can be restored by following measures (Loftas and Ross, 1995):

- Reforested land (not a tree plantation with bare soil)
- Gully erosion can be halted by check dams, and trees can be planted on gully banks
- Steep land is bench-terraced
- Contour cultivation practised on lower land
- Bunds are built to control SR
- New reservoirs supply power to nearby villages
- Shelter belts reduce wind erosion, and pastures are improved or upgraded
- Crop rotation practised in strips along contours
- Tree crops grown on eyebrow terraces on steep land

For proper land management and sustainable use of soil and water resources, on-site erosion needs to be assessed. A wide range of methods can be used, which can define the origin of Sl and categorize the severity of Sl (Lal, 1998). Numerous studies conducted field experiments to assess Sl in different land uses and suggested sound and practical measures to reduce the

severity of Sl (Janeau et al., 2014; Lacombe et al., 2018; Miyata et al., 2009; Neave and Rayburg, 2007; Neyret et al., 2020; Nouwakpo et al., 2018; Patin et al., 2018). The results suggested leaving or planting more vegetation in monoculture lands which noticeably contribute the most to Sl (Ahmad et al., 2020; Fernández-Moya et al., 2014; Nearing et al., 2017). Understory and plant residues on the soil surface are known to efficiently attenuate the effect of splash and thus soil detachment (Cerdà et al., 2018; Durán Zuazo et al., 2006; Ehigiator and Anyata, 2011; Li et al., 2014; Roose, 1996). In northern Thailand, soil erosion in rubber tree plantations decreased when understory was grown (Neyret et al., 2020). Indeed, in northern Lao PDR headwater catchments, the runoff coefficient is approximately 55% under teak trees at the plot scale (Lacombe et al., 2018), whereas it nearly doubled from 16% to 31% within 13 years at the catchment scale (Ribolzi et al., 2017), resulting from the absence of understory in the teak tree plantation area. Ahmad et al. (2020) suggested that intercropping is another good practice of growing more than one crop in the same field simultaneously to reduce soil erosion. Rather than using countermeasure on-site, several studies suggested that vegetated buffer strips at the riparian zone also limit Sl on the hillslope scale and contribute to the reduction of sediment export to the stream (Alemu et al., 2017; Cao et al., 2018; Dong et al., 2018; Gumiere et al., 2011; Kuglerová et al., 2014; Vigiak et al., 2008), and mitigates water quality problem downstream (Petersen et al., 2020).

2.2. WATER AND SOIL EROSION PROCESSES

2.2.1. *Water flow processes from local scale to catchment scale: overland flow, throughflow, groundwater flow*

Water flow processes can be described on three scales: plot scale (from the very beginning of water flow generation), hillslope scale, and catchment scale (**Figure 2.3**).

At the plot scale (**Figure 2.3a)**, when rain falls onto the land, rain water starts moving due to gravity. Some of it seeps into the ground based on the soil surface condition (vegetation and residue cover, etc.). The seeping water fills the soil pore and remains available for the plant. This water may subsequently be evaporated or flow laterally close to the surface as throughflow, or else it may percolate downwards under gravity to the water table. Some water flows down gradient as SR: infiltration-excess overland flow or saturation-excess overland flow. Infiltration-excess overland flow occurs when the rainfall intensity on a surface exceeds the rate at which water can infiltrate the ground (infiltration capacity). This is also called flooding excess overland flow, Hortonian overland flow (Horton, 1933), or unsaturated overland flow. This more commonly happens in arid and semi-arid regions or on the bare soil,

where rainfall intensities are high, and soil infiltration capacity is reduced by soil crusting or paved areas (Vaezi et al., 2010). Saturation-excess overland flow happens when the soil is saturated, and rain continues to fall; the rainfall immediately produces SR (Dunne and Black, 1970). The level of antecedent soil moisture is one factor influencing the time until the soil is saturated (Robinson and Ward, 2017).

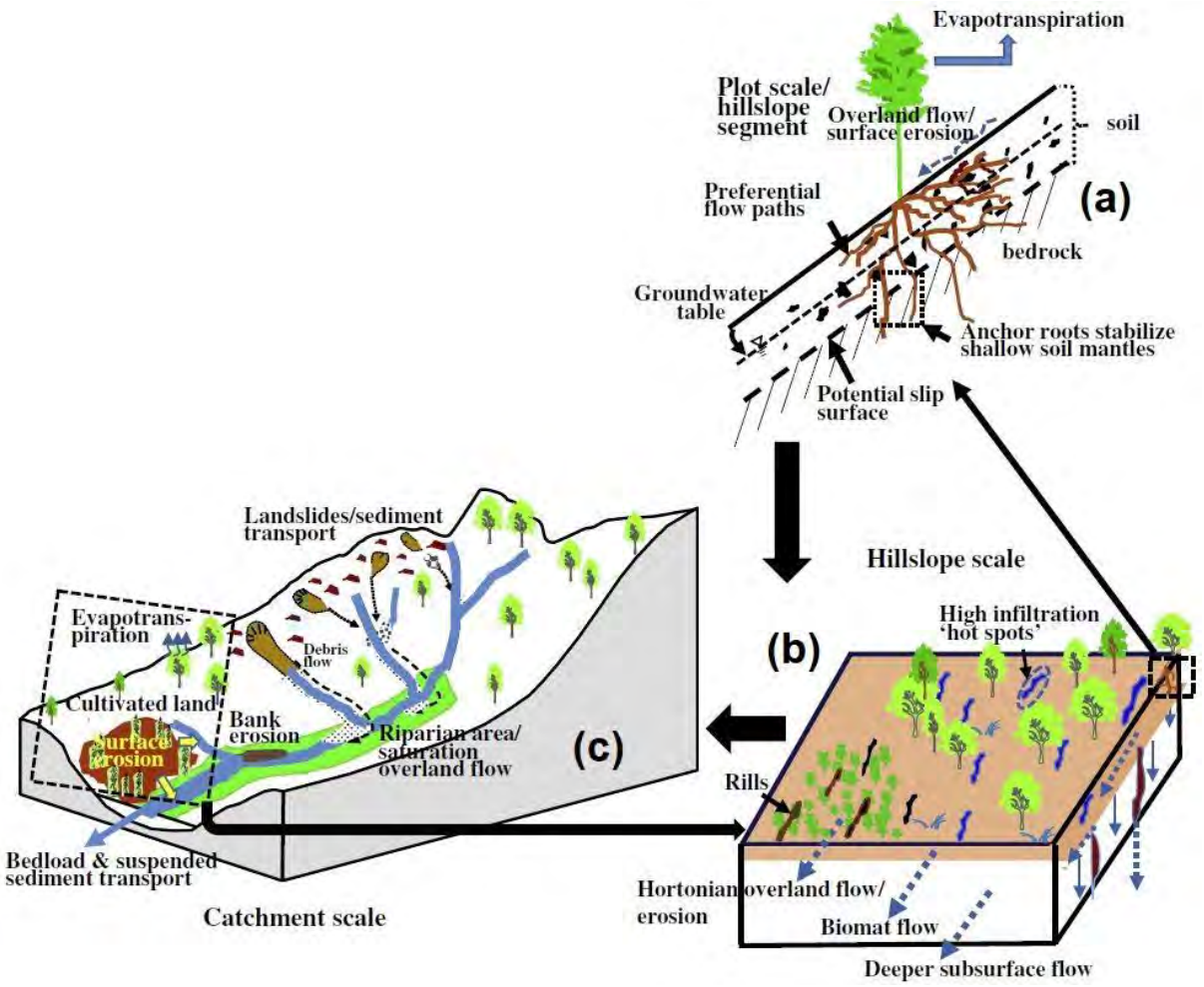

Figure 2.3: Water flow processes at (a) plot scale, (b) hillslope scale, and (c) catchment scale (Source: Sidle et al. (2017))

On the hillslope scale (**Figure 2.3b**), the processes involve the sheet flows happening inter rills, rill flow, exfiltration, throughflow and groundwater flow (Sidle et al., 2017). Sheet flow is formed by a thin, continuous film of overland flow on relatively smooth soil or rock surfaces. This flow then concentrates into the small channel called rill. The water flowing through these may not all contribute to the streamflow, but it may infiltrate latter when it is trapped by the obstacles, for example, vegetation cover at the downstream or riparian area (Fiener and Auerswald, 2006; Le Bissonnais et al., 2004). Simultaneously, it may be reduced in other

possible ways: a small portion of it may evapotranspire; water may become temporarily stored in microtopographic depressions; and a portion of it may infiltrate as it flows overland. Water infiltrating the soil surface and then moving laterally through the upper soil horizons towards the stream channels is known as throughflow. Throughflow is likely to happen when the lateral hydraulic conductivity of the surface soil horizons greatly exceeds the overall vertical hydraulic conductivity through the soil profile (Hewlett and Hibbert, 1967; Weyman, 1970). Subsequently, during prolonged or intense rainfall on a hillslope, water entering the upper layer of the profile more rapidly than its vertical drain through the lower layer, will accumulate and form a perched saturated layer from which water will escape laterally in the direction of greater hydraulic conductivity. However, some rainfall may percolate through the soil to the underlying groundwater, and so eventually reach the main stream as groundwater flow (Robinson and Ward, 2017).

Water flow processes on the catchment scale (**Figure 2.3c**) include overland flow, through flow, groundwater flow and stream flows connected from the upper part of the catchment and the sub-catchments (Robinson and Ward, 2017). All the flow will then accumulate into the same exit of the catchment called outlet.

The hydrological processes may be affected by various meteorological factors (Arnaez et al., 2007; USGS, 2021):

- Rainfall intensity
- Rainfall amount
- Rainfall duration
- Distribution of rainfall over the drainage basin
- Precipitation that occurred earlier and resulting soil moisture
- Other meteorological and climatic conditions that affect evapotranspiration, such as temperature, wind, relative humidity, and season

The other biophysical characteristics affecting the hydrological processes (Ai et al., 2015; Damian Ruiz Sinoga et al., 2010; USGS, 2021) are:

- Land use
- Vegetation
- Soil type

- Drainage area
- Basin shape
- Elevation
- Topography, especially the slope of the land
- Drainage network patterns
- Ponds, lakes, reservoirs, sinks, etc. in the basin, which prevent or delay runoff from continuing downstream

2.2.2. *Soil erosion and sediment transport processes*

Five types of soil erosion by water are categorized as following (Bhat et al., 2019):

- Raindrop erosion: raindrops striking on the surface of land cause detachment of soil particles and are carried with flowing water. It is also known as splash erosion.
- Sheet erosion: it is defined as detachment of the fairly uniform layer of soil from the land surface by the action of rainfall and runoff.
- Rill erosion: the elimination of the soil by the flowing water, forming areas of small branched canals.
- Gully erosion: the advanced stage of the erosion of the furrow. It is the last phase of water erosion.
- Stream bank erosion: the sourcing of material from the bottom and side of a stream or waterway and the clipping of bank by flowing water.

A mechanical erosion by water defined by a process comprising three mechanisms (Valentin and Rajot, 2018):

- fragmentation or detachment under the effect of very diverse agents: impact of raindrops and runoff and mass movements (stream bank erosion and landslide);
- transport of loose particles;
- sedimentation or deposition

Soil erosion processes can be described on three scales: plot scale (from very beginning of water flow generation), hillslope scale, and catchment scale (**Figure 2.3**).

On the plot scale (**Figure 2.3a)**, the dominant erosion mechanism is splash and sediments are washed, i.e. transported, by runoff (Kinnell, 2005). When rain falls onto the land, especially on the bare soil, rain detaches soil particles though splash effect. Then surface runoff transports those detached soil particles due to gravity. Surface runoff flow can also lift the loose particles or aggregates up and entrain them downhill when the energy of flow is sufficiently large. The soil particles can settle quickly, often in the plot, while the finer particles can be transported in suspension over long distances. This settlement of sediment is called deposition and happens due to gravity and frictional forces (Chaplot and Poesen, 2012), especially by understory and grass.

On the hillslope scale (**Figure 2.3b**), the deposition of detached soil particles may occur through gravity and prevailing friction (Chaplot and Poesen, 2012) and through riparian buffer (Cooper et al., 1987; Ding et al., 2011; Verstraeten et al., 2006; Vigiak et al., 2008). On this scale, linear erosion can occur through gullies (Chaplot et al., 2005b). Sediment deposition and linear erosion may be affected by hillslope topography (Buckley, 2010; Sabzevari and Talebi, 2019). On convergent hillslope (micro-catchment), the sediment flow may concentrate and bypass the riparian buffer through gullies (Verstraeten et al., 2006; Wenger, 1999), especially under heavy rainfalls (de Rouw et al., 2018).

Catchment scale involves sediment deposition and resuspension (**Figure 2.3c**). Sediments transported from hillslope could be trapped in the headwater wetland (Cao et al., 2018; Goddard and Elder, 1997; Schmadel et al., 2019), which is considered as sediment storage (Phillips, 1989). Deposited sediment can be resuspended under extreme event rainfall (Robotham et al., 2021; Thothong et al., 2011). The soil particles may be continuously transported through rills and then through gullies and at last may be accumulated into the channel on the catchment scale. Furthermore, high rainfall can resuspend those particles depositing in the bed of river channels (Ribolzi et al., 2016). On this scale, two more processes can significantly increase soil loss at the outlet of a catchment: landslides and stream bank erosion (Valentin and Rajot, 2018). Slope saturation by water is a primary cause of landslides, which can occur in the form of intense rainfall and changes in ground-water levels (Highland, 2004). The landslide trigger corresponds to a threshold combining several factors: an increase in mass (due to heavy rain), on a steep slope with a water-saturated sliding surface, often between two different soil horizons or even between two rocks (Valentin and Rajot, 2018). Stream bank erosion results from erosion of the foot of banks by turbulent stream flows, or from local saturation of the banks that collapse after a flood, or from a seepage zone linked to soil water exfiltration (Valentin and Rajot, 2018).

The factors influencing soil erosion depends on scale. Those factors are the erosivity of the eroding agent (amount of rainfall, rainfall intensity, kinetic energy), the erodibility of the soil (soil surface features), the slope of the land and the properties of the plant cover (Morgan, 2005). Moreover, soil erosion is also affected by length of slope and topography (Bhat et al., 2019). Soil erosion mostly happens when soil surface is not protected due to the absence of vegetation and residue cover (Loftas and Ross, 1995; Neave and Rayburg, 2007; Rey et al., 2004). Rainfall or throughfall detaches bare soil which is then washed by surface runoff (Valentin and Rajot, 2018). Clearing forests, growing crops on steep slopes or large field without protection, can all leave soil exposed to erosion (Ehigiator and Anyata, 2011; Valentin et al., 2005).

Multi-scale research studies seem a promising approach to detect and quantify the relative contribution of erosion processes (e.g., splash, sheet, concentrated flow, stream bank and stream bed mobilization, and resuspension) that dominate at various spatial scales (De Vente and Poesen, 2005; J. W. Poesen and Hooke, 1997; Van Noordwijk et al., 2004; Verbist et al., 2010).

2.3. TOPSOIL SURFACE FEATURES

Soil particles and their texture define the soil structure and the aggregation characterizing the soil surface features. Soil surface features also depend essentially on vegetation cover, rainfall depth, density and number of layers of vegetation, and residue (Valentin, 2018). Physical soil crusts are characterized by very low macroporosity. They seal the surface of the soil, hence the term seal, which is used to designate crusts in their wet state. Because of their hardness when dry, they tend to protect soils from *in situ* water erosion. However, as they encourage runoff, they increase the risk of downstream erosion in rills or gullies. Several types of physical crusts can be distinguished as following (Valentin and Bresson, 1992) and are shown in **Figure 2.4**:

- Structural crusts: formed *in situ* on the soil
- Gravel crusts: defined by coarse fragments embedded in a structural crust
- Erosion crusts: defined by their smooth surface aspect and resulting from the erosion by water of structural crusts
- Depositional crusts: resulting from the deposition of fine particles in puddles
- Saline crusts and efflorescence
- Biological soil crusts (or Biocrusts): resulting from the assemblage of many organisms

Figure 2.4: Free aggregates and coarse elements, structural crust (embedded aggregates), erosion crust and gravel crust (embedded coarse fragments) (source: (Valentin, 2018))

2.4. LAND USE CHANGE

Concerns about land use and cover change appeared in the research agenda on global environmental change several decades ago with the realization that land surface processes influence climate (Dale, 1997), agricultural productivity and environmental water quality (Lal, 1998). Population increase leads to increase food and fiber demand, thus increasing agricultural land (Lambin et al., 2003). These demands lead to deforestation representing one of the largest issues in global land use; forests have been converted into commercial croplands and tree plantations (Pimm, 2007; Tracy Van et al., 2016) such as rubber tree, oil palm tree, teak tree, etc. In 2010, teak tree plantations accounted for around 4 million ha, of which 83% was in Asia, 11% in Africa, 6% in tropical America, and less than 1% in Oceania (Kollert and Cherubini, 2012). However, in 2015, teak tree plantation was almost 7 million ha (Midgley et al., 2015). The increase in the global demand for food and fresh water and the associated land use changes or misuses exacerbate soil erosion by water (Chaplot et al., 2007).

First and foremost, through deforestation and forest degradation, tropical land cover changes have numerous adverse effects on both biotic and abiotic systems (Corlett, 2014; Myers, 1988; Rieley and Page, 2005). Furthermore, deforestation and land cover changes in tropical regions are often connected to complicated political and socio-environmental controversies involving stakeholders from all over the world (Dennis et al., 2005; Sheil et al., 2009). Carbon emissions and transboundary air pollution from forest conversion fires are typical examples of issues that may easily cause tension in international and global level politics (Chaplot et al., 2007; Miettinen et al., 2011).

In the sloping land of Southeast Asia, land use changes are rapid due to strong demographic, economic and political pressures. In many locations, the primary forest has been cleared for slash and burn cultivation or more intensified systems based on the use of pesticides, fertilizers and machinery. At the onset of the rainy season, the tilled soil is left bare. It tends to crust and generate runoff, which then concentrates linear erosion. Changes, especially those linked to land use, are even more extreme in areas where slash and burn systems predominate. These areas now suffer a reduction of the fallow period and an intensification of agriculture. In Laos, up to 1 million people may be involved in shifting cultivation, making up 40 percent of the land area dedicated to the country's principal crop, rice (Angelsen and Kaimowitz, 2004). Despite the crucial need for a sound assessment of processes linked to such regional changes, available data remain scarce and are usually based on a single process observed at a specific scale (Chaplot et al., 2005a).

Aside from the rice, other plantations for biomass, latex, and timber production have significantly increased through the shifting from rice cultivation. Over the last decades, Southeast Asia has experienced the expansion of rubber tree plantations into previously forested areas (Neyret et al., 2020). In Cambodia, land use has begun to change to agricultural crops such as palm oil, rubber, cassava, and kapok, which add more pressure to the forestland (Nut et al., 2021). In Lao PDR, the government promotes the plantation of trees, especially teak trees, by smallholders (Newby et al., 2012). In Luang Prabang province of northern Lao PDR, teak tree plantations increased from 500 ha in 1990 to more than 15000 ha by 2017 (Kolmert, 2001; Midgley et al., 2007; Smith et al., 2017). In the Houay Pano catchment located in the northern Lao PDR, the proportion of secondary forests in the catchment decreased between 2002 and 2014 and cropping land was continuously being converted to timber tree such as teak tree (Ribolzi et al., 2017). From 2008, it continuously increased, almost linearly, to reach a maximum of 36% of the catchment area in 2014 as teak plantation becomes more and more popular for its valuable timber in the world market. After the gradual conversion of rice-based shifting cultivation to teak tree plantation-based systems, overland flow contribution to stream flow increased from 16 to 31% and sediment yield raised from 98 to 609 $T \cdot km^{-2}$ (Ribolzi et al., 2017) (**Figure 2.5**). The teak tree plantation is characterized by limited understory vegetation cover, which enhances soil erosion. This change in land use to the improper-managed agricultural lands may lead to the unsustainability and soil degradation in the cultivated areas. Furthermore, this change will then need more extent of land in the natural forest after the

abandon of the degraded agricultural land. However, the sustainability of land use management in the mixed land use dominated by teak tree plantation is not yet fully assessed.

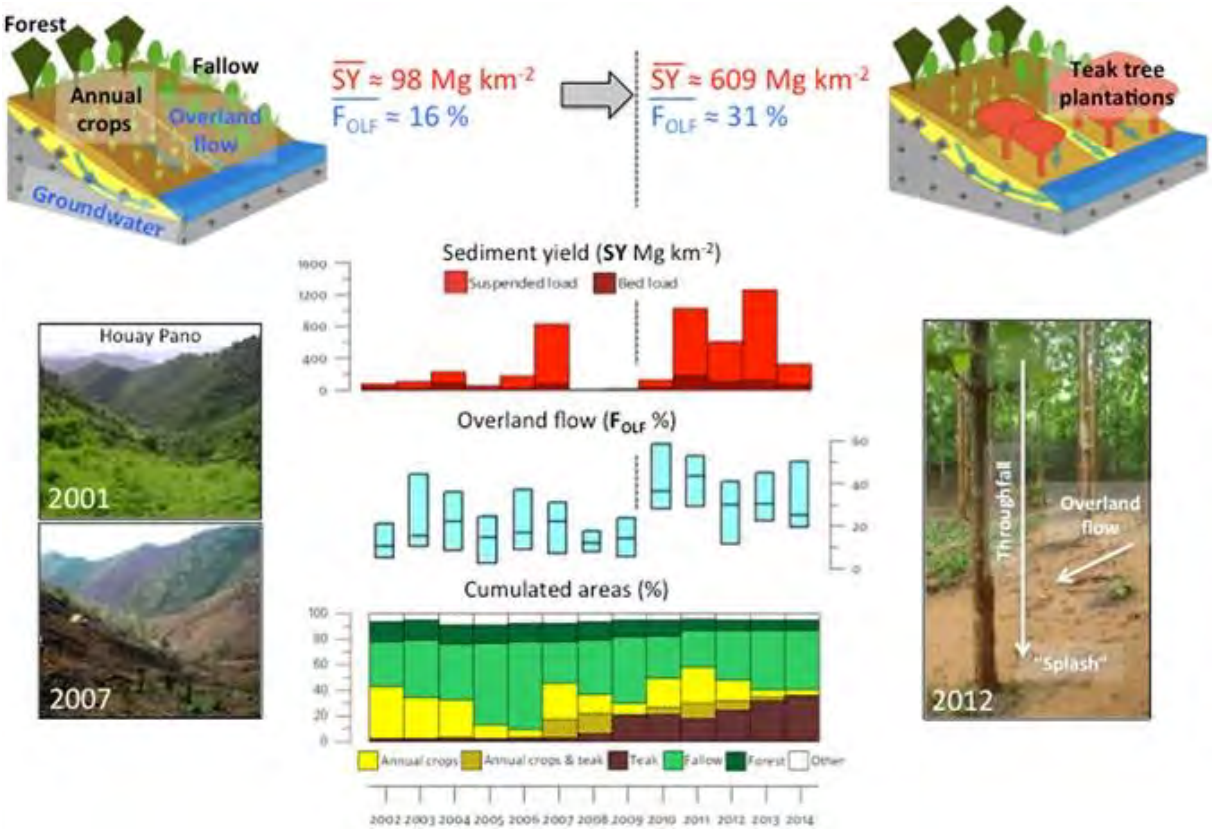

Figure 2.5: Houay Pano catchment after gradual conversion of rice-based shifting cultivation to teak planation-based systems (Source: Ribolzi et al. (2017)).

2.5. NATURAL FOREST AND BIODIVERSITY: ROLES OF THE UNDERSTORY AND THE RIPARIAN ZONES

Understory layer is an important biodiversity reservoir of the forest that contains more than 80 % of the vascular plant diversity (Gilliam, 2007). In addition, understory plants provide food, shelter and habitat, especially for arthropods (Boch et al., 2013) and large herbivores (Gill and Beardall, 2001; Smolko et al., 2018). More importantly, in terms of biodiversity conservation, the understory can also have an important functional role, regulating ecosystem processes (or functions), for instance via its impact on forest regeneration (George and Bazzaz, 2003), water cycling (Thrippleton et al., 2018), and nutrient and carbon dynamics (Elliott et al., 2015; Muller, 2003). The understory changes substantially the soil surface feature, thereby allowing more infiltration (Barmuta et al., 2009) and hence decreasing SR. The understory also limits soil erosion by reducing the rain splash effect and overland flow (Lacombe et al., 2018). However,

the number of studies that provide a proper quantification of the importance of the understory in determining ecosystem functions in forests is still limited.

Riparian zones extend from the edges of water bodies to upland cultivation. Riparian biodiversity is created and maintained by inherent nutrient, sediment and biogeochemical processes, variable energy and disturbance regimes, complex habitat, herbivory and other biotic processes (Naiman et al., 2013). Riparian zones are energy sources for adjoining aquatic systems via plant litter and arthropods falling into streams. Riparian zones intercept and retain SR, sediment, and nutrients from upland runoff (Cao et al., 2018; Ding et al., 2011; Dong et al., 2018; Vigiak et al., 2008). The preservation of riparian vegetation in the surrounding highland streams was associated with the overall better riparian condition, floristic quality, and water quality such as lower turbidity, lower total suspended solids, lower orthophosphate, and higher dissolved oxygen (Alemu et al., 2017). The preservation of riparian vegetation is strongly recommended in tropical highland streams surrounded by intensive agriculture to trap eroded soil particles and help reduce off-site water pollution, which in return provides sustainable benefit to the farmers (Morgan, 2005). However, the role of riparian grass in the tree plantation, especially teak tree plantation, where is prone to soil erosion is not yet studied.

2.6. SUSTAINABILITY OF AGROECOSYSTEM

Agroecosystems are natural ecosystems modified to produce food and fiber (Hodgson, 2012) and timber (L Soto-Pinto and Armijo-Florentino, 2014). An agroecosystem is not restricted to the immediate site of agricultural activity (e.g. the farm), but rather includes the region that is impacted by this activity, usually by changes to the complexity of species assemblages and energy flows, as well as to the net nutrient balance (Martin-Clouaire, 2018).

Forests and agroforestry systems play a fundamental role in the economy of rural communities contributing multiple benefits according to different agroecosystem features (Santoro et al., 2020). Jose (2009) confirmed that agroforestry provides four major ecosystem services and environmental benefits: (1) carbon sequestration, (2) biodiversity conservation, (3) soil enrichment and (4) air and downstream water quality. In Mexico, a group of farmers involved in a program established a sort of Taungya system to get food, timber, other products and services, including the environmental service of carbon sequestration (De Jong et al., 1997; Lorena Soto-Pinto et al., 2009). Ahmad et al. (2020) highlighted that a cover crop canopy of the understory cultivated under timber trees could reduce the soil erosion from cultivated fields during the peak season. The cover crop consists of sowing of legume and edible crop, which

will provide a ground cover acting as an umbrella that can reduce raindrop impact, reduce water velocities, decrease runoff, and increase water infiltration in the soil. Therefore, cover crops are one of the ways to reduce soil erosion. The combination of involved models in the agroecosystems, for example, food web models, crop models, decision models, and spatial models, is highlighted for the sound management and sustainable use of the agricultural land (Tixier et al., 2013). Several studies suggested keeping and planting the undergrowth (cash crop or edible crop) in the teak tree plantation for maintaining the ecological function for sustainable forestry (Imron et al., 2018; ITTO, 2004; Neyret et al., 2020; Pachas et al., 2019; Patin et al., 2018). However, the agronomic aspect and ecosystem services of the intercropping such as teak tree plantation with other cash crop are not yet studied in terms of sustainability of agroecosystem.

2.7. HYDROLOGICAL AND SEDIMENTARY MODELLING

To predict the SR and Sl in the catchment, many approaches have been used, from microplot scale to large catchment scales, by using simple physical equation models, statistical models, or empirical models (Chuenchum et al., 2020; Ganasri and Ramesh, 2016; Giang et al., 2017; Patin et al., 2018; Sok et al., 2020; Ziegler et al., 2001). Those models include SWAT (G. Arnold et al., 2012), KINEROS2 (C. Goodrich et al., 2012), RULSE (Renard and Ferreira, 1993), TEST (Van Dijk and Bruijnzeel, 2004), etc. Most models require a lot of data and are applied on large spatial scales and the annual scale. SWAT is not suitable for local scale and requires a lot of parameters for calibration. In the model calibration, many significantly different parameter sets can produce statistically similar model performance criteria used as an objective function (Abbaspour, 2021; Beven*, 2001). Such a condition leads to the equifinality (Hamilton, 2007), which may not represent the real situation in the field as the parameter values are not verified with the observation. Therefore, models with the calibration requiring many parameters may lead to uncertainty and produce misleading results. RUSLE is used to estimate the average long-term risk of erosion on arable land. It is suitable for the hillslope scale and is not designed for modelling soil erosion and sediment transport under individual rainfall events. Moreover, it does not consider typical erosion processes such as splash erosion, linear erosion, soil transport and soil deposition as a dynamic process (Benavidez et al., 2018). KINEROS2 is a distributed model applicable from plot to watershed scales (C. Goodrich et al., 2012). It is an event-based model that estimates runoff, erosion, and sediment transport in overland flow (hillslope) and the channel. However, it also utilizes several parameters to be calibrated. Parsimonious models such as GR2M (Mouelhi et al., 2006) and GR4J (C. Perrin et al., 2003)

utilize a few parameters for the calibration; however, the models are capable to assess the hydrological behaviour of a catchment. Likewise, TEST was developed by Van Dijk and Bruijnzeel (2004), also requires a few parameters. The model describes rainfall-driven transport by splash and shallow overland flow as a function of vegetation and soil surface cover. This model was successfully applied by Patin et al. (2018) on the plot and annual scale. It requires measured sediment yield of rainfall events for the calibration. Two parameters and a few data are required for this model, which can reduce the uncertainty caused by over parametrization and risk of equifinality (Hamilton, 2007). The parameters for the calibration are areal percentages of vegetation and residue at the ground surface.

2.8. PROBLEM STATEMENTS AND OBJECTIVES

In the mountainous region of northern Lao PDR, areas of widespread agricultural practices are known to increase SR, soil erosion, and in-stream suspended sediment concentrations compared to areas dominated by natural forest (Patin et al., 2012; Valentin et al., 2008). Increase in commercial perennial monocultures, such as teak tree plantations, leads to a drastic SR increase (Lacombe et al., 2016) and exacerbates Sl along hillslopes and at catchment scale (Lacombe et al., 2018; Ribolzi et al., 2017). In teak tree plantations, such as the old teak trees (high timbers with broad leaves) growing in the Houay Pano catchment, SR and soil erosion are likely related to recurrent understory and leaf litter suppression by burning at the end of the dry season, leaving the soil bare and exposed to the kinetic energy of the raindrops (Patin et al., 2018). Land use, understory cover, and soil surface condition, are the main drivers influencing the infiltration of water into the soil (Chaplot et al., 2007; Ribolzi et al., 2011b). Understory and plant residues on soil surface are known to efficiently attenuate the effect of splash and thus soil detachment whilst riparian grass is known as an attenuating factor of reduced Sl by trapping the sediment and preventing sediment from flowing to the stream. However, their roles are not yet investigated in details on how they will mitigate soil erosion from the microplot, to the hillslope, and to the catchment scales. The key scientific questions of this thesis are:

- Does the understory attenuate the Sl in the teak tree plantation? And how much is the Sl reduced by the understory?
- Does riparian grass efficiently reduce the quantity of sediment exported to the stream? And how much is its trapping efficiency of water and sediment?
- What is the difference between hydro-sedimentary behaviour of these two micro-catchments?

- Does scale impact on the hydro-sedimentary condition, connectivity and yield?
- What are the factors characterizing the processes of the sediment exportation on various scales? And how much does each process contribute to the sediment exportation?

In this thesis, we hypothesize that keeping understory and riparian grass limit Sl and prevent the sediment flow into the stream in the teak tree plantations. H. We also hypothesize that scale impacts on the hydro-sedimentary condition by reducing SR and Sl from the microplot, to the hillslope, and to the catchment scale. The synthesized conceptual diagram of the research questions is shown in **Figure 2.6** and **Figure 2.7**.

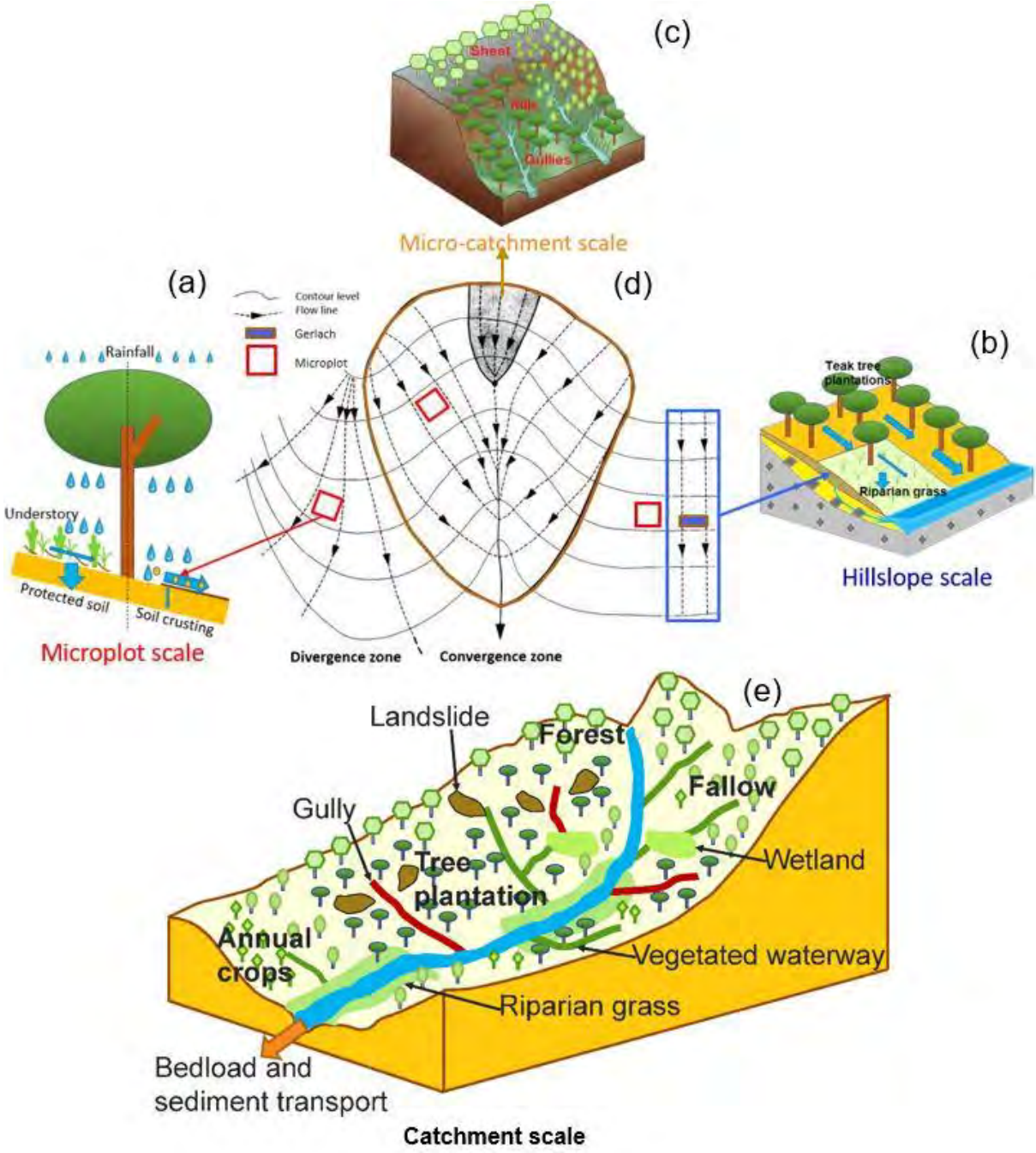

Figure 2.6: Synthesized processes of surface runoff (SR) and soil loss/sediment exportation (Sl) on multiple scales: (a) Microplot scale, (b) hillslope scale, including (c) micro-catchment scale, (e) catchment scale, and (d) sketch representing SR and Sl monitoring on microplot and hillslope scales including micro-catchment scale.

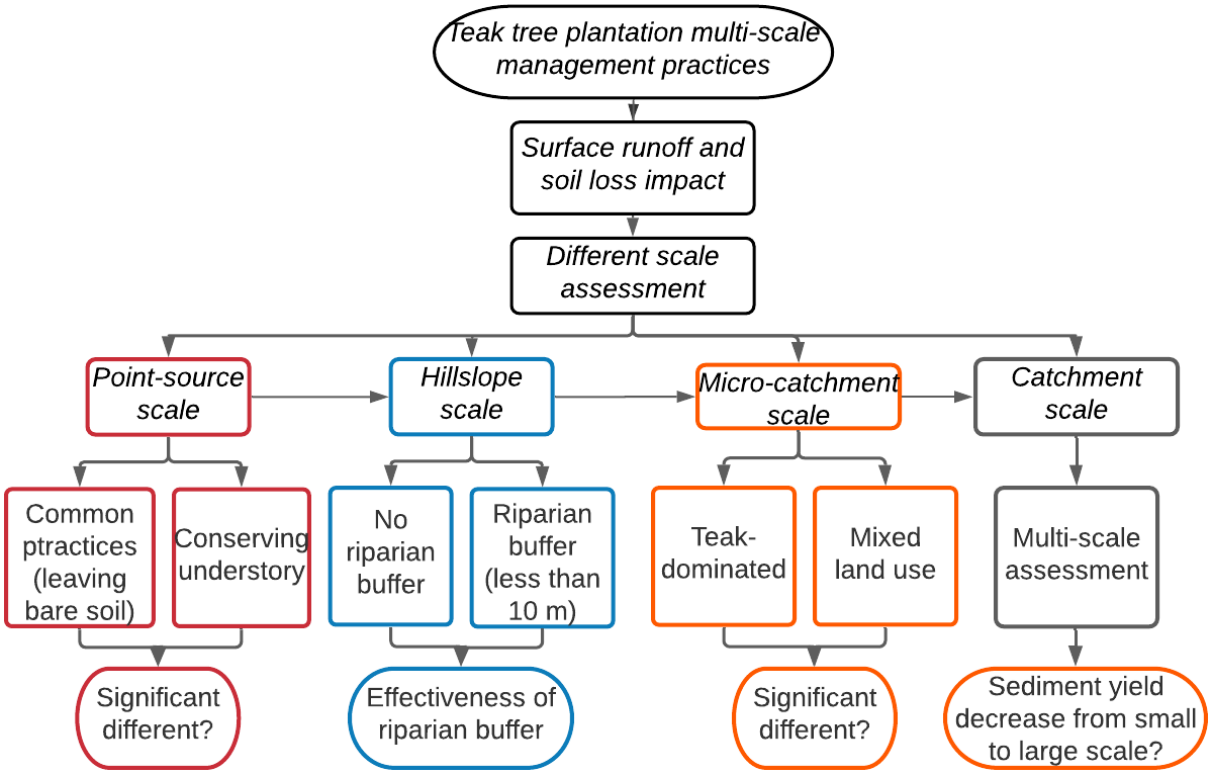

Figure 2.7: Synthesized conceptual diagram of multi-scale assessment of land management practice impacts on SR and Sl (using microplot, hillslope, micro-catchment, and catchment scales) in the teak-cultivated catchment.

Hence, the objectives of the thesis are:

1. To find the best land management practices to contribute to sustainable agricultural production in the teak tree plantations of Ban Kokngew, norther Lao PDR. In this context, the three specific objectives of our 1 m2 microplot experiment performed during the June to October monsoon period of 2017 are to: (1) assess the effects on SR and Sl of four understory management practices, namely teak with no understory (TNU; control treatment), teak with low density of understory (TLU), teak with high density of understory (THU), and teak with broom grass (TBG); (2) suggest soil erosion mitigation management practices; and (3) identify a field visual indicator allowing a rapid appraisal of soil erosion intensity.

2. To assess impacts of current management practices on SR and Sl on the hillslope adjacent to the riparian zone of the Houay Pano catchment, northern Lao PDR. In this context, three specific objectives of our 1 m2 microplot and Gerlach trap experiment during the rainy season of 2014 are to: (1) assess the effects of riparian grass in teak cultivated land on SR and Sl; (2) assess the trapping efficiency of riparian buffers for water (WTE), sediment (STE), and sediment concentration (SCTE); and (3) model Sl, WTE, STE, and SCTE.

3. To assess the multi-scale effect of teak tree plantation on SR and sediment yield in mixed land uses of Houay Pano catchment, northern Lao PDR. In this context, the specific objectives of using multi-scale experiment performed during the rainy season of 2014 are to: (1) compare SR and sediment yield from mixed-land-use and teak-dominated micro-catchments; and (2) assess the scale impacts on SR and sediment yield from microplot, to micro-catchment, and to catchment scale.

Chapter 3. Methodology

"Better to do something imperfectly than to do nothing perfectly" – Robert H. Schuller

Chapter 3

Methodology

3.1. STUDY AREA

3.1.1. *Geographical characteristics*

The study site was located in the mountainous region in Luang Prabang province of the northern Lao PDR (**Figure 3.1**). Northern Lao PDR is located almost entirely in the Mekong River basin. It covers 30% of total surface area of Lao PDR stretching to the northern border with China and to the eastern border with Vietnam with mountains of 1000 – 3000 m above sea level (Fujisaka, 1991). We focused on two sites in the province: one was situated in Ban Kokngew village; another was situated in Houay Pano catchment. The distance between these two sites is approximately 4 km.

The site in Ban Kokngew is situated near Nam Khan River with the altitude ranging from 330 to 380 m with the average slope of 42%. Soil of Ban Kokngew consists of Acrisol and Cambisol. In this site, we conducted microplot experiment to assess surface runoff and soil loss. Teak tree is planted in Ban Kokngew with different land managements: teak with no understory, teak with low density of understory, teak with high density of understory, and teak with broom grass.

Houay Pano headwater catchment is 10 km from Luang Prabang City (**Figure 3.1**). The land use of this catchment consists mainly of fallow and teak tree plantation in 2014. This catchment is an experimental catchment and a long-term critical zone observatory (Multi-scale TROPIcal CatchmentS or M-TROPICS; https://mtropics.obs-mip.fr/) and can be considered as being representative of the montane agro-ecosystems of South-East Asia. Altitude within the catchment is 435 – 716 m, and the slope gradient is 1 – 135 % (mean=52 %) (Boithias et al., 2021). Soil types of Houay Pano catchment are classified in three major orders: Entisol, Ultisol and Alfisol. Three hydrological stations are located at the outlets of the 2 micro-catchment (S7 and S8) and at the outlet of the Houay Pano catchment (S4). These stations aimed at recording the water level to estimate the discharge and to collect sediment samples.

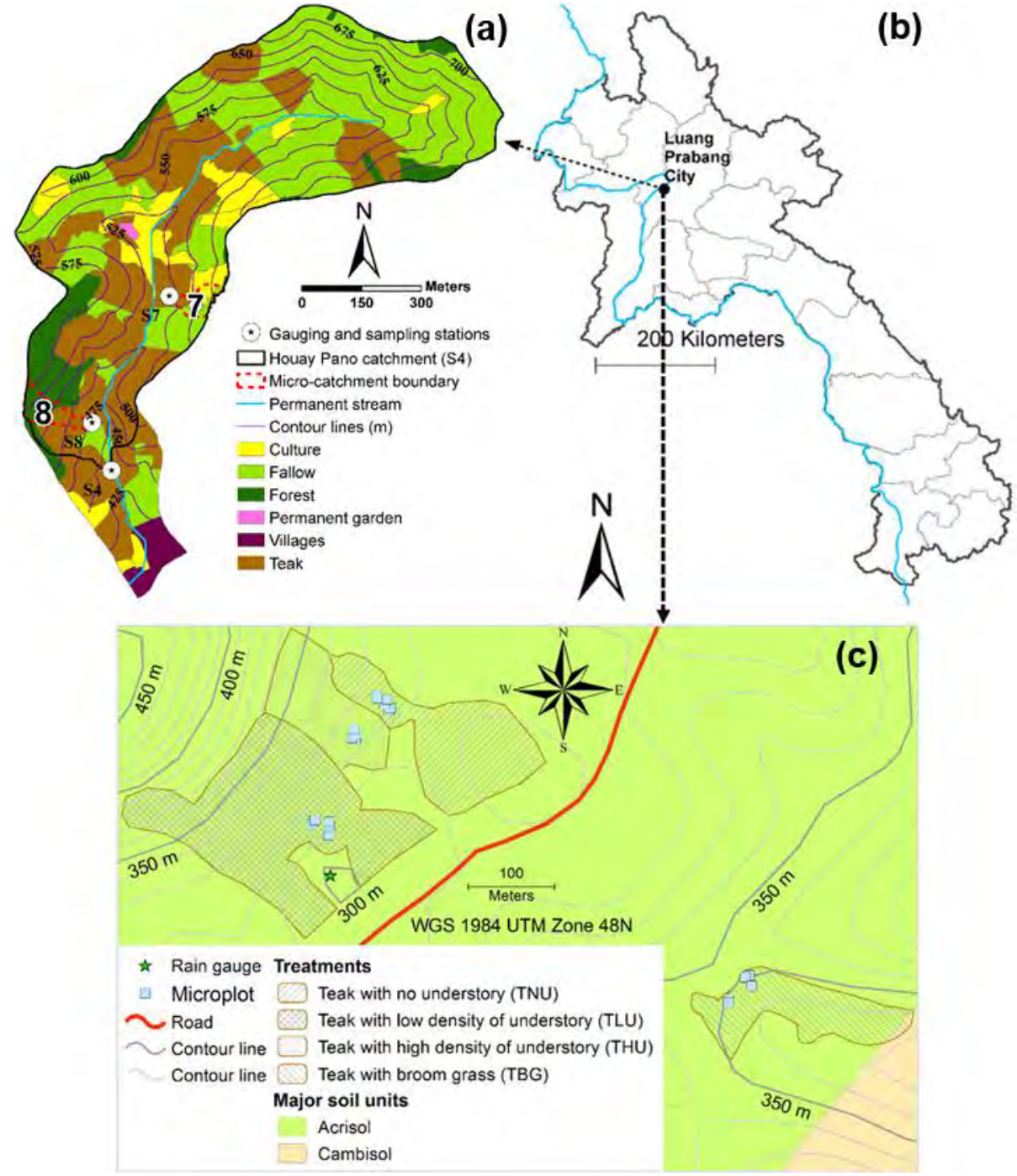

Figure 3.1: (a) Land use of 2014 of Houay Pano catchment with gauging and sampling stations of S4, S7, and S8; (b) microplot site in different treatment of teak tree plantation at Ban Kokngew; and (c) experimental sites located in Luang Prabang province of the northern Lao PDR.

3.1.2. *Climate condition*

The climate of the study sites is sub-tropical humid and is characterized by a monsoon regime with a dry season from November to May, and a wet season from June to October. The mean annual temperature is 23.4 °C. Mean annual rainfall is 1366 mm, about 71 % of which falls during the wet season (Boithias et al., 2021).

Extreme events with high rainfall usually led to landslides within the catchment (about 10% of the catchment area based on Boithias et al. (2021) from 2001 to 2019.

3.1.3. *Hydrological condition*

The flow mainly depends on rainfalls which generates the surface flow and infiltration without any significance of subsurface flow (i.e., groundwater flow) in the micro-catchment. However, groundwater flow is observed in S4 (Ribolzi et al., 2017). The groundwater flow significantly contributes to the decrease of concentration of suspended sediment during the rainfall. The hydrological variables are highly seasonal and the catchment is subject to extreme meteorological and hydrological events (Boithias et al., 2021). Floods during 2015 were described by villagers as unprecedented, and severe damage occurred as a result of tropical storm Haima in 2011 (ADB, 2016). However, in our study, there was also an extreme rainfall which resulted in a devastated flood.

3.2. EXPERIMENTAL METHODS: MICROPLOT, GERLACH, S4, S7 AND S8 STATIONS

3.2.1. *Microplot*

The use of microplots aimed at estimating surface runoff (SR, mm) and soil loss (Sl, $g \cdot m^{-2}$) generated in a square metre of each land use on the microplot scale. Microplot metal frames are connected to a covered and buried 170 L bucket through a pipe for SR and detached soil collection (**Figure 3.2a**). We collect SR and empty the buckets after every major rainfall event, or a significant rainfall triggering the sampling. An aliquot of SR is sampled from the bucket. The concentration of suspended sediment accumulated between two emptyings is measured after flocculation with a 10 $g \cdot L^{-1}$ concentrated aluminium sulfate solution, filtration with 0.7 µm acetate filters, and evaporation at 105 °C for 48 h. We then calculate soil detachment per square metre by multiplying the accumulated Sl concentration by the accumulated SR volume, considering that each metal frame is 1 m^2. Seasonal SR and Sl are the cumulated SR and SL, respectively, of all the samplings during the rainy season.

3.2.2. *Gerlach traps*

The use of Gerlach trap (Gerlach, 1967) aimed at trapping water and sediment to estimate the WTE, STE, and SCTE on the hillslope scale. Gerlach traps were installed in two columns of downslope. Gerlach trap consists of a Gerlach trough (0.5-m length, 0.2-m width, and 0.1-m height with a hinged lid; (**Figure 3.2b**), a plastic pipe, and a bucket. We installed the Gerlach on the slopping area and connected it to a plastic bucket downhill through the pipe. The bucket was 0.45 m high with the bottom and top diameters of 0.32 and 0.38 m, respectively. We set up three replicates Gerlach in each land use from the upslope to downslope of the focused teak tree plantation.

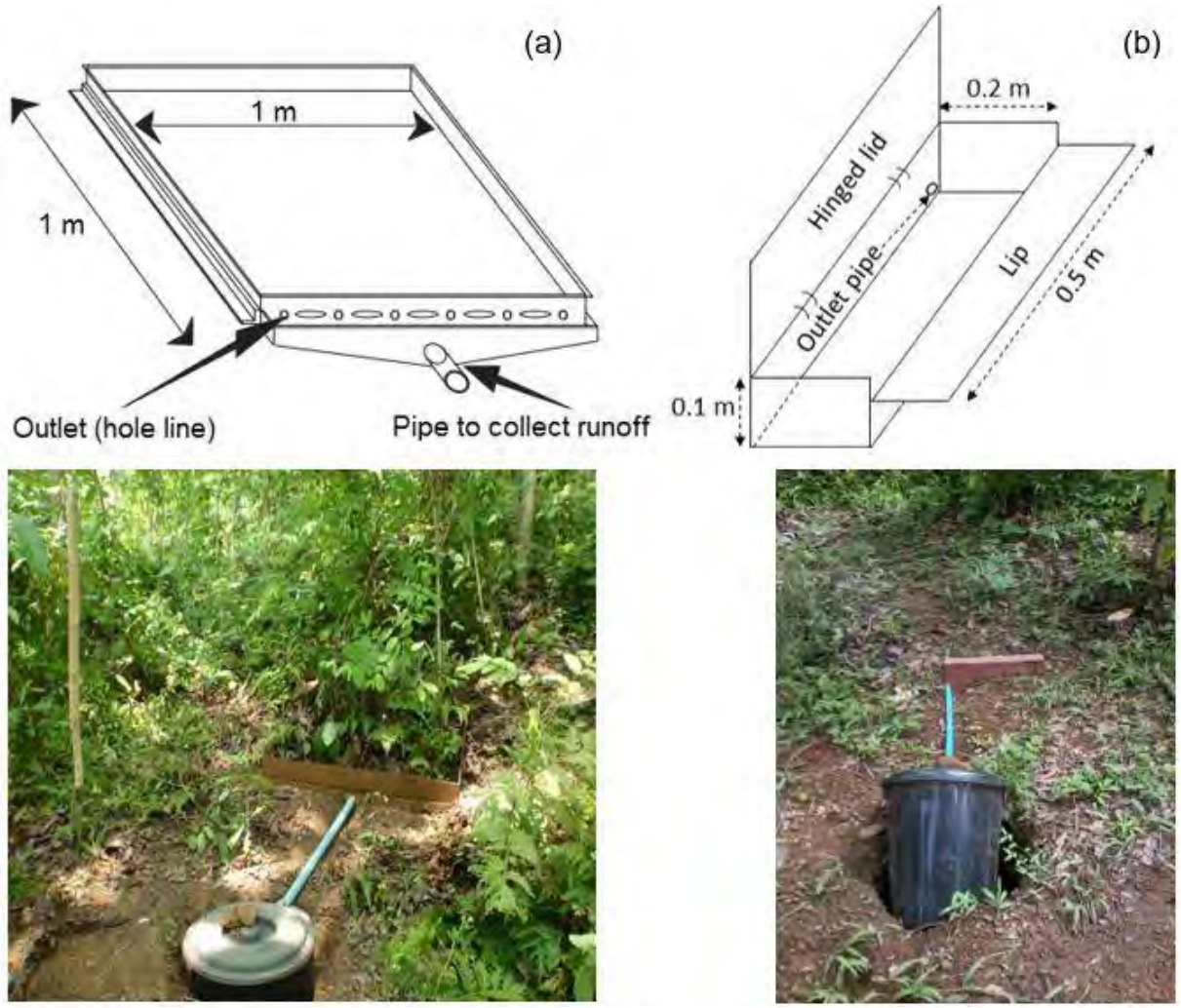

Figure 3.2: (a) Microplot (1 m^{-2}) and (b) Gerlach trap (1 m)

3.2.3. *S4, S7, and S8 stations*

A storage attached with combined V-notch and rectangular weirs was installed at the outlets of the micro-catchments (S7 and S8) and the catchment (S4) to estimate SR, suspended sediment (also Sl), and bed load.

We measured stream water level at the gauging stations of each catchment with a compound V-notch and rectangle notch weir (Boithias et al., 2021; Nouvelot, 1993) equipped with a water level recorder connected to a data logger, with 1-mm vertical precision. Water level is scanned every 30 s and recorded if a variation of ±1 mm is detected with in a period of 3 min (**Figure 3.3**). The discharge was then calculated based on the shape of the flow and water level using V-Shaped and rectangular weir formulas. SR is then calculated based on the discharge, except for S4 which requires baseflow separation to quantify SR and groundwater contributing to the total depth of flow (see **Chapter 6**).

We collected samples of stream water 10 cm below the river water surface at the gauging stations (S4, S7, and S8) in clean, 600 ml plastic bottles, using an automatic sampler. The automatic sampler is triggered by the water level recorder to collect water after every 2-cm water level change during flood rising and every 4-cm water level change during flood recession. We measured the concentration of suspended sediment in each sample after flocculation with a 10 $g \cdot L^{-1}$ concentrated aluminium sulfate solution, filtration with 0.7 µm acetate filters, and evaporation at 105 °C for 48 h. Suspended sediment mass is then divided by the sample volume to get the suspended sediment concentration.

We measured bed load by trapping the sediment in the stilling basin of the S4 weir. Each month or each time the stilling basin is full of sediment we use buckets to measure both the volumes of deposited soft sediment and of stones. The volume of stones bigger than the buckets is estimated from their dimensions, manually measured with a tape measure. We then calculate the average bulk density of the total of deposited sediment, assuming a density of 1.00 for soft sediment and of 2.65 for stones. After collection, we oven-dry the soft sediment samples; the dry weight of sediment samples is subsequently divided by the catchment area to express bed load in $t \cdot ha^{-1}$.

Sl is calculated using the total depth of flow, suspended sediment concentration and the bed load, which is detailed in **Chapter 6**.

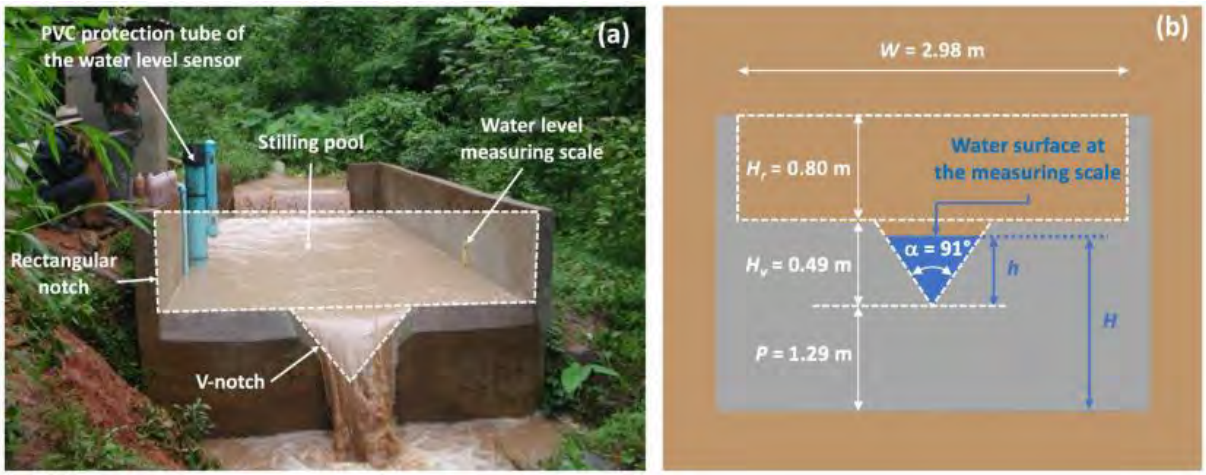

Figure 3.3: (a) Hydrometric station at the outlets of micro-catchment (S7 and S8) and the Houay Pano catchment (S4) during a stormflow event; (b) metrics of the compound weir (V-notch and rectangular notch): width of the channel (W), height of the rectangular notch (H_r), height of the V-notch (H_v), V-notch angle (α), height of the V-notch crest (P), water level at the measuring scale (H), and head (h) with h=H-P (Source: Boithias et al. (2021)).

3.3. MEASUREMENT OF SOIL SURFACE FEATURES, UNDERSTORY, GRASS AND TREE

Areal percentage of soil surface features and grass (*Microstegium sp.*) were assessed in each replicate of the microplot at the beginning and in the middle of the rainy season by visual inspections using the method proposed by Casenave and Valentin (1992) and extensively used in surface runoff and soil loss assessment (Lacombe et al., 2016; Lacombe et al., 2018; Neyret et al., 2020; Patin et al., 2012; Patin et al., 2018; Ribolzi et al., 2017; Ribolzi et al., 2018; Ribolzi et al., 2011b). We calculated the average of each soil surface feature for each land use by first calculating the averages of the two measurements dates per land use, and then by calculating the averages among the replicates per land use, which are detailed in **Chapter 4** and **Chapter 5**.

We considered two categories of understory: one consisting of weed and low vegetation and another consisting of purposely planted broom grass (Thysanolaena latifolia) monocrop. We described the structure of the understory by combining the use of visual inspections (areal percentage assessment) and measuring tapes (girth, height). We estimated the mean understory height and cover in a representative area of 18 m2 encompassing the three microplot replicates at the beginning and the end of the rainy season.

We measured teak tree height, teak cover, and stem diameter at 1.6 m height in 10 × 10 m plots enclosing the microplots.

3.4. ESTIMATION OF WATER AND SEDIMENT TRAPPING EFFICIENCIES

We estimated trapping efficiency based on the SR and Sl collected by Gerlach traps. Trapping efficiency (TE, dimensionless) was calculated for runoff water volumes (water trapping efficiency [WTE]), suspended sediment concentration (sediment concentration trapping efficiency [SCTE]), and for sediment trapping efficiency [STE]) as the portion of inflow trapped between the upper and the lower rim (McKergow et al., 2004; Vigiak et al., 2008). The formula for calculating trapping efficiency is provided in **Eq. 3.1**:

$$TE = \frac{(X_{in} - X_{out})}{X_{in}} \qquad \textbf{Eq. 3.1}$$

where X_{in} is the water flow amount in litre per linear metre of contour line ($L.m^{-1}$ for WTE), the average suspended sediment concentration ($g.L^{-1}$ for SCTE) or the mass of suspended sediment in gram per linear metre of contour line ($g.m^{-1}$ for STE), and X_{out} is the water flow amount (for WTE), the average suspended sediment concentration (for SCTE) or the mass of suspended sediment (for STE) of the lower Gerlach (outflow).

3.5. MODELLING SOIL EROSION

TEST model (Van Dijk and Bruijnzeel, 2004) was selected and applied in this research thesis as the measured data of the study area meet the requirement of this model. A justified Sl model of Patin et al. (2018) which is adapted from Van Dijk and Bruijnzeel (2004) is given as (**Eq. 3.2**):

$$Sl = D \cdot \Sigma(KE \cdot Rc) \cdot \exp(-a \cdot Gra) \cdot \exp(-b \cdot Res) \qquad \textbf{Eq. 3.2}$$

where Sl is the soil loss on the microplot scale ($g \cdot m^{-2}$), D is the effective soil detachability ($g \cdot J^{-1}$); KE is the rainfall kinetic energy ($J \cdot m^{-2}$); Rc is the runoff coefficient (%); Gra is the areal percentage of grass (%); Res is the areal percentage of residues (%); a and b are the decay coefficients of Gra and Res, respectively.

KE is calculated based on the rainfall kinetic energy content e_k which was modelled by the expression (Kinnell, 1981; Van Dijk et al., 2002) in **Eq. 3.3**:

$$e_k = e_{kmax} \cdot (1 - \alpha \cdot \exp(-\gamma \cdot R)) \qquad \textbf{Eq. 3.3}$$

where e_{kmax} is the maximum energy content, α and γ are empirical constants, and R is the rainfall intensity ($mm \cdot h^{-1}$). The total kinetic energy was then expressed as (**Eq. 3.4**):

$$KE = \Sigma(e_k \cdot R \cdot \Delta t) \qquad \textbf{Eq. 3.4}$$

where Δt is the rainfall time step (h).

To predict Sl on the hillslope and the catchment scale, additional parameters will be introduced into the model (**Eq. 3.2**). From the microplot to the catchment scale, several hydro-sedimentary processes and factors involved in the driving SR and Sl. Those processes include splash detachment, wash effect, accumulation by linear erosion, and deposition. On the microplot scale, the model is based on the detachment driven by the splash and wash effects which can be attenuated by grass and residues. Splash and wash effect involved KE and Rc. However, in **Chapter 4**, we applied a simple model describing Sl as function of Rc suggested by Patin et al. (2018). In **Chapter 5**, we applied **Eq. 3.2** describing Sl as function KE, Rc, Gra, and Res. On the hillslope scale including micro-catchment and on the catchment scale we introduced two more factors: intensifying factor as linear erosion and attenuating factor as sediment deposition. The process of linear erosion involves the erosion driven by the gully. The process of deposition including trapping factors by riparian zone, vegetated waterway, and headwater wetland. In **Chapter 6**, we developed a new model to predict Sl on the hillslope and catchment scale by upscaling the model used in **Chapter 5**, which describes Sl as function of KE, Rc, Gra, Res, gully feature, and trapping features.

[This page intentionally left blank]

Chapter 4. Understory limits surface runoff and soil loss in teak tree plantations of Northern Lao PDR

"I walk slowly, but I never walk backward" – Abraham Lincoln

Chapter 4

Understory limits surface runoff and soil loss in teak tree plantations of Northern Lao PDR[1]

This scientific chapter evaluated the impacts of understory on surface runoff and soil loss in the teak tree planation of the northern Lao PDR. The finding suggested that decision makers or famers should maintain understory and avoid understory and plant residue layers burning to minimize surface runoff and soil loss in steep slope areas such as montane regions of South East Asia. This study was published in the journal of Water (MDPI) on 19 August 2020.

Abstract: Many mountainous regions of the humid tropics experience serious soil erosion following rapid changes in land use. In northern Lao People's Democratic Republic (PDR), the replacement of traditional crops by tree plantations, such as teak trees, has led to a dramatic increase in floods and soil loss and to the degradation of basic soil ecosystem services such as water filtration by soil, fertility maintenance, etc. In this study, we hypothesized that conserving understory under teak trees would protect soil, limit surface runoff, and help reduce soil erosion. Using 1 m2 microplots installed in four teak tree plantations in northern Lao PDR over the rainy season of 2017, this study aimed to: (1) assess the effects on surface runoff and soil loss of four understory management practices, namely teak with no understory (TNU; control treatment), teak with low density of understory (TLU), teak with high density of understory (THU), and teak with broom grass, Thysanolaena latifolia (TBG); (2) suggest soil erosion mitigation management practices; and (3) identify a field visual indicator allowing a rapid appraisal of soil erosion intensity. We monitored surface runoff and soil loss, and measured teak tree and understory characteristics (height and percentage of cover) and soil surface features. We estimated the relationships among these variables through statistics and regression analyses. THU and TBG had the smallest runoff coefficient (23% for both) and soil loss (465 and 381 g·m−2, respectively). The runoff coefficient and soil loss in TLU were 35% and 1115 g·m−2, respectively. TNU had the highest runoff coefficient and soil loss (60%, 5455 g·m−2) associated to the highest crusting rate (82%). Hence, the soil loss in TBG was 14-times less

[1] This chapter is based on Song L, Boithias L, Sengtaheuanghoung O, Oeurng C, Valentin C, Souksavath B, Sounyafong P, de Rouw A, Soulileuth B, Silvera N, Lattanavongkot B, Pierret A, Ribolzi O. 2020. Understory limits surface runoff and soil loss in teak tree plantations of Northern Lao PDR. Water 12, 2327. https://doi.org/10.3390/w12092327.

than in TNU and teak tree plantation owners could divide soil loss by 14 by keeping understory, such as broom grass, within teak tree plantations. Indeed, a high runoff coefficient and soil loss in TNU was explained by the kinetic energy of rain drops falling from the broad leaves of the tall teak trees down to bare soil, devoid of plant residues, thus leading to severe soil surface crusting and soil detachment. The areal percentage of pedestal features was a reliable indicator of soil erosion intensity. Overall, promoting understory, such as broom grass, in teak tree plantations would: (1) limit surface runoff and improve soil infiltrability, thus increase soil water stock available for both root absorption and groundwater recharge; and (2) mitigate soil loss while favoring soil fertility conservation.

4.1. INTRODUCTION

Mountain areas of the humid tropics are characterized by steep slopes and heavy rains (Gerstengarbe and Werner, 2008). Hence these regions are prone to high surface runoff and soil erosion (Descroix et al., 2008). Conversion of natural forest to e.g., agricultural land exacerbates runoff production and soil erosion, leading to physicochemical and biological changes of the altered ecosystems (Nandi and Luffman, 2012; Valentin et al., 2008).

On-site effects of increased soil erosion include the reduction of soil quality impacting the sustainability of agricultural production (Valentin and Rajot, 2018), and economics, due to the loss of ecosystem services (Sartori et al., 2019). The tremendously higher rate of soil loss compared to its formation rate threatens food production and environmental quality (water, soil, and air) (Panagos et al., 2015; Pimentel, 2006; Pimentel and Burgess, 2013).

Off-site effects comprise floods, depletion of groundwater recharge, degradation of stream environments, and downstream sedimentation (Owens et al., 2005; Valentin and Rajot, 2018). In addition, the adsorption of organic and inorganic matter on soil particles and suspended sediments plays a leading role in the transport of nutrients (Yuan et al., 2019), radionuclides (Chartin et al., 2013), metals (Turner et al., 2008), pesticides (Domagalski and Kuivila, 1993), and bacterial pathogens (Gateuille et al., 2014; Ribolzi et al., 2011a). Higher contamination of rivers by fecal bacteria is often correlated to higher in-stream suspended sediment concentration (Boithias et al., 2016a; Kim et al., 2018). Sediment loads cause massive accumulation of fine sediments to river beds and cause the siltation of irrigation canals and dam reservoirs (Efthimiou et al., 2016; Thothong et al., 2011; Zarris et al., 2011), thus reducing their life spans. All of these on-site effects lead to high economic and ecological costs (i.e., sedimentation, flooding,

landslides, water eutrophication, biodiversity loss, land abandonment, destruction of infrastructures) (Sartori et al., 2019).

Natural forests are known for their protective effect against erosion (Sidle et al., 2006). Forests have favorable hydrodynamic properties for surface infiltration (Patin et al., 2012), subsurface drainage (Ziegler et al., 2004) due to the biological activity, and the development of macropores in the litter and underneath. A fraction of rainfall, known as throughfall, is intercepted by the canopy and the underlying vegetative strata (Ziegler et al., 2009). The amount of water and the kinetic energy of drops corresponding to throughfall is lower than that of rainfall, thus reducing soil erosion. Kinetic energy is the main factor initiating soil erosion; raindrops hit the soil surface and disaggregate the soil structure (Valentin, 2018) resulting in redistribution of soil material by splash effect (Valentin and Rajot, 2018) . Kinetic energy is controlled by rainfall (amount, drop size, fall velocity), vegetation characteristics (height, cover, residues) (Goebes et al., 2015), and slope (Valentin, 2018).

In the mountainous region of northern Lao People's Democratic Republic (PDR), widespread agricultural practices are known to increase surface runoff, soil erosion, and in-stream suspended sediment concentrations compared to natural forest (Patin et al., 2012; Valentin et al., 2008). In particular, commercial perennial monocultures, such as teak tree plantations, lead to a drastic surface runoff increase (Lacombe et al., 2016) and exacerbate soil loss along hillslopes (Lacombe et al., 2018; Ribolzi et al., 2017). In teak tree plantations, such as the old teak trees (high timbers with broad leaves) growing in the Houay Pano catchment, surface runoff and soil erosion are likely related to recurrent understory and leaf litter suppression by burning at the end of the dry season, leaving the soil bare and exposed to the kinetic energy of the raindrops (Patin et al., 2018).

Land use, understory cover, and soil surface condition, are the main drivers influencing the infiltration of water into the soil (Chaplot et al., 2007; Ribolzi et al., 2011b). Living plant roots modify both mechanical and hydrological characteristics of the soil matrix and negatively influence the soil erodibility (Shinohara et al., 2016; Vannoppen et al., 2015). Understory and plant residues on soil surface are known to efficiently attenuate the effect of splash and thus soil detachment (Cerdà et al., 2018; Durán Zuazo et al., 2006; Ehigiator and Anyata, 2011; Li et al., 2014; Roose, 1996). Soil surface features have a strong impact on surface runoff and soil erosion: soil aggregation limits surface runoff generation and soil loss (J. Poesen, 1989; Valentin and Ruiz Figueroa, 1987), while crusted soils can be self-protecting from erosion

because of their high surface shear stress resistance, but they also promote surface runoff, hence downstream erosion, especially on non-crusted areas (Lacombe et al., 2018; Valentin, 2018). For example, in northern Lao PDR, splash in teak tree plantations increases soil erosion, and the absence of understory enhances the effect of splash (Ribolzi et al., 2017). By adapting the model developed by (Van Dijk et al., 2003), Patin et al. (2018) showed that plant residues and weed cover at soil surface were the main attenuation factors of soil erosion. In northern Thailand, soil erosion in rubber tree plantations decreased when understory was grown (Neyret et al., 2020). Indeed, in northern Lao PDR headwater catchments, the runoff coefficient is approximately 55% under teak trees at the plot scale (Lacombe et al., 2018), whereas it nearly doubled from 16% to 31% within 13 years at the catchment scale (Ribolzi et al., 2017), resulting from the absence of understory in the teak tree plantation area. In particular, mature teak trees with limited understory were shown to export respectively 5.5- and 31-times more water and soil than broom grass (*Thysanolaena latifolia*) at the plot scale (Lacombe et al., 2018).

Hence, in this paper, we hypothesized that conserving understory such as broom grass, which provides income to farmers through broom making and selling (Pachas et al., 2020), protects soil, limits surface runoff, and helps to reduce soil erosion in teak tree plantations. The overarching goal of this study, conducted in the teak tree plantations of Ban Kokngew, northern Lao PDR, was thus to find the best strategy to contribute to sustainable agricultural production. In this context, the three objectives of our 1 m2 microplot experiment performed during the June to October monsoon period of 2017 were to: (1) assess the effects on surface runoff and soil loss of four understory management practices, namely teak with no understory (TNU; control treatment), teak with low density of understory (TLU), teak with high density of understory (THU), and teak with broom grass (TBG); (2) suggest soil erosion mitigation management practices; and (3) identify a field visual indicator allowing a rapid appraisal of soil erosion intensity.

4.2. MATERIALS AND METHODS

4.2.1. *Study area and experimental plots*

We conducted the experiment in 2017 in teak tree plantations surrounding Ban Kokngew, a village located in Luang Prabang Province, northern Lao PDR, and predominantly situated over Acrisol soil and Carboniferous and Permian limestones (**Figure 4.1**). The climate is sub-tropical humid and is characterized by a monsoon regime with a dry season from November to May, and a rainy from June to October. Mean annual rainfall recorded at Luang Prabang from 1960 to 2006 was 1268 mm, about 76% of which falls during the rainy season. The mean annual

temperature is 25.3 °C. Mean annual reference evapotranspiration is 1116 mm. The study area belongs to the mountainous region of northern Laos PDR. More specifically, the area is located within the "Luang Prabang mountain rain forest" ecoregion (Olson et al., 2001). The area has been experiencing dramatic land use changes in the last decade with the introduction of the teak tree plantations (Pachas et al., 2019; Ribolzi et al., 2017).

We selected this area because it presents, over short distances, diversely managed teak tree plantations. This area used to be shifting cultivation land. This last decade, teak has gradually replaced most of the fields and spontaneous forest regrowth because of land degradation, lack of labor and the expectation of profitability. Teak timber is valued for its durability and water resistance; it is used for furniture and construction in the rapidly developing city of Luang Prabang. Farmers spontaneously adopted different management practices within their plantations, and we selected four sites corresponding to actual contrasted situations that we intended to test and compare.

Aside from the most common situation which is teak with no understory (TNU), i.e., teak tree plantations where soil is kept bare, often by burning the leaf litter and understory, and which represented our control situation, we considered the three following alternative treatments: teak trees grown with high density understory (THU), teak trees grown with low density and/or periodically pruned understory (TLU), and teak trees grown with broom grass, *Thysanolaena latifolia* (TBG). In each treatment, we set up 1 m2 microplots (**Figure 4.2**) with six replicates per treatment.

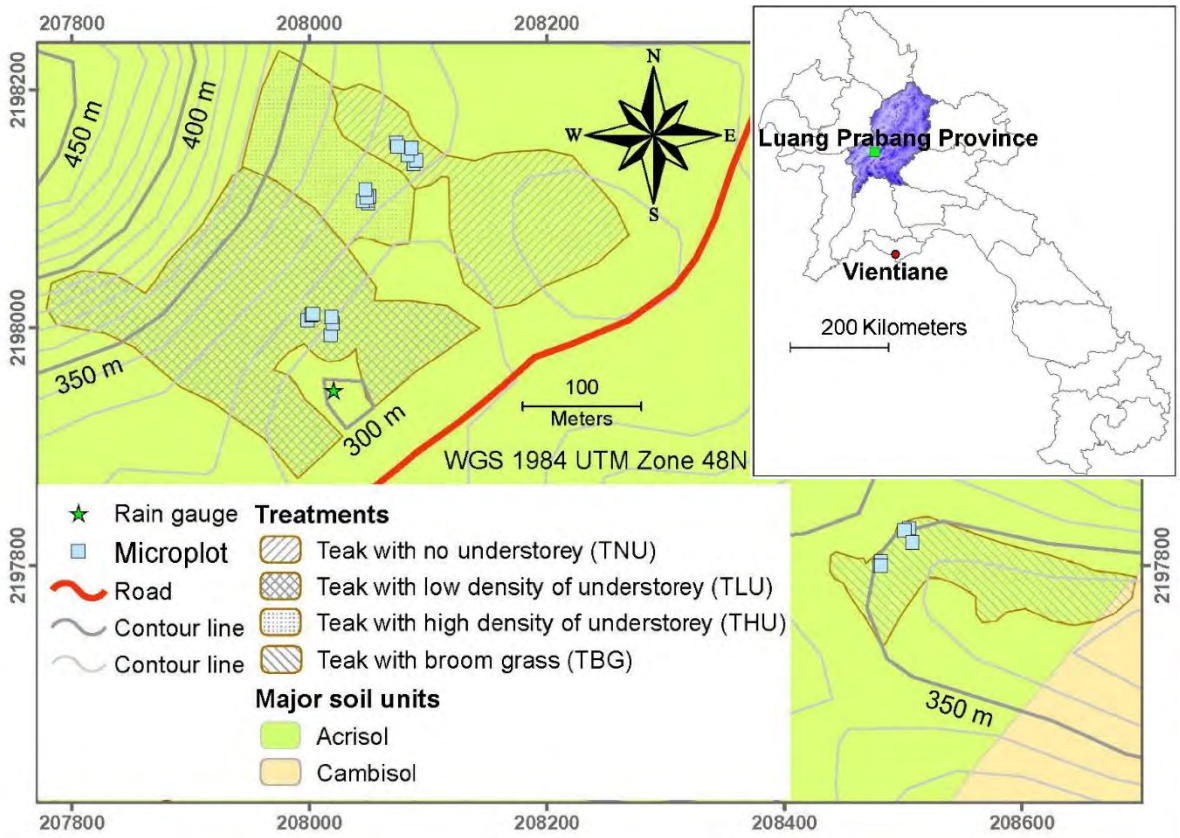

Figure 4.1: Study site in Ban Kokngew, Luang Prabang Province, Lao PDR, with location of experimental microplots, treatments, and soil types.

The age of the teak trees in the four treatments varied between 12 years in TBG and 18 years in TLU (**Table 4.1**). Elevation above sea level ranged between 316 m in TLU and 358 m in TBG, whereas TNU and THU were both at 325 m. The slopes of the microplots ranged between 39% in TNU and 46% in TBG. The slope difference between TNU and TBG was not considered a limitation for the comparison of treatments in this study since the effect of slope is known to be imperceptible for these slope ranges (Patin et al., 2018). The size of the teak tree plantations was 1.87 ha, 3.78 ha, 1.21 ha, and 1.32 ha in TNU, TLU, THU, and TBG, respectively. We installed a rain gauge near the treatments TNU, TLU, and THU, and approximately 500 m from TBG (**Figure 4.1**).

Table 4.1: Characteristics of the four experimental sites in 2017, measured on 14 December 2017, in Ban Kokngew, Luang Prabang, Lao PDR. TNU: teak with no understory; TLU: teak with low density of understory; THU: teak with high density of understory; TBG: teak with broom grass.

Treatment	Teak height (m)	Teak stem diameter (cm)	Teak cover (%)	Tree density (tree.ha^{-1})	Teak age (years)	Altitude (m)	Slope (%)	Latitude (°)	Longitude (°)
TNU	22	15.3	35	1,200	15	325	39.2	19.8577	102.21269
TLU	22	17.0	30	1,000	18	316	40.7	19.85641	102.21202
THU	20	15.4	70	800	15	325	41.5	19.85735	102.21237
TBG	20	16.4	60	1,000	12	358	45.5	19.85475	102.21666

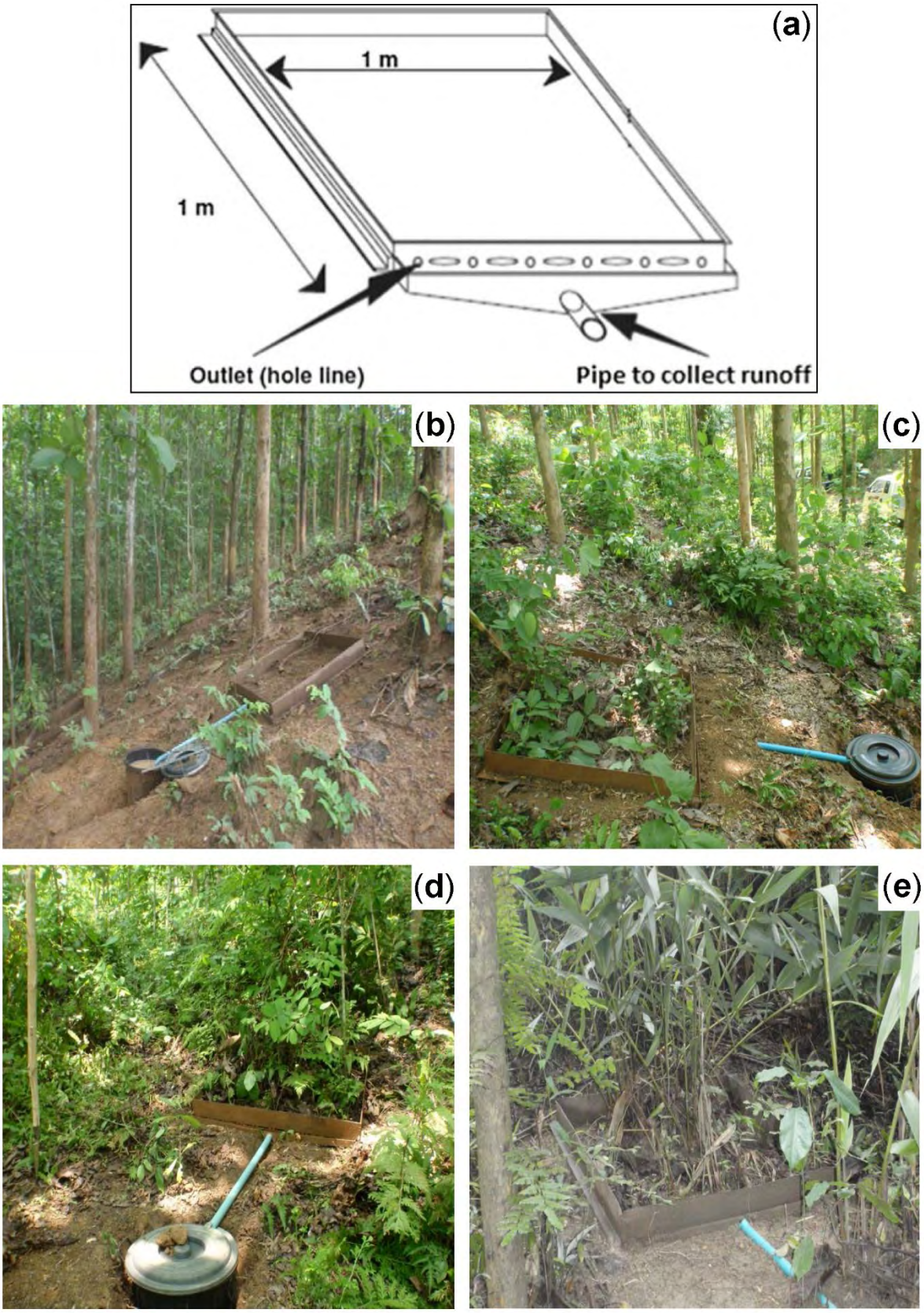

Figure 4.2: (a) Sketch of microplot of 1 × 1 m metal frame connected to a bucket through a pipe for surface runoff and sediment collection (sour: [31]). (b) Microplot of TNU: teak with no understory. (c) Microplot of TLU: teak with low density of understory. (d) Microplot of

THU: teak with high density of understory. (e) Microplot of TBG: teak with broom grass. Microplots were installed on 9 and 10 May 2017, in Bank Kokngew, Luang Prabang Province, Lao PDR.

4.2.2. *Teak trees and understory structure assessment*

We measured teak tree height, canopy cover, and stem diameter at 1.6 m height in 10 × 10 m plots enclosing the microplots. At the time of measurement, on 14 December 2017, i.e., during the dry season, some teak trees were already shedding their leaves (30% and 35% cover in TLU and TNU, respectively) but in other plantations, many teak leaves were still attached (70% and 60% cover in THU and TBG, respectively). Average teak heights ranged from 20 m to 22 m. Average diameter at 1.6 m height was 16 cm. The original planting density had been 2000 tree·ha^{-1} in TNU and TBG, from which the actual density was obtained by thinning 40% and 50%, respectively. The original planting density had been 1600 tree·ha^{-1} in THU and only 1200 tree·ha^{-1} in TLU; here the actual densities were obtained by thinning 50% and 16%, respectively (**Table 4.1**).

We considered two categories of understory: one consisting of weed and low vegetation, hereafter referred to as "understory" and another consisting of purposely planted broom grass (*Thysanolaena latifolia*) monocrop, hereafter referred to as "broom grass". Both kinds of understories are spontaneous vegetation, but farmers enhance broom grass propagation by cutting. The TBG treatment in this study was made of replanted broom grass. Farmers cut the inflorescences of broom grass to make brooms and regularly prune the grass. We described the structure of the understory in each of the four selected treatments during the 2017 rainy season by combining the use of visual inspections (percentage of cover assessment) and measuring tapes (girth, height). We estimated the mean understory height and cover in a representative area of 18 m2 encompassing the three microplot replicates on 4 June and 27 October 2017.

4.2.3. *Rainfall measurements*

We measured rainfall by using a rain gauge (Campbell BWS200 equipped with ARG100, 0.2 mm capacity tipping-bucket; **Figure 4.1**).

4.2.4. *Surface runoff, soil loss, and soil surface features assessment*

We collected surface runoff through a small channel at the lower side of each microplot, connected to a large plastic bucket by a plastic pipe (**Figure 4.2a**). The height of the buckets was 0.45 m while their diameter at the bottom was 0.32 m and the diameter at the top was 0.38 m. We emptied the buckets after every major event, or after a sequence of two to ten smaller

rainfall events. We calculated the runoff coefficient as the ratio between the total surface runoff depth and the total rainfall depth, expressed in percentage. We also computed a cumulated runoff coefficient over the rainy season.

Soil loss is the total weight of sediment collected each time the buckets were emptied. It was measured after flocculation, filtration, and oven dehydration. We calculated suspended sediment concentration by dividing sediment mass by surface runoff depth and we cumulated soil loss over the rainy season.

Soil surface features were assessed at the beginning (4 June) and at the end (27 October) of the rainy season using the method proposed by Casenave and Valentin (1992) and extensively used by Casenave and Valentin (1992), Valentin (2018), Lacombe et al. (2016), Ribolzi et al. (2017), Lacombe et al. (2018), Patin et al. (2018), Ribolzi et al. (2011b), Chaplot et al. (2007), Neyret et al. (2020), Ribolzi et al. (2018), Janeau et al. (2003), Valentin and Casenave (1992), Lacombe et al. (2015), Janeau et al. (2014), and Vigiak et al. (2008). We calculated the average of each soil surface feature for each treatment by first calculating the averages of the two measurements dates per treatment, and then by calculating the averages among the six replicates per treatment. Surface features include understory, residues (leaves, branches, and seeds), constructions by soil macro-organisms like earthworms and termites, moss and algae, charcoals, free aggregates, free gravel, and three types of crust: structural, erosion, and gravel crusts. In these soils, structural crusts result from the packing of highly stable micro-aggregates (Janeau et al., 2003; Ribolzi et al., 2011b). Compacted by raindrops and smoothed by surface runoff, this structural crust gradually transforms into an erosion crust characterized by a thin and very compacted smooth plasmic layer (Valentin and Bresson, 1992). When they include gravels, structural or erosion crusts become a gravel crust (Valentin and Casenave, 1992). Additionally, we assessed the percentage areas of soil corresponding to pedestal features (Valentin and Rajot, 2018).

4.2.5. *Statistical analysis and modelling*

We performed non-parametric Wilcoxon tests (R version 3.5.3, The R Foundation for Statistical Computing) to compare the distribution between paired groups of the four treatments for three variables (surface runoff depth, suspended sediment concentration, and runoff coefficient).

We conducted a correlation analysis between the measured variables, namely Rc: seasonal runoff coefficient; Sl: seasonal soil loss; and soil surface features expressed in areal percentage: Fa: free aggregates; Fg: free gravel; Tc: total crust; Sc: structural crust; Ec: erosion crust; Gc: gravel crust; Cha: charcoals; Res; residues; Wor: worm casts; Alg: algae; Mos: mosses; Ped:

pedestals; Und: understory. To meet the distributional and variance assumptions required for linear statistical models (Quinn and Keough, 2002), we transformed the variables prior to the analysis; variables expressed in percent were normalized using the arcsine of the square root, which is a classical transformation for percentages, while Sl was scaled with logarithm transformation (Patin et al., 2018). The main objective of these transformations was to make each distribution symmetrical. After transformation, we calculated Pearson correlation coefficients and significance levels (XLSTAT Premium version 20.1.1., Addinsoft, Paris, France) in order to test the correlation between variables.

We also calculated partial least squares regression (PLSR) analysis (Abdi, 2010) on the measured variables (XLSTAT Premium version 20.1.1.) in order to model Rc and Sl depending on soil surface features: Fa: free aggregates; Fg: free gravel; Tc: total crust; Cha: charcoals; Res; residues; Wor: worm casts; Alg: algae; Mos: mosses; Ped: pedestals; Und: understory. PLSR has the advantage to be little sensitive to multi-collinearity and can be used with datasets where the number of observations is close to the number of variables, or even smaller. The importance of each projected variable is estimated by the variable importance in the projection number (VIP). In order to limit the uncertainty related to the variables that bring little information to the model, and consequently to limit the distortion of the results, we discarded the VIP values below 0.8 (Wold, 1995; Zaldívar Santamaría et al., 2019).

4.3. RESULTS

4.3.1. *Rainfall*

Accumulated rainy season rainfall was 1133 mm from 4 June to 15 October 2017. A total of 22 major rainfall events occurred during the same period (**Supporting Figure 4-1**). Minimum rainfall depth was 17 mm whereas maximum was 93 mm. Average rainfall depth was 52 mm. About 36% of the major rainfall events occurred in July, which represents 33% of the accumulated rainy season rainfall depth.

4.3.2. *Height and cover of teak trees and understory*

The average height of the teak trees ranged from 20 m in THU and TBG to 22 m in TNU and TLU. Teak cover was 30% and 35% in TLU and TNU, respectively, and was 60% and 70% in TBG and THU, respectively. The average height of understory varied between 0.6 m in TNU and 4 m in TLU. Understory cover varied between 30% in TNU and 90% in THU (**Figure 4.3**).

4.3.3. *Soil surface features and pedestal features*

The average height of pedestal features ranged from 1.2 cm in TBG to 2.1 cm in TNU (**Figure 4.4a** and **4.4b**). The pedestal features cover was high in TNU (50%) compared to the other treatments (3 – 6%; **Figure 4.4b**).

Figure 4.4c illustrates the percentage area of total crust (erosion crust, structural crust, and gravel crust), free aggregates, free gravel, charcoals, and residues in each treatment. Soil surface across the treatments excluding TNU shared similar conditions, such as total crust (8.5%), free aggregates (32.5%), and residues (58.5%). On the contrary, TNU exhibited high total crust (82.5%), free gravel (9.3%), and little residues (2.91%). Structural crust accounts for more than 90% of total crust in each treatment and charcoals are negligible (less than 0.03%). Nevertheless, erosion crust was 0.54% in TNU, and negligible in the other three treatments (less than 0.05%).

Figure 4.5 shows the relationship between the percentage of cover of pedestal features and both surface runoff (logarithm model, R^2 = 0.82) and soil loss (linear model, R^2 = 0.91). The percentage of cover of pedestal features exhibits a consistent increase with increasing surface runoff and soil loss.

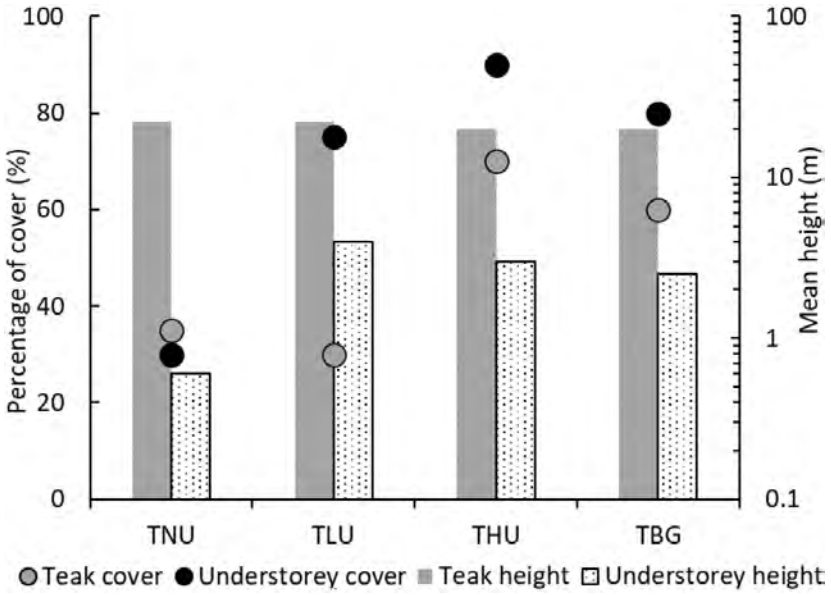

Figure 4.3: Percentage of cover (%) by teak trees and understory, and mean height (m) of teak trees and understory in each treatment measured on 14 December 2017, in Ban Kokngew, Luang Prabang Province, Lao PDR. TNU: Teak with no understory; TLU: teak with low density of understory; THU: teak with high density of understory; TBG: teak with broom grass.

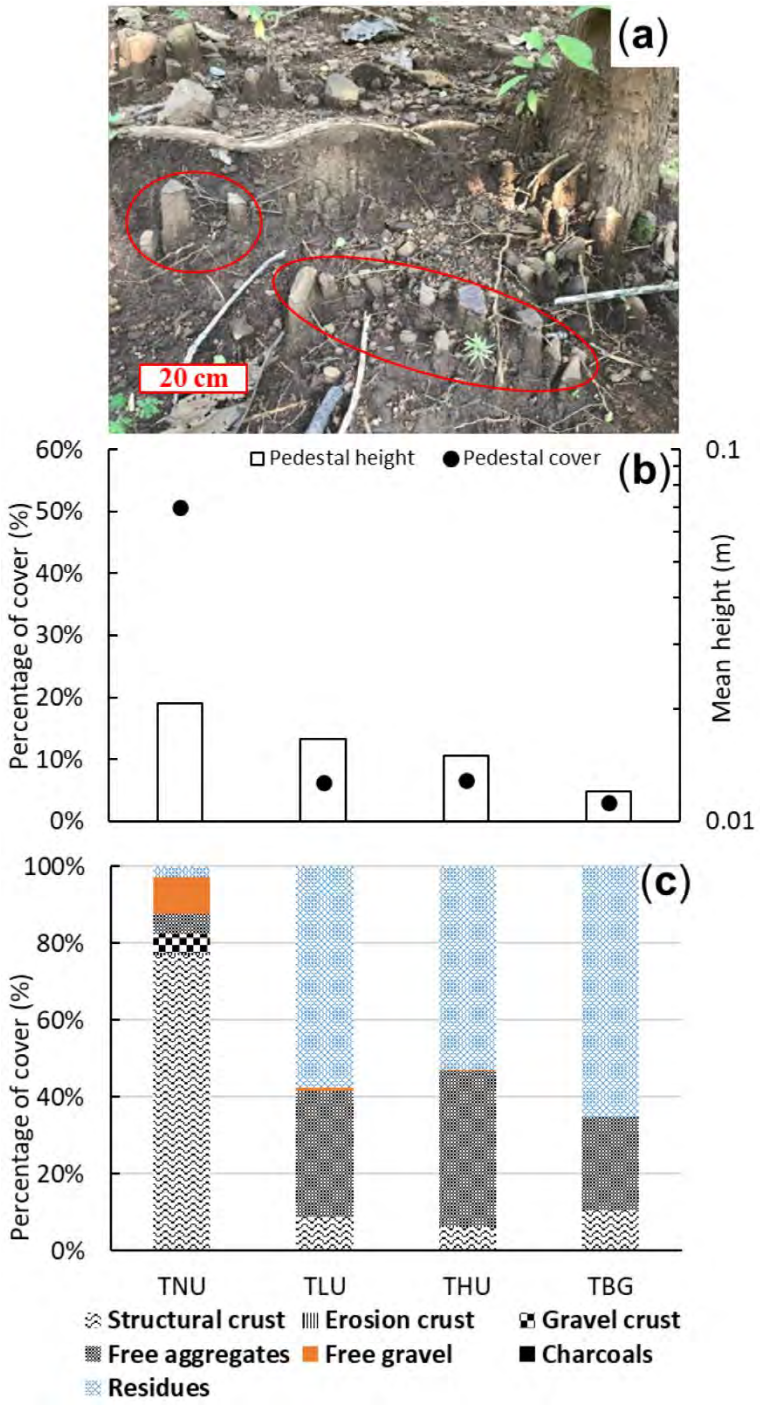

Figure 4.4: (a) Example of pedestal features circled by red lines. (b) Percentage of cover of pedestal features (%) and pedestal features' height (m; logarithmic scale). (c) Cumulative percentage areas (%) of soil surface features in 2017 in Bak Kokngew, Luang Prabang Province, Lao PDR. TNU: Teak with no understory; TLU: teak with low density of understory; THU: teak with high density of understory; TBG: teak with broom grass.

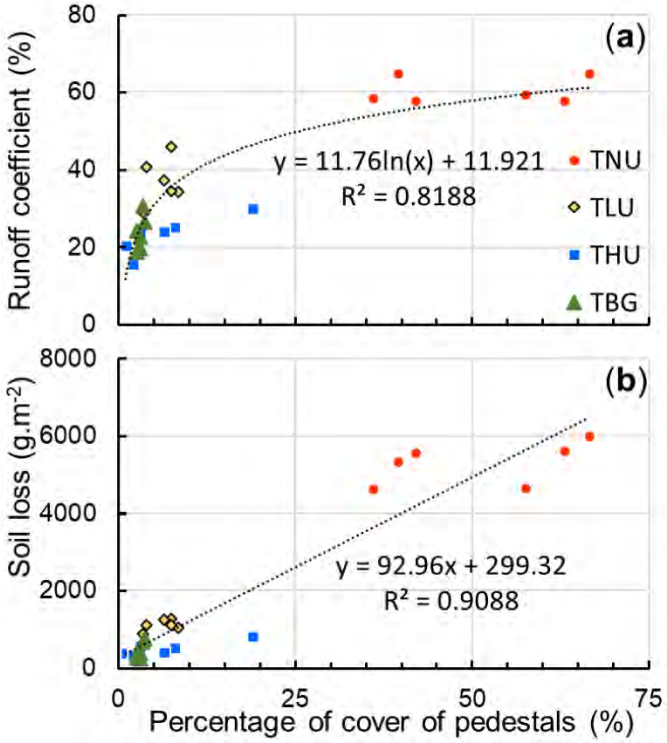

Figure 4.5: (a) Relationship between runoff coefficient (%) and percentage of cover of pedestal features (%). (b) Relationship between soil loss ($g \cdot m^{-2}$) and percentage of cover of pedestal features (%) measured in 2017 in Bak Kokngew, Luang Prabang Province, Lao PDR. TNU: Teak with no understory; TLU: teak with low density of understory; THU: teak with high density of understory; TBG: teak with broom grass.

4.3.4. *Relationship between surface runoff and soil loss across four treatments*

Figure 4.6 depicts the linear correlation between accumulated surface runoff and accumulated soil loss on log scale during the rainy season in 2017 for all the replicates. Total surface runoff averaged over the rainy season ranged from approximately 170 mm in THU and TBG to 480 mm in TLU, while it reached up to 680 mm in TNU. The average value in the four treatments was 370 mm. TBG and THU provided the same amount of surface runoff. Soil loss varied between 249 $g \cdot m^{-2}$ in TBG to 6012 $g \cdot m^{-2}$ in TNU, with an average of 1848 $g \cdot m^{-2}$ in all treatments. The highest sediment concentration was 9.60 $g \cdot L^{-1}$ in TNU, while the other three treatments had an average of 2.34 $g \cdot L^{-1}$.

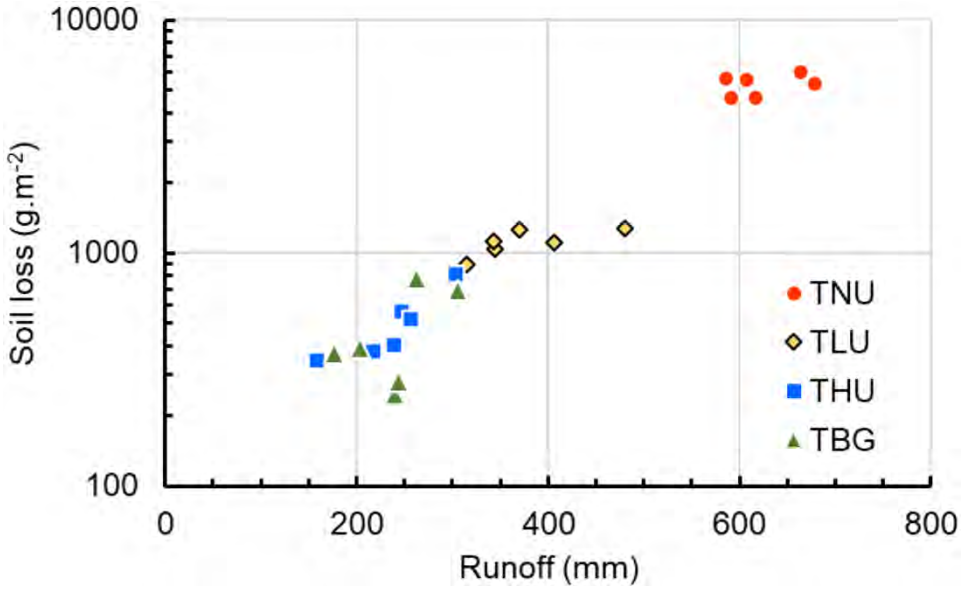

Figure 4.6: Surface runoff (mm) and soil loss (g·m^{-2}, logarithmic scale) measured from 4 June to 15 October 2017, in the four treatments with six replicates in Ban Kokngew, Luang Prabang Province, Lao PDR. TNU: teak with no understory; TLU: teak with low density of understory; THU: teak with high density of understory; TBG: teak with broom grass.

4.3.5. *Effect of understory on soil loss and surface runoff generation*

The Wilcoxon test applied to the cumulative surface runoff, the average suspended sediment concentration, and the runoff coefficient for the four treatments highlighted three significantly (p-value > 0.05) different categories of treatments: from the little erosive treatments (THU and TBG) to highly erosive treatments (TNU; **Figure 4.7**).

The surface runoff pattern matched the rainfall pattern, while the soil detachment pattern did not perfectly match rainfall pattern (**Supporting Figure 4-1**). The highest median values of surface runoff and runoff coefficient (44 mm mostly in TNU and about 110% in TBG and TNU, respectively) were observed from 15 July to 15 August and this pattern was less clear for soil loss. We found the maximum median value of soil loss in TNU (551 g·m^{-2}). For one replicate of TNU, the soil loss reached 1054 g·m^{-2} (8 July).

Supporting Figure 4-2 shows the cumulative surface runoff and cumulative soil loss in relation to cumulative rainfall over the 2017 rainy season for the different treatments. Surface runoff and soil loss in TBG were 242 mm and 381 g·m^{-2}, respectively. Surface runoff and soil loss in THU were 242 mm and 465 g·m^{-2}, respectively. Surface runoff and soil loss in TLU were 358 mm and 1115 g·m^{-2}, respectively. TNU produced more surface runoff (612 mm) and much more soil loss (5455 g·m^{-2}) than the other treatments. Hence, the surface runoff in TNU was approximately 2.5-times higher than in THU and TBG, and 1.7-time higher than in TLU. The

soil loss in TNU was 13- and 14-times higher than in THU and TBG, respectively. TNU had the sharpest rise of soil loss among all the treatments. Median runoff coefficients for TBG, THU, TLU, and TNU were 23%, 23%, 25%, and 60%, respectively.

4.3.6. *Runoff coefficients and soil loss in relation to soil surface features and understory cover*

Table 4.2 shows the relationship between the surface runoff coefficient, soil loss, and soil surface features areal percentages. Erosion crust, charcoals, worm casts, algae, and mosses show weak correlations with the surface runoff coefficient while the other soil surface features and understory cover provided Pearson correlation coefficient (r) above 0.7. The features with lower r had lower percentages, which may cause poor relation with the surface runoff coefficient. Free aggregates, residues and understory had a strong and negative correlation with surface runoff with r between –0.72 and –0.91. Free gravel, total crust, structural crust, gravel crust, and pedestal features cover exhibited a strong correlation with surface runoff (r = 0.84, 0.89, 0.89, 0.98, and 0.89, respectively). We also found a strong correlation between soil loss and surface runoff (r = 0.97). Soil surface features and understory cover exhibited significant inter-correlation except for charcoals, worm casts, algae, and mosses, which were weakly related to other types of soil surface features or understory cover.

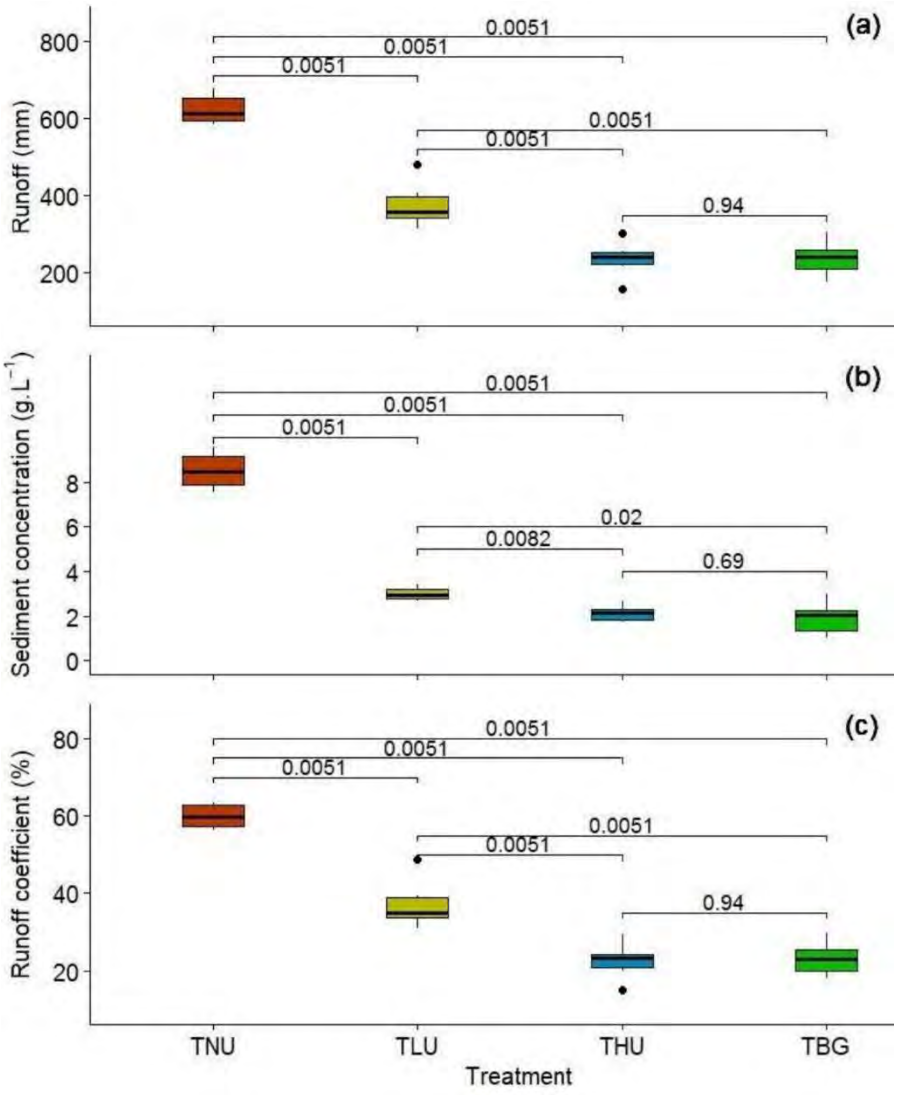

Figure 4.7: Boxplots of (a) cumulative surface runoff (mm), (b) average suspended sediment concentration ($g \cdot L^{-1}$), and (c) runoff coefficient (%) in each treatment measured from 4 June to 15 October 2017, in Ban Kokngew, Luang Prabang Province, Lao People's Democratic Republic. Each rainfall bar represents the accumulated rainfall over the period prior to the sampling. Each boxplot contains the extreme of the lower whisker (vertical line), the lower hinge (thin line), the median (bold line), the upper hinge (thin line), the extreme of the upper whisker (vertical line), and the outliers (black dots) with p-values from Wilcoxon tests between two groups of treatments. The whiskers extend to the most extreme data point, which is no more than 1.5-times the interquartile range from the box. TNU: teak with no understory; TLU: teak with low density of understory; THU: teak with high density of understory; TBG: teak with broom grass. The runoff coefficient is the ratio in percentage between total surface runoff depth and total rainfall depth.

Table 4.2: Correlation (Pearson coefficient) between seasonal runoff coefficient (Rc), seasonal soil loss (Sl), and soil surface features: Fa: free aggregates; Fg: free gravel; Tc: total crust; Sc: structural crust; Ec: erosion crust; Gc: gravel crust; Cha: charcoals; Res; residues; Wor: worm casts; Alg: algae; Mos: mosses; Ped: pedestals; Und: understory. All variables were measured in 2017 in Ban Kokngew, Luang Prabang Province, Lao PDR.

	Rc	Sl	Fa	Fg	Tc	Sc	Ec	Gc	Cha	Res	Wor	Alg	Mos	Ped
Sl	0.97****													
Fa	-0.72****	-0.77****												
Fg	0.84****	0.86****	-0.72****											
Tc	0.89****	0.90****	-0.87****	0.84****										
Sc	0.89****	0.90****	-0.87****	0.83****	0.99****									
Ec	0.62**	0.64***	-0.58**	0.44*	0.67***	0.66***								
Gc	0.87****	0.90****	-0.78****	0.90****	0.91****	0.90****	0.70***							
Cha	0.48*	0.44*	-0.39	0.32	0.52**	0.52**	0.49*	0.43*						
Res	-0.87****	-0.89****	0.77****	-0.88****	-0.97****	-0.97****	-0.66***	-0.94****	-0.53**					
Wor	-0.47*	-0.42*	-0.07	-0.46*	-0.27	-0.27	-0.15	-0.37	-0.13	0.39				
Alg	0.55**	0.53**	-0.31	0.49*	0.45*	0.45*	0.16	0.44*	0.28	-0.47*	-0.23			
Mos	-0.26	-0.34	0.27	-0.25	-0.39	-0.38	-0.32	-0.37	-0.10	0.42*	0.26	-0.13		
Ped	0.89****	0.91****	-0.80****	0.82****	0.94****	0.94****	0.73****	0.91****	0.54**	-0.92****	-0.30	0.38	-0.31	
Und	-0.91****	-0.93****	0.89****	-0.86****	-0.98****	-0.98****	-0.63**	-0.91****	-0.49*	0.95****	0.26	-0.47*	0.36	-0.92****

Significance level: **** $p < 0.0001$; *** $p < 0.001$; ** $p < 0.01$; * $p < 0.0$

Figure 4.8a shows PLSR biplot of inter-correlation between runoff coefficient, soil loss, understory, and soil surface features. The runoff coefficient and soil loss were positively correlated with total crust, pedestal features cover, free gravel, charcoals, and algae, but were negatively correlated with understory, residues, and free gravel. Worm casts and mosses had no significant relation with the other variables.

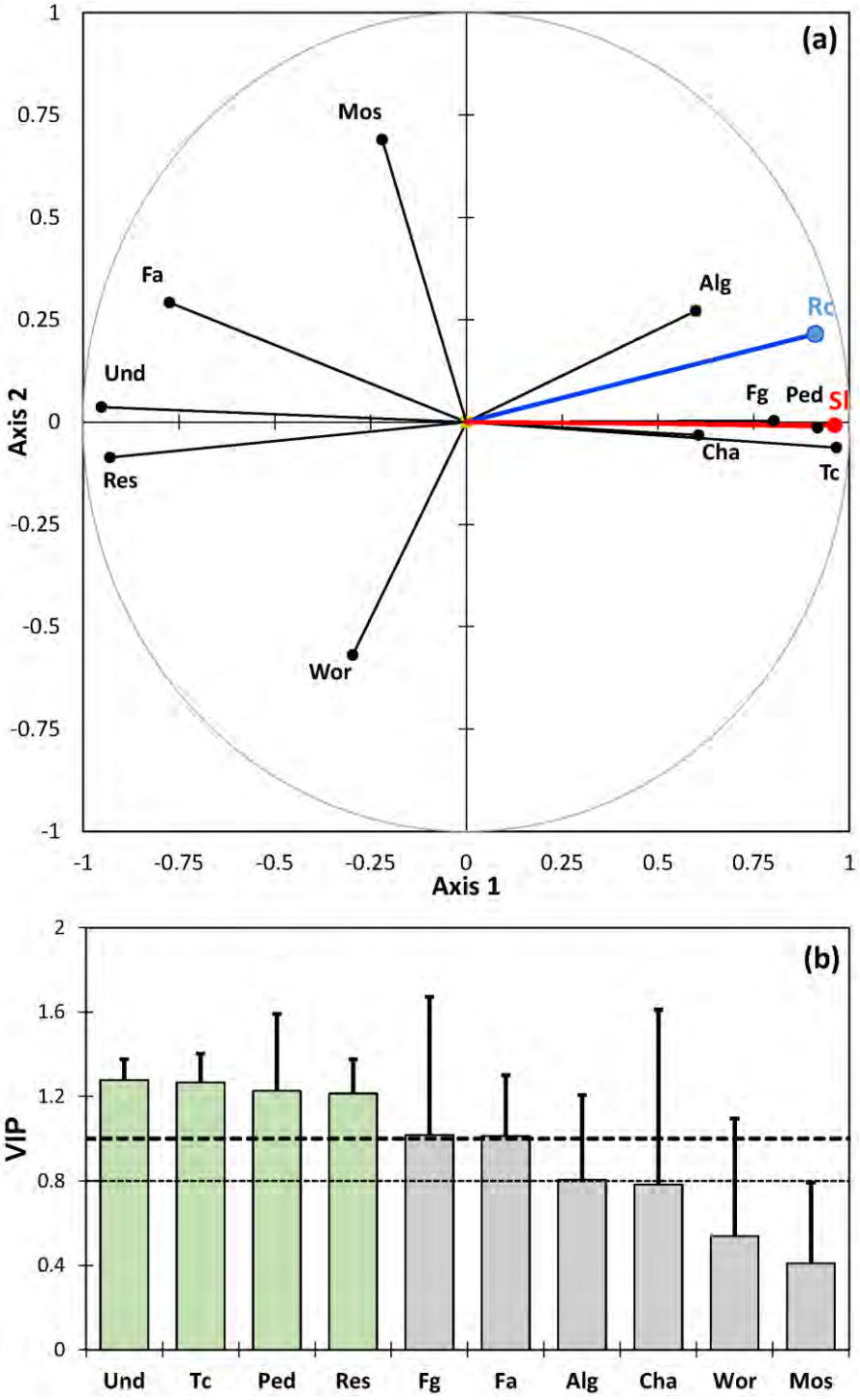

Figure 4.8: (a) Partial least squares regression (PLSR) biplot for seasonal surface runoff coefficient (Rc) and seasonal soil loss (Sl) in relation with soil surface features and understory.

(b) Variable importance for the projection (VIP) score plot of each variable contributing the most to the models of Rc and Sl. Und: understory; Tc: total crust; Ped: pedestals; Res; residues; Fg: free gravel; Fa: free aggregates; Alg: algae; Cha: charcoals; Wor: worm casts; Mos: mosses. All variables were measured in 2017 in Ban Kokngew, Luang Prabang Province, Lao PDR.

Figure 4.8b displays the score plot of variable importance in projection (VIP) for each soil surface feature and understory treatment. This plot allows the rapid identification of the variables that contribute the most to the models of runoff coefficient and soil loss (**Supporting Figure 4-3**). Understory, total crust, pedestal features cover, and residues, were considered the most important variables and therefore the best predictors in the model. The coefficient of each variable contributing to the models' equation are listed in **Supporting Table 4-1**.

Figure 4.9 shows the observed and the modelled soil loss proposed by (Patin et al., 2018). The soil loss is a function of the runoff coefficient with the equation $\ln(Sl) = -1.30 + 2.36 \ln(Rc)$, where Sl is the soil loss and Rc is the runoff coefficient. The model provided significant statistics ($R^2 = 0.91$, p-value < 0.0001) and is a promising framework for the prediction of soil loss based on the runoff coefficient.

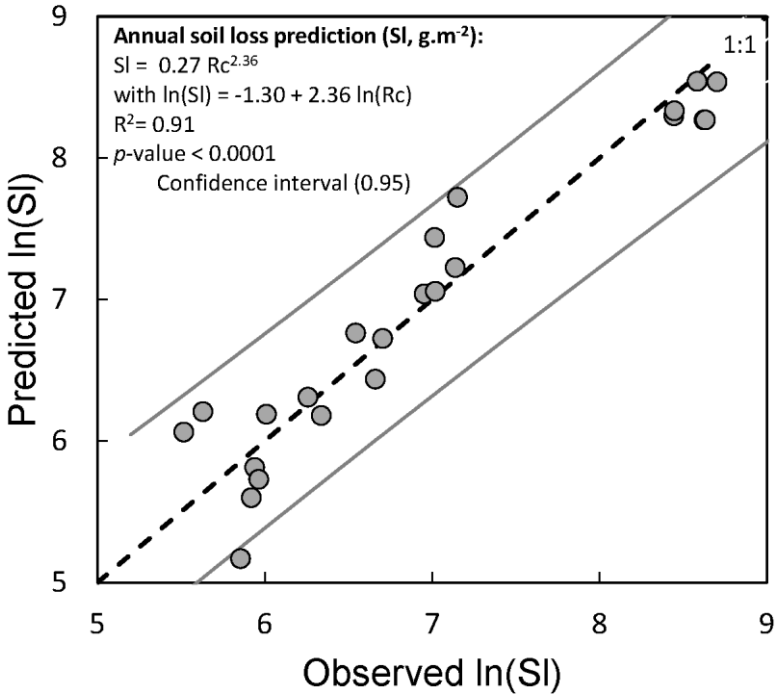

Figure 4.9: Observed and modelled seasonal soil loss. Each point represents the seasonal soil loss of the 24 microplots. Values (in $g \cdot m^{-2}$) were predicted using the simple formulation $\ln(Sl) = -1.30 + 2.36 \ln(Rc)$, where Rc is the seasonal runoff coefficient and Sl is the seasonal soil loss, as proposed by Patin et al. (2018). Observed Rc and Sl were measured from 4 June to 15 October 2017, in Ban Kokngew, Luang Prabang Province, Lao PDR.

4.4. DISCUSSION

4.4.1. *Understory limits surface runoff and soil erosion*

Soil loss is strongly related to surface runoff (**Figure 4.6** and **Figure** 4.8, and **Table 4.2**). Soil loss increased with increasing surface runoff, especially in TNU, which produced the most surface runoff, over the rainy season (**Supporting Figure 4-1**). Patin et al. (2018) successfully applied the Terrace Erosion and Sediment Transport (TEST) model developed by Van Dijk et al. (2003) to estimate soil detachment observed for various land covers in the Houay Pano catchment, northern Lao PDR. They also proposed a simple soil loss model describing the soil loss as a function of the runoff coefficient. We applied this simplified model and also found that seasonal surface runoff coefficient is a reliable predictor of the seasonal soil loss (**Figure 4.9**). This result shows that, at the plot scale, surface runoff is statistically the main process responsible for the transfer of solid particles. Our results show that under the studied conditions, sediment production, which is high, is not the limiting factor to soil loss. We found that soil loss had a strong correlation with structural crust and a strong negative correlation with free aggregates and residues. Overall, these findings are in accordance with the findings reported by Lacombe et al. (2018), namely that soil loss increases with an increasing surface runoff coefficient proportionally predicted by structural crust. The percentage of erosion crust is one of the main drivers of soil erosion (Lacombe et al., 2018). At the plot scale, soil detachment firstly depends on splash (Valentin and Rajot, 2018). The packing of the soil particles, which is due to the compaction by large drops, leads to crust forming (Valentin and Rajot, 2018). Soil detachment by splash eventually leads to pedestal features (Valentin and Rajot, 2018). We found that the structural crust represents in average 93–100% of the total crust, similar to the 91% reported by Lacombe et al. (2018) for mature teak trees. Consistently, the percentage of pedestal features cover (Figure 4.4a) and total crust (82% of the percentage area of soil surface feature; Figure 4.4b) was relatively high in TNU. The highest surface runoff and soil loss were observed in TNU, due to the highly crusted area together resulting from less residues cover and the absence of understory cover. Hence, runoff generation occurs on the crusted soil area which restricts infiltration (Bu et al., 2014; Fox et al., 2004), depending on the presence of plant residues at soil surface and understory (Neave and Rayburg, 2007; Rey et al., 2004). Residues do not only prevent crust formation (Neave and Rayburg, 2007), but also favor the biological activity of organisms which decompose organic matter from the residues, especially macro-faunal communities (also referred to as soil engineers) (Angelsen and Kaimowitz, 2004). This biological process contributes to increase the infiltration rate through the development of soil

biological porosity and breakdown of soil crusts resulting from previous inappropriate land use (Blanco and Lo, 2012; Rey et al., 2004). The surface runoff coefficient is a function of structural crust (Lacombe et al., 2018) and our results confirmed this finding (**Table 4.2**). A similar result was obtained by (Fox et al., 2004; Kosmas et al., 1997; Podwojewski et al., 2008) who found that a soil crusted area enhances surface runoff and soil erosion. Crusted soil has less influence on soil detachment due to its physical protection (Chaplot et al., 2007). This implies that structural crust is not the main cause of soil erosion but the main driver of surface runoff generation (Lacombe et al., 2018). Once generated, surface runoff carries towards downstream the soil particles detached by splash (Valentin and Rajot, 2018).

Our models based on PLSR analysis confirmed the importance of each soil surface feature, including understory cover, in predicting seasonal surface runoff coefficient and seasonal soil loss at the plot scale (**Supporting Figure 4-3** and **Supporting Table 4-1**). High soil detachment and surface runoff could be alleviated by the physical protection of both understory covers including broom grass and plant residues (originating from teak leaves and understory). Soil splash depends on understory cover and on the percentage of cover by residues (Valentin and Rajot, 2018), while surface runoff decreases when understory cover increases (Nouwakpo et al., 2018). The understory and a thick residue layer reduce the rain splash effect and allow a high rate of infiltration, which then reduces surface runoff and soil erosion (Calder et al., 1993). The soil is protected by understory, which dissipates the high raindrops' kinetic energy under teak trees (Valentin and Rajot, 2018). In the absence of understory, the height of trees plays a decisive role with respect to soil detachment (**Figure 4.3**). Tall tree canopy in dense tree plantations intercepts the raindrops. Since teak tree leaves are broad, leaves dramatically increase the diameter of raindrops with throughflow, hence their kinetic energy and erosivity (Geißler et al., 2012; Goebes et al., 2015; Lacombe et al., 2018). Plant residue attenuates the effect of rain splash and reduces the percentage area of total crust (Lacombe et al., 2018). A number of authors have shown that the removal of understory by slashing and burning induces increased surface runoff and soil erosion (Blanco and Lo, 2012; Fernández-Moya et al., 2014; Lacombe et al., 2015; Le et al., 2020).

Runoff coefficients in the four treatments varied in time and increased in the middle of the rainy season (July 2017, **Supporting Figure 4-1**), which is explained by antecedent rainfall, i.e., the rain falling before any rainfall event of interest (Jadidoleslam et al., 2019). Rainfall events happen more frequently in the middle of the rainy season. Since there is less time between two subsequent rainfall events to dry the soil, soil moisture increases, and soils get saturated or

nearly saturated by water. Consequently, surface runoff generation is enhanced, and the runoff coefficients increase in the middle of the rainy season. Surface runoff in TNU plots were much higher than in all other treatments over the rainy season (**Supporting Figure 4-1**). The runoff coefficient in TNU was higher than in the other treatments since the very beginning of the season despite the low soil moisture and the low hydraulic conductivity of soil. Overall, the runoff coefficient in TNU was the highest with 59.7% (**Supporting Figure 4-2**), which is comparable to the values found by Lacombe et al. (2018) in mature teak tree plantations with similar conditions of understory. On the contrary, the runoff coefficients of THU and TBG were around 23% (**Supporting Figure 4-2**), which is comparable to the overall runoff coefficient calculated for the treatments associating young teak trees with a variety of understory in Lacombe et al. (2018).

The least erosive treatment in this study, i.e., TBG (381 $g \cdot m^{-2}$), produced soil loss about 7.5-times higher than the broom grass treatment in Houay Dou catchment in northern Lao PDR (Lacombe et al., 2018). The difference between our finding and broom grass treatment in Lacombe et al. (2018) can be explained by the lower residue cover and the greater height of teak trees in our study, and by the fact that broom grass canopy was less dense because it was grown under the shadow of the teak trees and frequently harvested. Our values in TBG treatment were also greater than the values reported by (Phan Ha et al., 2012; Podwojewski et al., 2008) in northern Vietnam, with similar understory, topography, and climate, but with different vegetation types, namely mixed tree plantation and fallow, respectively. Similarly, the most erosive treatment in this study, i.e., TNU (5455 $g \cdot m^{-2}$), produced soil loss about 3.5-times higher than the mature teak tree treatment in Lacombe et al. (2018). The values in TNU were also higher than the values reported by (Chaplot et al., 2007; Lacombe et al., 2018; Podwojewski et al., 2008) in the same region with similar understory conditions. Such discrepancies may be related to soil surface conditions or plant and understory characteristics (height, plant density, percentage of cover), which were usually discussed in this study. However, values 5.4-times higher were measured by (Santamaría Leandro, 1992) in Costa Rica, where antecedent land use as rangeland most likely greatly and durably reduced soil hydraulic conductivity (Fernández-Moya et al., 2014). Overall, the soil loss in TBG was 14-times less than in TNU. Hence, teak tree plantation owners could divide soil loss by 14 by keeping understory, such as broom grass, within teak tree plantations.

Considering the finding of our study at the plot scale, the farmers would also have saved about 40 – 50 $ton \cdot ha^{-1}$ of soil over the 2017 rainy season if they had grown understory under teak

trees. However, this result must be qualified since the value cannot be extrapolated at scales larger than the plot scale, such as the catchment scale, because erosion processes at catchment scale are different (suspended sediments deposition or resuspension, gully formation on steep slope). At the catchment scale, a supplementary mitigation measure to trap water and eroded soil particles before entering the river network would be riparian buffers and vegetation filter strips (Cao et al., 2018; Vigiak et al., 2008).

4.4.2. *Broom grass grown in teak tree plantations: Agronomic aspects and ecosystem services*

Tree spacing is a determinant factor of teak tree productivity (Blanco and Lo, 2012). In our study, densities of 800 – 1200 tree·ha^{-1} (Pachas et al., 2019) (**Table 4.1**) were relatively high compared to densities reported for other plantation areas (< 800 tree·ha^{-1}) (Blanco and Lo, 2012; Koonkhunthod et al., 2007; Kumar et al., 2016). Planting trees at lower densities in our study site should be seriously considered as not only would it warrant higher productivity (Blanco and Lo, 2012), possibly higher than in natural forest (40 tree·ha^{-1}) (Koonkhunthod et al., 2007), but it would also allow growing intercropped understory adding economic value to the overall plantation yield.

The introduction of agroforestry into agricultural practices ensures an increased food security by a restored soil fertility for food crops (Schroeder, 1993) and a sustainable production of wood (Angelsen and Kaimowitz, 2004). Broom grass is neither a food nor a feed crop but similar to agroforestry systems, it is grown under trees. Thus, the management practice may possibly increase the overall productivity (biomass, economic yield (Pachas et al., 2020; Pachas et al., 2019) of the plot, by making an optimal use of the resources (water and nutrients), that would otherwise not be utilized by a single crop, consumed by plant species at different soil layers depending on their root length (Chitra-Tarak et al., 2018). Although it seems to be more productive when grown in full light (Lacombe et al., 2018), broom grass can be grown under teak trees, similar to other shade-tolerant crops, such as patchouli (Kumar et al., 2016).

Growing broom grass in teak tree plantations may supply a range of ecosystem services that is not limited to the supply of raw material for brooms and to the prevention of high surface runoff and soil loss in teak tree plantations. At the plot scale, the litter from broom grass leaves may increase top soil organic matter content (Angelsen and Kaimowitz, 2004), thus improving soil structure, soil nutrient availability (Blanco and Lo, 2012), soil carbon sequestration (Balmford and Whitten, 2003), and increasing water infiltration and soil moisture retention (Neyret et al.,

2020; Rey et al., 2004). Diversifying vegetation strata may diversify the habitats for bird species and other forest-dependent species (Harvey and Villalobos, 2007; Koonkhunthod et al., 2007; Wunderle Jr, 1997), thus increasing predator biodiversity (Imron et al., 2018; R. Perrin, 1976) and reducing the need for chemical inputs (insecticides, herbicides, etc.) in e.g., surrounding annual crop plots. At the catchment scale, favoring water infiltration and reducing surface runoff may mitigate natural disasters (floods and droughts) (Balmford and Whitten, 2003; Blanco and Lo, 2012) and increase the transfer time of contaminants deposited at the soil surface (Monaghan et al., 2016). Decreasing the sediment supply to the stream network would increase the life span of dam reservoirs (Annandale, 2006) and avoid dredging costs (Boithias et al., 2016b; Crowder, 1987; McHenry, 1974), an issue of particular concern along the Mekong River where the number of dams is dramatically increasing (Arias et al., 2014; Dang et al., 2018).

4.4.3. *Percentage of cover of pedestal feature: an indicator of soil erosion*

Both the PLSR model and the simplified model proposed by Patin et al. (2018) that we presented in this study provided promising results to predict soil loss. Nevertheless, such models require input data from experimental microplots which are rather difficult and time consuming to be implemented, particularly within the framework of a large-scale approach. It would be more practical to use simple indicators that are known to be proxies of soil loss, such as soil surface features and/or understory characteristics (**Table 4.2**). On one hand, understory cover varies throughout the year, which causes difficulties in visual observation and inconsistent estimation. On the other hand, observing soil surface features (such as total crust, free aggregates, free gravel, residues, etc.) requires some expertise. However, among soils surface features, pedestal feature cover is a reliable proxy of soil erosion intensity in the field (**Figure 4.4a**) that is easy to assess visually. The estimated soil loss depth in 2017, based on bulk density of 1 $g \cdot cm^3$ for Acrisol (Phan Ha et al., 2012), was 0.53±0.05 cm. Hence, lay people could use the proxy of the percentage of cover of pedestal features to identify the impact of the agricultural management of their land on soil degradation through surface runoff and soil loss.

4.5. CONCLUSIONS

We investigated the impact of different types of understory on surface runoff and soil loss in a teak tree plantation of the mountainous region of northern Lao PDR. We analyzed the relationship between understory management, soil surface features (including pedestal features), and surface runoff and soil loss at the plot scale. This paper clearly demonstrates that

teak tree plantations, especially in steep sloping lands, can be prone to considerable soil loss if not properly managed. Our main findings, which are graphically synthesized in **Figure 4.10**, are that:

- Understory cover acts as an umbrella that protects soil surface from rain splash despite the height of teak trees and the large size of their leaves which contribute to produce raindrops of high kinetic energy. Teak tree plantation owners could divide soil loss by 14 by keeping understory, such as broom grass, within teak tree plantations. Hence, growing understory under teak trees is a mitigation management practice that can be reliably promoted to limit surface runoff and soil erosion.
- Residues from both teak tree leaves and understory not only protect the soil but also enhance the infiltrability of water into the soil. In contrast, the main driver of surface runoff and soil erosion is the percentage of crusted area.
- Understory such as broom grass provides several benefits to the relevant stakeholders in the area, in terms of incomes and ecosystem services. For example, the farmers can sell the brooms made from broom grass.
- The percentage of cover of pedestal features appears as a good indicator of soil erosion that farmers and teak tree plantations owners could easily use to assess the degradation of their land.

In such a context, to minimize surface runoff and soil erosion in steep slope areas such as the montane regions of south–east Asia, decision makers should, if not legally enforce the maintenance of understory strata in teak tree plantation, at least recommend the plantations owners to maintain understory and avoid understory and plant residue layers burning.

At the plot scale, our findings are relevant to farmers concerned about soil loss and soil fertility in their teak tree plots. At catchment scale, they are relevant to decision makers concerned with the management of costs (such as the cost of water treatment, and/or infrastructure rehabilitation such as dam reservoir dredging) resulting from soil loss induced by upslope activities such as tree plantations and improper agricultural land management. In addition to maintaining the understory strata, encouraging the use of e.g., riparian zone buffers along the streams (Ahmad et al., 2020; Bhat et al., 2019) could also be recommended to trap soil particles from the cultivated hillslopes and favor runoff infiltration, and thus ensure the sustainability of the system.

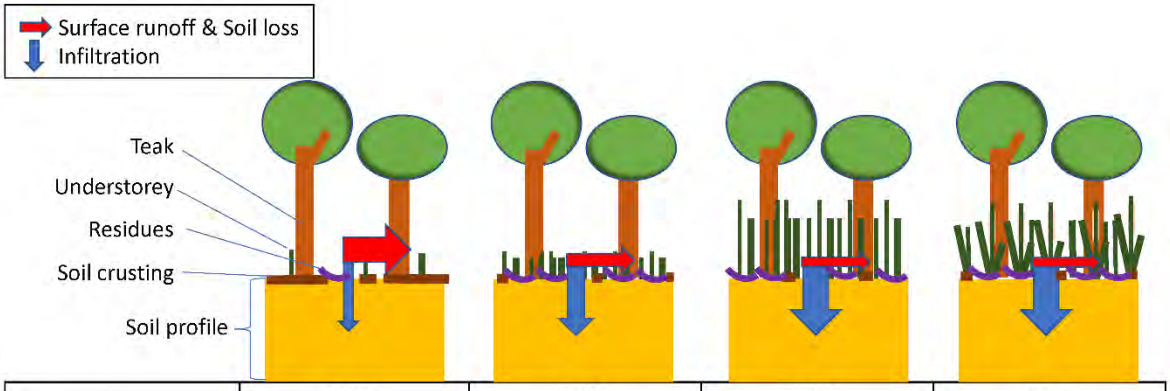

	TNU	TLU	THU	TBG
Runoff coefficient (%)	60	35	23	23
Soil loss (g.m^{-2})	5455	1115	465	381
Understorey cover (%)	30	75	90	80
Residues (%)	3	58	53	65
Crusting rate (%)	82	9	6	11

Figure 4.10: Graphical abstract. TNU: teak with no understory; TLU: teak with low density of understory; THU: teak with high density of understory; TBG: teak with broom grass.

4.6. SUPPORTING MATERIALS

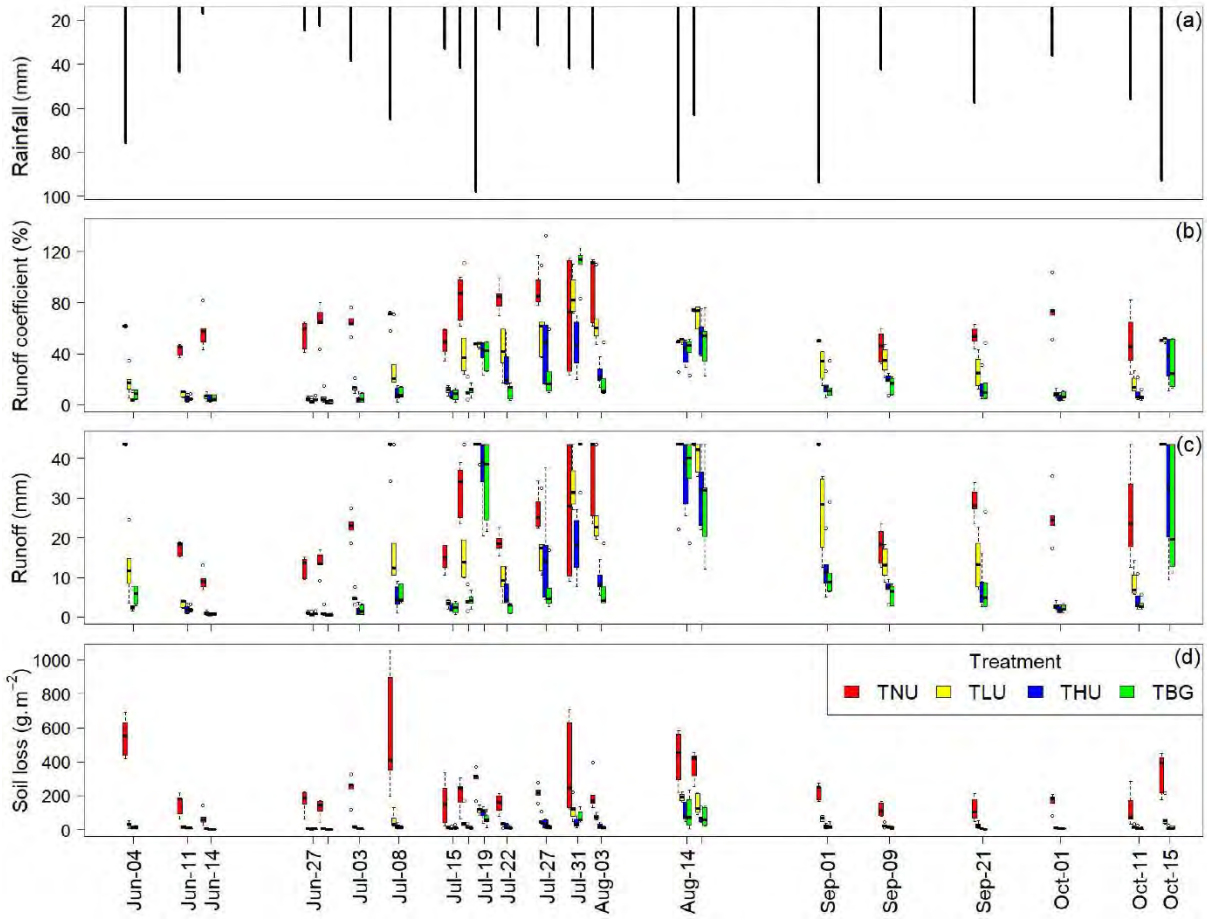

Supporting Figure 4-1: (a) Cumulated rainfall (mm). (b) boxplots of runoff coefficient (%). (c) boxplots of surface runoff (mm). (d) boxplot of soil loss ($g \cdot m^{-2}$) in each treatment measured from 4 June to 15 October 2017, in Ban Kokngew, Luang Prabang Province, Lao PDR. TNU: teak with no understory; TLU: teak with low density of understory; THU: teak with high density of understory; TBG: teak with broom grass. Each rainfall bar represents the accumulated rainfall over the period previous to the sampling. Each boxplot contains the extreme of the lower whisker (dashed line), the lower hinge (thin line), the median (bold line), the upper hinge (thin line), and the extreme of the upper whisker (dashed line). The whiskers extend to the most extreme data point, which is no more than 1.5-times the interquartile range from the box.

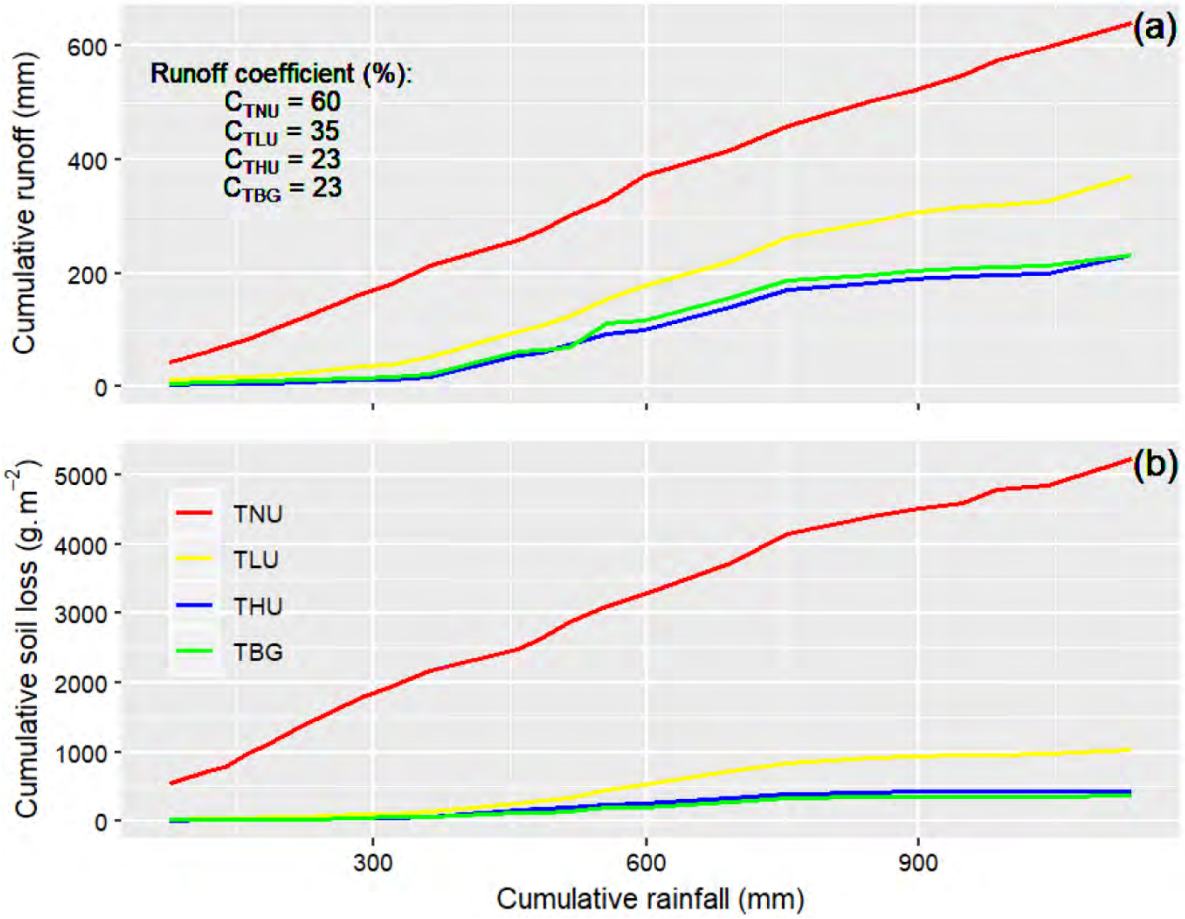

Supporting Figure 4-2: (a) Cumulative surface runoff (mm) versus cumulative rainfall and runoff coefficient (%, total surface runoff divided by total rainfall), and (b) cumulative soil loss (g·m^{-2}) versus cumulative rainfall (mm), measured from 4 June to 15 October 2017, in Ban Kokngew, Luang Prabang Province, Lao PDR. TNU: teak with no understory; TLU: teak with low density of understory; THU: teak with high density of understory; TBG: teak with broom grass.

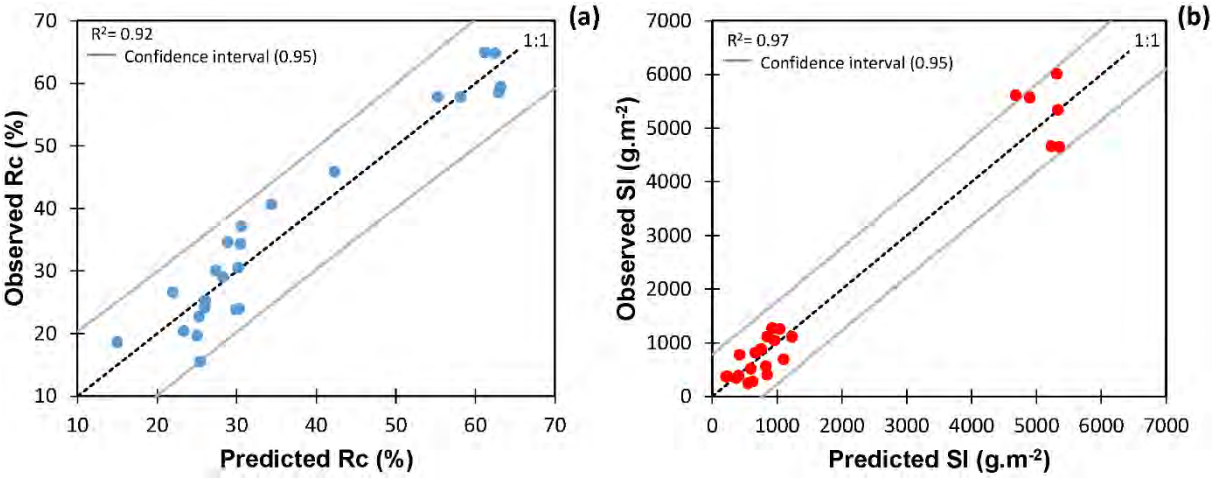

Supporting Figure 4-3: Observed and modelled seasonal runoff coefficient (Rc; in %) and seasonal soil loss (Sl; in $g \cdot m^{-2}$) from partial least squares (PLS) regression method. Observed Rc and Sl were measured from 4 June to 15 October 2017, in Ban Kokngew, Luang Prabang Province, Lao PDR.

Supporting Table 4-1: Coefficients of each variable in the runoff coefficient (%) and soil loss ($g \cdot m^{-2}$) partial least squares (PLS) models. SD: standard deviation; Fa: free aggregates; Fg: free gravel; Tc: total crust; Cha: charcoals; Res: residues; Wor: worm casts; Alg: algae; Mos: mosses; Ped: pedestals; Und: understory.

Variable	Runoff coefficient (%)				Soil loss ($g.m^{-2}$)			
	Coefficient	SD	Lower limit	Upper limit	Coefficient	SD	Lower limit	Upper limit
Constant	43.53	3	37	50	2916.84	166	2573	3261
Fa	-0.10	0	0	0	-18.46	3	-25	-12
Fg	0.31	0	0	1	53.96	16	22	86
Tc	0.07	0	0	0	10.35	1	8	13
Cha	54.79	42	-32	142	7692.58	3965	-531	15916
Res	-0.09	0	0	0	-12.40	1	-15	-10
Wor	-0.74	0	-1	0	-26.93	16	-60	7
Alg	41.56	21	-1	84	3191.76	736	1666	4718
Mos	3.41	5	-7	14	-84.62	83	-256	87
Ped	0.13	0	0	0	16.11	3	10	22
Und	-0.13	0	0	0	-14.34	1	-17	-12

Constants and coefficients of each variable of the proposed model of runoff coefficient and soil loss using PLS model.

[This page intentionally left blank]

Chapter 5. Erosion control in teak tree plantation: trapping efficiency of surface runoff and sediment by riparian grass buffers in the humid tropics

"The way to get started is to quit talking and begin doing." – *Walt Disney*

Chapter 5

Erosion control in teak tree plantation: trapping efficiency of surface runoff and sediment by riparian grass buffers in the humid tropics

This scientific chapter assessed the impact of riparian grass on surface runoff and soil and assessed its efficiency in trapping surface runoff and sediment on the teak-cultivated hillslope. The finding suggested that the decision makers or farmers should at least leave 6-m riparian grass buffer to limit water and sediment fluxes discharging downstream.

Abstract: Riparian vegetation acts as a trap by capturing surface runoff (SR) and sediment derived from soil erosion along cultivated hillslopes. It has been shown that teak tree plantations can be prone to soil loss (Sl), particularly under mountainous humid tropical conditions, and the effect of riparian buffer in such an environment has not been yet investigated. This study aimed to: (1) assess the effects of riparian grass (*Microstegium sp.*) in teak cultivated land on SR and Sl; (2) assess the trapping efficiency of riparian buffer for water (WTE), sediment load (STE), and sediment concentration (SCTE); (3) model Sl, WTE, STE, and SCTE. Field measurements were carried out on an experimental catchment located in northern Lao PDR during the rainy season 2014. Runoff coefficient (Rc), Sl, and soil surface features, including the areal percentages of both residues (Res), grass (Gra), and soil crusts were measured using triplicates of 1-m^2 microplots installed in contrasted land uses of the riparian zone: teak with no understory (TNU); grass with a few teaks planted inside (GWT); and grass nearby teak trees (GNT). WTE, STE, and SCTE were estimated using triplicates of 0.5-m Gerlach traps installed upstream and downstream of riparian buffers of 3-m and 6-m length: grass with teaks (GT); grass (G); and teak with no understory (T, uphill of GT and G). TNU had annual value of Rc (55%) and Sl (5791 $g \cdot m^{-2}$) higher than those of GWT (13%, 250 $g \cdot m^{-2}$), and GNT (19%, 159 $g \cdot m^{-2}$). Riparian grass had significant positive WTE, STE and SCTE, with higher efficiency of 6-m length buffer compared to the 3-m length buffer. An event scale process-oriented model, i.e., the product of rainfall kinetic energy, Rc, and two non-linear attenuation factors (involving Res and Gra), well predicted Sl observations ($R^2 = 0.91$). Good agreements were found between observed and predicted WTE, STE SCTE values using Partial Last Square Regression models ($R^2 = 0.99$; 0.96; and 0.94, respectively) with SR, Res, Gra and soil crusts having the highest score of variable importance in projection. Importantly, trapping efficiency during heavy storms (24-hour rainfall > 54.8 mm) appears to be less effective. However, leaving riparian buffers of

at least 6 m is suggested to limit surface water and sediment fluxes discharging downstream during small storms (24-hour rainfall < 54.8 mm) in the context of teak tree cultivated hillslopes.

5.1. INTRODUCTION

Soil erosion by water is globally found a severe hazard, generally caused by natural phenomena, it can be strongly aggravated by anthropogenic activities, some agricultural practices in particular (Wuepper et al., 2020). Commonly known human factors are deforestation, overgrazing, and intensive and extensive cultivation (Ahmad et al., 2020). In return, soil erosion aggravation due to improper agricultural practices leads to crop productivity losses globally and subsequently impacts the world economy and threaten food security (Sartori et al 2019). Mountainous areas are more vulnerable to soil erosion because of the steep slope (Ahmad et al., 2020; Bhat et al., 2019; Huon et al., 2017; Sharma et al., 2017). Soil erosion is particularly intense in the tropical mountainous region, such as Southeast Asia (Borrelli et al., 2017), where heavy storms may result in the supply of large quantities of suspended sediment to streams (Sidle et al., 2006). Teak tree plantations on steep slope significantly increase soil erosion (Patin et al., 2018; Ribolzi et al., 2017; Song et al., 2020) and in-stream particulate matter concentration (Patin et al., 2018; Ribolzi et al., 2017; Song et al., 2020).

Improper management of the understory in the teak tree plantations in the mountainous area of northern Lao PDR (Laos) has enhanced the severity of sediment mass transported towards the rivers (Ribolzi et al., 2017). Song et al. (2020) found that keeping the understory limited surface runoff and soil loss in the teak tree plantations. Conserving grass in the riparian buffer is a promising alternative measure for trapping surface runoff and sediment (Alemu et al., 2017; Bereswill et al., 2014; Dong et al., 2018; Gumiere et al., 2011; Mekonnen et al., 2014; Pan et al., 2018) from the upland, including uplands of the humid tropics (Vigiak et al., 2008), which may further protect the downstream water quality (Angelsen and Kaimowitz, 2004; Cao et al., 2018; Ding et al., 2011; Dosskey et al., 2010; Vidon and Hill, 2004). In fragmented landscapes in northern Vietnam, based on a modelling study, Ziegler et al. (2006) found that buffer lengths of 17 – 47 m (effective slope lengths) on gentle slope were sufficient to trap surface runoff (trapping efficiency of 65-85%). They suggested to leave buffer length even longer for larger storms.

However, buffers lengths as suggested by Ziegler et al. (2006) may not be economically realistic hence accepted by farmers in the context of small headwater catchments of South East Asia

(Lestrelin and Giordano, 2007). Indeed, a buffer zone of the recommended length could represent more than a quarter of the total hillslope length (e.g., Boithias et al. (2021), which constitutes a considerable loss of cultivated land. In northern Lao PDR, only few famers plant teak trees with understory and maintain riparian vegetation. In these exceptional cases, riparian buffer lengths range between 4 and 23 m (de Rouw et al., 2018), hence shorter than the recommended lengths of Ziegler et al. (2006) for water flux.

Therefore, in this study, we tested the trapping efficiency of two riparian grass (*Microstegium sp.*) buffer lengths, based on *in situ* observations in teak tree plantations, and focusing not only on surface runoff, but also on suspended sediment flux. We thus calculated the water trapping efficiency (WTE), the sediment trapping efficiency (STE), and the sediment concentration trapping efficiency (SCTE). We hypothesized that keeping 3-m and 6-m buffer lengths of riparian grass would trap surface runoff and suspended sediment for a wide range of rainfall depths and intensities.

Patin et al. (2018) successfully applied the Terrace Erosion and Sediment Transport (TEST) model developed by Van Dijk et al. (2003) to estimate soil detachment observed for various land covers on the annual scale in the Houay Pano catchment, northern Lao PDR. In this study, this model is tested in riparian zone situation for estimating soil loss on the event scale. Here, we hypothesized that soil loss is enhanced by rainfall kinetic energy and runoff coefficient, and mitigated by residues and grass which were suggested in **Chapter 4** as mitigation factors of soil loss.

The overall goal of this study was to assess the effect of riprian grass of surface runoff and soil loss on the hillsope of teak tree plantation. Field measurements were carried out during the rainy season 2014, on the Houay Pano experimental catchment located in northern Lao PDR (Boithias et al., 2021). The specific objectives of this study were:

- To assess the effects of riparian grass in teak cultivated land on surface runoff and soil loss;
- To assess the trapping efficiency of riparian buffers for water (WTE), sediment load (STE), and sediment concentration (SCTE);
- To model soil loss, WTE, STE, and SCTE.

5.2. MATERIAL AND METHODS

5.2.1. *Study area*

The experimental site was set up in the riparian buffer with and without grass on the downslope of teak tree plantations located in the Houay Pano headwater catchment (Boithias et al., 2021), 10 km from Luang Prabang City in northern Lao PDR (**Figure 5.1**). This catchment is typical of the transition from an agrarian based on shifting cultivation to a commercial tree plantation system of Northern Lao PDR (Ribolzi et al., 2017). The climate is sub-tropical humid and is characterized by a monsoon regime with a dry season from November to May, and a wet season from June to October. The mean annual temperature is 23.4 °C. Mean annual rainfall is 1366 mm, about 71 % of which falls during the wet season. Altitude within the catchment is 435 – 716 m, and the slope gradient is 1 – 135 % (mean=52 %).

The average heights of teak trees were 8 and 2 m in teak with no understory (TNU) and grass with a few teaks planted inside (GWT), respectively. Teak tree cover percentage was 92% and 33% in TNU and GWT, respectively. No teak trees were growing in grass nearby teak trees (GNT). The average height of the grass ranged from 0.32 m in TNU to 0.78 m in GNT. The grass cover percentage varied between 7% in TNU and 45% in GNT (**Supporting Figure 5-1a**).

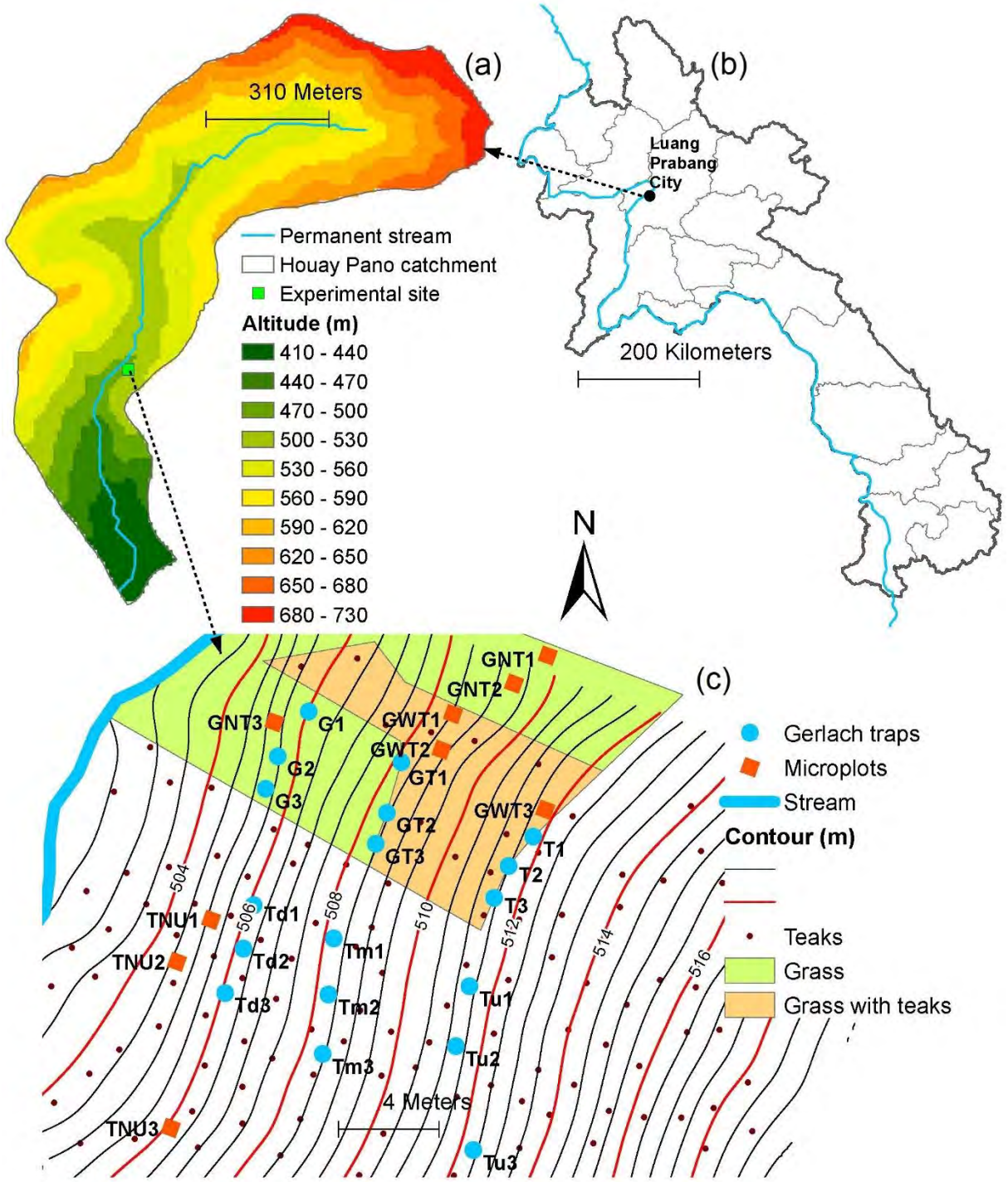

Figure 5.1: (c) Experimental site of 1-m² microplots and 1-m Gerlach traps during the rainy season of 2014 in (a) Houay Pano catchment (upper left) located in northern (b) Lao PDR. Microplots: TNU: teak with no understory; GNT: grass nearby teak trees; GWT: grass with a few teaks planted inside. Gerlach traps: T: teak with no understory (upland of GT and G); GT: grass with teak; G: grass; Tu: teak with no understory (up); Tm: teak with no understory (middle); Td: teak with no understory (down).

5.2.2. *Field experimentation, measurement, and calculation*

5.2.2.1. Microplots and Gerlach traps installation

In the selected site, we selected three land uses (**Figure 5.1**) representing the different conditions of the riparian area. Some area of the riparian grass contained a few teak trees. We made the observation under the teak tree plantation where no riparian grass grew as control treatment by capturing surface runoff and soil loss to be compared with those in the riparian grasses.

We conducted the experimentation in the riparian area by using microplots and Gerlach traps (Gerlach, 1967) (**Figure 5.2**) collecting samples from 6 July to 22 September 2014. We did not collect samples of Gerlach traps for the first rainfall event because the installation of Gerlach traps was not yet done. Totally, there were 20 and 19 samplings of the microplots and Gerlach traps, respectively.

Surface runoff (SR, mm) and soil loss (Sl, $g \cdot m^{-2}$) were monitored using microplots set up in three land uses (3 replicates in each land use): TNU as a control treatment, GWT, and GNT. Microplot consists of 1-m^2 metal frame with 0.15-m height inserted into the soil at a depth of about 0.1 m, connected to a large plastic bucket downhill by a plastic pipe (**Figure 5.2a**). The bucket was 0.45 m high with the bottom and top diameters of 0.32 and 0.38 m, respectively. We set up three replicates in each installation of TNU, GWT, GNT (except TNU for which TNU1 turned out to not be representative of the TNU land use) with the average slope gradient of 53, 70, and 69%, respectively.

Incoming and outgoing fluxes (surface runoff, sediment concentration, and sediment) across riparian sites were monitored using 0.50-m-wide Gerlach traps (Gerlach, 1967) which were applied in several researches (Comino et al., 2016; Kagabo et al., 2013; Thomaz, 2009; Vigiak et al., 2008). Gerlach traps were installed in two columns of downslope. First column involved Gerlach traps installed in teak with no understory (T), grass with teaks (GT), and grass (G). Second column involved the installation of Gerlach traps in teak with no understory at the upslope (Tu), teak with no understory in the middle (Tm), and teak with no understory at the downslope (Td). In each column, we installed Gerlach traps on the boundary between TNU and GWT, GWT and GNT (3-m buffer of riparian grass), and between GNT and stream (6-m buffer of riparian grass).

Gerlach trap consists of a Gerlach trough (0.5-m length, 0.2-m width, and 0.1-m height with a hinged lid; **Figure 5.2b**), a plastic pipe, and a bucket. We installed the Gerlach on the slopping area and connected it to a plastic bucket downhill through the pipe. The bucket was 0.45 m high

with the bottom and top diameters of 0.32 and 0.38 m, respectively. We set up three replicates in each installation of T, GT, G, Tu, Tm, and Td, with the average slope gradient of 66, 49, 77, 73, 55, and 59%, respectively.

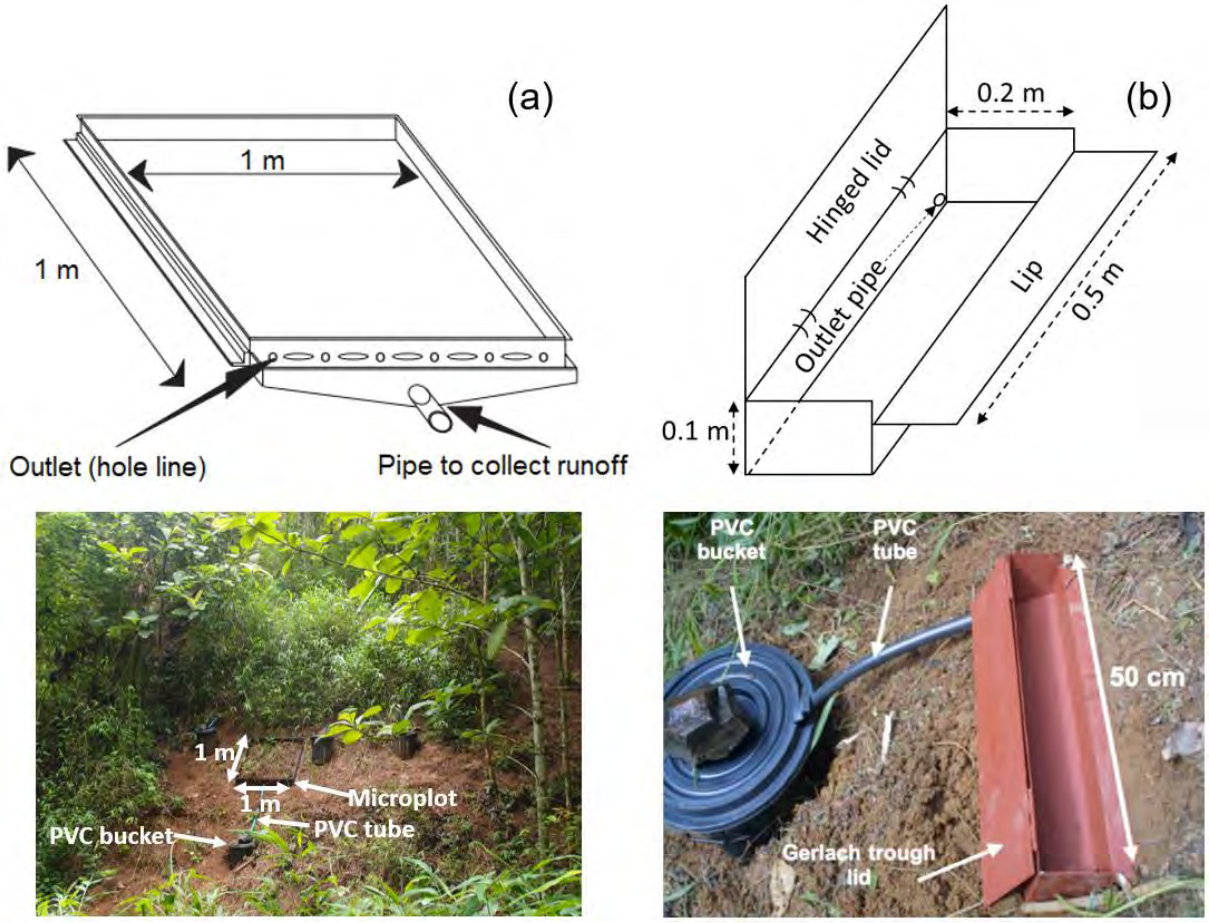

Figure 5.2: Experimental design: (a) diagram showing microplot and (b) Gerlach trap. Microplots and Gerlach traps were installed during the 2014 rainy season in Houay Pano catchment, northern Lao PDR. Microplots (red): TNU: teak with no understory; GNT: grass nearby teak trees; GWT: grass with a few teaks planted inside. Gerlach traps (blue): T: teak with no understory (upland of GT and G); GT: grass with teaks; G: grass; Tu: teak with no understory (up); Tm: teak with no understory (middle); Td: teak with no understory (down).

5.2.2.2. Rainfall measurement, rainfall kinetic energy and erosivity assessment

Rainfall within the Houay Pano catchment is measured since 2001 by the M-TROPICS long-term critical zone observatory (Boithias et al., 2021). A Campbell BWS200 rain gauge equipped with ARG100 (0.2 mm capacity tipping-bucket) was used in 2014. We used 6-min rainfall from 1 January 2001 to 31 December 2019 to analyze rainfall patterns (see section **5.2.3**). We used 6-min rainfall from 1 January to 31 December 2014 to analyse the outcomes of microplot and Gerlach traps. In both cases, daily rainfall was cumulated from 6 AM to 6 AM.

Three kinds of rainfall depth were estimated: rainfall depth within 24 hours prior to the sampling (24_R), significant rainfall depth triggering sampling (Sign_R), and accumulated rainfall depth between two samplings (Acc_R). Seasonal rainfall during the experiment was also calculated. We used Acc_R to analyze the outcomes of microplots and Gerlach traps. We calculated Acc_R by summing up the rainfall between two samplings. We calculated 24_R by summing up backward the rainfall within 24 hours from each sampling time. We calculated Sign_R by summing up the rainfall of the event which triggered the sampling in the buckets.

Rainfall kinetic energy (KE) was computed with the formula and parameters suggested by Patin et al. (2018) for both open space with grass (KEo) and teak tree (KEt). The term of rainfall kinetic energy is even used under the teak tree for the convenient call throughout the text. Three kinds of rainfall kinetic energy were estimated: rainfall depth within 24 hours prior to the sampling (24_KE), significant rainfall depth triggering sampling (Sign_KE), and accumulated rainfall depth between two samplings (Acc_KE). Erosivity Index (EI30) was computed with the total rainfall kinetic energy and maximum 30-min rainfall intensity (I30). We calculated erosivity index for the open space with grass (EI30_o) and for teak tree (EI30_t) using KEo and KEt, respectively, for each Sign_R. We used I30 and EI30 in order to assess the characteristics of each cumulative rainfall, and to assess their relations with the other variables of interest in this study.

5.2.2.3. Grass and soil surface features assessment

Areal percentage of grass and soil surface features were assessed in each replicate of the microplot at the beginning (14 June) and in the middle (27 August) of the 2014 rainy season by visual inspections using the method proposed by Casenave and Valentin (1992) and extensively used in surface runoff and soil loss assessment (Lacombe et al., 2016; Lacombe et al., 2018; Neyret et al., 2020; Patin et al., 2012; Patin et al., 2018; Ribolzi et al., 2017; Ribolzi et al., 2018; Ribolzi et al., 2011b; Song et al., 2020). We calculated the average of each soil surface feature for each land use by first calculating the averages of the two measurements dates per land use, and then by calculating the averages among the three replicates per land use. Surface features include areal percentages of grass (Gra, %), residues (Res, %; leaves, branches, seeds), worm casts (Wor, %; constructions by soil macro-organisms like earthworms and termites), mosses (Mos, %), algae (Alg, %), charcoals (Cha, %), free aggregates (Fa, %), free gravel (Fg, %), pedestals (Ped, %), and soil crusts: total crust (Tc, %), structural crust (Sc, %), erosion crust (Ec, %), and gravel crust (Gc, %). In addition to the areal percentage of the pedestal (Ped), we measured pedestal height (Pedm, m) by using a ruler.

We used the average value of the measurement of teak, grass and soil surface features for the overall analyses.

5.2.2.4. Water sample collection

For both microplot and Gerlach, we sampled water and sediment after every major event (events whose rainfall triggered the sampling). We collected the sample in the buckets using a 650-mL plastic bottle after thoroughly stirring the water until the sediment was homogenous. For each sampling, we also measured the volume of the remaining water sample with a plastic measuring beaker to calculate the total runoff volume and total suspended sediment mass. After each sample collection and measurements of total runoff in the buckets, we emptied the buckets.

5.2.2.5. Runoff coefficient, soil loss, and trapping efficiency calculations

For microplots, we calculated the runoff coefficient (Rc, %) as the ratio between total surface runoff depth and total rainfall depth, both cumulated between two samplings (Rc) and over the whole wet season (seasonal Rc).

Sediment mass of each sample was measured after flocculation, filtration and oven dehydration of the water samples. We calculated suspended sediment concentration (SSC) by dividing suspended sediment mass by the surface runoff depth of the sample. The total weight of suspended sediment in the bucket (Sl) was derived from the multiplication of SSC of the sample by the total surface runoff depth in the bucket. We also cumulated suspended sediment, i.e., soil loss, over the whole rainy season (seasonal Sl).

We calculated the entering surface runoff (Run, $L \cdot m^{-1}$), entering sediment concentration (Con, $g \cdot L^{-1}$), and entering sediment (Sed, $g \cdot m^{-1}$) into each land use. Run, Con, and Sed mean surface runoff, suspended sediment concentration, and suspended sediment, respectively, coming from the upslope and entering the land use we focus TE analyses. We calculated seasonal Run and seasonal Sed by summing up Run and Sed, respectively, of all the 19 events. Seasonal Con was calculated by dividing the seasonal Sed by seasonal Run.

For the Gerlach traps, TE (dimensionless) was calculated for surface runoff water volumes (WTE, dimensionless), for suspended sediment concentration (SCTE, dimensionless), and for sediment load (STE, dimensionless) as the portion of inflow trapped between the upper and the lower rim (McKergow et al., 2004), following **Eq. 5.1**:

$$TE = \frac{(X_{in} - X_{out})}{X_{in}} \qquad \textbf{Eq. 5.1}$$

where X_{in} is the surface runoff in litre per linear metre of contour line ($L \cdot m^{-1}$) for WTE, the average SSC ($g \cdot L^{-1}$) for SCTE, or the mass of suspended sediment in gram per linear metre of contour line ($g \cdot m^{-1}$) for STE of the upper Gerlach trap (inflow), and X_{out} is the SR for WTE, the average SSC for SCTE, or the mass of suspended sediment for STE of the lower Gerlach trap (outflow).

We calculated WTE, SCTE, and STE for each length of buffer as following: T-GT of 3-m buffer, GT-G of 3-m buffer, T-G of 6-m buffer, Tu-Tm of 3-m buffer, Tm-Td of 3-m buffer, and Tu-Td of 6-m buffer. We calculated WTE, SCTE, and STE for both event and seasonal scale.

5.2.3. *Statistical analysis and modelling*

To classify rainfall events, we first calculated the return periods of rainfall with the maximum daily rainfall from 2001 to 2019 which followed a lognormal distribution, the best fitted model compared with Pearson type 3 and GEV distributions (**Supporting Figure 5-2**). We then classified the 20 significant 24_R into 4 categories based on the calculated return periods (1.005, 1.111, and 2 years): small (S), medium (M), large (L), and extreme (E) daily rainfalls.

We performed non-parametric Wilcoxon tests (R version 3.5.3) to compare the distribution between paired-groups of the three land uses (TNU, GWT and GNT) for SR, SSC, and Rc measured using microplots, and for surface runoff and soil loss measured using the Gerlach traps. In order to check that TE was significantly greater than zero, we performed Wilcoxon signed-rank test. In the same way, in order to check the effect of the buffer length on TE, Wilcoxon rank sum test was performed to evaluate if TE of a 6-m buffer is greater than TE of a 3-m buffer. Wilcoxon test was performed on seasonal TE, TE of all events combined, and TE of individual events.

We conducted a correlation analysis between the measured variables, namely seasonal Rc, seasonal Sl, and soil surface features expressed in areal percentage. We calculated Spearman's rank correlation coefficients and significance levels by using XLSTAT version 20.4.1 (Addinsoft, 2021) between the variables measured at the microplot scale (**Table 5.2**) and at the Gerlach trap scale including trapping efficiencies (**Table 5.5**).

Patin et al. (2018) adjusted the model developed by Van Dijk and Bruijnzeel (2004) and Van Dijk et al. (2003) to estimate soil loss on an annual scale in **Eq. 5.2**:

$$\ln(Sl) = \ln(D) + a \cdot \ln(KE \cdot Rc) - b \cdot Gra - c \cdot Res \qquad \textbf{Eq. 5.2}$$

where D is the effective soil detachability ($g \cdot J^{-1}$), KE is the rainfall kinetic energy ($J \cdot m^{-2}$), Rc is the runoff coefficient (%), Gra is the areal percentage of grass (%), Res is the areal percentage of residues (%), a is the coefficient of ln(KE·Rc), and b and c are the decay coefficients of Gra and Res, respectively. In this study, the model was adapted to the riparian zone situation. We applied this method to our dataset by recalculating coefficients, to build a new model on the event scale using the Sl values of the 20 events. To build the model, we used the linear regression method to calculate the value of ln(D), a, b, and c.

We employed Partial Least Square Regression (PLSR) (Abdi, 2010) method by using XLSTAT version 20.4.1 (Addinsoft, 2021) to model seasonal WTE, SCTE, and STE depending on rainfall characteristics (seasonal rainfall: Rain; and KE), soil surface features (Fa, Tc, Sc, Ec, Gc, Cha, Res, Wor, Alg, Mos, Ped, and Gra), seasonal Rc, entering surface runoff (Run), entering sediment concentration (Con), and topographical conditions such as slope (slope), rugosity (Rugo), and length of buffer (Length).

5.3. RESULTS

5.3.1. *Rainfall, rainfall kinetic energy, and erosivity*

The 2014 rainfall amount was 1 366 mm, of which 863 mm (63% of the annual rainfall) occurred during the sampling period.

24_R exceeded 30 $mm \cdot d^{-1}$ for eight major events and Sign_R surpassed 30 $mm \cdot d^{-1}$ for six major events. Acc_R surpassed 50 $mm \cdot d^{-1}$ for six major events. Eight major events had I30 greater than 20 $mm \cdot h^{-1}$ (**Table 5.1**). KEo exceeded 400 $J \cdot m^{-2}$ for seven major events. KEt exceeded 400 $J \cdot m^{-2}$ for ten major events. EI30 exceeded 100 $MJ \cdot mm \cdot ha^{-1} \cdot h^{-1}$ for seven and nine major events under open space with grass and under teak trees, respectively. The highest observed 24_R (189.4 mm) classified as extreme is the only centennial occurrence. The other 24_R have not reached the 2-year return period as thirteen (events 1, 2, 3, 7, 9, 10, 11, 12, 13, 14, 16, 17, and 20) and six (events 4, 5, 6, 8, 15, and 18) major events were classified as small and medium, respectively. The medium class is consistent with seven major events (events 4, 5, 6, 8, 15, 18, and 19) whose intensity were higher than 50 $mm \cdot h^{-1}$ (**Figure 5.3**).

Table 5.1: Rainfall characteristics during the sampling period, from 6 July to 22 September 2014, in Houay Pano catchment. Sig_Date: date during which significant rainfall (rainfall triggering the sampling) happened; 24_R: 24-hour rainfall (rainfall within 24 hour prior to the sampling); Sign_R: significant rainfall triggering sampling; Acc_R: accumulated rainfall between two samplings; KEo: rainfall kinetic energy for open space with grass for a single significant event; KEt: rainfall kinetic energy for teak trees for a single significant event; I30: maximum 30-min rainfall intensity; EI30_o: erosivity index for open space with grass; EI30_t: erosivity index for teak trees. Rainfall event classes are ranked based on the return period of the daily rainfall. Rainfall event were classified as small (S), medium (M), large (L), and extreme (E) daily rainfall (24_R).

Event	Class	Sig_Date	24_R (mm)	Sign_R (mm)	Acc_R (mm)	KEo ($J \cdot m^{-2}$)	KEt ($J \cdot m^{-2}$)	I30 ($mm \cdot h^{-1}$)	EI30_o ($MJ \cdot mm \cdot ha^{-1} \cdot h^{-1}$)	EI30_t ($MJ \cdot mm \cdot ha^{-1} \cdot h^{-1}$)
1	S	7/6/2014	14	9.4	14	139.0	294.9	16	22.2	47.2
2	S	7/8/2014	15	11.4	15	158.7	349.1	12	19.0	41.9
3	S	7/13/2014	18.8	9.2	30	169.8	291.8	17.6	29.9	51.4
4	M	7/19/2014	39.8	30.8	50	641.4	982.6	52	333.5	510.9
5	M	7/23/2014	46.4	42.8	62	835.0	1341.6	56.8	474.3	762.0
6	M	7/25/2014	46.8	46.6	50	897.8	1532.5	39.2	351.9	600.7
7	S	7/27/2014	24.2	14.4	21.8	172.7	385.0	10	17.3	38.5
8	M	7/30/2014	36.2	34	39	631.2	1104.5	43.2	272.7	477.2
9	S	8/2/2014	19.2	13.2	19.2	164.1	350.4	12.4	20.3	43.5
10	S	8/6/2014	12.8	6.6	37.8	90.9	191.6	10.4	9.5	19.9
11	S	8/7/2014	17.2	7.4	17.4	129.8	231.6	12.8	16.6	29.6
12	S	8/15/2014	28.2	8.2	46.8	132.6	263.4	16	21.2	42.1
13	S	8/16/2014	23.4	10.4	16	171.0	334.1	19.6	33.5	65.5
14	S	8/20/2014	30	30	30.2	389.3	821.1	18	70.1	147.8
15	M	8/29/2014	46.8	22.4	64.2	482.0	735.8	43.2	208.2	317.9
16	S	9/5/2014	22.6	21	43	325.7	651.8	25.6	83.4	166.9
17	S	9/6/2014	10.2	8.6	14	151.7	269.7	16	28.1	51.6
18	M	9/14/2014	49.2	49	50.4	506.0	780.0	46.4	234.8	361.9
19	E	9/17/2014	189.4	182.8	192.6	3800.3	5904.9	88.4	3359.4	5220.0
20	S	9/22/2014	26.2	26.2	49.4	309.4	680.9	15.6	30.9	68.1

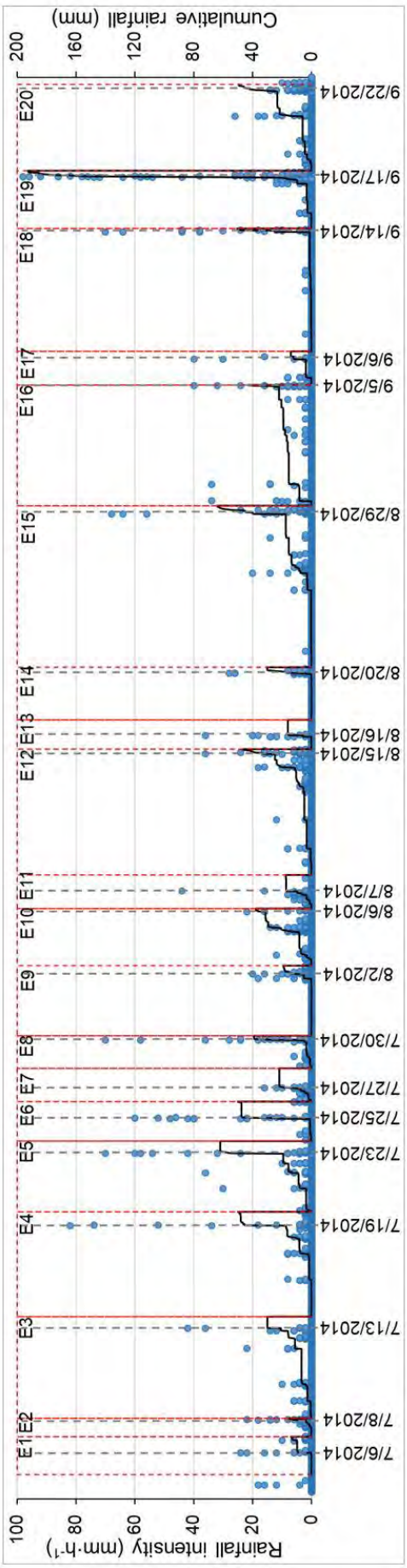

Figure 5.3: Rainfall intensity ($mm \cdot h^{-1}$) and cumulative rainfall (mm) for 20 samplings. Each blue dotted line refers to each significant rainfall event that triggered the sampling. Each dotted red rectangle represents rainfalls between each sampling. E: event that triggered the sampling.

5.3.2. *Surface runoff and soil loss observations using microplots*

The average height of pedestal features varied from 0.5 cm in GNT to 4 cm in TNU. The areal percentage of pedestal features was 73% in TNU, 0.5% in GNT, and 8% in GWT (**Supporting Figure 5-1a**).

Supporting Figure 5-1c represents the percentage area of total crust (sum of the erosion, structural, and gravel crusts), free aggregates, free gravel, charcoals, and residues in each land use. Soil surface feature shows similar patterns in GNT and GWT, such as total crust (2%), free aggregates (40 – 50%), and residues (47 – 56%). By contrast, in TNU total crust was 90%, free aggregates were 6% and residues were 4%. Structural crust accounts for 100% of the total crust in GNT and GWT and for 81% in TNU.

Figure 5.4 exhibits the relationship between seasonal Rc and seasonal Sl on log scale during the rainy season in 2014 for all the replicates in each land use. Average seasonal Rc over the period of the experiment was about 13% in GWT and 19% in GNT, and 55% in TNU. Average seasonal Sl was 159 g·m^{-2} in GNT, 250 g·m^{-2} in GWT, and 5 791 g·m^{-2} in TNU, with an average of 2067 g·m^{-2} in all land uses.

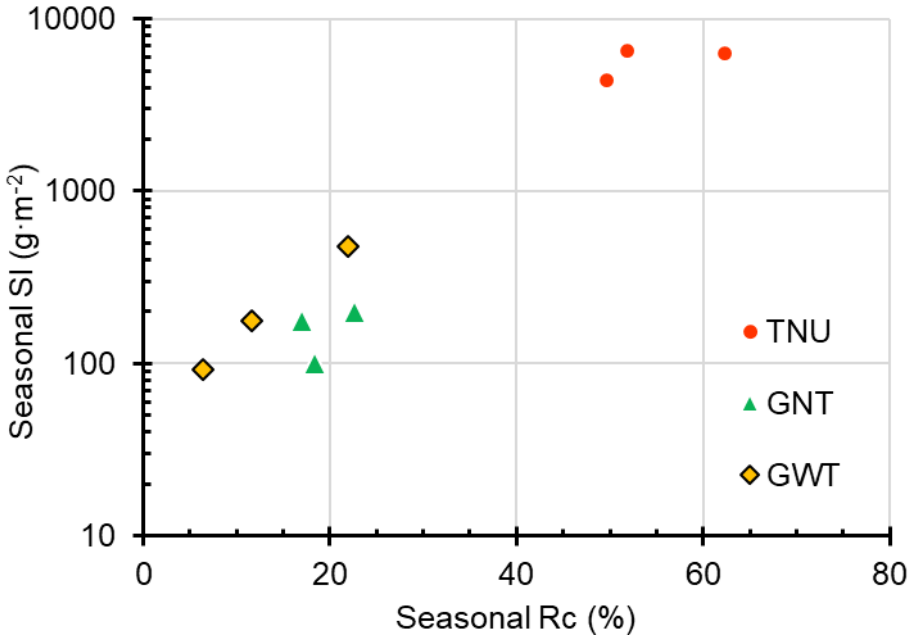

Figure 5.4: Microplots: seasonal runoff coefficient (seasonal Rc, %) and seasonal soil loss (seasonal Sl, g·m^{-2}, logarithmic scale) from 6 July to 22 September 2014, for the three land uses with 3 replicates in Houay Pano catchment, northern Lao PDR. TNU: teak with no understory; GNT: grass nearby teak trees; GWT: grass with a few teaks planted inside. Runoff coefficient is the ratio in percentage between total surface runoff depth and total rainfall depth.

The Wilcoxon test applied to SR revealed two significantly different (p-value > 0.05) categories of land use (**Figure 5.5**): the least erosive (GNT and GWT) and the highly erosive land use (TNU). The Wilcoxon test applied to the average SSC provided three categories of land use: the least erosive (GNT), the moderately erosive (GWT), and the highly erosive (TNU). The Wilcoxon test applied to Rc provided three categories of land uses: the least erosive (GWT), the moderately erosive (GNT), and the highly erosive (TNU).

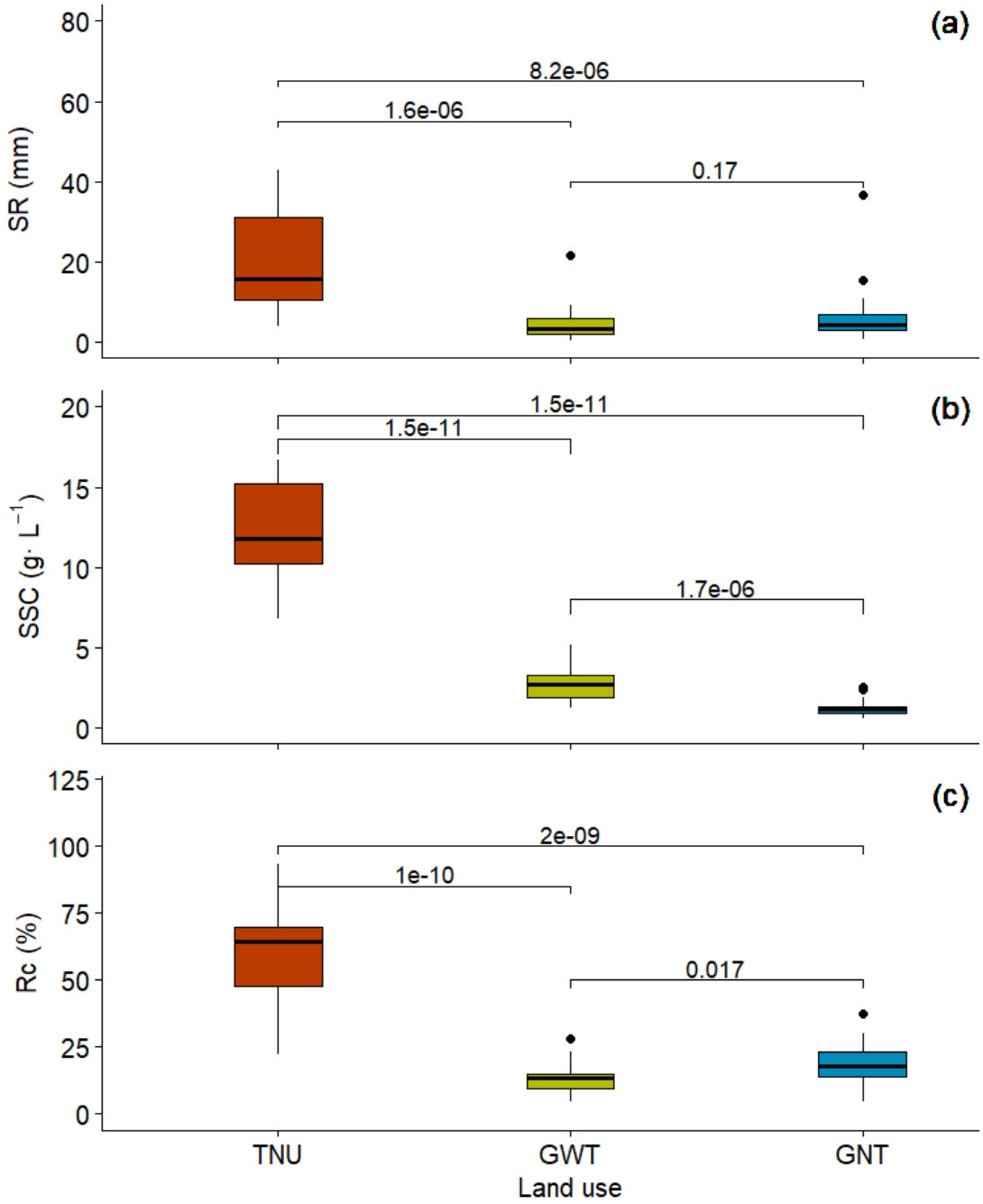

Figure 5.5: Microplots: boxplots of (a) surface runoff (SR, mm), (b) suspended sediment concentration (SSC, g·L^{-1}), and (c) runoff coefficient (Rc, %) for individual events and each land use from 6 July to 22 September 2014, with p-value of Wilcoxon test between two groups

of land uses in Houay Pano catchment, northern Lao PDR. TNU: teak with no understory; GNT: grass nearby teak trees; GWT: grass with a few teaks planted inside. Each boxplot contains the extreme of the lower whisker (vertical line), the lower hinge (thin line), the median (bold line), the upper hinge (thin line), the extreme of the upper whisker (vertical line), and the outliers (black dots) with *p*-value of Wilcoxon test between two groups of land uses. The whiskers extend to the most extreme data point which is no more than 1.5 times the interquartile range from the box. Runoff coefficient is the ratio in percentage between total surface runoff depth and total rainfall depth.

Supporting Figure 5-3 illustrates the cumulative SR and cumulative Sl in relation to cumulative rainfall between 6 July to 22 September 2014, for the three land uses in microplots. Cumulative SR was the highest in TNU (415 mm), which also showed the highest cumulative Sl (5791 $g \cdot m^{-2}$). The cumulative SR in TNU is 3 and 4.5 times higher than in GNT and GWT, respectively. The cumulative Sl in TNU is 36 and 23 times higher than in GNT and GWT. TNU had the sharpest rise of Sl among all the land uses. Mean Rc for TNU, GNT, and GWT were 55%, 19%, and 13%, respectively.

Table 5.2 shows the relationship between Rc, Sl, and soil surface features areal percentages. Ec, Gc, Res, and Wor show correlation with Rc with the absolute Spearman's rank correlation coefficients (r) above 0.83 (*p*-value < 0.05). Res and Wor exhibited a negative correlation with Rc with r equal to -0.88 and -0.83, respectively (*p*-value < 0.05). Areal percentage of Ec, and Gc had a positive correlation with Rc (r = 0.84; *p*-value < 0.05). Sl had a positive correlation with Rc (r = 0.92; *p*-value < 0.05). Soil surface features were correlated between them except for Fg, Alg and Mos. Even though Gra doesn't show correlations with Rc (r = -0.55, *p*-value > 0.05), it was negatively correlated with Sl, Fa, Tc, Sc, Ec, Gc and Ped (r = -0.73, 0.79, -0.86, -0.77, -0.75, -0.75, -0.95, respectively; *p*-value < 0.05).

Table 5.2: Spearman's rank correlation coefficients between variables observed on microplots, namely: seasonal runoff coefficient (Rc), seasonal soil loss (Sl), and areal percentages of soil surface features: Fa: free aggregates; Fg: free gravel; Tc: total crust; Sc: structural crust; Ec: erosion crust; Gc: gravel crust; Cha: charcoals; Res: residues; Wor: worm casts; Alg: algae; Mos: mosses; Ped: pedestals; Gra: grass. All variables were measured in 2014 in Houay Pano catchment, northern Lao PDR.

Variables	Rc	Sl	Fa	Fg	Tc	Sc	Ec	Gc	Cha	Res	Wor	Alg	Mos	Ped
Sl	**0.92 ***													
Fa	-0.50	-0.66												
Fg	0.35	0.44	-0.61											
Tc	0.61	**0.80 ***	**-0.96 ***	0.66										
Sc	0.56	**0.75 ***	**-0.94 ***	0.50	**0.95 ***									
Ec	**0.84 ***	**0.82 ***	**-0.81 ***	0.48	**0.83 ***	**0.77 ***								
Gc	**0.84 ***	**0.82 ***	**-0.81 ***	0.48	**0.83 ***	**0.77 ***	**1.00 ***							
Cha	0.50	0.59	-0.65	0.01	0.60	**0.74 ***	0.60	0.60						
Res	**-0.88 ***	**-0.74 ***	0.40	-0.12	-0.46	-0.41	**-0.84 ***	**-0.84 ***	-0.55					
Wor	**-0.83 ***	**-0.85 ***	0.66	-0.24	-0.68	-0.68	**-0.78 ***	**-0.78 ***	**-0.71 ***	**0.72 ***				
Alg	-0.27	-0.07	0.30	-0.37	-0.14	-0.14	-0.37	-0.37	-0.28	0.32	0.37			
Mos	0.17	0.04	-0.39	-0.13	0.26	0.36	0.53	0.53	0.37	-0.40	-0.20	-0.30		
Ped	0.60	**0.73 ***	**-0.85 ***	0.35	**0.88 ***	**0.83 ***	**0.85 ***	**0.85 ***	0.50	-0.54	**-0.69 ***	0.02	0.48	
Gra	-0.55	**-0.73 ***	**0.79 ***	-0.33	**-0.86 ***	**-0.77 ***	**-0.75 ***	**-0.75 ***	-0.48	0.49	0.58	-0.23	-0.30	**-0.95 ***

Significance: * p-value < 0.05

Figure 5.6 shows the observed and the modelled soil loss on the event scale. The equation of soil loss is given in **Eq. 5.3**:

$$\ln(Sl) = -4.39 + 0.91 \cdot \ln(KE \cdot Rc) - 2.47 \cdot 10^{-2} \cdot Gra - 2.29 \cdot 10^{-2} \cdot Res \qquad \textbf{Eq. 5.3}$$

where Sl is the soil loss ($g \cdot m^{-2}$), KE is the rainfall kinetic energy ($J \cdot m^{-2}$), Rc is the runoff coefficient (%), Gra is the areal percentage of grass (%), and Res is the areal percentage of residue (%).

The model performance was $R^2 = 0.91$ for calibration and 0.92 for validation (p-value < 0.05).

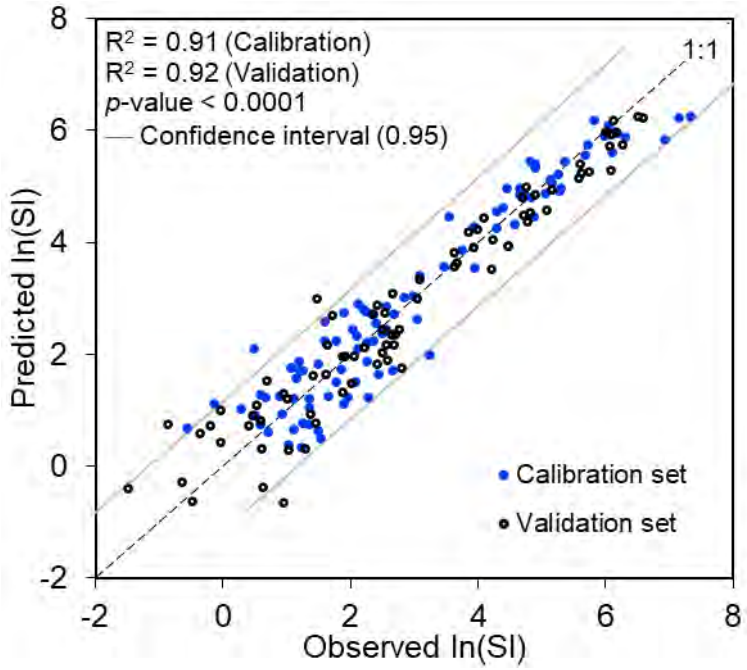

Figure 5.6: Microplots: observed and predicted soil loss (Sl, $g \cdot m^{-2}$) from 6 July to 22 September 2014, in Houay Pano catchment, northern Lao PDR. Each point represents the 20 samplings of soil loss of the 9 microplots.

5.3.3. *Water and sediment movement observations using Gerlach traps*

Surface runoff and soil loss exiting each land use for individual rainfall events were significantly higher in Tm and Td (3 to 22 and 7 to 675 times for surface runoff and soil loss, respectively) than in Tu, T, GT, and G (**Supporting Figure 5-4**). Wilcoxon test showed that the two groups of Tm and Td were not significantly different (p-value > 0.05) for both surface runoff and soil loss while the other land use pairings for soil loss were significantly different (

Supporting Table 5-1). However, T, GT, and Tu generated similar surface runoff (*p*-value > 0.05). Surface runoff and soil loss increased downhill from Tu to Tm and to Td while, in contrast, decreased from T to GT and T.

G released the least surface runoff and soil loss among the 6 land uses (**Figure 5.7**) over the rainy season. Td and Tm generated the highest surface runoff and soil loss followed by Tu, T, and GT.

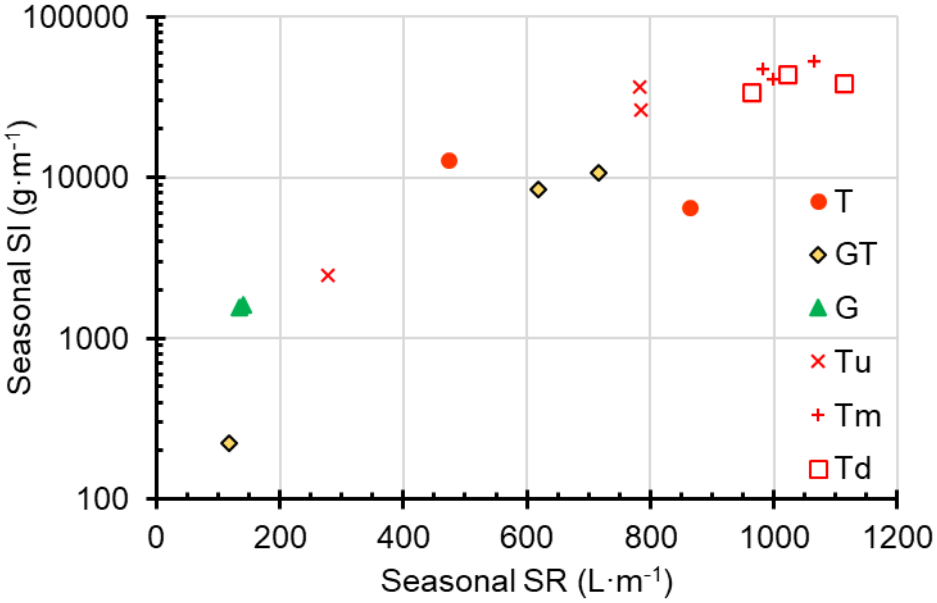

Figure 5.7: Gerlach traps: seasonal surface runoff (seasonal SR, $L \cdot m^{-1}$) and seasonal soil loss (seasonal Sl, $g \cdot m^{-1}$, logarithmic scale) from 8 July to 22 September 2014, for the 6 land uses with 3 replicates in Houay Pano catchment, northern Lao PDR. T: teak with no understory; GT: grass with teak; G: grass; Tu: teak with no understory (up); Tm: teak with no understory (middle); Td: teak with no understory (down).

Figure 5.8 shows seasonal WTE, SCTE, and STE (calculated using seasonal SR, average SSC, and seasonal Sl, respectively) for each length of buffer: 3 and 6 m (T-GT of 3-m buffer, GT-G of 3-m buffer, and T-G of 6-m buffer). T-G and G-GT showed the highest and positive WTE and STE. WTE and STE of T-GT were the lower than those of T-G and G-GT. SCTE showed similar value for each buffer length: T-GT, G-GT, and T-G. **Supporting Figure 5-5** shows WTE, SCTE, and STE (calculated using seasonal SR, average SSC, seasonal Sl, respectively) for each length of buffer: 3 and 6 m (Tu-Tm of 3-m buffer, Tm-Td of 3-m buffer, and Tu-Td of 6-m buffer). WTE, SCTE, and STE were almost the same for each buffer length: Tu-Tm, Tm-Td, and Tu-Td.

Table 5.3 provides the *p*-values of the Wilcoxon signed-rank test between trapping efficiencies (WTE, SCTE, and STE of T-G and T-GT) and the theoretical median of zero for the seasonal (using seasonal SR, average SSC, seasonal Sl, respectively), all events (combination of events), and each event. The *p*-values less than 0.05 mean that trapping efficiency is significantly positive. The seasonal was significantly positive in WTE and STE for T-G, but no significance was found for T-GT. For all events combined, WTE, SCTE, and STE were higher than zero for both T-GT and T-G (*p*-value < 0.05). On the event scale, most of the events yielded positive WTE, SCTE, and STE, especially for T-G. However, WTE, SCTE, and STE for T-GT were negative in half of the events. We observed more positive SCTE and STE in T-G than in T-GT.

Supporting Table 5-2 provides the results of the same test of GT-G, Tu-Tm, Tm-Td, and Tu-Td. WTE of GT-G was significantly positive. WTE, SCTE, and STE of GT-G were significantly positive in all events combined and in some individual events. Tu-Td, Tu-Tm, and Tm-Td provided significantly positive WTE, SCTE, and TE in few events.

Based on the *p*-value of rank sum test (upper-tailed test), WTE, SCTE and STE of T-G was significantly greater than those of T-GT in most of the events and in the all events (**Table 5.4**). For the accumulation, WTE of T-G was significantly greater than of T-GT. WTE, SCTE, and STE of Tu-Td were not significantly greater than those of Tu-Tm (**Supporting Table 5-3**).

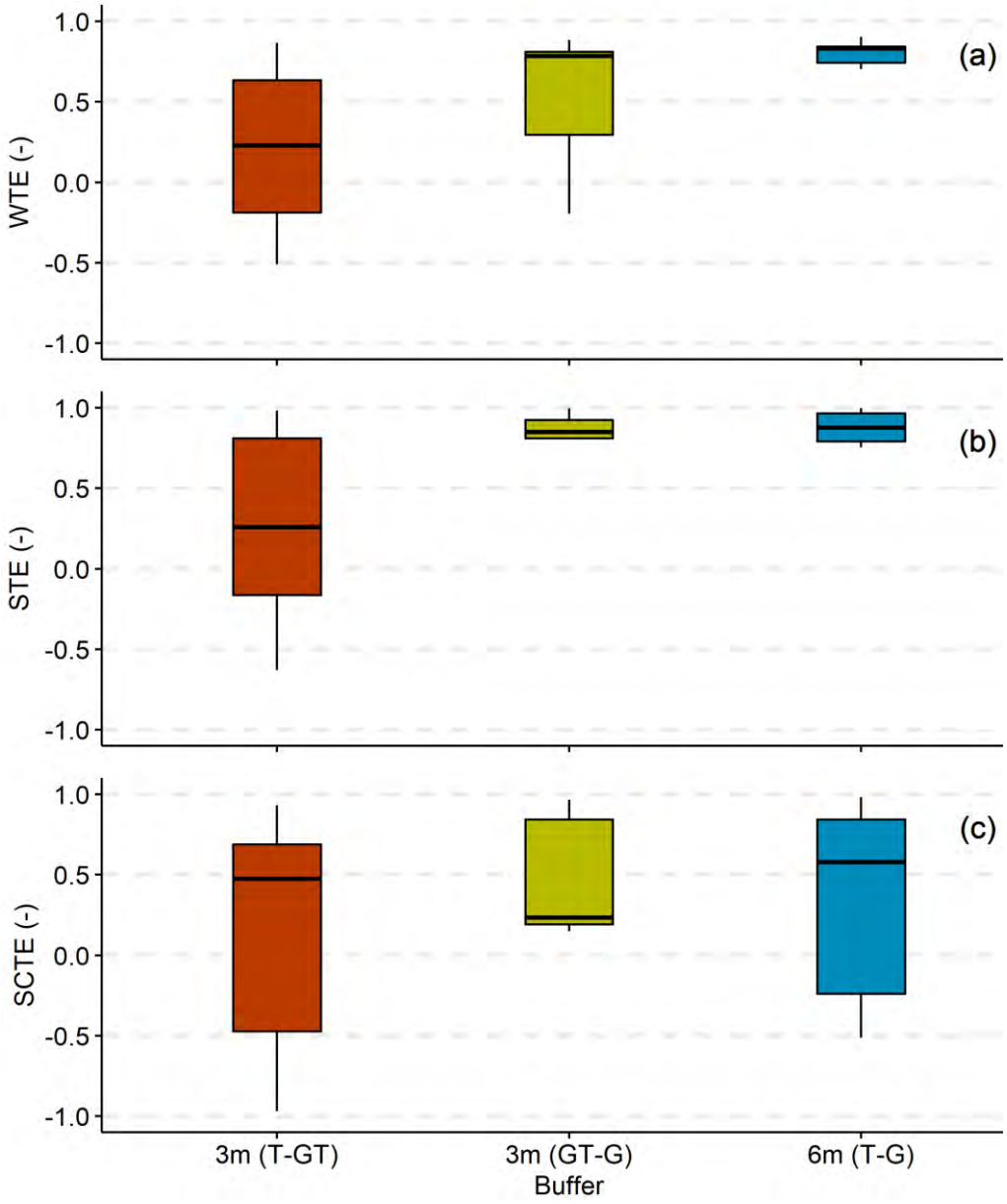

Figure 5.8: Gerlach traps: (a) water trapping efficiency (WTE), (b) sediment trapping efficiency (STE), and (c) suspended sediment concentration efficiency (SCTE) for each length of buffer and accumulation in 2014, Houay Pano catchment, northern Lao PDR from 8 July to 22 September 2014. T: teak with no understory; GT: grass with teak; and G: grass.

Table 5.3: *p*-value of Wilcoxon signed-rank test to accept the alternative hypothesis: median is greater than the theoretical median of zero. Sig_Date: date during which significant rainfall (rainfall triggering the sampling) happened; T: teak with no understory; and GT: grass with teak; G: grass; WTE: water trapping efficiency; SCTE: sediment concentration trapping efficiency; and STE: sediment trapping efficiency. Seasonal refers to calculations using seasonal surface runoff, seasonal sediment concentration, and seasonal soil loss, which were measured in Houay Pano catchment, northern Lao PDR from 8 July to 22 September 2014.

	Sig_Date	T-G (6m)			T-GT (3m)		
		WTE	**SCTE**	**STE**	**WTE**	**SCTE**	**STE**
Seasonal		**0.016**	0.078	**0.016**	0.281	0.500	0.219
All events		**<0.0001**	**<0.0001**	**<0.0001**	**<0.0001**	**<0.0001**	**<0.0001**
2	7/8/2014	**0.016**	0.078	**0.016**	0.063	0.813	0.063
3	7/13/2014	**0.016**	**0.016**	**0.016**	**0.016**	0.656	**0.016**
4	7/19/2014	**0.016**	**0.016**	**0.016**	**0.016**	**0.016**	**0.016**
5	7/23/2014	**0.016**	**0.016**	**0.016**	**0.016**	**0.016**	**0.016**
6	7/25/2014	**0.016**	**0.016**	**0.016**	0.578	0.281	0.578
7	7/27/2014	0.078	**0.018**	**0.016**	0.578	**0.016**	**0.016**
8	7/30/2014	**0.016**	**0.016**	**0.016**	0.500	0.500	0.422
9	8/2/2014	**0.016**	**0.016**	**0.016**	**0.016**	0.078	**0.016**
10	8/6/2014	**0.030**	0.281	**0.031**	0.656	**0.016**	**0.016**
11	8/7/2014	**0.016**	**0.016**	**0.018**	**0.031**	**0.047**	**0.031**
12	8/15/2014	**0.016**	**0.016**	**0.016**	0.156	**0.016**	**0.016**
13	8/16/2014	**0.016**	0.281	**0.016**	0.281	0.078	0.219
14	8/20/2014	**0.016**	**0.016**	**0.016**	**0.016**	0.156	**0.031**
15	8/29/2014	**0.016**	0.264	**0.016**	**0.016**	0.078	**0.047**
16	9/5/2014	0.125	0.125	0.125	0.250	0.750	0.625
17	9/6/2014	**0.016**	**0.016**	**0.016**	0.719	**0.016**	0.281
18	9/14/2014	0.125	0.125	0.125	0.625	0.750	0.625
19	9/17/2014	0.438	0.063	0.063	0.844	0.578	0.422
20	9/22/2014	0.422	0.578	0.578	0.781	**0.016**	0.578

Table 5.4: *p*-value of Wilcoxon rank sum test (upper-tailed test) to accept the alternative hypothesis: the medians of T-G (6m) is greater than the medians of T-GT (3m). Sig_Date: date during which significant rainfall (rainfall triggering the sampling) happened; T: teak with no understory; and GT: grass with teaks; G: grass; WTE: water trapping efficiency; SCTE: sediment concentration trapping efficiency; and STE: sediment trapping efficiency. Seasonal refers to calculations using seasonal surface runoff, seasonal sediment concentration, and seasonal soil loss, which were measured in Houay Pano catchment, northern Lao PDR from 8 July to 22 September 2014.

	Sig_Date	T-G (6m) vs T-GT (3m)		
		WTE	**SCTE**	**STE**
Seasonal		**0.047**	0.197	0.066
All events		**< 0.0001**	**< 0.0001**	**< 0.0001**
2	7/8/2014	0.967	**0.033**	0.057
3	7/13/2014	0.706	**0.001**	**0.001**
4	7/19/2014	0.155	**0.001**	**0.001**
5	7/23/2014	0.650	**0.013**	**0.013**
6	7/25/2014	**0.047**	**0.002**	**0.001**
7	7/27/2014	0.277	**0.002**	**0.001**
8	7/30/2014	**0.013**	**0.021**	**0.013**
9	8/2/2014	0.242	**0.001**	**0.008**
10	8/6/2014	0.090	0.706	0.242
11	8/7/2014	**0.032**	**0.002**	**0.002**
12	8/15/2014	0.090	**0.090**	**0.004**
13	8/16/2014	**0.047**	0.242	0.120
14	8/20/2014	**0.001**	**0.066**	**0.013**
15	8/29/2014	0.066	0.141	**0.047**
16	9/5/2014	0.350	**0.050**	0.100
17	9/6/2014	**0.032**	0.120	**0.032**
18	9/14/2014	0.100	0.200	0.200
19	9/17/2014	0.238	0.305	0.129
20	9/22/2014	0.350	0.706	0.409

The surface runoff and soil loss patterns matched the rainfall pattern (**Supporting Figure 5-6** and **Supporting Figure 5-7**). The highest medians of surface runoff of T, GT, and G were 84, 87, and 46 $L \cdot m^{-1}$, respectively, on 29 August, 30 July, and 17 September 2014, respectively. The highest medians of soil loss of T, GT, and G were 4033, 3993, and 753 $g \cdot m^{-1}$, respectively, in the extreme event of 17 September 2014. The highest median of surface runoff among Tm and Td (93 $L \cdot m^{-1}$ in Tm and Td) was observed on 17 August 2014 as the one of Tu (83 $L \cdot m^{-1}$) was on 5 September 2014. The highest median of soil loss among Tu and Tm (3219 and 8123

$g \cdot m^{-1}$, respectively) was observed in 19 July 2014 as the one of Td (6458 $g \cdot m^{-1}$) was observed in 25 July 2014.

Table 5.5 shows the relationship between trapping efficiencies, rainfall characteristics, topographical conditions, soil surface features and other related variables on the event scale.

WTE was positively correlated to SCTE, STE, Run, slope, Fa, Fg, Res, Wor, Alg, and Gra (Spearman's rank correlation coefficients $r > 0.23$, p-value < 0.05). WTE was negatively correlated to Rugo, Con, Rc, Tc, Sc, Ec, Gc, Cha, Mos, and Ped ($r < -0.46$, p-value < 0.05). SCTE was positively correlated to STE, slope, Fa, Fg, Fes, Wor, and Gra ($r > 0.3$, p-value < 0.05). SCTE was negatively correlated to Rugo, Con, Rc, Acc_KE, Tc, Sc, Ec, Gc, Cha, Mos, and Ped ($r < -0.22$, p-value < 0.05). STE was positively correlated to slope, Fa, Fg, Res, Wor, Alg, and Gra ($r > 0.26$, p-value < 0.05). STE was negatively correlated to Rugo, Con, Rc, Tc, Sc, Ec, Gc, Cha, Mos, and Ped ($r < -0.38$, p-value < 0.05).

Figure 5.9 shows PLSR biplot of correlation between WTE (a), SCTE (b), STE (c), rainfall characteristics, topographical condition and soil surface features, and their scores in the plot of variable importance in projection (VIP) contributing to the prediction of WTE (d), SCTE (e), and STE (f), and the models of WTE (g), SCTE (h), and STE (i). Considering axis t1, WTE ($r = 0.84$) was positively associated with Res ($r = 0.97$), Gra ($r = 0.91$), Wor ($r = 0.98$), and Fa ($r = 0.99$), but were negatively associated with Run ($r = -0.73$), Con ($r = -0.91$), Mos ($r = -0.99$), Ped ($r = -0.99$), Rugo ($r = -0.97$), soil crust (Tc, Sc, Ec, and Gc; $r = -0.99$), Cha ($r = -0.99$), KE ($r = -0.74$), and Rc ($r = -0.73$). Considering axis t2, WTE ($r = 0.48$) is positively associated with Rain ($r = 0.53$). These variables, except for KE, got scores above 1 in the VIP plot and were considered as important and the best predictors in the model of WTE ($R^2 = 0.99$). The other variables such as length of buffer, slope, Fg, and Alg had no significant relation to WTE.

SCTE ($r = 0.62$) was positively associated with Res ($r = 0.99$), Wor ($r = 0.99$), Fa ($r = 0.96$), and Gra ($r = 0.77$) along axis t1, and with Rain ($r = 0.92$) and Run ($r = 0.84$) along axis t2. SCTE was negatively associated with Rugo ($r = -0.99$), Ped ($r = -0.97$), soil crust ($r = -0.98$), Mos ($r = -0.93$), Cha ($r = -0.98$), Rc ($r = -0.88$), and Con ($r = -0.77$) along axis t1. The other variables had no significant relation with SCTE. However, Run, Rain, Con, Fg and Alg had scores greater than 1 in the VIP and are the best predictors of the model of SCTE ($R^2 = 0.94$). However, VIP scores of the rest of variables (Length of buffer: Length, KE, Slope, Rugo, Gra, Res, Wor, Ec, Gc, Cha, Tc, Sc, Mos, Ped, Fa, and Rc) were approximately equal to 8.

STE (r = 0.70) was positively associated with Res (r = 0.99), Gra (r = 0.86), Wor (r = 0.99), and Fa (r = 0.99) along axis t1, and with Rain (r = 0.97) along axis t2. STE was negatively associated with soil crust (r = -0.99), Cha (r = -0.99), Rc (r = -0.95), Mos (r = -0.98), Ped (r = -0.99), Rugo (r = -0.99), Run (r = -0.70), and Con (r = -0.89) along axis t1. According to VIP plot, Run, Rain, and Con, were the best predictors of the model of STE (R^2 = 0.96). VIP scores of the other variables excluding Length and Slope were greater than 0.8.

Table 5.5: Spearman's rank correlation coefficients between trapping efficiencies, rain characteristics, topography and soil surface features on the event scale. WTE: water trapping efficiency; SCTE: suspended sediment concentration trapping efficiency; STE: sediment trapping efficiency; Rugo: rugosity; Acc_R: accumulated rainfall between two samplings; 24_R: rainfall within 24 hours prior to the sampling; Sign_R: significant rainfall triggering sampling; Run: entering surface runoff; Con: entering sediment concentration; Length: length of buffer; Slope: slope of buffer; Rc: runoff coefficient; Acc_KE: accumulated rainfall kinetic energy; 24_KE: 24-hour rainfall kinetic energy prior to the sampling; Sign_KE: significant rainfall kinetic energy that rainfall triggered the sampling; Imax: maximum rainfall intensity; I30: maximum 30-min rainfall intensity; Fa: free aggregates; Fg: free gravel; Tc: total crust; Sc: structural crust; Ec: erosion crust; Gc: gravel crust; Cha: charcoals; Res: residues; Wor: worm casts; Alg: algae; Mos: mosses; Ped: pedestal; Gra: grass. All variables were measured in 2014 in Houay Pano catchment, northern Lao PDR.

Variables	WTE	SCTE	STE
SCTE	**0.42****		
STE	**0.80****	**0.83****	
Rugo	**-0.71****	**-0.58****	**-0.77****
Acc_R	0.06	-0.13	-0.03
24_R	0.07	-0.12	-0.02
Sign_R	0.10	-0.05	0.03
Run	**0.23***	-0.15	-0.01
Con	**-0.50****	**-0.25****	**-0.38****
Length	0.07	0.09	0.06
Slope	**0.34****	**0.31****	**0.33****
Rc	**-0.46****	**-0.35****	**-0.44****
Acc_KE	-0.01	**-0.22***	-0.13
24_KE	0.02	-0.15	-0.07
Sign_KE	0.01	-0.12	-0.05
Imax	0.14	-0.04	0.02
I30	0.17	-0.09	0.03
EI30	0.06	-0.15	-0.06
Fa	**0.72****	**0.61****	**0.73****

Fg	**0.32****	**0.30****	**0.31****
Tc	**-0.72****	**-0.61****	**-0.73****
Sc	**-0.72****	**-0.61****	**-0.73****
Ec	**-0.72****	**-0.60****	**-0.74****
Gc	**-0.72****	**-0.60****	**-0.74****
Cha	**-0.72****	**-0.60****	**-0.74****
Res	**0.65****	**0.53****	**0.68****
Wor	**0.65****	**0.53****	**0.68****
Alg	**0.23***	0.16	**0.26****
Mos	**-0.72****	**-0.61****	**-0.73****
Ped	**-0.72****	**-0.61****	**-0.73****
Gra	**0.72****	**0.61****	**0.73****

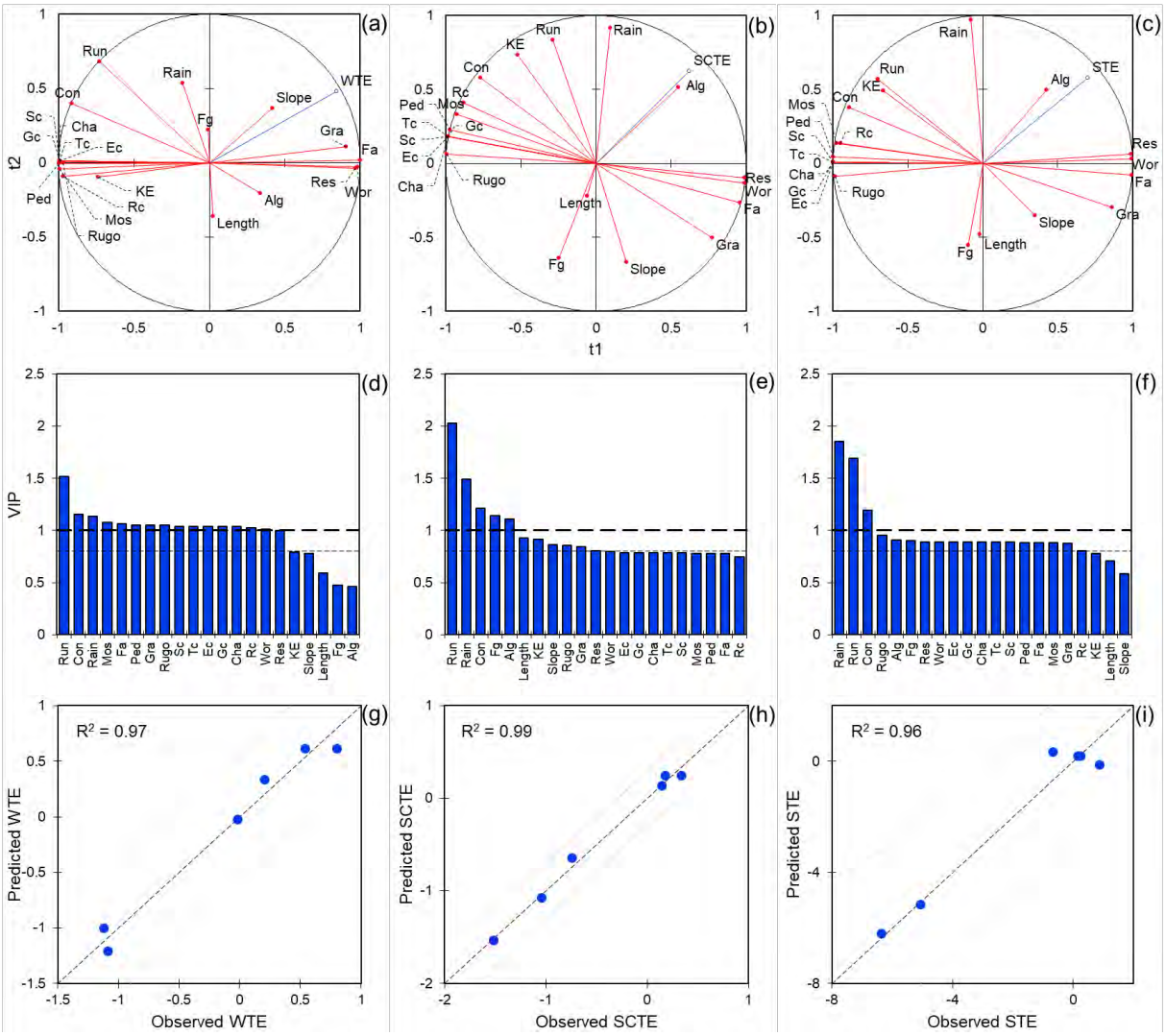

Figure 5.9: Partial least squares regression (PLSR) biplot for (a) seasonal water trapping efficiency (WTE), (b) seasonal suspended sediment concentration trapping efficiency (SCTE), and (c) seasonal sediment trapping efficiency (STE) in relation with rain characteristics,

topography and soil surface features. Variable importance in projection (VIP) score plot of each variable of (d) WTE, (e) SCTE, and (f) STE, which contributed the most to the models of (g) WTE, (h) SCTE and (i) STE, respectively. Rugo: rugosity; Rain: seasonal rainfall; Run: entering runoff; Con: entering sediment concentration; Length: length of buffer; Slope: slope of buffer; Rc: runoff coefficient; KE: rainfall kinetic energy; Fa: free aggregates; Fg: free gravel; Tc: total crust; Sc: structural crust; Ec: erosion crust; Gc: gravel crust; Cha: charcoals; Res: residues; Wor: worm casts; Alg: algae; Mos: mosses; Ped: pedestal; Gra: grass. All variables were measured in 2014 in Houay Pano catchment, northern Lao PDR.

5.4. DISCUSSION

5.4.1. *Riparian vegetation limits soil loss and surface runoff on the microplot scale*

Rain splash detaches and transports the soil particles, possibly lifting the loose particles along with the water flow (Valentin and Rajot, 2018), when the flow energy is sufficiently large to detach the soil particles from the bulk soil. However, riparian vegetation which acts as an umbrella may protect soil surface against this mechanism, hence limits surface runoff and soil loss.

Soil loss is strongly related to surface runoff ($r = 0.92$, p-value < 0.05) (**Figure 5.4** and **Figure 5.7**, and **Table 5.2**). Soil loss increased with increasing surface runoff, especially in teak with no understory. We found that soil loss was positively correlated with areal percentages of soil crust and pedestal ($r > 0.73$, p-value < 0.05), and was negatively correlated with areal percentages of residues, worm casts and grass ($r < -0.73$, p-value < 0.05). Areal percentage of soil crust in teak with no understory is higher than in grass nearby teak trees and grass with a few teaks planted inside (**Supporting Figure 5-1**): it causes more surface runoff and soil loss (Song et al., 2020) and restricts infiltration (Bu et al., 2014). Overall, these findings are in accordance with the findings reported by Song et al. (2020), Lacombe et al. (2018), and Patin et al. (2018), namely that soil loss increases with an increasing runoff coefficient proportionally predicted by soil crust, and soil loss is inversely proportional to areal percentages of residues and grass.

Surface runoff in grass nearby teak trees and grass with a few teaks planted inside were 3 and 4 times, respectively, less than in teak with no understory. Rain may be attenuated by grass cover and residues at the soil surface layer which act as barriers and allow more times for the rain infiltrating hence lead to less surface runoff. Nevertheless, the soil loss in grass nearby teak trees and grass with a few teaks planted inside were 36 and 23 times, respectively, less than in

teak with no understory. Hence, soil loss in teak tree plantation could be divided by 23 by leaving riparian grass under the teak tree plantation. This index is higher than the value found by Song et al. (2020) in teak tree plantation with the understory of broom grass that soil loss in teak tree plantation with broom grass was 14 times less than in teak tree plantation with bare soil. This is explained by the density of both teak trees and the understory. The density of riparian grass may be wider than the density of broom grass in the study of Song et al. (2020), i.e., riparian grass may be widely spread over a wide area and broom grass might have more bare space for soil detachment. However, the areal percentage of grass (18.5%) in grass nearby teak trees was almost one fourth less than the areal percentage (80%) in teak with broom grass of Song et al. (2020). Areal percentage (33%) and height (2.2 m) of teak trees in grass with a few teaks planted inside was low compared to the areal percentage (60%) and height (20 m) of teak trees in teak with broom grass of Song et al. (2020). Low areal percentage of teak trees causing less rainfall interception together with short teak trees lead to smaller rainfall kinetic energy generated by the throughfall from teak tree leaves, which causes the soil detachment (Lacombe et al., 2018). Rainfall kinetic energy under teak tree is high due to broad leaves of teak trees which accumulate the rain through interception which then produce larger raindrops. Soil loss in grass nearby teak trees is 3 times higher than soil loss in broom grass measured by Lacombe et al. (2018). Soil loss in grass nearby teak trees is 3 times less than soil loss in broom grass but equal to the soil loss in grass measured by Patin et al. (2018). Areal percentage of residues could explain that residues in grass nearby teak trees, broom grass of Lacombe et al. (2018), broom grass and grass of Patin et al. (2018) were 50, 81, 7, 61%, respectively. Teak with no understory (residues = 3%) generated soil loss 4 and 2 times higher than teak trees (residues = 40%) of Lacombe et al. (2018) and teak trees (residues = 26%) of Patin et al. (2018), respectively. Soil loss in teak with no understory (5791 $g \cdot m^{-2}$) is comparable to the soil loss in teak trees (5455 $g \cdot m^{-2}$) of Song et al. (2020) with the same value of residues.

We applied on the event scale the **Eq. 5.2**, and found that rainfall kinetic energy, runoff coefficient, areal percentages of grass, and residues, were also reliable predictors of the soil loss on the event scale (**Figure 5.6**). Our model coefficients are different from those of Patin et al. (2018), except for the coefficient of the product of rainfall kinetic energy with runoff coefficient which is equal, and close to 1. Coefficients of areal percentages of grass and residues (2.47×10^{-2} and 2.29×10^{-2}, respectively) in our study are smaller than in Patin et al. (2018) (1.00 and 0.65, respectively). However, the two variables are important for the efficiency of the model because the model was much improved by these two variables. The R^2 of our model and of Patin et al.

(2018) are 0.91 and 0.75, respectively. The difference may be explained by the fact that the model of Patin et al. (2018) included about thirty land uses and thirteen years of the experiments and our model used only 3 land uses and 20 events of a single year.

5.4.2. *Effectiveness of grass in trapping water and sediment*

Buffer of riparian grass forms a physical barrier that slows surface flow rates. The decrease in surface runoff reduces the energy, which makes suspended sediment in the surface runoff deposits. Then riparian grass mechanically traps sediment and debris. Roots maintain soil structure and physically restrain otherwise erodible soil. Flow rates are generally slower for sheet flow than for channelized flow. Therefore, where vegetation helps resist the formation of channels, water will flow more slowly, allowing more time for settling of sediments and infiltration (Castelle et al., 1994).

On the hillslope scale, teak tree plantation without riparian grass showed negative trapping efficiency of both surface runoff and sediment concentration, meaning that surface runoff and the mass of sediment exported increase downhill. Median water trapping efficiency and sediment concentration trapping efficiency were significantly greater than zero (p-value < 0.05) and were up to 0.86 and 0.88 for the 6 m of riparian grass buffer length, respectively. This positive trapping efficiency may be initially because of the increasing hydraulic roughness of the riparian grass filter which decelerates surface runoff and subsequently increases the infiltration rate (Borin et al., 2005; Deletic and Fletcher, 2006; Le Bissonnais et al., 2004). A study conducted by Vigiak et al. (2008) in 2005 and 2006 in the Houay Pano catchment showed that mean water trapping efficiency and sediment concentration trapping efficiency were 0.06 (p-value > 0.05) and -0.27, respectively, with riparian grass buffer length between 5 and 12 m. Our study showed higher mean water trapping efficiency and sediment concentration trapping efficiency of 0.69 and 0.58 (p-value), respectively. Receiving inflow from different uphill plantation may cause these high differences as trapping efficiency riparian grass of Vigiak et al. (2008) was the mean of three sites with different upslope land uses.

5.4.3. *Buffer length effectiveness on the hillslope*

Riparian grass buffer effectively trapped suspended sediment on the event scale (**Table 5.3**). Regarding the seasonal scale, there was only significant trapping efficiency for water trapping efficiency and sediment trapping efficiency of 6 m of buffer length. 3 m of buffer length was effective in trapping water and sediment for most of the small rainfall. 6 m of buffer length was effective in trapping water and sediment under medium class of rainfall. 6 m of buffer length

traps more surface runoff and sediment than 3 m of buffer length (**Table 5.4**). A range of buffer lengths from 3 to 200 m was found to be effective, depending on site-specific conditions (Castelle et al., 1994). The effectiveness of the grass in trapping water and sediment substantially varies with buffer lengths (Ziegler et al., 2006). However, in the context of Houay Pano catchment, the farmers may accept to leave the riparian buffer of less than 10 meters for their limit of cultivation due to the steep slope (63%). Hence, leaving 6 m of buffer length of riparian grass is suggested downhill in the teak tree plantation.

5.4.4. *Factors affecting trapping efficiency on the hillslope*

Our study revealed that trapping efficiency of riparian grass was associated with a meteorological factor (rainfall), physical factors (areal percentages of residues, grass, worm casts, free aggregates, mosses, pedestals, rugosity, soil crust, charcoals), and hydrological factor (entering surface runoff, entering sediment concentration, and runoff coefficient). On the seasonal scale, rain showed its positive association with trapping efficiency (**Figure 5.9**). This could be explained by the fact that larger rainfall led to more water and sediment trapped by each buffer and less rainfall led to less trapped water and sediment. On the event scale, based on Table 1 and 3, rain expressed the contrasting relation with trapping efficiency. On extreme and some medium events, trapping efficiency were not significant and even negative, especially for 3-m buffer length. Even during some small event, trapping efficiency could be insignificant. This can be explained by antecedent rainfall conditions, which lead to a higher soil moisture content, limit water infiltration, and increase surface runoff (Jadidoleslam et al., 2019), hence the trapping efficiency of e.g. event 20 could have been affected by the one of event 19. This reflects that entering surface runoff, entering sediment concentration, and runoff coefficient affect trapping efficiency. In section **5.4.3**, we highlighted the differences between the values of trapping efficiency of riparian grass in our study and in Vigiak et al. (2008): these differences implied that land use influences the trapping efficiency. Some factors are associated together, for instance, physical factors and hydrological factors. The other factors that may influence trapping efficiency are factors affecting hydrological factors. Those influencing factors are rainfall intensity, rainfall duration and time interval between rainfall events, and slope (Martíni et al., 2020). We found that slope was correlated with trapping efficiency ($r = 0.33$, p-value < 0.01). Maximum 30-min rainfall intensity, rainfall kinetic energy, and erosivity index showed the same patterns as rainfall for each event, meaning that these variables may also be considered as the controlling factors of trapping efficiency (**Table 5.1**). However, the trapping efficiencies were not correlated with maximum 30-min rainfall intensity, rainfall kinetic energy, erosivity

index, nor rainfall (**Table 5.5**), except that accumulated rainfall kinetic energy was negatively correlated with sediment concentration trapping efficiency (p-value < 0.05). Here, the combination of some small rainfall events together with the rainfall event that triggered the sampling could explain the lack of correlation. It is suggested to assess trapping efficiency for each single event to better characterize factors affecting trapping efficiency such as meteorological and hydrological conditions.

5.4.5. *Insight from the plot- and hillslope scales modelling approaches*

Our model on the plot scale confirmed the importance of rainfall kinetic energy, runoff coefficient, and areal percentages of grass and residues, in predicting soil loss on the event scale (**Figure 5.6**). High soil detachment could be alleviated by the conservation of grass and plant residues (from teak leaves and riparian grass) under the teak tree canopy. In contrast, rainfall kinetic energy and runoff coefficient are the factors enhancing the soil loss (Lacombe et al., 2018), while aggravated by soil crust generated on bare soil (Valentin and Rajot, 2018). Therefore, preventive measure by conserving grass under teak trees should be favoured.

On the hillslope scale, trapping efficiency was associated with factors hindering or aggravating soil erosion. The PLS regression model on seasonal scale revealed that water trapping efficiency, sediment concentration trapping efficiency, and sediment trapping efficiency had positive correlation with areal percentages of residues, grass, worm casts, free aggregates, and seasonal rainfall (**Figure 5.9**). The trapping efficiency had negative correlation with entering surface runoff, entering sediment concentration, runoff coefficient, and areal percentages of mosses, pedestals, rugosity, soil crust, and charcoals. Similar to the plot scale, the protecting factors at the hillslope scale such as residues and grass play an important role in trapping surface runoff and sediment, meaning reducing surface runoff and soil loss. However, at the hillslope scale, more aggravating factors engaged in the runoff and erosion process such as entering surface runoff and entering sediment concentration. This implies the engagement of upstream flux in the larger spatial scale. A similar finding of Vigiak et al. (2008) in Houay Pano catchment revealed that the trapping efficiency of the riparian grass depends on incoming flowrates. Rugosity reduced trapping efficiency in this study because it represents the pedestal features, which result from splash process during detachment (Song et al., 2020).

In terms of land use management, residues and grass at the soil surface are important in for trapping and reducing water and sediment exportation. It is suggested conserving grass cover in the teak tree plantations to limit upstream flux of water and sediment, hence increase the

trapping efficiency of the riparian buffer downstream. Applying the two management practices by conserving grass in teak tree plantation and in the riparian zone may mitigate soil erosion and its negative effects, even under heavy rainfall in the context of limited riparian buffers in Houay Pano catchment. Therefore, these erosion control measures would regulate water balance in the catchment and prevent soil and nutrient loss, water pollution, reservoir siltation, etc., for the environmental sustainability in the catchment.

5.5. CONCLUSIONS

We assessed the effect of riparian grass buffers on surface runoff, soil loss, sediment exportation, and water and sediment trapping efficiencies in the teak tree plantations of the mountainous region of northern Lao PDR. Our findings are:

- Keeping grass in the riparian zone limited surface runoff and reduced soil loss.
- Riparian grass effectively trapped surface runoff and sediment for buffer lengths less than 6 m but it is less effective for extreme rainfall (24-hour rainfall > 54.8 mm).
- Soil loss in teak tree plantations could be divided by 23 by leaving riparian grass.
- Soil loss is predicted by rainfall kinetic energy, runoff coefficient, areal percentage of grass and residues.

The study conducted at the plot scale (Song et al., 2020) in a teak tree plantation suggested that keeping the understory effectively reduced surface runoff and soil loss. To improve management practice in teak tree plantations in mountainous tropical areas, we provide in this study the additional suggestion of leaving riparian grass buffers of at least 6 m to capture soil loss originating from the uplands and to ensure the sustainability of the agricultural productivity and of the ecosystem at the hillslope scale. Riparian grass buffers may be more effective when integrated with a management practice that keeps understory in the teak tree plantation. Therefore, the understanding of riparian grass behaviour in soil trapping in a large scale is important to suggest countermeasures against soil degradation in the agricultural land. Further research is now needed to assess if riparian grass may play an important role in reducing surface runoff and soil loss on the catchment scale.

5.6. SUPPORTING MATERIALS

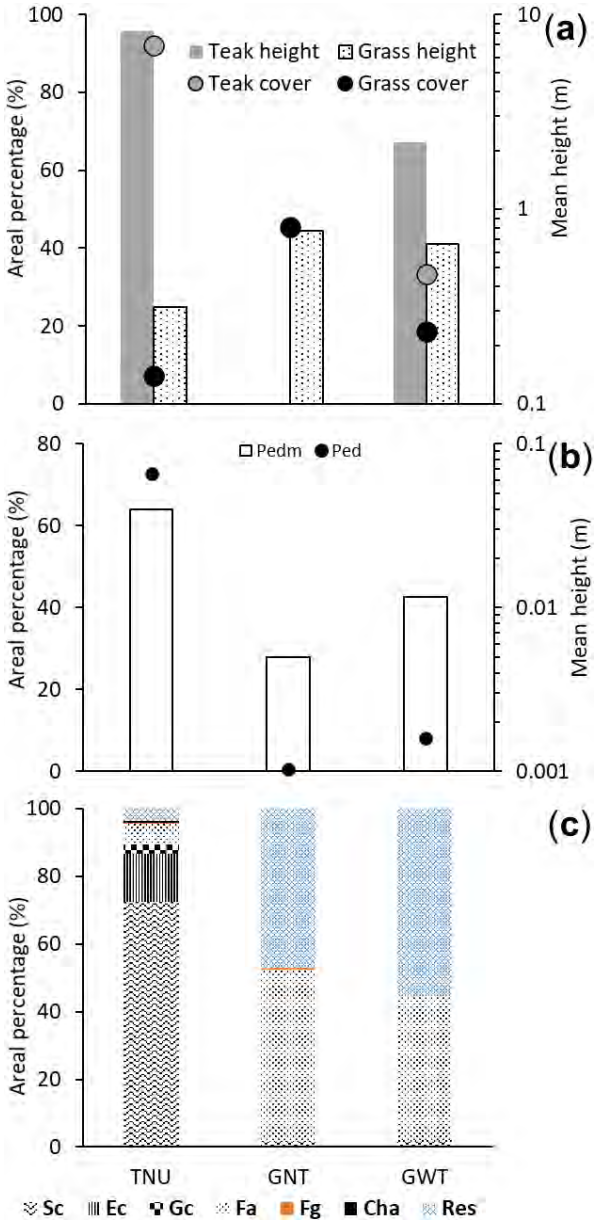

Supporting Figure 5-1: Microplots: (a) areal percentage (%) of teak trees and grass, and mean height (m) of teak trees and grass; (b) areal percentage of pedestal (Ped, %) and pedestal height (Pedm, m, logarithmic scale); (c) cumulative percentage areas (%) of the soil surface features. All the areal percentages were measured on 14 June and 27 August 2014, in Houay Pano catchment, northern Lao PDR. TNU: teak with no understory; GNT: grass nearby teak trees; GWT: grass with a few teaks planted inside; Ped: areal percentage of the pedestal; Pedm: pedestal height; Sc: structural crust; Ec: erosion crust; Gc: gravel crust; Fa: free aggregates; Fg: free gravel; Cha: charcoals; Res: residues.

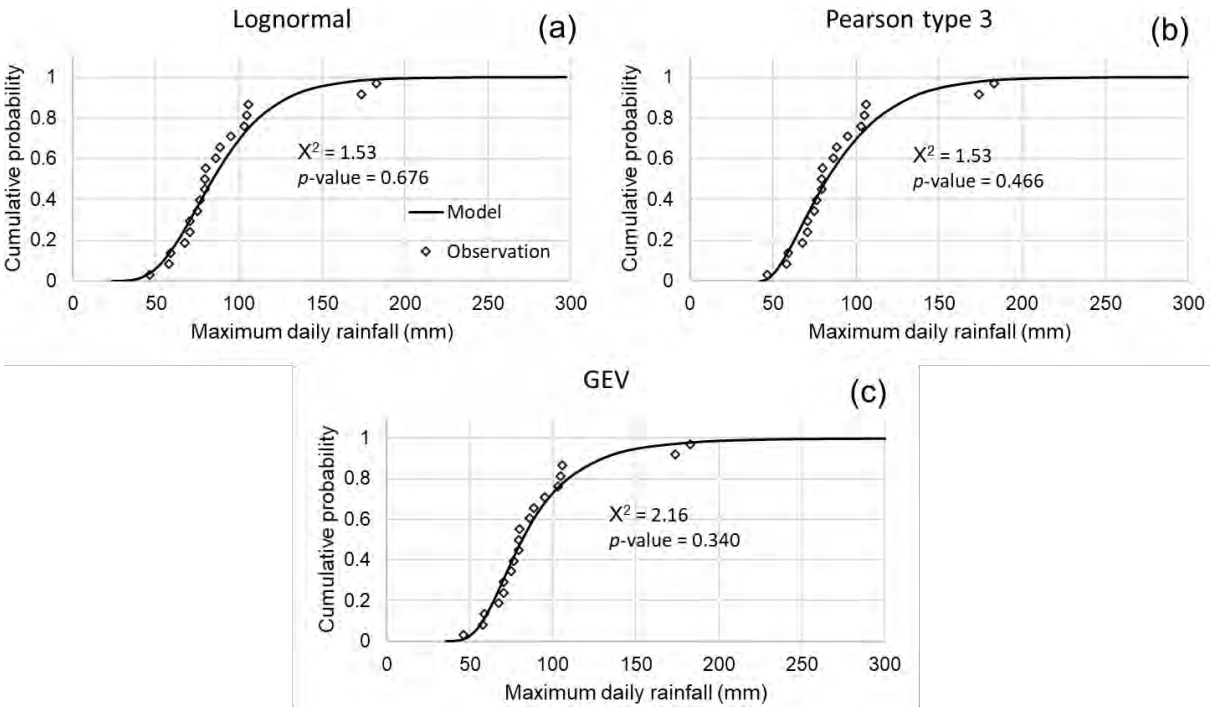

Supporting Figure 5-2: Observed maximum daily rainfall (mm) between 2001 and 2019 and different fitting model: (a) lognormal distribution, (b) Pearson type 3 distribution, and (c) GEV distribution. GEV: Generalized extreme value; X2: Chi-squared value (lower value represents better fitness); and higher p-value indicated better fitness.

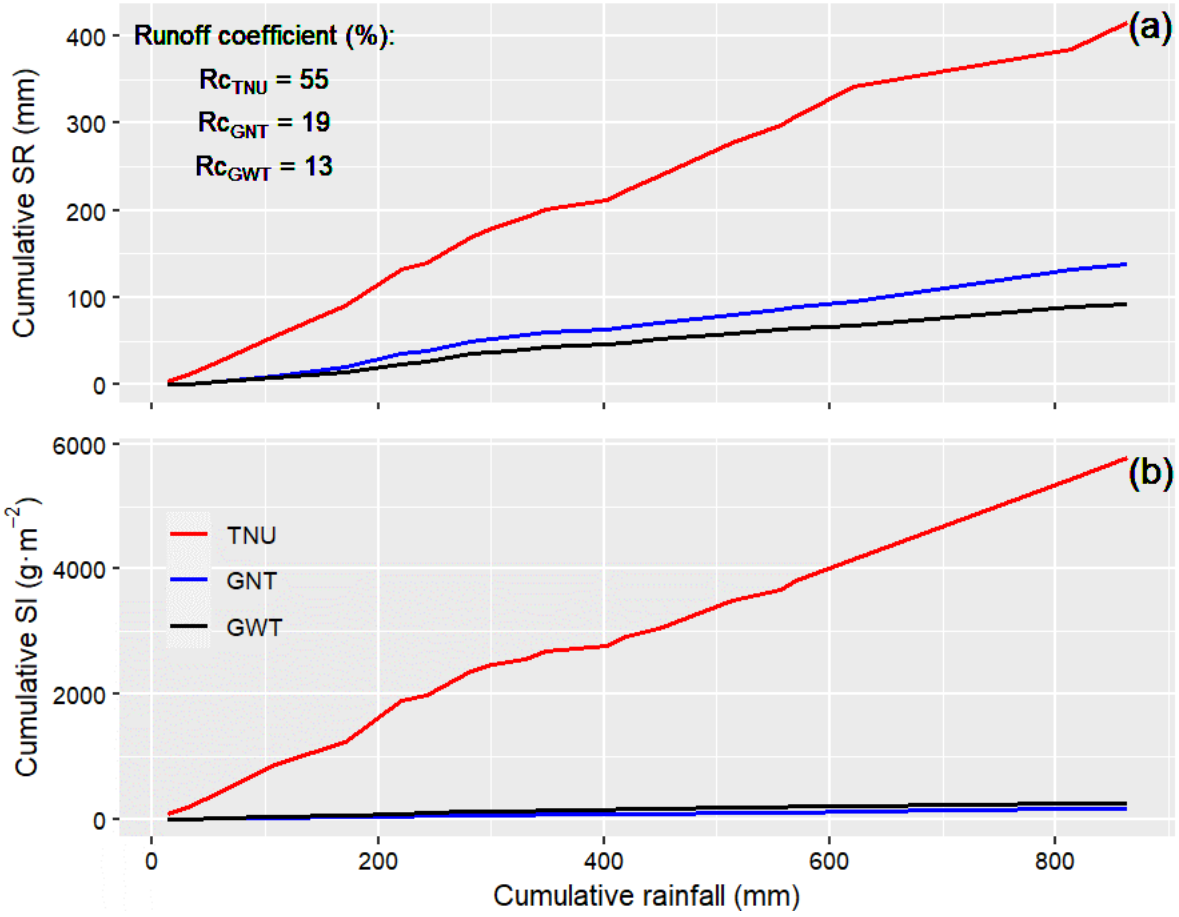

Supporting Figure 5-3: Microplots: (a) cumulative surface runoff (SR, mm) versus cumulative rainfall (mm), and runoff coefficient (%, total surface runoff divided by total rainfall), and (b) cumulative soil loss (Sl, g·m-2) versus cumulative rainfall (mm) from 6 July to 22 September 2014, in Houay Pano catchment, northern Lao PDR. TNU: teak with no understory; GNT: grass nearby teak trees; GWT: grass with a few teaks planted inside.

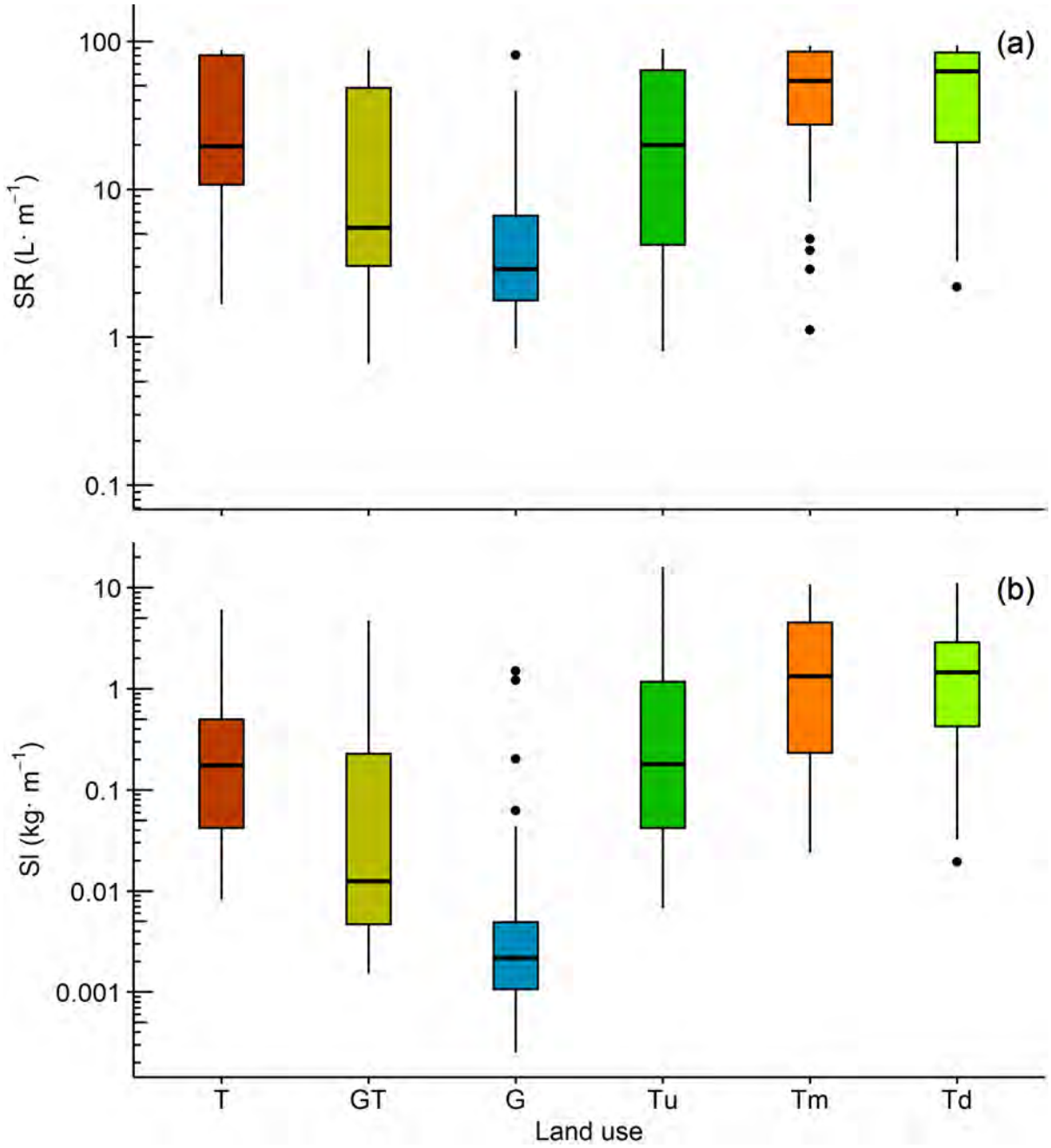

Supporting Figure 5-4: Gerlach traps: boxplots of (a) surface runoff (SR, $L \cdot m^{-1}$) and (b) soil loss (Sl, $kg \cdot m^{-1}$) for the six land uses with 3 replicates along the 19 sampled events from July 7th to September 22nd, 2014, in Houay Pano catchment, northern Lao PDR. T: teak with no understory (upland of GT and G); GT: grass with teak; G: grass; Tu: teak with no understory (up); Tm: teak with no understory (middle); Td: teak with no understory (down). Each boxplot contains the extreme of the lower whisker (vertical line), the lower hinge (thin line), the median (bold line), the upper hinge (thin line), the extreme of the upper whisker (vertical line), and the outliers (black dots) with p-value of Wilcoxon test between two groups of treatments. The

whiskers extend to the most extreme data point which is no more than 1.5 times the interquartile range from the box.

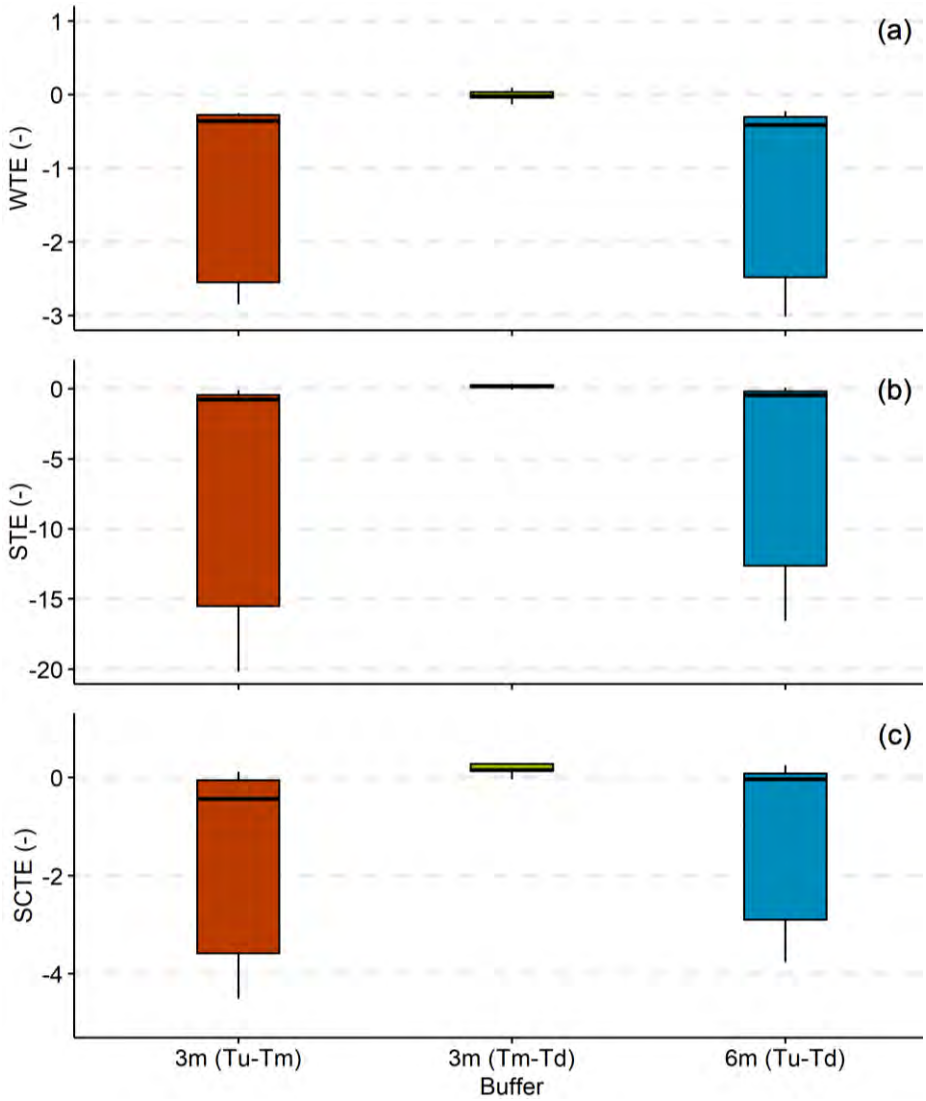

Supporting Figure 5-5: Gerlach traps: (a) water trapping efficiency (WTE), (b) sediment trapping efficiency (STE), and (c) suspended sediment concentration efficiency (SCTE) for each length of buffer and accumulation in 2014, Houay Pano catchment, northern Lao PDR from July 7th to September 22nd, 2014. Tu: teak with no understory (up); Tm: teak with no understory (middle); and Td: teak with no understory (down).

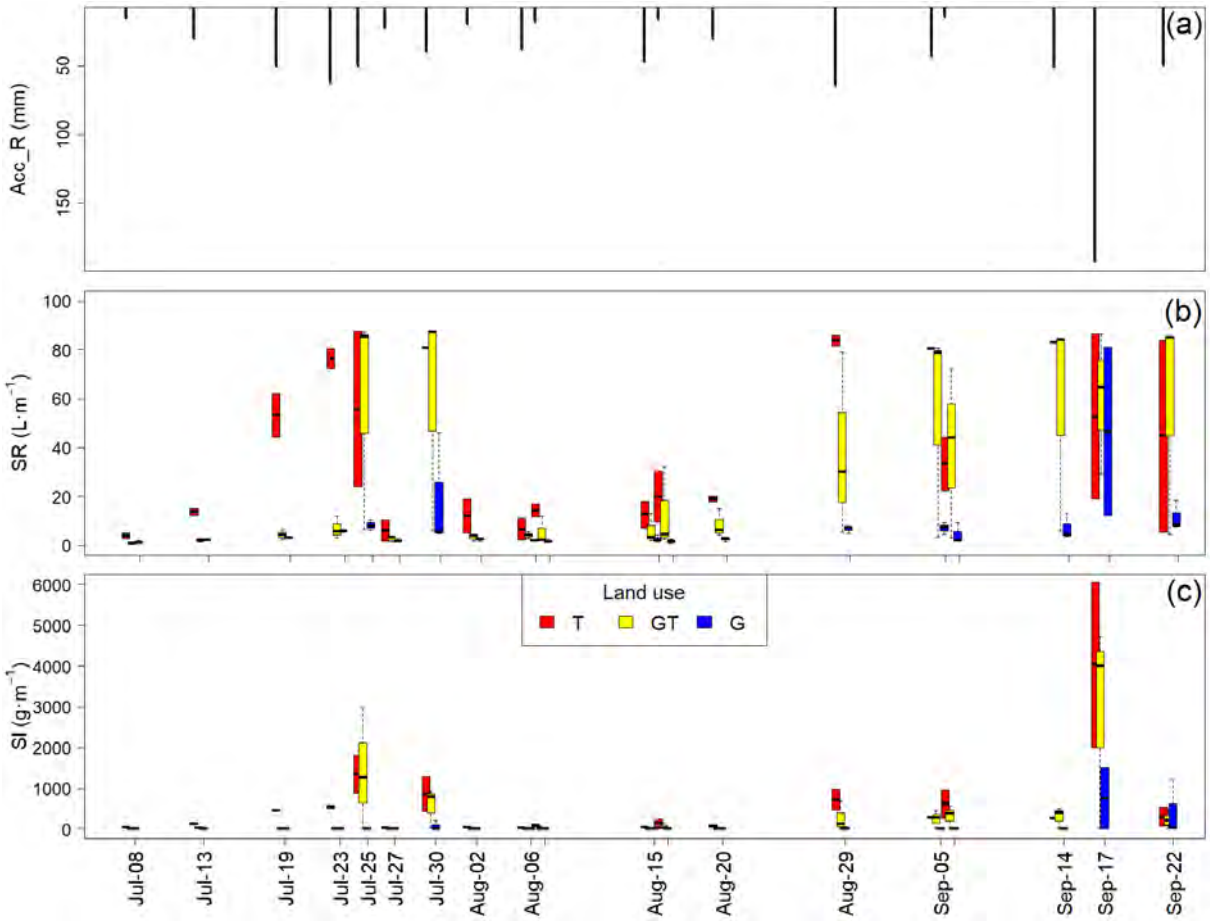

Supporting Figure 5-6. Gerlach traps: (a) accumulated rainfall between two samplings (Acc_R, mm); boxplot of (b) surface runoff (SR, $L \cdot m^{-1}$), and (c) soil loss (Sl, $g \cdot m^{-1}$) for three land uses from 8 July to 22 September 2014, in Houay Pano catchment, northern Lao PDR. T: teak with no understory; GT: grass with teaks; G: grass. Each rainfall bar represents the cumulative rainfall over two to twenty-three rainfall events, or after every major event (event whose rainfall triggered the sampling). Each boxplot contains the extreme of the lower whisker (dashed line), the lower hinge (thin line), the median (bold line), the upper hinge (thin line), and the extreme of the upper whisker (dashed line). The whiskers extend to the most extreme data point, which is no more than 1.5 times the interquartile range from the box.

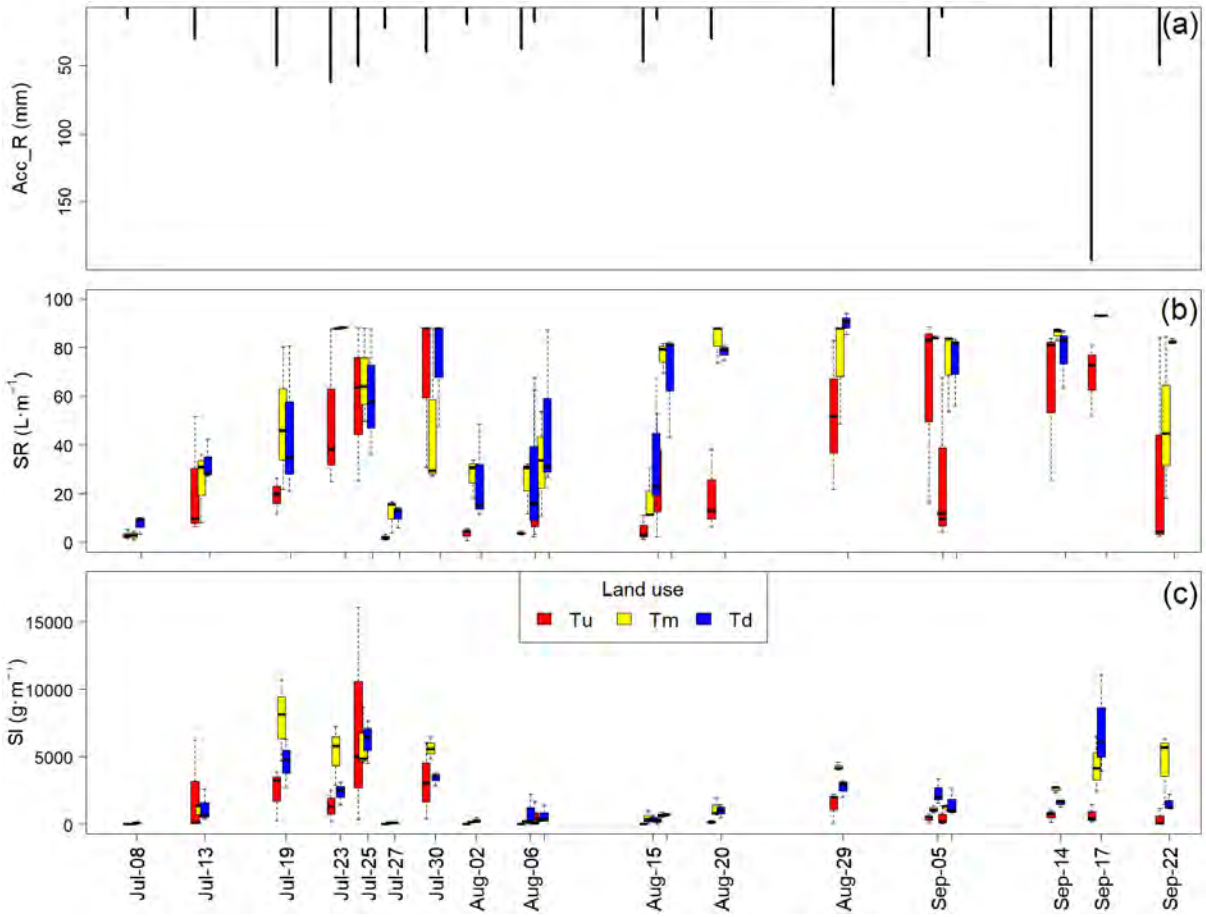

Supporting Figure 5-7: Gerlach traps: (a) accumulated rainfall (Acc_R, mm); boxplot of (b) surface runoff (SR, $L \cdot m^{-1}$), and (c) soil loss (Sl, $g \cdot m^{-1}$) for three land uses from July 8th to September 22nd, 2014 in Houay Pano catchment, northern Lao PDR. Tu: teak with no understory (up); Tm: teak with no understory (middle); and Td: teak with no understory (down). Each rainfall bar represents the cumulative rainfall over two to twenty-three rainfall events, or after every major event. Each boxplot contains the extreme of the lower whisker (dashed line), the lower hinge (thin line), the median (bold line), the upper hinge (thin line), and the extreme of the upper whisker (dashed line). The whiskers extend to the most extreme data point, which is no more than 1.5 times the interquartile range from the box.

Supporting Table 5-1: *p*-value of Wilcoxon test for significant difference of seasonal surface runoff (seasonal SR, $L \cdot m^{-1}$) and seasonal soil loss (seasonal Sl, $g \cdot m^{-1}$) between two groups of treatments. T: teak with no understory; GT: grass with teak; G: grass near teak; Tu: teak with no understory (up); Tm: teak with no understory (middle); and Td: teak with no understory (down).

		T	GT	G	Tu	Tm
Seasonal SR	**GT**	**<0.05**				
	G	**<0.05**	**<0.05**			
	Tu	0.310	0.120	**<0.05**		
	Tm	**<0.05**	**<0.05**	**<0.05**	**<0.05**	
	Td	**<0.05**	**<0.05**	**<0.05**	**<0.05**	1.000
Seasonal Sl	**GT**	**<0.05**				
	G	**<0.05**	**<0.05**			
	Tu	0.520	**<0.05**	**<0.05**		
	Tm	**<0.05**	**<0.05**	**<0.05**	**<0.05**	
	Td	**<0.05**	**<0.05**	**<0.05**	**<0.05**	0.810

Supporting Table 5-2: *p*-value of Wilcoxon signed-rank test to accept the alternative hypothesis: median is greater than the theoretical median of zero. Sig_Date: date during which significant rainfall (rainfall triggering the sampling) happened; GT: grass with teak; G: grass near teak; Tu: teak with no understory (up); Tm: teak with no understory (middle); Td: teak with no understory (down); WTE: water trapping efficiency; SCTE: sediment concentration trapping efficiency; and STE: sediment trapping efficiency. Seasonal refers to calculations using seasonal surface runoff, seasonal sediment concentration, and seasonal soil loss, which were measured in Houay Pano catchment, northern Lao PDR from July 8th to September 22nd, 2014.

	Sig. Date	GT-G (3m)			Tu-Td (6m)			Tu-Tm (3m)			Tm-Td (3m)		
		WTE	**SCTE**	**STE**	**WTE**	**SCTE**	**STE**	**WTE**	**SCTE**	**STE**	**WTE**	**SCTE**	**STE**
Seasonal		**0.010**	0.285	0.285	1.000	0.898	0.996	1.000	0.994	1.000	0.787	**0.004**	**0.006**
All event		**<0.0001**	**<0.0001**	**<0.0001**	1.000	1.000	1.000	1.000	1.000	1.000	0.980	0.969	0.915
2	7/8/2014	1.000	**0.016**	**0.047**	0.998	0.545	0.994	0.674	0.736	0.820	0.996	0.715	0.990
3	7/13/2014	0.820	**0.002**	**0.002**	0.980	0.875	0.980	0.898	0.898	0.898	0.898	0.455	0.936
4	7/19/2014	0.125	**0.002**	**0.002**	0.996	0.820	0.990	0.996	0.918	1.000	0.590	0.213	**0.014**
5	7/23/2014	0.752	**0.006**	0.064	0.996	0.951	0.986	0.986	0.990	1.000	0.988	**0.004**	**0.004**
6	7/25/2014	**0.020**	**0.002**	**0.002**	0.715	0.898	0.820	0.850	0.787	0.820	0.326	0.875	0.752
7	7/27/2014	0.181	**0.004**	**0.002**	1.000	**0.002**	1.000	1.000	**0.002**	0.990	0.500	1.000	0.936
8	7/30/2014	0.064	**0.010**	0.064	0.633	0.936	0.787	0.064	0.998	0.986	0.994	**0.006**	**0.002**
9	8/2/2014	0.213	**0.002**	**0.002**	1.000	0.715	1.000	1.000	**0.002**	1.000	0.326	1.000	0.936
10	8/6/2014	**0.002**	0.875	0.410	0.980	1.000	0.980	1.000	0.213	1.000	0.633	1.000	0.820
11	8/7/2014	**0.010**	**0.002**	**0.004**	0.986	0.918	0.980	0.951	0.936	0.980	0.936	0.590	0.752
12	8/15/2014	0.102	**0.037**	**0.002**	1.000	1.000	1.000	0.994	1.000	1.000	0.986	0.326	0.850
13	8/16/2014	**0.004**	0.590	0.082	0.998	0.594	1.000	1.000	0.077	1.000	0.410	0.989	0.898
14	8/20/2014	**0.002**	0.082	**0.004**	1.000	0.989	1.000	1.000	0.951	1.000	0.064	0.545	0.500
15	8/29/2014	**0.020**	0.317	0.064	1.000	0.875	0.996	0.980	1.000	1.000	0.990	**0.002**	**0.002**
16	9/5/2014	0.326	**0.002**	**0.006**	**0.002**	1.000	1.000	0.820	1.000	1.000	**0.002**	1.000	1.000
17	9/6/2014	0.064	0.082	0.064	0.998	0.590	0.994	0.998	0.248	0.990	0.500	0.633	0.590
18	9/14/2014	0.064	0.102	0.150	0.898	0.997	1.000	0.998	1.000	1.000	**0.037**	**0.004**	**0.002**
19	9/17/2014	0.344	0.281	0.219	0.997	1.000	1.000	0.997	1.000	1.000	1.000	0.980	0.980
20	9/22/2014	0.180	0.850	0.850	0.980	0.990	0.998	0.986	1.000	1.000	0.980	**0.002**	**0.010**

Supporting Table 5-3: *p*-value of Wilcoxon rank sum test (upper-tailed test) to accept the alternative hypothesis: the medians of Tu-Td (6m) is greater than the medians of Tu-Tm (3m). Sig. Date: date during which significant rainfall (rainfall triggering the sampling) happened; Tu: teak with no understory (up); Tm: teak with no understory (middle); Td: teak with no understory (down); WTE: water trapping efficiency; SCTE: sediment concentration trapping efficiency; and STE: sediment trapping efficiency. Seasonal refers to calculations using seasonal surface runoff, seasonal sediment concentration, and seasonal soil loss, which were measured in Houay Pano catchment, northern Lao PDR from July 8th to September 22nd, 2014.

		Sig. Date	**Tu-Td (6m) vs Tu-Tm (3m)**		
			WTE	**SCTE**	**STE**
Seasonal			0.602	0.111	0.149
All event			0.605	0.317	0.521
	2	7/8/2014	0.988	0.568	0.980
	3	7/13/2014	0.667	0.432	0.602
	4	7/19/2014	0.365	0.218	0.129
	5	7/23/2014	0.762	0.057	0.081
	6	7/25/2014	0.302	0.602	0.466
	7	7/27/2014	0.432	0.980	0.905
	8	7/30/2014	0.988	**0.016**	0.111
	9	8/2/2014	0.302	0.980	0.871
	10	8/6/2014	0.333	1.000	0.500
	11	8/7/2014	0.635	0.432	0.667
	12	8/15/2014	0.905	0.500	0.602
	13	8/16/2014	0.568	0.847	0.667
	14	8/20/2014	0.365	0.365	0.398
	15	8/29/2014	0.830	**0.039**	**0.025**
	16	9/5/2014	**< 0.0001**	1.000	0.969
	17	9/6/2014	0.365	0.432	0.398
	18	9/14/2014	0.170	**0.002**	**0.025**
	19	9/17/2014	0.610	0.807	0.782
	20	9/22/2014	0.830	**< 0.0001**	0.081

[This page intentionally left blank]

Chapter 6. Multiscale assessment of the effect of teak-tree plantation on surface runoff and sediment yield in mixed land-use mountainous tropical catchment

"The greatest threat to our planet is the belief that someone else will save it" – Robert Swan

Chapter 6

Multiscale assessment of the effect of teak-tree plantation on surface runoff and sediment yield in mixed land-use mountainous tropical catchment

The findings on the microplot scale described in ***Chapter 4*** *highlighted massive soil loss generated in teak tree plantations with no proper management of the understory. In* ***Chapter 5****, we suggested that, without any measure of local soil erosion reduction, at least riparian grass should be left to capture sediment from the uphill to prevent soil exportation and water pollution downstream. In this scientific chapter, we evaluate the multiscale hydro-sedimentary behaviour of a 0.6 km² mixed land-use mountainous tropical catchment, including teak tree plantations*

Abstract: The increase of the area planted with teak trees in the tropical mountainous catchments of Lao PDR has been shown to enhance soil erosion on both the plot and the hillslope scales, involving processes of detachment, inter rill erosion, linear erosion, and deposition. On the catchment scale, the processes involved in soil loss and sediment exportation are deposition and resuspension, in addition to the processes involved on the smaller spatial scales. However, the multiscale impact of teak tree plantations on soil erosion and on sediment exportation is not yet known. Hence, this study aimed to: (1) compare the surface runoff (SR) and the soil loss (Sl) occurring in both mixed-land-use and teak-tree-dominated micro-catchments scale; (2) assess the impact of the spatial scale when assessing SR and Sl on the microplot, hillslope (here two micro-catchments), and catchment scales; (3) model soil loss on the hillslope and catchment scale; and (4) quantify contributions of each erosion process to sediment yield. Field experiments were carried out during the 2014 rainy season on the microplots (1x1 m^2) installed in 6 land uses: fallow of 2 years, fallow of 5 years, secondary forest, teak with no understory, teak with understory, and upland rice; the micro-catchments (0.6 ha) S7, with mixed land uses, and S8, dominated by teak trees; and the catchment (60.2 ha) S4, outlet of the Houay Pano experimental catchment located in northern Lao PDR. We measured rainfall, SR, Sl, soil surface features including the areal percentage of both residues and grass, area of each land use; fraction of headwater wetland, vegetated waterway, and riparian buffer (proportional to the total area of the catchment). Our results highlighted that, on the hillslope scale, seasonal SR and seasonal Sl in the teak-tree-dominated micro-catchment (187.95 mm and 3635 $g \cdot m^{-2}$, respectively) were significantly higher (p-value < 0.001) than those in the mixed-land-use micro-catchment (24.12 mm and 95 $g \cdot m^{-2}$, respectively). The seasonal soil loss decreased from 275 and 661 $g \cdot m^{-2}$ (weighting of S7 and S4, respectively) on

the microplot scale, to 95 $g \cdot m^{-2}$ (S7) on the micro-catchment scale, and increased to 236 $g \cdot m^{-2}$ (S4) on the catchment scale. In contrast, soil loss increased from 1065 $g \cdot m^{-2}$ (weighting of S8) on the microplot scale, to 3635 $g \cdot m^{-2}$ (S8) on the micro-catchment scale, which can be explained by the additional linear erosion along the gully. Upscaling sediment transfer from the microplot to micro-catchment and catchment scales improved our soil loss prediction by taking into account erosion on the plot scale, linear erosion, and sediment deposition throughout the catchment. Our Sl model yielded a R^2 of 0.92 but was limited to reproduce the extreme event of September 17. Sl during this extreme event may be explained by the extreme flood event and by the occurred landslides, which may have become an important source of sediment resuspension. The model predicted that Sl was mostly contributed by inter rill erosion (443 $g \cdot m^{-2}$), but later deposed throughout the catchment (S4). This contribution was in contrast to Sl of the micro-catchment dominated by teak tree plantation (S8) with similar rates of inter rill (424 $g \cdot m^{-2}$) and linear erosions (482 $g \cdot m^{-2}$) and without sediment deposition.

6.1. INTRODUCTION

Soil erosion, especially by water, is known as one of the most environmental concerning problems in the world under the changing climate (Borrelli et al., 2020; Oldeman, 1994). Southeast Asia was predicted as one of the regions the most prone to soil erosion due to the cropland expansion (Borrelli et al., 2017) and land mismanagement (Bhat et al., 2019). In Lao PDR, many researches focus on soil erosion, which is generally triggered by land and soil management and enhanced by steep topographies and heavy tropical rainfall (Chaplot and Poesen, 2012; Lacombe et al., 2018; Patin et al., 2018; Ribolzi et al., 2017). Those researches mainly assessed soil loss in various land uses. Lacombe et al. (2018) highlighted two remarkable land uses, i.e., teak trees with no understory generating high soil loss and broom grass as understory protecting soil against erosion at the plot scale. Furthermore, Patin et al. (2018) also emphasized that high soil loss occurred under teak tree plantations. Ribolzi et al. (2017) assessed the long-term effect of the land use conversion of traditional slash-and-burn agricultural systems, with long fallow periods, to teak tree plantations dominated agricultural systems, by quantifying the annual overland flow and sediment yield. The results at catchment scale showed a substantial increase of overland flow (16 to 31%) and sediment yield (98 to 609 $Mg \cdot km^{-2}$) when land is converted from shifting cultivation into teak tree plantation between 2002 and 2014. In 0 and Chapter 5, on both microplot and hillslope scale, we also suggested that teak tree plantation without understory caused higher soil loss compared to the other land

uses. However, multi-scale assessment of sediment exportation from mixed land-use catchment dominated by teak tree plantations is not yet performed.

Soil erosion processes are complex and dynamic, from the plot to the catchment scale. On the plot scale, both rain splash and surface runoff may cause soil detachment and transport. Rain splash detaches and transports the soil particles, possibly lifting the loose particles along with the water flow (Valentin and Rajot, 2018), when the flow energy is sufficiently large to detach the soil particles from the bulk soil. On the hillslope scale, the deposition of detached soil particles may occur through gravity and prevailing friction (Chaplot and Poesen, 2012) and through riparian buffer (Cooper et al., 1987; Ding et al., 2011; Verstraeten et al., 2006; Vigiak et al., 2008), and linear erosion may occur through gullies (Chaplot et al., 2005b). Sediment deposition and linear erosion may be affected by hillslope topography (Buckley, 2010; Sabzevari and Talebi, 2019). Riparian buffer may efficiently trap the sediment when the hillslope is divergent and parallel as the surface runoff flowing through this these shapes is not concentrated. On convergent hillslope, the sediment flow may concentrate and by pass the riparian buffer through gullies (Verstraeten et al., 2006; Wenger, 1999), especially under heavy rainfalls (de Rouw et al., 2018). Catchment scale involves sediment deposition and resuspension. Sediments transported from hillslope could be trapped in the headwater wetland (Cao et al., 2018; Goddard and Elder, 1997; Schmadel et al., 2019), which is considered as sediment storage (Phillips, 1989). Deposited sediment can be resuspended under extreme event rainfall (Robotham et al., 2021; Thothong et al., 2011). The soil particles may be continuously transported through rills and then through gullies and at last may be accumulated into the channel on the catchment scale. High rainfall can resuspend those particles depositing in the bed of river channels (Ribolzi et al., 2016). However, in case of teak tree plantation dominated land uses, the relative contributions of each process occurring on each spatial scale were not yet assessed.

The hydro-sedimentary processes may be intensified or attenuated by several factors such as rainfall characteristics, land use, catchment morphology (convergence, divergence), presence of a wetland, vegetation, landslide, and soil surface features known to control soil erosion (Lacombe et al., 2018; Nadeu et al., 2015; Ribolzi et al., 2018; Yin et al., 2015; Zhang et al., 2018). These factors play important roles in characterizing the dominant processes on each scale. The dominant processes include inter rill erosion on plot scale, linear erosion (rill and gully) on hillslope scale, and deposition on hillslope and catchment scale. In **Chapter 5**, a soil loss model was successfully applied and able to predict the soil loss on the plot scale. Four

factors including rainfall kinetic energy, runoff coefficient, and areal percentages of vegetation and residues were taken into account, which are dominant on the plot scale. However, applying this model on larger scales is challenging and upscaling of this model is needed to predict soil loss on various scale. Blöschl and Sivapalan (1995) suggests that, when upscaling, we should develop models to focus on the dominant processes that control hydrological response in different environments and at different scales.

In this study, we formulated two hypotheses for the effect of teak-tree plantation surface runoff and soil loss in a mixed land-use mountainous tropical catchment. First hypothesis is that land dominated by teak tree plantations impacts on surface runoff, soil loss, and erosion processes in the micro-catchment. Second hypothesis is that surface runoff and sediment yield decrease from plot to catchment scale based on dominant processes on each scale. Using field measurements carried out during the rainy season 2014, on the Houay Pano experimental catchment located in northern Lao PDR (Boithias et al., 2021); hence, the specific objectives of this study were: (1) compare the surface runoff (SR) and the soil loss (Sl) occurring in both mixed-land-use and teak-tree-dominated micro-catchments scale; (2) assess the impact of the spatial scale when assessing SR and Sl on the microplot, hillslope (here two micro-catchments), and catchment scales; (3) model soil loss on the hillslope and catchment scale; and (4) quantify contributions of each erosion process to sediment yield.

6.2. MATERIALS AND METHODS

6.2.1. *Study area*

The Houay Pano headwater catchment is a 60.2 ha experimental site (Boithias et al., 2021) belonging to the Multi-scale TROPIcal CatchmentS critical zone observatory (M-TROPICS CZO; https://mtropics.obs-mip.fr/). The catchment is located in the mountainous region of northern Lao PDR, 10 km South from Luang Prabang City. It is part of the Mekong river basin (**Figure 6.1**). The climate is sub-tropical humid and is characterized by a monsoon regime with a dry season from November to May, and a wet season from June to October. The mean annual temperature is 23.4 °C. Mean annual rainfall is 1366 mm, about 71 % of which falls during the wet season. Altitude within the catchment is 435 – 716 m, and the slope gradient is 1 – 135 % (mean=52 %) (Boithias et al., 2021).

This catchment can be considered as being representative of the montane agro-ecosystems of South-East Asia. The land use of this catchment consists of fallow (from 1 to 15 years old, classified as fallow of 1 – 3 years (Fa2) and fallow of 4 – 15 years (Fa5)), teak tree with no

understory (TNU, understory < 80%), teak with understory (TWU, understory > 80%), secondary forest (For), annual crop (URH: upland rice) (**Table 6.1**), banana, broom grass, temporarily unit, and fish pond. Banana (3.95%), broom grass (0.57%), temporarily unit (0.38%), and fish pond (0.2%) had small proportions to the catchment area which are considered as negligible and thus not reported in **Table 6.1**.

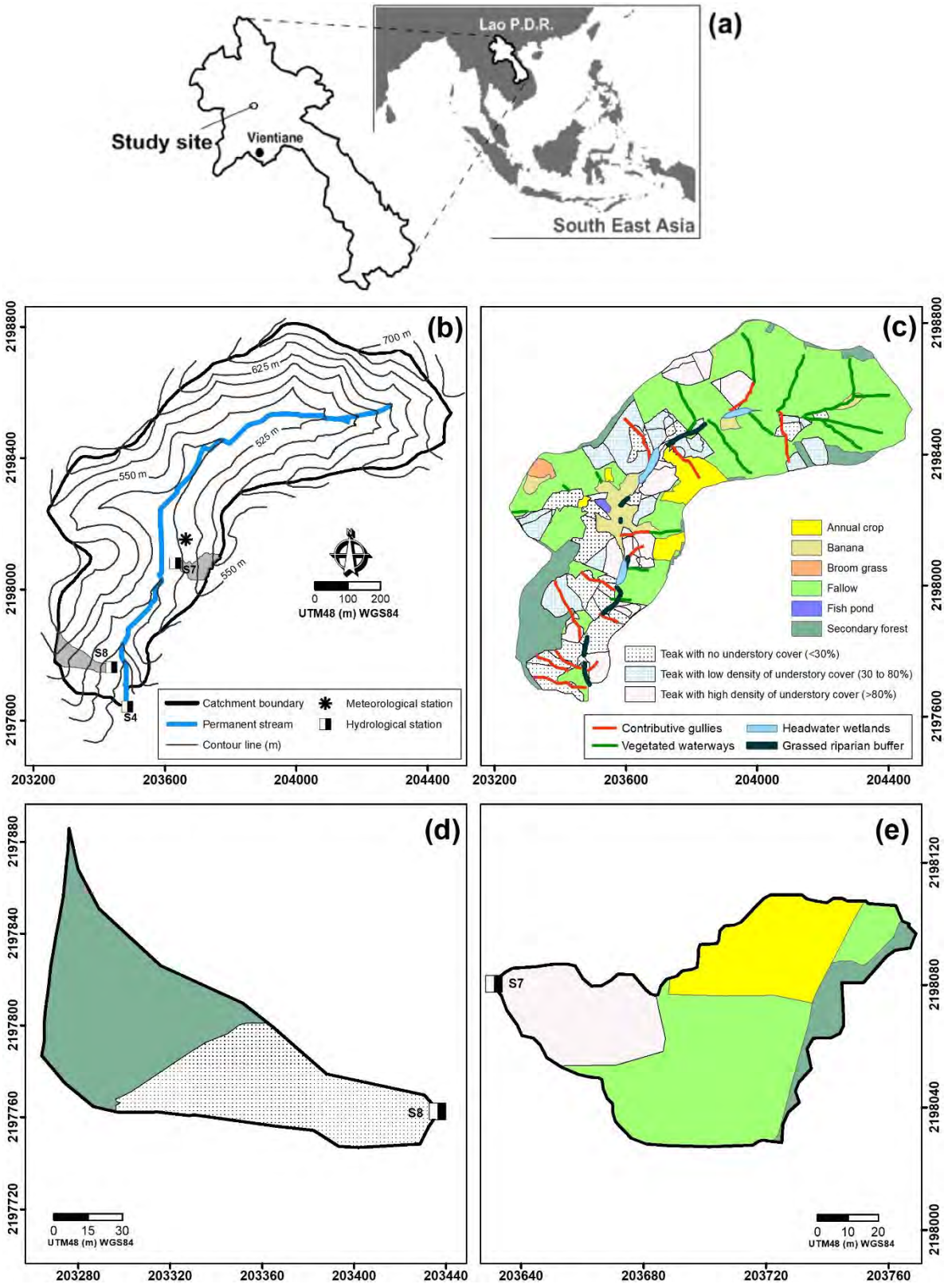

Figure 6.1: (a) Study site located in northern Lao PDR; (b) topographical map of the Houay Pano catchment (S4) and location of micro-catchments (S7 and S8); land use in 2014: (c) S4; (d) S8; (e) S7.

Table 6.1: Area (ha) of each catchment and percentages of each land use in each catchment. TNU: teak with no understory; TWU: teak with understory; For: secondary forest; URH: upland rice hillslope; Fa5: fallow of 4 – 15 years; Fa2: fallow of 1 – 3 years.

Catchment	Area (ha)	TNU (%)	TWU (%)	For (%)	URH (%)	Fa5 (%)	Fa2 (%)
S7	0.62		22.40	7.30	22.19	38.89	9.22
S8	0.57	41.50		58.50			
S4	60.2	25.54	7.83	8.69	4.10	14.51	33.36

6.2.2. *Field experimentation*

Rates of surface runoff (SR) and soil loss (Sl) were evaluated on different spatial scales by hypothesizing that the dominant hydro-sedimentary processes driving SR and Sl, are different on microplot, micro-catchment (hillslope), or on catchment scales. Sl represents both terms of soil loss on the microplot scale and sediment yield on the micro-catchment and catchment scales. The term micro-catchment refers to the hillslope spatial scale, with a convergent shape which possibly leads to the forming of gullies or small ephemeral streams.

We investigated SR and Sl on the plot scale using 1×1 m² microplots, where erosion is associated mainly with splash detachment by rain. Three replicated microplots were installed in each one of the six land uses, i.e., Fa2, Fa5, TNU, TWU, For, and URH.

On the hillslope scale, we installed a weir at the outlets of the two micro-catchments (S7 and S8, with the surface area of 0.62 and 0.57 ha, respectively) to monitor surface runoff and suspended sediment concentration, and thus Sl at the micro-catchment scale (**Figure 6.1**). These two micro-catchments were also selected to compare the effect of land use on Sl: S7 and S8 were with mixed land uses and dominated by teak, respectively. These two micro-catchments were selected because they had the same characteristics for meteorology, surface area, morphology, and type of soil.

On the catchment scale, we installed a weir at the outlet of the catchment (S4, with the surface area of 60.2 ha) to investigate discharge (including SR and groundwater flow) and Sl and the processes which control soil erosion (linear erosion and deposition) on the catchment scale.

6.2.3. *Measurement and calculation methods*

6.2.3.1. Rainfall measurement

We measured rainfall (Rfa) with the rain gauge of the automatic meteorological station (**Figure 6.1**) located within the catchment. Rainfall of 2014 was recorded at 6-min time intervals using a Campbell BWS200 rain gauge equipped with ARG100 (0.2 mm capacity tipping-bucket).

6.2.3.2. Microplot monitoring

Microplot metal frames were connected to a covered and buried 170 L bucket through a pipe for SR and Sl collection (see section **5.2.2.1**). We collected SR and emptied the buckets after every major rainfall event, or after a series of 2 to 10 smaller rainfall events. 19 rainfall events were observed during the experimental period lasting from 8 July to 22 September 2014. A sample of surface runoff was collected from the bucket. The concentration of soil loss accumulated between two emptyings was measured after flocculation, filtration, and oven dehydration, following a procedure similar to that used for suspended sediment concentration. We then calculated soil detachment per square metre by multiplying the accumulated soil loss concentration by the accumulated surface runoff volume, considering that each metal frame is 1 m^2.

Seasonal runoff and seasonal soil loss are accumulated surface runoff and accumulated soil loss, respectively, during the experimental period.

6.2.3.3. Discharge measurement

We measured stream water level at the gauging stations of the catchment (S4, S7, and S8) with a compound V-notch and rectangle notch weir (Boithias et al., 2021; Nouvelot, 1993) equipped with a water level recorder connected to a data logger, with 1-mm vertical precision **(Figure 6.2**). Water level was scanned every 30 s and recorded if a variation of ±1 mm was detected within a period of 3 min. The discharge was then calculated based on the shape of the flow and water level using V-Shaped and rectangular weir formulas.

Figure 6.2: A storage attached with combined V-notch and rectangular weir for sediment, bed load, and discharge measurement

Both baseflow and SR contribute to the flow in S4 during rainfall events. We used a tracer-based approach to separate storm hydrographs into 'event water' and 'pre-event water'. This approach relies on a simple mixing model with two end-members and electrical conductance (EC) at 25°C as a tracer. It is of relatively low cost compared to, e.g. isotopic tracers and was successfully tested in the study catchment (Ribolzi et al., 2018). Based on previous field observations and measurements performed in the same study catchment (Patin et al., 2012; Ribolzi et al., 2011b; Vigiak et al., 2008), the two end-members of the model (i.e., overland flow EC end-member in event water, and groundwater EC end-member in pre-event water) can be interpreted in terms of hydrological processes. Event water mainly includes infiltration excess that produces overland flow along hillslopes. Pre-event water relates to groundwater that feeds the stream during the storm event, plus the water in the stream channel prior to the storm event, which is also related to groundwater outflows. As suggested by Collins and Neal (1998), we verified the linearity between EC and the concentration of a conservative tracer to control the relevance of the EC-based approach in our context (Ribolzi et al., 2018). The mixing model applied to individual samples is described by the following equations (**Eq. 6.1** and **Eq. 6.2**):

$$Q = Q_{OF} + Q_{GW} \qquad \textbf{Eq. 6.1}$$

$$Q \cdot EC = Q_{OF} \cdot EC_{OF} + Q_{GW} \cdot EC_{GW} \qquad \textbf{Eq. 6.2}$$

where Q is the instantaneous stream water discharge at the catchment outlet ($L \cdot s^{-1}$), Q_{OF} is the instantaneous discharge of overland flow, i.e., event water or surface runoff ($L \cdot s^{-1}$), Q_{GW} is the instantaneous discharge of groundwater, i.e., pre-event water or sub-surface flow ($L \cdot s^{-1}$), EC is the instantaneous electrical conductivity measured in the stream ($\mu S \cdot cm^{-1}$), EC_{OF} is the electrical conductivity in overland flow (overland flow EC end-member; $\mu S \cdot cm^{-1}$), approximated from electrical conductivity measurements in samples of overland flow collected at the soil surface on hillslopes draining to the stream, and EC_{GW} is the electrical conductivity in groundwater (groundwater EC end-member; $\mu S \cdot cm^{-1}$), approximated from the stream electrical conductivity at the beginning of the flood event, since groundwater is the only supply of water to the stream during inter-storm flow periods (Ribolzi et al., 2005). For each individual sample, we calculated the relative contributions of Q_{OF} and of Q_{GW} to Q based on **Eq. 6.2**, namely Q_{OF} % and of Q_{GW}% (in %).

6.2.3.4. Suspended sediment measurement

We collected samples of stream water 10 cm below the river water surface at the S7, S8, and S4 gauging station in clean, 600-ml plastic bottles, using an automatic sampler (Automatic Pumping Type Sediment Sampler, ICRISAT; **Figure 6.3**). 19 flood events were sampled that corresponds to the 19 samplings using the microplots. The automatic sampler was triggered by the water level recorder to collect water after every 2-cm water level change during flood rising and every 4-cm water level change during flood recession. We measured the concentration of suspended sediment concentration in each sample after flocculation with a 10 $g \cdot L^{-1}$ concentrated aluminium sulphate solution, filtration with 0.7 µm acetate filters, and evaporation at 105 °C for 48 h. Suspended sediment mass was then divided by the sample volume to calculate the suspended sediment concentration.

For predicting the missing data of suspended sediment, we used specific maximum discharge ($l \cdot s^{-}1 \cdot ha^{-1}$) and measured suspended sediment to fit an equation of their relation (power regression) and predict the suspended sediment of missing events according to the measured maximum discharge.

Figure 6.3: Automatic sampler with 600-ml plastic bottles

6.2.3.5. Bed load measurement

We measured bed load of micro-catchment and catchment by trapping the sediment in the stilling basin of the weirs of S4, S7, and S8 (Boithias et al., 2021). Each month or each time the stilling basin is full of sediment we used buckets to measure both the volumes of deposited soft sediment and of stones. The volume of stones bigger than the buckets was estimated from their dimensions, manually measured with a tape measure. We then calculated the average bulk density of the total of deposited sediment, assuming a density of 1.00 for soft sediment and of 2.65 for stones. After collection, we oven-dried the soft sediment samples; the dry weight of sediment samples was subsequently divided by the catchment area to express bed load in $T \cdot ha^{-1}$.

6.2.3.6. Soil loss calculation on micro-catchment and catchment scales

To calculate Sl of each event in the micro-catchment and catchment, we weighted the bed load using the suspended sediment of each event before each bed load collection and then added up each fraction of bed load to Sl of each event.

Contribution of bed load to Sl of each event is weighted using the suspended sediment of each event before the bed load collection. Sl of an event is then the sum of weighted bed load of each event and the corresponding suspended sediment.

6.2.3.7. Land use monitoring

Detailed land-use surveys were conducted within the catchment in 2014 with a handheld GPS (Boithias et al., 2021). We classified land use into six classes, namely: URH; Fa2; Fa5, For,

TNU and TWU (**Table 6.1**). We grouped the land uses with teak based on the areal percentage of the understory. TNU had an areal percentage of understory smaller than 80% and TWU had an areal percentage of understory higher than 80% (**Figure 6.1**).

6.2.3.8. Weighting surface runoff and soil loss

We used SR and Sl in the microplots observed under each land use to weight Sl in S4, S7, and S8 using the percentages of their land uses, to calculate SR and Sl for S4, S7, and S8.

6.2.4. *Statistical analyses and modelling*

We performed non-parametric Wilcoxon rank sum test (XLSTAT version 20.4.1; (Addinsoft, 2021)) to check if both SR and Sl in S8 are greater than those in S7.

We used the spatially variable infiltration model (SVI) of Yu et al. (1997) and surface runoff equation of Patin et al. (2012) to predict the surface runoff (**Eq. 6.3**). For each land use, we used the median and geometrical standard deviation of maximum infiltration rate (Im) calculated by Patin et al. (2012) for our calculation.

$$SR = \sum_{R \in R_e} (R - I_m \cdot (1 - \exp(-R/I_m))) \cdot \Delta t \qquad \textbf{Eq. 6.3}$$

where R is the rainfall intensity (mm·h-1); Re is the rainfall event; SR is the total runoff volume (mm) of Re; Im is the maximum infiltration rate (mm·h-1); Δt is the time step of rainfall record. Then we calculated runoff coefficient (Rc) by dividing SR by the total rainfall of Re.

We then calculated rainfall kinetic energy (KE) by applying the equation of Lacombe et al. (2018) provided in **Eq. 6.4**:

$$KE = A \cdot \ln(R) - B \qquad \textbf{Eq. 6.4}$$

where A is the coefficient and B is a constant. The value of A and B depends on the land use (Lacombe et al., 2018); values of A and B are provided in **Table 6.2**.

We then replaced all the calculated values of SR and KE into the **Eq. 6.5** (Model 1 with inter rill erosion) to calculate Sl by taking value of the effective soil detachability (D) and the coefficient values of a and b from **Chapter 5**.

$$Sl = D \cdot \Sigma(KE \cdot R_C) \cdot \exp(-a \cdot Gra) \cdot \exp(-b \cdot Res) \qquad \textbf{Eq. 6.5}$$

where Sl is the soil loss (g·m-2); D is the effective soil detachability (g·J-1); KE is the rainfall kinetic energy (J·m-2); Rc is the runoff coefficient (%); Gra is the areal percentage of grass (%); Res is the areal percentage of residues (%); a and b are the decay coefficients of Gra and

Res, respectively. D, a, and b are equal to exp(-4.39), -2.47·10-2 and 2.29·10-2, respectively, which were calibrated for the event scale in **Chapter 5**.

Table 6.2: Surface feature characteristic, coefficients of KE, and maximum infiltrability. gd: geometric standard deviation.

		TNU	TWU	For	URH	Fa5	Fa2
Crust (%)	Average	72.67	5.67	0.75	57.5	2	8.67
Gra (%)	Average	16	53	12	12	49	7
Res (%)	Average	12	24	76	2	69	13
KE coefficient	A	5.9758	5.9758	6.5847	2.1138	6.5847	6.5847
	B	4.435	4.435	1.3151	11.218	1.3151	1.3151
Im (mm/h)	Median	18	35	74	19	74	74
	gd	4.9	3.8	3.3	2.8	3.3	3.3

Monte Carlo method were used to repeat 10000 random calculations of the parameters to simulate Sl using Model 1 (**Eq. 6.5**)

To improve Model 1, we upscaled it by taking into account catchment scale factors. Generally, on both hillslope and catchment scales, other processes intensify or attenuate the overall Sl. For example, rill and gully erosion (linear erosion) intensify overall Sl, while deposition of sediment attenuates the overall Sl (Chaplot et al., 2005b; Robotham et al., 2021; Schmadel et al., 2019). We introduced those attenuating and intensifying factors into the **Eq. 6.5**. Hence, the new upscale model, i.e., Model 2, with the attenuating and intensifying factors is given in **Eq. 6.6**.

$$Sl = M_1 \cdot F_{LE} \cdot F_{TE} \qquad \textbf{Eq. 6.6}$$

where M_1 is Model 1 (**Eq. 6.5**), and F_{LE} and F_{TE} are the areal fractions of linear erosion and sediment deposition, respectively.

The intensifying factor, which enhances linear erosion, takes into account the fraction of gully area on the hillslope or on the catchment scales (**Eq. 6.7**).

$$F_{LE}=F_{GR} \qquad \textbf{Eq. 6.7}$$

where F_{GR} is the areal fraction of gully, respectively, on the hillslope or on the catchment scales.

The attenuating factors, which enhance sediment deposition, include headwater wetland, vegetated waterway, and riparian buffer. We summed up the fraction of those factors by calculating their areal fractions to the total area (micro-catchment or catchment) (**Eq. 6.8**).

$$F_{TE} = F_{HW} + F_{VW} + F_{RB} \quad \textbf{Eq. 6.8}$$

where F_{HW} is the areal fraction of headwater wetland; F_{VW} is the areal fraction of vegetated waterway; and F_{RB} is the areal fraction of riparian buffer, on the hillslope or on the catchment scales.

Hence, the equation of Model 2 for Sl is given in **Eq. 6.9**:

$$Sl = D \cdot \Sigma(KE \cdot R_C) \cdot \exp(-a \cdot Gra) \cdot \exp(-b \cdot Res) \cdot \exp(c \cdot F_{LE}) \cdot \exp(-d \cdot F_{TE}) \quad \textbf{Eq. 6.9}$$

where c is the intensifying coefficient of F_{LE}; d are the decay coefficients of F_{TE}. We applied Model 2 to our dataset by recalculating coefficients to build a new model on the event scale using the Sl values of the 19 events by keeping constant the coefficient of the Model 1.

For the calibration of Model 2, we first introduced F_{LE} into Model 1 and calibrated the coefficient of this parameter using the data of S8. S8 contained gullies only, which contributed to F_{LE}. We used this method to reduce the model uncertainty (Abbaspour, 2021), which leads to erroneous and misleading results when different parameter sets of the model reach the same objective function. After the coefficient of F_{LE} was calibrated, we then introduced the second parameter, F_{TE}, which represents the characteristics of S4. We calibrated the coefficient of F_{TE} by fixing the calibrated parameter of F_{LE} fixed. We applied the two calibrated coefficients of F_{LE} and F_{TE} to the model taking into account all the catchments, i.e., S8, S7, and S4, to validate the model performance.

6.2.5. *Assumptions*

- We assumed that Im of secondary forest was equal to Im of fallow to calculate the surface runoff using the runoff volume equation of Patin et al. (2012). And we assumed that Im of fallow of all years had the same rate.
- As areal percentages of broom grass, temporarily unit, banana, and fish pond are small compared to the areal percentages of the other land uses, we neglected these land uses in the calculation.
- We assumed that the annual crops consisted of upland rice only.
- We assumed that KE in upland rice is equal to KE of non-intercepted rainfall in order to use the equation of KE provided by Lacombe et al. (2018).
- We assumed that, in S4, areal percentages of residues and grass of 1- and 3-year fallow are equal to the areal percentage of residues and grass of Fa2, respectively. Areal

percentage of residues and grass of 4-, 6-, 7-, 12-, and 15-year fallow are supposed to be equal to the areal percentage of residues and grass of Fa5.

- We assumed that small events between large events triggering the samplings are negligible for S8, S7, and S4.

6.3. RESULTS

6.3.1. *Surface runoff and soil loss at the microplot scale*

The 2014 Rfa was 1366 mm, of which 536 mm (39% of the annual Rfa) occurred during the sampling period of the microplot from 8 July to 22 September 2014. An extreme Rfa was recorded on 17 September 2014 with 182.8 mm (during 13 h). Seasonal Rc of Fa2, Fa5, For, TNU, TWU, and URH were 10%, 14%, 23%, 55%, 28%, and 37%, respectively.

The median of SR in Fa2, Fa5, For, TNU, TWU, and URH were 1.8, 2.91, 4,11, 11.5, 3.04, and 4.53 mm, respectively. The median of Sl in Fa2, Fa5, For, TNU, TWU, and URH were 1, 2, 7, 74, 5, and 11 $g \cdot m^{-2}$, respectively. The SR and Sl in TNU recorded during the extreme event of September 17 were 42.33 mm and 517 $g \cdot m^{-2}$, respectively. The SR in Fa2, Fa5, For, TWU, and URH recorded during the same extreme event were 17.6, 21.27, 31.47, 43, and 43 mm, respectively. The Sl in Fa2, Fa5, For, TWU, and URH recorded during the extreme event were 15, 15, 54, 50, and 271 $g \cdot m^{-2}$, respectively.

Figure 6.4 shows the observed cumulative SR and cumulative Sl in relation to cumulative Rfa over the 2014 rainy season for monitored in the plots, the two micro-catchments, and the catchment. For the microplots, seasonal SR (294.19 mm) and Sl (2216 $g \cdot m^{-2}$) in TNU were higher than those in the other land uses. URH ranked second with seasonal SR of 200.31 mm and Sl of 795 $g \cdot m^{-2}$. Land uses generating the least seasonal SR and seasonal Sl were Fa2 (54.90 mm and 43 $g \cdot m^{-2}$, respectively) and Fa5 (77.05 mm and 74 $g \cdot m^{-2}$, respectively). Land uses generating the medium seasonal SR and seasonal Sl were TWU (150.44 mm and 213 $g \cdot m^{-2}$, respectively) and For (125.77 mm and 249 $g \cdot m^{-2}$, respectively).

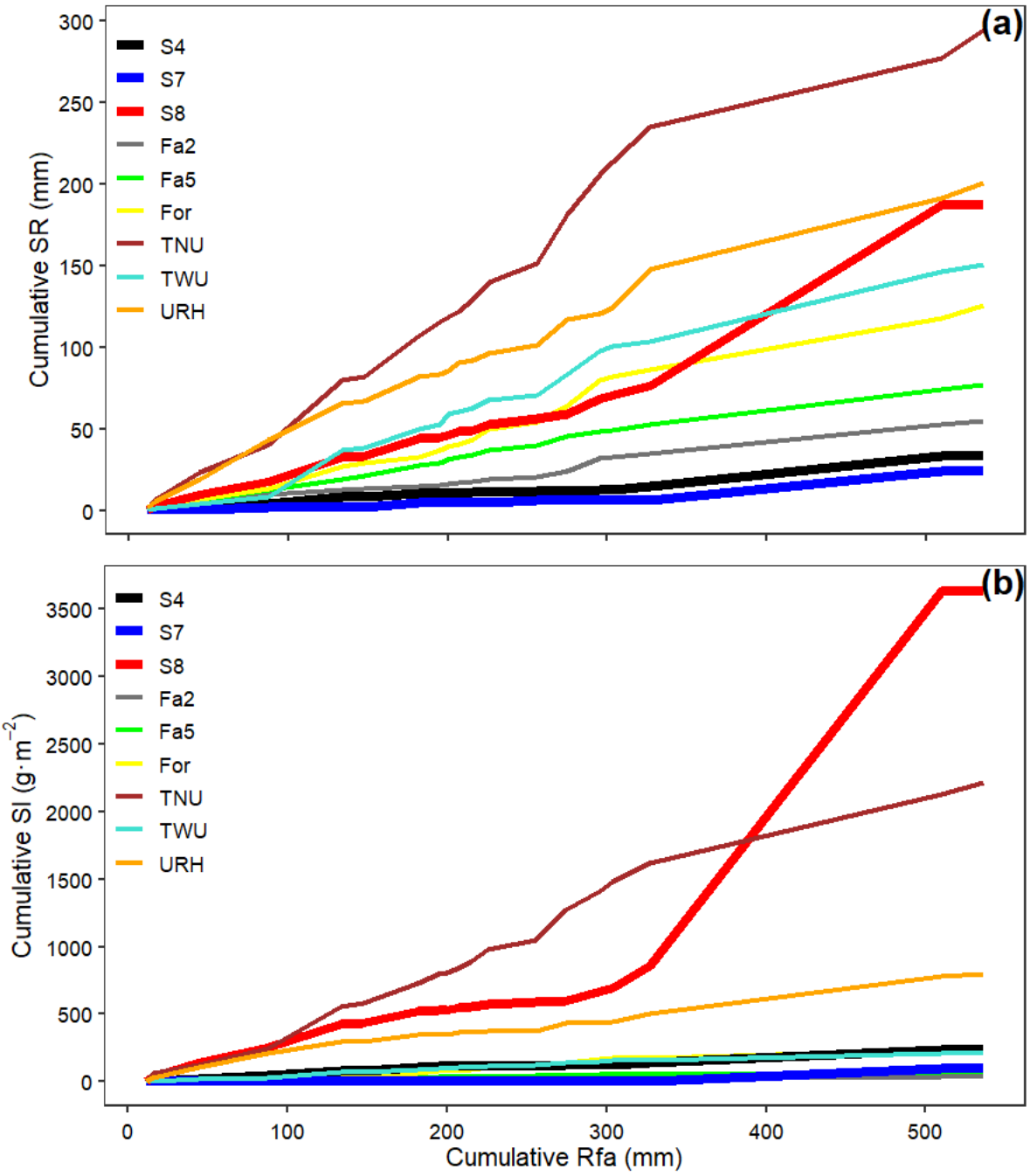

Figure 6.4: (a) Cumulative surface runoff (SR; mm) versus cumulative rainfall (Rfa, mm), and (b) cumulative soil loss (Sl; g·m^{-2}) versus cumulative Rfa, in the catchment (S4), the micro-catchments (S7 and S8), and the microplots (Fa2, Fa5, For, TNU, TWU, and URH), measured from 8 July to 22 September 2014, in Houay Pano catchment, northern Lao PDR. Fa2: fallow of 1 – 3 years; Fa5: fallow of 4 – 15 years; For: forest; TNU: teak without understory; TWU: teak with understory; URH: upland rice.

6.3.2. *Surface runoff and soil loss on micro-catchment scale and comparison of S7 and S8*

Seasonal SR and seasonal Sl in S8 (187.95 mm and 3635 $g \cdot m^{-2}$, respectively) were higher than in S7 (24.12 mm and 95 $g \cdot m^{-2}$, respectively) (**Figure 6.4**). SR (p-value < 0.0001) and Sl (p-value < 0.0001) in S8 were both significantly higher than in S7. The median of SR in S7 and S8 were 0.04 and 2.66 mm, respectively (**Figure 6.5**). The median of Sl in S7 and S8 were 0.03 and 21 $g \cdot m^{-2}$, respectively. SR and Sl for the extreme rainfall event in S8 were 111.22 mm and 2778 $g \cdot m^{-2}$, respectively, while the highest SR and Sl in S7 were 17,65 mm and 88 $g \cdot m^{-2}$, respectively.

6.3.3. *Surface runoff and soil loss at the catchment scale (S4)*

Seasonal SR and Sl in S4 were 33.32 mm and 236 $g \cdot m^{-2}$, respectively (**Figure 6.4**). The median SR and Sl in S4 were 0.41 mm and 2 $g \cdot m^{-2}$, respectively. SR and Sl for the extreme rainfall event were 18.02 mm and 93 $g \cdot m^{-2}$, respectively.

6.3.4. *Comparison of soil loss between scales*

Figure 6.5 shows the measured Sl compared to the weighted Sl in S8, S7, and S4. **Figure 6.5a, c, and e** included the extreme event as **Figure 6.5b, d, and f** excluded the extreme event. In S8, the median measured Sl (21 $g \cdot m^{-2}$) was not significantly different from the weighted Sl (35 $g \cdot m^{-2}$) with p-value > 0.372. In S7, the median measured Sl (0.03 $g \cdot m^{-2}$) was less than the weighted Sl (7 $g \cdot m^{-2}$) with the p-value < 0.0001. In S4, the median measured Sl (2 $g \cdot m^{-2}$) was less than the weighted Sl (22 $g \cdot m^{-2}$) with p-value < 0.001.

For the extreme event, in S8, measured Sl (2778 $g \cdot m^{-2}$) was more than 11 times higher than weighted Sl (246 $g \cdot m^{-2}$). However, in S7, the weighted Sl (83 $g \cdot m^{-2}$) was similar to the measured Sl (83 $g \cdot m^{-2}$). In S4, the measured Sl (159 $g \cdot m^{-2}$) was higher than the measured Sl (94 $g \cdot m^{-2}$).

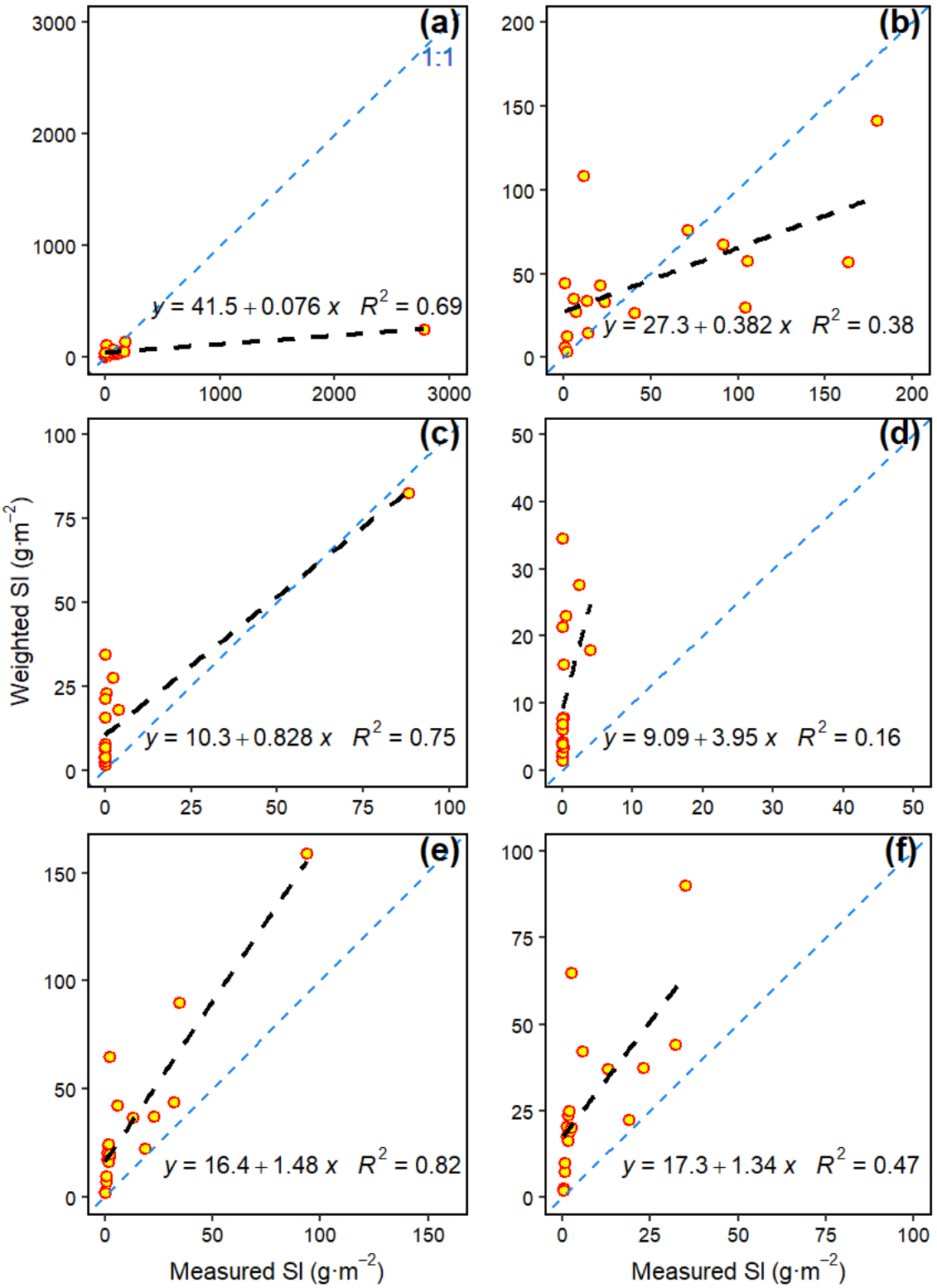

Figure 6.5: Measured and weighted soil loss (Sl; g·m^{-2}) of S8 (a, b), S7 (c, d), and S4 (e, f). a, c, and e included the extreme event of 17 September 2014, where a landslide occurred within the catchment, while b, d, and f excluded this extreme event.

Figure 6.6 compares the measured Sl with the predicted Sl (Model 1 with the application of Monte Carlo method) in S8 (a), S7 (b), and S4 (c). For S8, the predicted Sl was underestimated compared to the measured Sl. For S7 and S4, the predicted Sl was overestimated compared to the measured Sl. Seasonal Sl in S4 was smaller than in S8 but higher than in S7 (**Figure 6.4**).

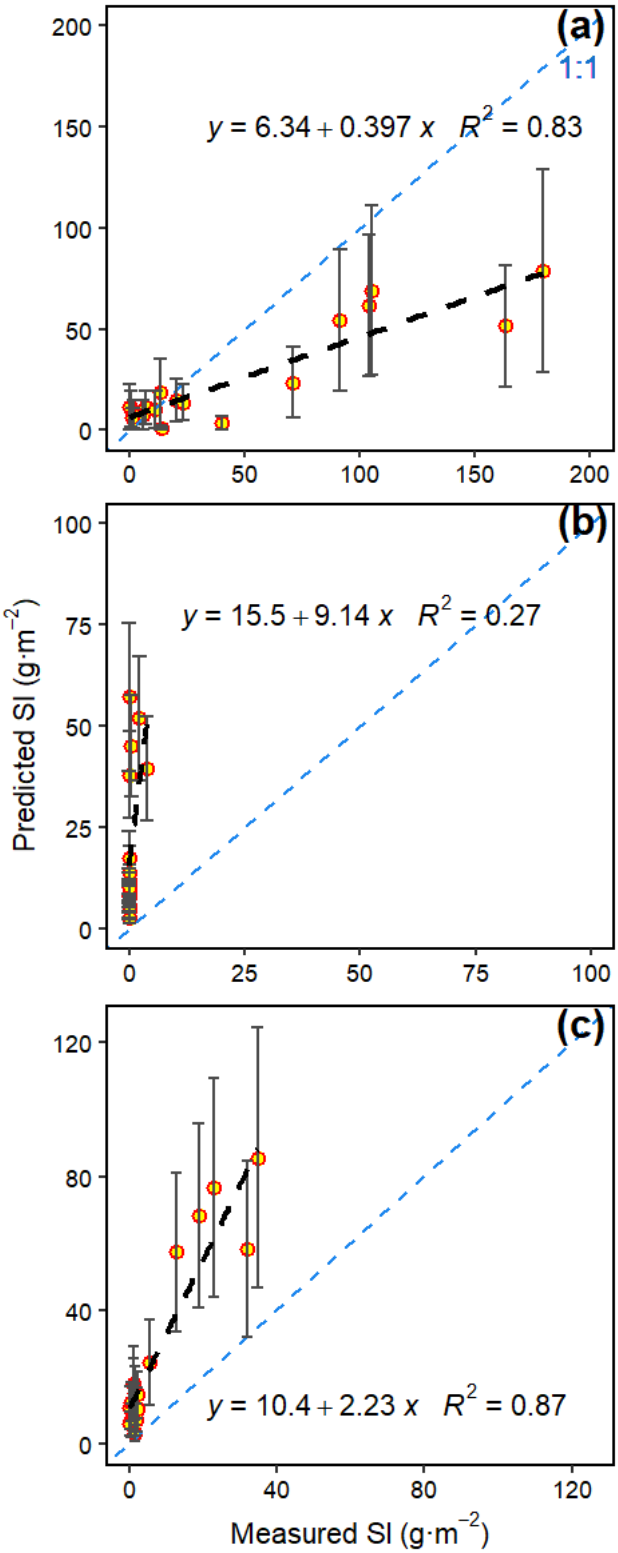

Figure 6.6: Measured and predicted soil loss (Sl; $g \cdot m^{-2}$) of (a) S8, (b) S7, and (c) S4 without the extreme event. Predicted Sl was based on Model 1 using the Monte Carlo method. Measured Sl were monitored at the outlets of the catchment S4, and of the micro-catchment S7 and S8, from 8 July to 22 September 2014, in Houay Pano catchment, northern Lao PDR.

6.3.5. *Soil loss model improvement and upscaling*

Figure 6.7 compares the measured Sl with the predicted Sl by Model 1 (a) and Model 2 (b) on the micro-catchment (S7 and S8) and catchment (S4) scales. Sl was underestimated by Model 1. However, after upscaling Model 1 by adding linear erosion and deposition factors of hillslope and catchment scales into Model 1 (R^2 = 0.48), Model 2 predicted Sl with an R^2 of 0.92. The equation of soil loss of Model 2 is given in **Eq. 6.10**:

$$\ln(Sl) = -4.39 + 0.91 \cdot \ln(KE \cdot Rc) - 2.47 \cdot 10^{-2} \cdot Gra - 2.29 \cdot 10^{-2} \cdot Res + 76.63 \cdot F_{LE} - 21.05 \cdot F_{TE} \quad \textbf{Eq. 6.10}$$

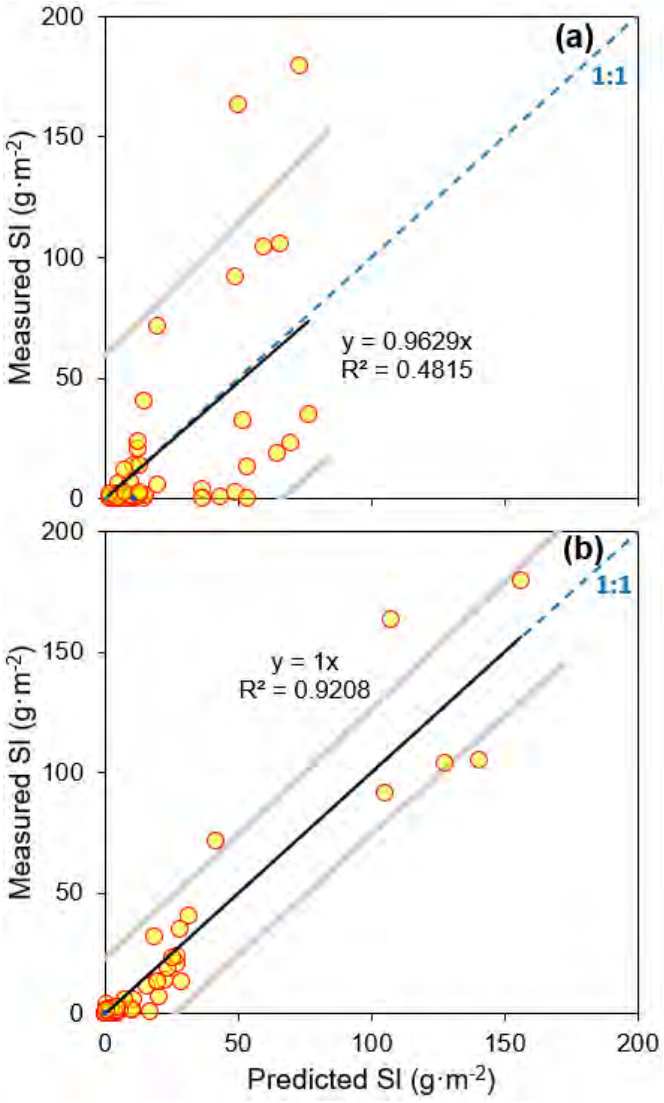

Figure 6.7: Measured and predicted sediment yield (Sl; g·m^{-2}): (a) Model 1 (inter rill erosion (**Chapter 5**)) and (b) Model 2 (Model 1 with linear erosion and sediment deposition processes). Measured Sl were monitored at the outlets of the catchment S4, and of the micro-catchment S7 and S8, from 8 July to 22 September 2014, in Houay Pano catchment, northern Lao PDR.

6.4. DISCUSSION

6.4.1. *Teak tree plantation impact on surface runoff and soil loss at the micro-catchment scale*

Surface runoff and soil loss in S8 are significantly higher than those in S7 (p-value < 0.0001). Seasonal surface runoff and seasonal soil loss in S8 were respectively 8 and 38 times higher than seasonal surface runoff and seasonal soil loss in S7. During the extreme event of 17 September 2014, the soil loss occurred in S8 was 32 times higher than the soil loss in S7. However, excluding this extreme event, seasonal soil loss in S8 was 122 times higher than the seasonal soil loss in S7.

This could be firstly explained by the area of teak trees with no understory in S8, which caused high soil detachment by the raindrops on the microplot scale (see **Chapter 4**). Furthermore, in S7, there were vegetated waterways which might attenuate the soil erosion and make the sediment deposing. In the same year of 2014, on the microplot scale in the Houay Pano catchment, seasonal soil loss in TNU was 53 and 30 times greater than seasonal soil loss of Fa2, and Fa5, respectively. The bare soil in TNU is susceptible to erosion from both soil detachment by splash and transport with surface runoff (Ehigiator and Anyata, 2011; Lacombe et al., 2018; Neyret et al., 2020; Patin et al., 2018; Ribolzi et al., 2017) due to soil surface crusting which limits the infiltration and enhances overland flow (Patin et al., 2012; Valentin et al., 2008). In addition, the observation at the microplot scale in the same catchment showed that the infiltration rate under fallow is higher than the infiltration rate under teak trees (Patin et al., 2012): fallow dissipates rainfall kinetic energy, thus limits soil surface crusting (Ribolzi et al., 2017). In addition, in S8, we observed linear erosion by the gully (**Figure 6.8**): the gully accumulates detached soil and might enhance the soil loss as gully erosion exports the sediment from the hillslope (Chaplot et al., 2005b; Chaplot and Poesen, 2012; Valentin et al., 2005).

Figure 6.8: Eroded gullies in Houay Pano catchment

6.4.2. *Surface runoff and sediment yield from microplot to hillslope and catchment scale*

The seasonal surface runoff decreased from 195, 122, and 135 mm (weighting of S8, S7, and S4, respectively) in the microplot, to 188 mm (S8) and 24 mm (S7) on the hillslope, and to 33 mm (S4) on the catchment scale. The infiltration rate higher in the fallow than in the teak tree plantation may explain the lower surface runoff in S7 (Patin et al., 2012). The higher crusting rate in S8 (**Table 6.2**) would limit the infiltration and enhance surface runoff (explained in **0**), which may cause the small decrease in surface runoff from the microplot to the hillslope scale.

The seasonal sediment yield decreased from 662 and 275 $g \cdot m^{-2}$ (weighting of S4 and S7, respectively) in the microplot, to 95 $g \cdot m^{-2}$ (S7) on the hillslope, and increased to 236 $g \cdot m^{-2}$ (S4) on the catchment scale. Chaplot et al. (2005c) suggested that sediment could be deposited on the hillslope resulting from the high infiltration rate limiting the transport of sediment. In contrast, soil loss increased from 1065 $g \cdot m^{-2}$ (weighting of S8) in the microplot to 3634 $g \cdot m^{-2}$ (S8) on the hillslope scale. The increase in seasonal soil loss in S8 on the hillslope scale can be due to the large contribution of soil loss caused by the teak tree plantation (Ribolzi et al., 2017). Many authors suggested that the sediment yield from a hillslope or a catchment is likely to be less than the total soil loss from the microplots (Chaplot and Poesen, 2012; Polyakov and Lal,

2008; Roehl, 1962; Walling, 1983), because of additional processes occurring on the hillslope and catchment scales, with only a relatively small proportion of the detached and transported soil material getting out of the catchment (Beven et al., 2005; De Vente et al., 2007; Parsons et al., 2008; Walling et al., 2006).

The sediment yield (236 $Mg \cdot km^{-2}$) of the catchment (S4) was low compared to those reported in the region dominated by tropical monsoon and with intensive agricultural activities such as Thailand (5100 $Mg \cdot km^{-2}$) (Janeau et al., 2002), the Philippines (2700 $Mg \cdot km^{-2}$) (Zhang et al., 2018), and Malaysia (400 $Mg \cdot km^{-2}$) (Negishi et al., 2008), which can be explained: (a) only 19 individual rainfall events of the rainy season taken into account in our study and (b) more intensive cultivation and typhoons which high precipitation and landslides in those countries.

Model 1 has some limitations, since it takes into account the erosion at the microplot scale only. The result of applying this equation with the runoff formula of Patin et al. (2012) on the hillslope and catchment scales is not satisfying since the model was designed for the microplot scale (**Figure 6.6**). Bracken et al. (2015) suggested that scaling up erosion rates is difficult with some problem of extrapolation of erosion rate to explain the processes of transfer, and suggested that it is necessary to consider all the mechanisms of detachment and transport of sediment in the approaches of sediment connectivity. In the previous chapter and the other studies (Verstraeten et al., 2006; Vigiak et al., 2008), the riparian buffer showed its importance in trapping the sediment on the hillslope. Furthermore, Nakhle et al. (2021) highlighted that headwater wetlands play an important role in sediment deposition. Wenger (1999) highlighted that several research findings suggested that stream channel and gully erosion can be the major sources of sediment in watersheds, with a significant proportion of 80% of the total sediment yield. Underestimation of soil loss can be due to the failure to include soil loss by linear erosion in the gully (Vandaele and Poesen, 1995). We observed riparian buffer, vegetated waterway, headwater wetland, and gully in the catchment (**Figure 6.1** and **Figure 6.8**). Hence, we further improved our initial soil loss model (Model 1) by considering additional processes that don't happen in the microplot scale, i.e., linear erosion and deposition. Linear erosion by rill and gully is an intensifying factor which occurs on the hillslope scale. Headwater wetland, vegetated waterway, and riparian buffer are attenuating factors which cause the sediment deposing before flowing downstream. We were then able to improve Model 1 by considering those factors our improved soil loss model (Model 2) which covered all the processes controlling the sediment transfer.

Based on Model 2, we could differentiate the fractions of the erosion of both inter rill and linear erosion and the deposition. In S4, inter rill erosion (443 $g \cdot m^{-2}$) contributed the most to the soil loss (163 $g \cdot m^{-2}$) but was reduced through the deposition on the hillslope and catchment scales (328 $g \cdot m^{-2}$) as explained above (**Figure 6.9**). Linear erosion contributed less to the soil loss in the catchment. Different fractions of soil loss contributions were predicted in S8 and S7 (**Table 6.3**).

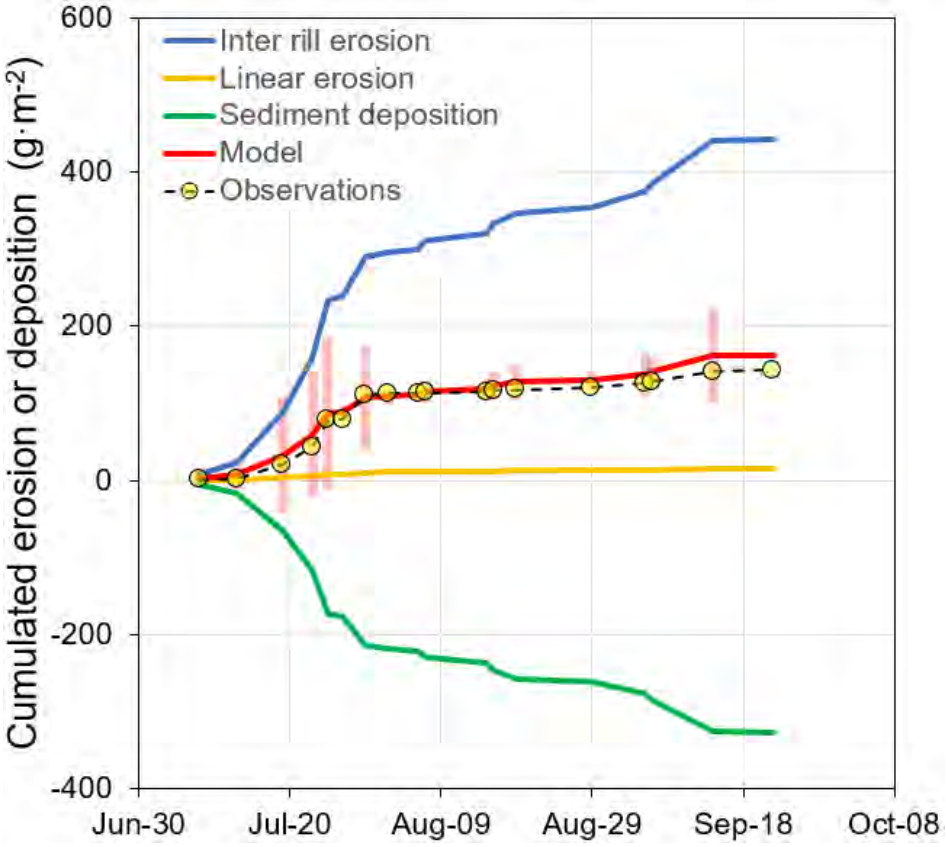

Figure 6.9: Cumulative erosion and deposition of the soil of the catchment scale (S4): inter rill erosion (blue), linear erosion (yellow), deposition (green), predicted soil loss (red), and measured soil loss (dashed line with yellow circles). Soil loss was measured from 8 July to 22 September 2014 in Houay Pano catchment, northern Lao PDR. Soil loss measured during the extreme rainfall event of 17 September 2014 was excluded.

Table 6.3: Observed and modelled sediment yield and erosion processes contributing to sediment yield excluding the extreme rainfall event of 17 September 2014.

$g \cdot m^{-2}$	S4	S8	S7
Observed sediment yield	143	857	7
Modeled sediment yield	163	905	9
Inter rill erosion	443	424	316
Linear erosion	16	482	0

Sediment deposition	328	0	307

In S8, soil loss from simulated inter rill erosion (424 $g \cdot m^{-2}$) was similar to the soil loss from simulated linear erosion (482 $g \cdot m^{-2}$), and no deposition was predicted. This similar contribution of inter rill and linear erosion was aligned with the finding of Chaplot et al. (2005b). In contrast, inter rill erosion in S7 was almost offset by sediment deposition with no contribution of linear erosion. Land use explained the different linear erosion in S7 and S8. Land use is suggested as the main controlling factors in the generation and development of the gully and can be a predictor of soil loss (Chaplot et al., 2005a; Chaplot et al., 2005b). Consistently, no gully was observed in S7.

Though Model 2 provided satisfactory results by considering more parameters that characterize the processes on the hillslope and on the catchment scales, the extreme rainfall event of 17 September 2014 was not taken into account in the model. In S8, a significant outlier is depicted, which can be explained by the extreme rainfall event which generated an extreme flood and several landslides within the micro-catchment (**Figure 6.10**). This extreme rainfall event contributed (2778 $g \cdot m^{-2}$) approximately 76% to the seasonal soil loss. Using Model 2, we calculated the soil loss of this event and found that soil loss was 694 $g \cdot m^{-2}$. The difference between the observed and the predicted soil loss of this event was 2084 $g \cdot m^{-2}$, which accounted for 57% of the seasonal soil loss. As mentioned above, landslides, resuspension of the sediment from the hillslope and from the streambed, and bank erosion during the flood may explain this large contribution. More frequent extreme rainfall events, with higher rainfall intensities per day, were observed in the Houay Pano catchment from 2014 to 2019 (Boithias et al., 2021), which possibly led to several landslides. During the period of our study, the extreme rainfall event on 17 September 2014 excluded from the model has daily rainfall of 182.8 mm (during 13 h). Landslide is known to contribute to the soil loss in the catchment during extreme events (Zhang et al., 2018). Large volumes of surface runoff can lead to the resuspension of high amount of deposited sediment in the catchment. Hence, considering the extreme events where landslides possibly occur is of importance, and this factor should, in the future, be integrated into the prediction of soil loss.

Figure 6.10: Landslide occurred behind the weir of S8 in the Houay Pano catchment

On the hillslope scale, sediment deposition and linear erosion by gully may be affected by the hillslope topography (Buckley, 2010; Sabzevari and Talebi, 2019) (also see **Chapter 2**). Finding of Verstraeten et al. (2006) showed that, on straight hillslope, sediment reduction by riparian buffer is large with the efficiency greater than 70%. Divergent and parallel hillslope may allow efficient sediment trapping by riparian buffers as surface runoff flowing through these shapes is not concentrated. On convergent hillslope, the sediment flow may concentrate and by pass the riparian buffer through gullies (Verstraeten et al., 2006; Wenger, 1999), especially under heave rainfalls (de Rouw et al., 2018). Sabzevari and Talebi (2019) suggested that hillslope topography significantly affects soil erosion and sediment yield. Hence, it will be useful to consider hillslope topography into the soil loss prediction in the future.

6.5. CONCLUSIONS

We investigated the effect of teak-tree plantation on surface runoff and soil loss/sediment yield on various spatial scales in a mixed land uses mountainous tropical catchment. Processes of sediment transfer from the plot to the catchment scale were assessed. Our main findings suggested that:

- On the hillslope scale, seasonal surface runoff and sediment yield in the teak-dominated micro-catchment (187.95 mm and 3635 $Mg \cdot km^{-2}$, respectively) were significantly higher (p-value < 0.001) than those in the mixed-land-use micro-catchment (24.12 mm and 95 $Mg \cdot km^{-2}$, respectively).
- The seasonal surface runoff and sediment yield decreased from 122 – 135 mm and 275 – 662 $Mg \cdot km^{-2}$, respectively, on the microplot scale; to 24 mm and 95 $Mg \cdot km^{-2}$, respectively, on the micro-catchment scale; and increased to 33 mm and 236 $Mg \cdot km^{-2}$, respectively, on the catchment scale. In contrast, sediment yield in the teak tree plantation increased from 1065 $Mg \cdot km^{-2}$ on the microplot scale, to 3635 $Mg \cdot km^{-2}$ on the micro-catchment scale, which can be explained by the additional linear erosion along the gully. This finding suggests that gully erosion in the teak tree-dominated catchment is significant and may be associated to the improper management practice of leaving bare soil under the teak tree.
- Upscaling sediment yield from the microplot to micro-catchment and catchment scales improved our soil loss prediction by taking into account erosion on the plot scale, linear erosion, and sediment deposition throughout the catchment. Our soil loss model yielded a R^2 of 0.92 but was limited to reproduce the extreme event of September 17. Soil loss during this extreme event may be explained by the extreme flood event and by the occurred landslides, which may have become an important source of sediment resuspension.
- The model predicted that sediment yield was mostly contributed by inter rill erosion (443 $Mg \cdot km^{-2}$), but later deposed throughout the catchment (S4) by attenuating factors such as riparian grass, headwater wetland, and vegetated waterway. This contribution was in contrast to soil loss of the micro-catchment dominated by teak tree plantation (S8) with similar rates of inter rill (424 $Mg \cdot km^{-2}$) and linear erosions (482 $Mg \cdot km^{-2}$) and without sediment deposition.

On the catchment scale, soil erosion and sediment exportation are influenced by natural and anthropogenic activities, such as land use (i.e., vegetation and management practices), soil properties, topography (Bonetti et al., 2019; Sabzevari and Talebi, 2019) and climate (e.g., rainfall characteristics (Arnaez et al., 2007; Assouline and Ben-Hur, 2006)). The hillslope topography should be taken into account in the study, which characterize the catchment and may affect the trapping and/or the transfer of sediment. Divergent and linear hillslope may enhance the sediment deposition by the mean of the trapping of riparian grass. Convergent hillslope may favour the formation of gullies which contribute to the linear erosion. In addition, the gully may act as a bypass and discharge the sediment into the stream, even if a riparian grass buffer is kept along the stream. Moreover, a study conducted in the same catchment (Houay Pano) by Chaplot et al. (2005b) reported that the formation of linear features accounted for most of the sediment exported from the catchments, as tillage and inter rill erosion only redistribute the sediments on the hillslope. However, in this study, both linear erosion by gully and inter rill erosion contributed to the sediment yield at the same rate. Hence, the effect of teak tree plantation on gully formation should be further assessed to confirm the increase in soil loss on the hillslope scale.

Chapter 7. Conclusions and perspectives

"Smile and enjoy life"

Chapter 7

Conclusions and perspectives

7.1. GENERAL CONCLUSIONS

This thesis focuses on the analyses of data collected on the microplot (1 m^{-2}), hillslope including micro-catchment (0.6 ha), and catchment (60 ha) scales. Surface runoff and soil loss were measured on the three observation scales, and using different *in situ* monitoring and modelling tools suitable for each spatial scale, in the teak tree-cultivated areas in the tropical mountainous region of northern Lao PDR.

On the microplot scale (**Figure 7.1a**), we assessed the effect of understory management on surface runoff and soil loss in the teak tree plantation. The teak tree plantation with no understory generated the highest seasonal surface runoff (612 mm) and seasonal soil loss (5455 $g \cdot m^{-2}$), while the teak tree plantation with understory, such as broom grass, had the smallest seasonal surface runoff (242 mm) and seasonal soil loss (381 – 465 $g \cdot m^{-2}$). The seasonal surface runoff and soil loss in the teak tree plantation with low density of understory were 358 mm and 1115 $g \cdot m^{-2}$, respectively. The highest seasonal surface runoff and soil loss in the teak tree plantation without understory is generally associated to the highest crusting rate (82%) caused by kinetic energy of rain drops falling from the broad leaves of the tall teak trees down to the bare soil devoid of plant residues hence leading to soil detachment. Hence, the soil loss in the teak tree plantation with understory was 14-times less than in teak tree plantation with no understory, and teak tree plantation owners could divide soil loss by 14 by keeping understory, such as broom grass, within their plantations. We suggested that the areal percentage of pedestal features was a reliable indicator of soil erosion intensity.

On the hillslope scale (**Figure 7.1b**), we assessed the ability of riparian grass buffers to mitigate surface runoff, soil loss, and water and sediment trapping efficiencies in the teak tree plantations with no understory. Our findings suggest that teak tree plantation with no understory generated the highest seasonal surface runoff (415 mm) and seasonal soil loss (5791 $g \cdot m^{-2}$), thus higher than seasonal surface runoff and soil loss in grass with a few teak trees inside (93 mm, 250 $g \cdot m^{-2}$) and in grass nearby teak trees (138 mm, 159 $g \cdot m^{-2}$). Seasonal soil loss in teak tree plantations could be divided by 23 by leaving riparian grass. On the event and microplot scale, soil loss was well predicted by rainfall kinetic energy, runoff coefficient, and areal percentage of grass and residues. Riparian grass effectively trapped surface runoff and sediment for buffer lengths less than 6 m. The water trapping efficiencies of 6-m buffer of riparian grass was significantly

higher than the one of 3-m buffer. The median water, sediment and sediment concentration trapping efficiencies of 6-m buffer of riparian grass reached 0.86, 0.98 and 0.88, respectively. However, the trapping efficiency was less effective for extreme rainfall events (24-hour rainfall > 54.8 mm).

On the micro-catchment scale (i.e., convergent hillslope; **Figure 7.1c**), we assessed the effect of land use on surface runoff and soil loss, and compared surface runoff and soil loss in a micro-catchment dominated by teak tree plantation and in a micro-catchment with mixed land uses. Seasonal surface runoff (188 mm) and seasonal sediment yield (3635 $Mg \cdot km^{-2}$) were significantly higher in the teak tree-dominated micro-catchment than in the mixed-land-use micro-catchment. The gully formed in the teak tree-dominated micro-catchment accumulated soil particles detached by splash effect and eroded soil particles in the gully itself. Based on the modelling result, the contribution of gully erosion (482 $Mg \cdot km^{-2}$) was approximately the same as the contribution of interrill erosion (424 $Mg \cdot km^{-2}$). The finding from the multi-scale assessment (microplot, micro-catchment, and catchment scales) suggested that amounts of seasonal surface runoff and sediment yield decreased from the microplot (122 – 135 mm and 275 – 662 $Mg \cdot km^{-2}$, respectively), to the micro-catchment (24 mm and 95 $Mg \cdot km^{-2}$), and increased to the catchment scales (33 mm, 236 $Mg \cdot km^{-2}$) (**Figure 7.1e**). In contrast, teak tree plantation generated higher sediment yield (1065 $Mg \cdot km^{-2}$) from the microplot to (3635 $Mg \cdot km^{-2}$) the micro-catchment scale. This finding suggests that gully erosion in the teak tree-dominated catchment is significant and may be associated to the improper management practice of leaving bare soil under the teak tree. Soil loss on the microplot scale is mainly associated with detachment by rain splash. On both the micro-catchment and the catchment scales, soil loss is controlled by entering fluxes of soil particles from the upslope position; intensifying factors, such as the linear erosion by gully; and attenuating factors, such as the deposition of suspended sediment (by trapping factors, e.g., riparian grass buffers) and the trapping by headwater wetlands and vegetated waterways. Our upscaled soil loss model was able to predict sediment yield on the catchment scale and to quantify the contribution of inter rill erosion, linear erosion, and sediment deposition to the sediment yield but was limited to reproduce the extreme event.

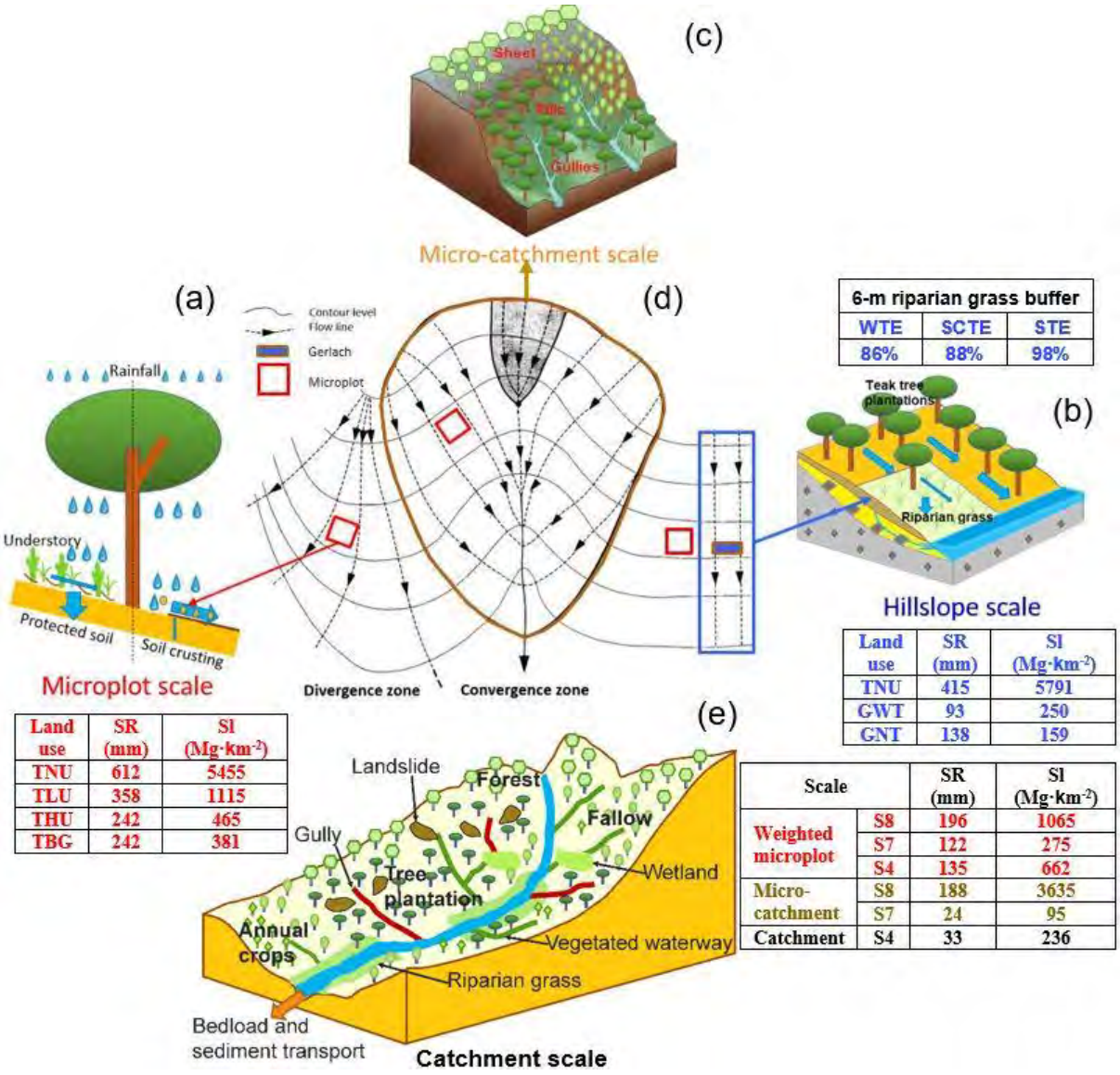

6-m riparian grass buffer		
WTE	SCTE	STE
86%	88%	98%

Land use	SR (mm)	Sl (Mg·km^{-2})
TNU	612	5455
TLU	358	1115
THU	242	465
TBG	242	381

Land use	SR (mm)	Sl (Mg·km^{-2})
TNU	415	5791
GWT	93	250
GNT	138	159

Scale		SR (mm)	Sl (Mg·km^{-2})
Weighted microplot	S8	196	1065
	S7	122	275
	S4	135	662
Micro-catchment	S8	188	3635
	S7	24	95
Catchment	S4	33	236

Figure 7.1: Synthesized surface runoff (SR, mm) and soil loss/sediment exportation (Sl, Mg·km^{-2}) on multiple scales: (a) Microplot scale, (b) hillslope scale, including (c) micro-catchment scale, (e) catchment scale, and (d) sketch representing SR and Sl monitoring on microplot and hillslope scales including micro-catchment scale. TNU: teak with no understory; TLU: teak with low density of understory; THU: teak with high density of understory; TBG: teak with broom grass; GWT: grass with few teaks planted inside; GNT: grass nearby teak trees; S8 and S7: micro-catchments; and S4: catchment (Houay Pano).

7.2. RECOMMENDATIONS AND PERSPECTIVES

The study conducted on the microplot scale suggests that promoting understory such as broom grass in teak tree plantations would effectively reduce surface runoff and soil loss on the plot scale. In such a context, to favour water infiltration and mitigate soil erosion in steep slope areas such as the montane regions of Southeast Asia, decision makers should, if not legally enforce the maintenance of understory strata in teak tree plantation, at least recommend the plantations owners to maintain understory and avoid the burning of understory and of plant residue.

In addition to maintaining the understory strata, encouraging the use of e.g., riparian zone buffers along the streams (Ahmad et al., 2020; Bhat et al., 2019) could also be recommended to trap soil particles from the cultivated hillslopes and favor surface runoff infiltration, and thus ensure the sustainability of the agro-ecosystem and its long-term productivity on the hillslope scale. To improve management practices in teak tree plantations in mountainous tropical areas, we provide in this study the additional suggestion of leaving riparian grass buffers of at least 6 m to capture soil loss originating from the uplands. Riparian grass buffers may be more effective when integrated with a management practice that keeps understory in the teak tree plantation to reduce on-site soil erosion and hence, to avoid high sediment load discharging into the river. Furthermore, the understanding of riparian grass behaviour in soil particle trapping on a large spatial scale is important to suggest countermeasures against soil degradation in the agricultural land. Further research is now needed to assess if riparian grass may play an important role in reducing surface runoff and soil loss on the catchment scale.

On the catchment scale, soil erosion and sediment exportation are influenced by natural and anthropogenic activities, such as land use (i.e. vegetation and management practices), soil properties, topography (Bonetti et al., 2019; Sabzevari and Talebi, 2019) and climate (e.g. rainfall characteristics (Arnaez et al., 2007; Assouline and Ben-Hur, 2006)). The hillslope topography should be taken into account in the study, which characterize the catchment and may affect the trapping and/or the transfer of sediment. Divergent and linear hillslope may enhance the sediment deposition by the mean of the trapping of riparian grass. Convergent hillslope may favour the formation of gullies which contribute to the linear erosion. In addition, the gully may act as a bypass and discharge the sediment into the stream, even if a riparian grass buffer is kept along the stream. Moreover, a study conducted in the same catchment (Houay Pano) by Chaplot et al. (2005b) reported that the formation of linear features accounted for most of the sediment exported from the catchments, as tillage and inter rill erosion only redistribute the sediments on the hillslope. However, in this study, both linear erosion by gully and inter rill

erosion contributed to the sediment yield at the same rate. Hence, the effect of teak tree plantation on gully formation should be further assessed to confirm the increase in soil loss on the hillslope scale.

The effect of extreme rainfall event on soil erosion was not assessed in this study. Nowadays, the carbon released into the atmosphere through deforestation is an issue of growing concern due to its potential contributions to global climate change (Achard et al., 2004; Defries et al., 2007; Defries et al., 2002; Eva et al., 2010; Houghton et al., 2000; Skutsch et al., 2007; van der Werf et al., 2009). The change in climate is expected to bring a more vigorous hydrological cycle, including more total rainfall and more frequent high intensity rainfall events around the globe (Borrelli et al., 2020; Nearing et al., 2004), which then increases the risk of soil erosion. Furthermore, a research conducted in the transnational watershed of Laos and Vietnam (Upper Ca River Watershed) predicted that soil erosion will significantly increase due to the warmer and wetter climate of the wet season triggered by climate change (Giang et al., 2017). Extreme events may also cause high sediment resuspension and landslides, which contribute to enormous loads of sediment downstream. Hence, a sound understanding of these factors as driving forces and characteristics of the system influencing soil erosion is vital. Further investigation by integrating all the factors including rainfall characteristics and landslides into the prediction of soil erosion and of sediment transfer is suggested to fully explain the connectivity of sediment transfer from a source to a sink within a catchment, i.e., from the local erosion to the outlet of the catchment. Soil erosion may in return contribute to global carbon release which changes the climate as soil acts as a sink for greenhouse gases (Bhat et al., 2019). This loop may interchange their impacts and intensify both climate change and soil erosion. To comate adverse effects of this loop, one of the suitable measures is to apply sustainable soil management practices as suggested in this study to limit soil erosion (Borrelli et al., 2017).

At the microplot scale, our findings are relevant to farmers concerned about soil loss and soil fertility in their teak tree plots. The farmer would earn additional incomes by practicing intercropping in the teak tree plantations, for example, keeping broom grass in the tree plantation. This practice will not only alleviate the loss of soil fertility, and the loss of soil as a support for agricultural production, but also add economic value to the overall plantation yield, and may supply a range of ecosystem services downstream. For example, at catchment scale, the practices of both keeping understory and riparian grass are relevant to decision makers concerned with the management of costs (such as the cost of water treatment, infrastructure rehabilitation such as dam reservoir dredging, and natural disaster mitigation) resulting from

soil loss induced by upslope activities such as tree plantations and improper agricultural land management.

The suggested measures provide on-site and off-site benefits to the agro-ecosystem; however, soil erosion mitigation measures may sometimes make the sediment yield worse on the catchment scale. For example, if there is no mitigation measure applied at the plot scale, the eroded soil particles from the uplands will settle down within the riparian area by mean of grass trapping. After a long period of time, this accumulated deposit of sediment may cause landslides, which contribute in turn to the overall sediment exportation. In the opposite, applying as much mitigation measures as to stop sediment exportation, may cause water in the river to be clear: so-called "hungry" water has an increased erosive potential of the river banks and bed. Furthermore, clear streamflow may not transport the nutrient-rich suspended sediment, and thus limit the supply of fertile inputs on the river banks, floodplains and in the river delta. A limited runoff may also induce saltwater intrusion in the delta, and affect groundwater quality and agricultural yields.

The findings based on the multi-scale assessment of this thesis will provide social and scientific communities quantitative results on soil erosion form the local scale to the catchment. The farmers and policy makers will gain more understanding of good land management practices and implement appropriate policy for the sustainability of their environment and benefits. The findings of this thesis research will contribute to further investigation of integration of all processes (i.e., interrill erosion, linear erosion, deposition, resuspension, and landslide) and controlling factors (i.e., understory, riparian grass, wetland, vegetated waterway, rainfall characteristics, and topography) described here into models.

Chapter 7

Conclusions et perspectives

7.3. CONCLUSIONS GÉNÉRALES

Cette thèse se concentre sur les analyses des données collectées à l'échelle de la micro-parcelle (1 m^{-2}), du versant, du micro-bassin (0,6 ha) et du bassin versant (60 ha). Le ruissellement de surface et la perte en sols ont été mesurés à l'aide des différents outils expérimentaux basés sur les échelles, les événements pluviométriques importants et les utilisations des terres, dans les zones cultivées en teck dans la région montagneuse tropicale du nord de la RDP lao.

À l'échelle de la micro-parcelle (**Figure 7.1a**), nous avons évalué l'effet du traitement avec différentes gestions du sous-couvert sur le ruissellement de surface et la perte en sols dans la plantation de teck. La plantation de teck sans sous-couvert a généré le ruissellement de surface (612 mm) et la perte en sols (5455 $g \cdot m^{-2}$) les plus élevés, car la plantation de teck avec sous-couvert tel que l'herbe à balai avait le plus petit ruissellement de surface (242 mm) et la perte en sols (381 – 465 $g \cdot m^{-2}$). Le ruissellement de surface et la perte en sols dans la plantation de teck à faible densité de sous-couvert étaient respectivement de 358 mm et 1115 $g \cdot m^{-2}$. Le ruissellement de surface et la perte en sols les plus élevés dans la plantation de teck sans sous-couvert sont généralement associés au taux de croûte le plus élevé (82 %) causé par l'énergie cinétique des gouttes de pluie tombant des larges feuilles des grands tecks jusqu'au sol nu dépourvu de résidus végétaux entraînant ainsi un détachement du sol. Par conséquent, la perte en sols dans la plantation de teck avec sous-couvert était 14 fois inférieure à celle de TNU et les propriétaires de plantations de teck pouvaient diviser la perte en sols par 14 en gardant le sous-couvert, comme l'herbe à balai, dans les plantations de teck. Nous avons suggéré que le pourcentage de surface des piédestals était un indicateur fiable de l'intensité de l'érosion du sol.

Sur le versant (**Figure 7.1b**), nous avons évalué l'impact des zones tampons d'herbes rivulaires sur le ruissellement de surface, la perte en sols et l'efficacité de piégeage de l'eau et des sédiments dans les plantations de teck sans sous-couvert. Nos résultats suggèrent que les plantations d'arbres de teck sans sous-couvert généraient toujours le ruissellement de surface le plus élevé (415 mm) et la perte en sols (5791 $g \cdot m^{-2}$) plus élevée que celles en herbe avec quelques tecks à l'intérieur (93 mm, 250 $g \cdot m^{-2}$) et en herbe à proximité de teck (138 mm, 159 $g \cdot m^{-2}$). La perte en sols dans les plantations de teck pourrait être divisée par 23 en laissant de l'herbe rivulaire. À l'échelle des événements et des micro-parcelles, la perte en sols était bien prédite par l'énergie cinétique des précipitations, le coefficient de ruissellement, le pourcentage

de surface d'herbe et de résidus. L'herbe rivulaire a piégé efficacement le ruissellement de surface et les sédiments sur des longueurs tampons même inférieures à 6 m. L'efficacité de piégeage de l'eau de la zone tampon de 6 m de la zone rivulaire était significativement plus élevée que celle de la zone tampon de 3 m. L'efficacité médiane de piégeage de l'eau et des sédiments d'une zone tampon de 6 m de l'herbe rivulaire pourrait atteindre respectivement 0,86 et 0,88. Cependant, il était moins efficace pour les précipitations extrêmes (précipitations sur 24 heures > 35,4 mm).

A l'échelle du micro-bassin (**Figure 7.1c**), nous évaluons l'effet de l'utilisation des terres dominée par la plantation de teck et la jachère. Le ruissellement de surface et l'exportation de sédiments étaient significativement plus élevés dans le micro-bassin dominé par le teck que dans celui dominé par la jachère. La ravine formée dans le micro-bassin dominé par le teck a accumulé le sol détaché par effet d'éclaboussure et a contribué à plus d'érosion dans la formation de la ravine. On prévoyait que l'érosion en ravines contribuerait au même taux que l'érosion en nappe. Les conclusions de l'évaluation à plusieurs échelles suggèrent que le ruissellement de surface et l'exportation de sédiments diminuent de la micro-parcelle au micro-bassin versant et à l'échelle du bassin versant (**Figure 7.1e**). En revanche, la plantation d'arbres en teck a généré une exportation de sédiments encore plus élevée de la micro-parcelle à l'échelle du micro-bassin versant. Cette découverte suggère que l'érosion en ravines dans le bassin versant dominé par le teck est importante et peut être associée à une mauvaise pratique de gestion consistant à laisser le sol nu sous le teck. L'érosion des sols à l'échelle de micro-parcelle est principalement associée au détachement par éclaboussures de pluie. À l'échelle du versant, l'érosion du sol est contrôlée en entrant les flux provenant de la position amont et le dépôt de sédiments par le facteur de piégeage de la zone tampon d'herbes rivulaires. À l'échelle du micro-bassin et du bassin versant, l'érosion des sols est contrôlée par des facteurs plus intensifs et atténuants tels que l'érosion linéaire par ravine, les facteurs de piégeage par les zones humides d'amont et les cours d'eau végétalisés. Notre modèle de perte en sols à grande échelle a pu prédire le rendement en sédiments à l'échelle du bassin versant et quantifier la contribution de l'érosion en nappe, de l'érosion linéaire et du dépôt de sédiments au rendement en sédiments, mais s'est limité à reproduire l'événement extrême.

7.4. RECOMMANDATIONS ET PERSPECTIVES

L'étude menée à l'échelle de la micro-parcelle a suggéré que la promotion du sous-couvert tel que l'herbe à balai dans les plantations de teck réduisait efficacement le ruissellement de surface et la perte en sols à l'échelle locale. Dans un tel contexte, pour améliorer les conditions hydrologiques et atténuer l'érosion des sols dans les zones à forte pente telles que les régions montagneuses de l'Asie du Sud-Est, les décideurs devraient, sinon imposer légalement le maintien des strates de sous-couvert dans les plantations de teck, au moins recommander les propriétaires de plantations pour entretenir le sous-couvert et éviter le brûlage des couches de sous-couvert et de résidus végétaux.

En plus de maintenir les strates du sous-couvert, il pourrait également être recommandé d'encourager l'utilisation de zones tampons rivulaires le long des cours d'eau (Ahmad et al., 2020; Bhat et al., 2019) pour piéger les particules de sol des pentes cultivées et favoriser l'infiltration, et ainsi assurer la pérennité de la productivité agricole et de l'écosystème à l'échelle du versant. Pour améliorer les pratiques de gestion dans les plantations de teck dans les zones tropicales montagneuses, nous proposons dans cette étude la suggestion supplémentaire de laisser des zones tampons d'herbes rivulaires d'au moins 6 m pour capturer la perte en sols provenant d'amont du versant. Les zones tampons d'herbe rivulaire peuvent être plus efficaces lorsqu'elles sont intégrées à une pratique de gestion qui maintient le sous-couvert dans la plantation de teck pour réduire l'érosion des sols sur place et éviter ainsi le déversement d'une charge sédimentaire élevée dans la rivière. De plus, la compréhension du comportement d'herbe rivulaire du piégeage du sol à grande échelle est importante pour suggérer des contre-mesures contre la dégradation des sols dans les terres agricoles. Des recherches supplémentaires sont maintenant nécessaires pour évaluer si l'herbe rivulaire peut jouer un rôle important dans la réduction du ruissellement de surface et de la perte en sols à l'échelle du bassin versant.

À l'échelle du bassin versant, l'érosion des sols et l'exportation de sédiments sont influencées par les activités naturelles et anthropiques, telles que l'utilisation des terres, les pratiques de gestion, la végétation, les propriétés du sol, le cours d'eau, la topographie et le climat, comme souligné précédemment par de nombreux auteurs (Borrelli et al., 2020; Chaplot et al., 2005b; Chaplot and Poesen, 2012; Lacombe et al., 2018; J. Poesen, 2018; Ribolzi et al., 2017; Sabzevari and Talebi, 2019; Valentin and Rajot, 2018; Zhang et al., 2018). La topographie du versant doit être prise en compte dans l'étude, car elle caractérise le bassin versant et peut affecter le piégeage et le transfert des sédiments. Les versants convexes et linéaires peuvent augmenter le dépôt de sédiments par le piégeage d'herbe rivulaire. Le versant concave peut être

sensible à la formation du ravin qui contribue à l'érosion linéaire et le ravin peut contourner le flux de sédiments dans le cours d'eau. Par ailleurs, une étude menée dans le même bassin versant (Houay Pano) par Chaplot et al. (2005b) ont signalé que la formation ou le développement de caractéristiques linéaires représentaient la plupart des sédiments exportés des bassins versants, car le labour et l'érosion en nappe ne redistribuent les sédiments que sur le versant. Cependant, dans cette étude, l'érosion linéaire par le ravin et l'érosion en nappe ont contribué au même taux à l'exportation de sédiments. Par conséquent, l'effet de la plantation de teck sur la formation de ravins devrait être évalué plus loin pour confirmer l'augmentation de la perte en sols sur le versant.

L'effet des précipitations extrêmes sur l'érosion des sols n'est pas encore évalué dans cette étude. De nos jours, en particulier, le carbone libéré dans l'atmosphère par la déforestation est un problème de plus en plus préoccupant en raison de ses contributions potentielles au changement climatique mondial (Achard et al., 2004; Defries et al., 2007; Defries et al., 2002; Eva et al., 2010; Houghton et al., 2000; Skutsch et al., 2007; van der Werf et al., 2009). Le changement climatique devrait entraîner un cycle hydrologique plus vigoureux, notamment des précipitations totales plus abondantes et des événements pluvieux de haute intensité plus fréquents dans le monde entier (Borrelli et al., 2020; Nearing et al., 2004), ce qui augmente alors la risque d'érosion des sols. En outre, une recherche menée dans le bassin versant transnational du Laos et du Vietnam a prédit que l'érosion des sols sera considérablement accrue en raison du climat plus chaud et plus humide de la saison humide déclenchée par le changement climatique (Giang et al., 2017). L'événement extrême peut également provoquer la remise en suspension des sédiments et des glissements de terrain qui contribuent d'énormes sédiments en aval. Par conséquent, une bonne compréhension de ces facteurs en tant que forces motrices et caractéristiques du système influençant l'érosion des sols est vitale. Une enquête plus approfondie en intégrant tous les facteurs dans la prédiction du transfert de sédiments est suggérée pour expliquer pleinement la continuité du transfert de sédiments d'une source à un puits dans un bassin versant, c'est-à-dire de l'érosion locale à l'exutoire du bassin versant.

À l'échelle de micro-parcelle, nos résultats sont pertinents pour les agriculteurs préoccupés par la perte en sols et la fertilité du sol dans leurs parcelles de teck. L'agriculteur gagnerait plus d'argent en appliquant des pratiques de culture intercalaire dans la plantation de teck, par exemple, en gardant l'herbe à balai dans la plantation d'arbres. Cette pratique non seulement atténuera la perte de fertilité des sols, mais ajoutera également une valeur économique au rendement global de la plantation et peut fournir une gamme de services écosystémiques en

aval. Par exemple, à l'échelle du bassin versant, les pratiques de conservation du sous-couvert et de l'herbe rivulaire sont pertinentes pour les décideurs concernés par la gestion des coûts (tels que le coût du traitement de l'eau, la réhabilitation des infrastructures telles que le dragage des réservoirs de barrage et l'atténuation des catastrophes naturelles) résultant de la perte en sols induite par les activités en amont telles que les plantations d'arbres et la mauvaise gestion des terres agricoles.

Les mesures suggérées offrent de nombreux avantages au système; cependant, les mesures d'atténuation du sol peuvent aggraver l'érosion du sol. Par exemple, s'il n'y a pas de mesure de l'érosion locale, les sédiments érodés d'amont du versant se déposeront dans la zone rivulaire au moyen du piégeage d'herbe. Après une longue période de temps, ce dépôt accumulé provoquera des glissements de terrain qui contribuent à l'érosion des sols. De plus, l'application de nombreuses mesures d'atténuation peut rendre l'eau de la rivière claire car aucune érosion en amont car l'eau claire peut provoquer l'érosion des berges. De plus, l'écoulement fluvial peut ne pas transporter et contribuer à des sédiments fertiles en aval le long de la rivière ainsi que dans le delta. Le ruissellement limite peut également induire une intrusion d'eau salée qui affecte la qualité des eaux souterraines et les rendements agricoles.

Les résultats basés sur l'évaluation multi-échelle de cette thèse fourniront aux communautés sociales et scientifiques des résultats quantitatifs sur l'érosion des sols de l'échelle locale au bassin versant. Les agriculteurs et les décideurs comprendront mieux les bonnes pratiques de gestion des terres et mettront en œuvre une politique appropriée pour la durabilité de leur environnement et de leurs avantages. Des études de recherche sont nécessaires pour examiner les limites de cette étude en intégrant davantage tous les facteurs décrits ici dans les modèles.

References

Abbaspour, K. (2021). The fallacy in the use of the "best-fit" solution in hydrologic modeling. *Science of the total environment*, 149713. doi:https://doi.org/10.1016/j.scitotenv.2021.149713

Abdi, H. (2010). Partial least squares regression and projection on latent structure regression (PLS Regression). *Wiley interdisciplinary reviews: computational statistics, 2*(1), 97-106. doi: https://doi.org/10.1002/wics.51

Achard, F., Eva, H. D., Mayaux, P., Stibig, H. J., & Belward, A. (2004). Improved estimates of net carbon emissions from land cover change in the tropics for the 1990s. *Global biogeochemical cycles, 18*(2).

ADB. (2016). *LAO: Northern Rural Infrastructure Development Sector Project – Due Diligence for Additional Financing - Climate Risk and Vulnerability Assessment*. Retrieved from https://www.adb.org/sites/default/files/linked-documents/42203-025-sd-05.pdf

Addinsoft. (2021). XLSTAT statistical and data analysis solution. New York, USA. Retrieved from https://www.xlstat.com

Ahmad, N. S. B. N., Mustafa, F. B., & Gideon, D. (2020). A systematic review of soil erosion control practices on the agricultural land in Asia. *International Soil and Water Conservation Research, 8*(2), 103-115. doi:https://doi.org/10.1016/j.iswcr.2020.04.001

Ai, N., Wei, T., Zhu, Q., Zhao, X. K., Zhao, W., Ma, H., & Xie, R. (2015). Factors affecting runoff and sediment yield on the semiarid loess area in Northern Shaanxi Province, China. *Physical Geography, 36*(6), 537-554. doi:10.1080/02723646.2015.1133189

Alemu, T., Bahrndorff, S., Hundera, K., Alemayehu, E., & Ambelu, A. (2017). Effect of riparian land use on environmental conditions and riparian vegetation in the east African highland streams. *Limnologica (Online), 66*, 1-11. doi:https://doi.org/10.1016/j.limno.2017.07.001

Angelsen, A., & Kaimowitz, D. (2004). Is agroforestry likely to reduce deforestation. In G. Schroth, G. A. d. Fonseca, C. A. Harvey, C. Gascon, H. L. Vasconcelos, & A.-M. N. Izac (Eds.), *Agroforestry and biodiversity conservation in tropical landscapes* (pp. 87-106). Washington, DC: Island Press.

Annandale, G. W. (2006). Reservoir sedimentation. In *Encyclopedia of Hydrological Sciences*.

Arias, M. E., Cochrane, T. A., Kummu, M., Lauri, H., Holtgrieve, G. W., Koponen, J., & Piman, T. (2014). Impacts of hydropower and climate change on drivers of ecological productivity of Southeast Asia's most important wetland. *Ecological modelling, 272*, 252-263. doi:https://doi.org/10.1016/j.ecolmodel.2013.10.015

Arnaez, J., Lasanta, T., Ruiz-Flaño, P., & Ortigosa, L. (2007). Factors affecting runoff and erosion under simulated rainfall in Mediterranean vineyards. *Soil and tillage research, 93*(2), 324-334. doi:https://doi.org/10.1016/j.still.2006.05.013

Assouline, S., & Ben-Hur, M. (2006). Effects of rainfall intensity and slope gradient on the dynamics of interrill erosion during soil surface sealing. *Catena, 66*(3), 211-220.

Balmford, A., & Whitten, T. (2003). Who should pay for tropical conservation, and how could the costs be met? *Oryx 37*(2), 238-250.

Barmuta, L., Watson, A., Clarke, A., & Clapcott, J. (2009). *The importance of headwater streams*. Retrieved from http://ecite.utas.edu.au/62231

Benavidez, R., Jackson, B., Maxwell, D., & Norton, K. (2018). A review of the (Revised) Universal Soil Loss Equation ((R)USLE): with a view to increasing its global applicability and improving soil loss estimates. *Hydrology and earth system sciences, 22*(11), 6059-6086. doi:10.5194/hess-22-6059-2018

Bereswill, R., Streloke, M., & Schulz, R. (2014). Risk mitigation measures for diffuse pesticide entry into aquatic ecosystems: proposal of a guide to identify appropriate measures on a catchment scale. *Integrated environmental assessment and management, 10*(2), 286-298. doi:https://doi-org.insu.bib.cnrs.fr/10.1002/ieam.1517

Beven, K., Heathwaite, L., Haygarth, P., Walling, D., Brazier, R., & Withers, P. (2005). On the concept of delivery of sediment and nutrients to stream channels. *Hydrological Processes: An International Journal, 19*(2), 551-556. doi:https://doi.org/10.1002/hyp.5796

Beven*, K. (2001). How far can we go in distributed hydrological modelling? *Hydrology and earth system sciences, 5*(1), 1-12. doi:https://doi.org/10.5194/hess-5-1-2001

Bhat, S. A., Dar, M. U. D., & Meena, R. S. (2019). Soil erosion and management strategies. In *Sustainable Management of Soil and Environment* (pp. 73-122): Springer. doi:https://doi.org/10.1007/978-981-13-8832-3_3

Blanco, J. A., & Lo, Y.-H. (2012). *Forest Ecosystems: More Than Just Trees*: BoD–Books on Demand. ISBN: 9535102028

Blöschl, G., & Sivapalan, M. (1995). Scale issues in hydrological modelling: A review. *Hydrological processes, 9*(3-4), 251-290. doi:https://doi.org/10.1002/hyp.3360090305

Boch, S., Berlinger, M., Fischer, M., Knop, E., Nentwig, W., Türke, M., & Prati, D. (2013). Fern and bryophyte endozoochory by slugs. *Oecologia, 172*(3), 817-822.

Boithias, L., Auda, Y., Audry, S., Bricquet, J.-P., Chanhphengxay, A., Chaplot, V., . . . Xayyathip, K. (2021). The Multiscale TROPIcal CatchmentS critical zone observatory M-TROPICS dataset II: land use, hydrology and sediment production monitoring in Houay Pano, northern Lao PDR. *Hydrological processes, 35*(5), e14126. doi:https://doi.org/10.1002/hyp.14126

Boithias, L., Choisy, M., Souliyaseng, N., Jourdren, M., Quet, F., Buisson, Y., . . . Ribolzi, O. (2016a). Hydrological Regime and Water Shortage as Drivers of the Seasonal Incidence of Diarrheal Diseases in a Tropical Montane Environment. *PLoS neglected tropical diseases, 10*(12), e0005195. doi:10.1371/journal.pntd.0005195

Boithias, L., Terrado, M., Corominas, L., Ziv, G., Kumar, V., Marques, M., . . . Acuna, V. (2016b). Analysis of the uncertainty in the monetary valuation of ecosystem services--A case study at the river basin scale. *Science of the total environment, 543*(Pt A), 683-690. doi:10.1016/j.scitotenv.2015.11.066

Bonetti, S., Richter, D. D., & Porporato, A. (2019). The effect of accelerated soil erosion on hillslope morphology. *Earth surface processes and landforms, 44*(15), 3007-3019. doi:https://doi.org/10.1002/esp.4694

Borin, M., Vianello, M., Morari, F., & Zanin, G. (2005). Effectiveness of buffer strips in removing pollutants in runoff from a cultivated field in North-East Italy. *Agriculture,*

ecosystems & environment, 105(1-2), 101-114. doi:https://doi.org/10.1016/j.agee.2004.05.011

Borrelli, P., Robinson, D. A., Fleischer, L. R., Lugato, E., Ballabio, C., Alewell, C., . . . Panagos, P. (2017). An assessment of the global impact of 21st century land use change on soil erosion. *Nature communications, 8*(1), 2013. doi:https://doi.org/10.1038/s41467-017-02142-7

Borrelli, P., Robinson, D. A., Panagos, P., Lugato, E., Yang, J. E., Alewell, C., . . . Ballabio, C. (2020). Land use and climate change impacts on global soil erosion by water (2015-2070). *Proceedings of the National Academy of Sciences, 117*(36), 21994-22001. doi:https://doi.org/10.1073/pnas.2001403117

Bracken, L. J., Turnbull, L., Wainwright, J., & Bogaart, P. (2015). Sediment connectivity: a framework for understanding sediment transfer at multiple scales. *Earth surface processes and landforms, 40*(2), 177-188. doi:https://doi.org/10.1002/esp.3635

Bu, C.-f., Wu, S.-f., & Yang, K.-b. (2014). Effects of physical soil crusts on infiltration and splash erosion in three typical Chinese soils. *International Journal of Sediment Research, 29*(4), 491-501. doi:https://doi.org/10.1016/S1001-6279(14)60062-7

Buckley, A. (2010). Understanding curvature rasters. Retrieved from https://www.esri.com/arcgis-blog/products/product/imagery/understanding-curvature-rasters/

C. Goodrich, D., S. Burns, I., L. Unkrich, C., J. Semmens, D., P. Guertin, D., Hernandez, M., . . . R. Levick, L. (2012). KINEROS2/AGWA: Model Use, Calibration, and Validation. *Transactions of the ASABE, 55*(4), 1561-1574. doi:https://doi.org/10.13031/2013.42264

Calder, I. R., Hall, R. L., & Prasanna, K. (1993). Hydrological impact of Eucalyptus plantation in India. *Journal of hydrology, 150*(2-4), 635-648.

Cao, X., Song, C., Xiao, J., & Zhou, Y. (2018). The optimal width and mechanism of riparian buffers for storm water nutrient removal in the Chinese eutrophic Lake Chaohu watershed. *Water, 10*(10), 1489. doi:https://doi.org/10.3390/w10101489

Casenave, A., & Valentin, C. (1992). A runoff capability classification system based on surface features criteria in semi-arid areas of West Africa. *Journal of hydrology, 130*(1-4), 231-249. doi:https://doi.org/10.1016/0022-1694(92)90112-9

Castelle, A. J., Johnson, A., & Conolly, C. (1994). Wetland and stream buffer size requirements—a review. *Journal of environmental quality, 23*(5), 878-882. doi: https://doi.org/10.2134/jeq1994.00472425002300050004x

Cerdà, A., Rodrigo-Comino, J., Giménez-Morera, A., Novara, A., Pulido, M., Kapović-Solomun, M., & Keesstra, S. D. (2018). Policies can help to apply successful strategies to control soil and water losses. The case of chipped pruned branches (CPB) in Mediterranean citrus plantations. *Land use policy, 75*, 734-745. doi:https://doi.org/10.1016/j.landusepol.2017.12.052

Chaplot, V., Giboire, G., Marchand, P., & Valentin, C. (2005a). Dynamic modelling for linear erosion initiation and development under climate and land-use changes in northern Laos. *Catena, 63*(2-3), 318-328. doi:https://doi.org/10.1016/j.catena.2005.06.008

Chaplot, V., Khampaseuth, X., Valentin, C., & Bissonnais, Y. L. (2007). Interrill erosion in the sloping lands of northern Laos subjected to shifting cultivation. *Earth surface processes and landforms, 32*(3), 415-428. doi:https://doi.org/10.1002/esp.1411

Chaplot, V., Le Brozec, E. C., Silvera, N., & Valentin, C. (2005b). Spatial and temporal assessment of linear erosion in catchments under sloping lands of northern Laos. *Catena, 63*(2-3), 167-184. doi:https://doi.org/10.1016/j.catena.2005.06.003

Chaplot, V., & Poesen, J. (2012). Sediment, soil organic carbon and runoff delivery at various spatial scales. *Catena, 88*(1), 46-56. doi:https://doi.org/10.1016/j.catena.2011.09.004

Chaplot, V., Rumpel, C., & Valentin, C. (2005c). Water erosion impact on soil and carbon redistributions within uplands of Mekong River. *Global biogeochemical cycles, 19*(4). doi:https://doi.org/10.1029/2005GB002493

Chartin, C., Evrard, O., Onda, Y., Patin, J., Lefèvre, I., Ottlé, C., . . . Bonté, P. (2013). Tracking the early dispersion of contaminated sediment along rivers draining the Fukushima radioactive pollution plume. *Anthropocene, 1*, 23-34. doi:10.1016/j.ancene.2013.07.001

Chitra-Tarak, R., Ruiz, L., Dattaraja, H. S., Kumar, M. M., Riotte, J., Suresh, H. S., . . . Sukumar, R. (2018). The roots of the drought: Hydrology and water uptake strategies mediate forest-wide demographic response to precipitation. *Journal of ecology, 106*(4), 1495-1507.

Chuenchum, P., Xu, M., & Tang, W. (2020). Estimation of soil erosion and sediment yield in the Lancang–Mekong river using the modified revised universal soil loss equation and GIS techniques. *Water, 12*(1), 135. doi:https://doi.org/10.3390/w12010135

Collins, R., & Neal, C. (1998). The hydrochemical impacts of terraced agriculture, Nepal. *Science of the total environment, 212*(2-3), 233-243. doi:https://doi.org/10.1016/S0048-9697(97)00342-2

Comino, J. R., Quiquerez, A., Follain, S., Raclot, D., Le Bissonnais, Y., Casalí, J., . . . Brevik, E. (2016). Soil erosion in sloping vineyards assessed by using botanical indicators and sediment collectors in the Ruwer-Mosel valley. *Agriculture, ecosystems & environment, 233*, 158-170.

Cooper, J., Gilliam, J., Daniels, R., & Robarge, W. (1987). Riparian areas as filters for agricultural sediment. *Soil Science Society of America Journal, 51*(2), 416-420.

Corlett, R. (2014). *The ecology of tropical East Asia*: Oxford University Press, USA. ISBN: 019968135X

Crowder, B. M. (1987). Economic costs of reservoir sedimentation: A regional approach to estimating cropland erosion damage. *Journal of soil and water conservation, 42*(3), 194-197.

Dale, V. H. (1997). The relationship between land-use change and climate change. *Ecological applications, 7*(3), 753-769.

Damian Ruiz Sinoga, J., Francisco Martinez Murillo, J., & Gabarron Galeote, M. A. (2010). *Factors affecting runoff and soil detachment in micro-plots under different climatic conditions (South of Spain)*. Paper presented at the EGU General Assembly 2010.

Dang, T. D., Cochrane, T. A., & Arias, M. E. (2018). Quantifying suspended sediment dynamics in mega deltas using remote sensing data: A case study of the Mekong floodplains. *International Journal of Applied Earth Observation and Geoinformation, 68*, 105-115. doi:10.1016/j.jag.2018.02.008

De Jong, B. H. J., Tipper, R., & Taylor, J. (1997). A framework for monitoring and evaluating carbon mitigation by farm forestry projects: Example of a demonstration project in

Chiapas, Mexico. *Mitigation and adaptation strategies for global change, 2*(2), 231-246. doi:10.1007/BF02437206

de Rouw, A., Ribolzi, O., Douillet, M., Tjantahosong, H., & Soulileuth, B. (2018). Weed seed dispersal via runoff water and eroded soil. *Agriculture, ecosystems & environment, 265*, 488-502. doi:https://doi.org/10.1016/j.agee.2018.05.026

De Vente, J., & Poesen, J. (2005). Predicting soil erosion and sediment yield at the basin scale: scale issues and semi-quantitative models. *Earth-science reviews, 71*(1-2), 95-125.

De Vente, J., Poesen, J., Arabkhedri, M., & Verstraeten, G. (2007). The sediment delivery problem revisited. *Progress in physical geography, 31*(2), 155-178. doi:https://doi.org/10.1177/0309133307076485

Defries, R., Achard, F., Brown, S., Herold, M., Murdiyarso, D., Schlamadinger, B., & de Souza Jr, C. (2007). Earth observations for estimating greenhouse gas emissions from deforestation in developing countries. *Environmental science & policy, 10*(4), 385-394.

Defries, R., Houghton, R. A., Hansen, M. C., Field, C. B., Skole, D., & Townshend, J. (2002). Carbon emissions from tropical deforestation and regrowth based on satellite observations for the 1980s and 1990s. *Proceedings of the National Academy of Sciences, 99*(22), 14256-14261.

Deletic, A., & Fletcher, T. D. (2006). Performance of grass filters used for stormwater treatment—a field and modelling study. *Journal of hydrology, 317*(3-4), 261-275. doi:https://doi.org/10.1016/j.jhydrol.2005.05.021

Dennis, R. A., Mayer, J., Applegate, G., Chokkalingam, U., Colfer, C. J. P., Kurniawan, I., . . . Ruchiat, Y. (2005). Fire, people and pixels: linking social science and remote sensing to understand underlying causes and impacts of fires in Indonesia. *Human Ecology, 33*(4), 465-504.

Descroix, L., González Barrios, J. L., Viramontes, D., Poulenard, J., Anaya, E., Esteves, M., & Estrada, J. (2008). Gully and sheet erosion on subtropical mountain slopes: Their respective roles and the scale effect. *Catena, 72*(3), 325-339. doi:10.1016/j.catena.2007.07.003

Ding, W., He, X., & Chen, W. (2011). *Runoff and sediment reduction by riparian buffer filters on steep slopes.* Paper presented at the 2011 International Conference on Computer Distributed Control and Intelligent Environmental Monitoring.

Domagalski, J. L., & Kuivila, K. M. (1993). Distributions of pesticides and organic contaminants between water and suspended sediment, San Francisco Bay, California. *Estuaries, 16*(3), 416-426. doi:10.2307/1352589

Dong, Y., Xiong, D., Su, Z. a., Yang, D., Zheng, X., Shi, L., & Poesen, J. (2018). Effects of vegetation buffer strips on concentrated flow hydraulics and gully bed erosion based on in situ scouring experiments. *Land degradation & development, 29*(6), 1672-1682. doi:https://doi.org/10.1002/ldr.2943

Dosskey, M. G., Vidon, P., Gurwick, N. P., Allan, C. J., Duval, T. P., & Lowrance, R. (2010). The role of riparian vegetation in protecting and improving chemical water quality in streams 1. *Journal of the American Water Resources Association, 46*(2), 261-277. doi:https://doi.org/10.1111/j.1752-1688.2010.00419.x

Douglas Jr., C. L., King, K. A., & Zuzel, J. F. (1998). Nitrogen and Phosphorus in Surface Runoff and Sediment from a Wheat-Pea Rotation in Northeastern Oregon. *Journal of*

environmental quality, 27(5), 1170-1177. doi:https://doi.org/10.2134/jeq1998.00472425002700050023x

Dunne, T., & Black, R. D. (1970). An experimental investigation of runoff production in permeable soils. *Water Resources Research, 6*(2), 478-490.

Durán Zuazo, V. H., Martínez, J. R. F., Pleguezuelo, C. R. R., Martínez Raya, A., & Rodríguez, B. C. (2006). Soil-erosion and runoff prevention by plant covers in a mountainous area (se spain): Implications for sustainable agriculture. *The Environmentalist, 26*(4), 309-319. doi:10.1007/s10669-006-0160-4

Efthimiou, N., Lykoudi, E., Panagoulia, D., & Karavitis, C. (2016). Assessment of soil susceptibility to erosion using the EPM and RUSLE Models: the case of Venetikos River Catchment. *Global NEST Journal, 18*(1), 164-179.

Ehigiator, O. A., & Anyata, B. U. (2011). Effects of land clearing techniques and tillage systems on runoff and soil erosion in a tropical rain forest in Nigeria. *Journal of environmental management, 92*(11), 2875-2880. doi:https://doi.org/10.1016/j.jenvman.2011.06.015

Eldridge, D. J., Wilson, B. R., & Oliver, I. (2003). *Regrowth and soil erosion in the semi-arid woodlands of New South Wales : a report to the Native Vegetation Advisory Council / David J. Eldridge, Brian R. Wilson [and] Ian Oliver*. Sydney: Centre for Natural Resources, NSW Dept. of Land and Water Conservation. ISBN: 0734753071 (Report)

073475308X (Supplement)

Elliott, K. J., Vose, J. M., Knoepp, J. D., Clinton, B. D., & Kloeppel, B. D. (2015). Functional role of the herbaceous layer in eastern deciduous forest ecosystems. *Ecosystems, 18*(2), 221-236.

Eva, H., Carboni, S., Achard, F., Stach, N., Durieux, L., Faure, J.-F., & Mollicone, D. (2010). Monitoring forest areas from continental to territorial levels using a sample of medium spatial resolution satellite imagery. *ISPRS Journal of Photogrammetry and Remote Sensing, 65*(2), 191-197.

Fernández-Moya, J., Alvarado, A., Forsythe, W., Ramírez, L., Algeet-Abarquero, N., & Marchamalo-Sacristán, M. (2014). Soil erosion under teak (Tectona grandis Lf) plantations: General patterns, assumptions and controversies. *Catena, 123*, 236-242.

Fiener, P., & Auerswald, K. (2006). Influence of scale and land use pattern on the efficacy of grassed waterways to control runoff. *Ecological Engineering, 27*(3), 208-218. doi:https://doi.org/10.1016/j.ecoleng.2006.02.005

Fondriest Environmental, I. (2014). Sediment Transport and Deposition. *Fundamentals of Environmental Measurements.* Retrieved from https://www.fondriest.com/environmental-measurements/parameters/hydrology/sediment-transport-deposition/

Fox, D., Bryan, R., & Fox, C. (2004). Changes in pore characteristics with depth for structural crusts. *Geoderma, 120*(1-2), 109-120. doi:https://doi.org/10.1016/j.geoderma.2003.08.010

Fujisaka, S. (1991). A diagnostic survey of shifting cultivation in northern Laos: targeting research to improve sustainability and productivity. *Agroforestry Systems, 13*(2), 95-109. doi:10.1007/BF00140235

G. Arnold, J., N. Moriasi, D., W. Gassman, P., C. Abbaspour, K., J. White, M., Srinivasan, R., . . . K. Jha, M. (2012). SWAT: Model Use, Calibration, and Validation. *Transactions of the ASABE, 55*(4), 1491-1508. doi:https://doi.org/10.13031/2013.42256

Ganasri, B. P., & Ramesh, H. (2016). Assessment of soil erosion by RUSLE model using remote sensing and GIS - A case study of Nethravathi Basin. *Geoscience Frontiers, 7*(6), 953-961. doi:https://doi.org/10.1016/j.gsf.2015.10.007

Gateuille, D., Evrard, O., Lefevre, I., Moreau-Guigon, E., Alliot, F., Chevreuil, M., & Mouchel, J. M. (2014). Mass balance and decontamination times of Polycyclic Aromatic Hydrocarbons in rural nested catchments of an early industrialized region (Seine River basin, France). *Science of the total environment, 470-471*, 608-617. doi:10.1016/j.scitotenv.2013.10.009

Geißler, C., Kühn, P., Böhnke, M., Bruelheide, H., Shi, X., & Scholten, T. (2012). Splash erosion potential under tree canopies in subtropical SE China. *Catena, 91*, 85-93. doi:https://doi.org/10.1016/j.catena.2010.10.009

George, L. O., & Bazzaz, F. A. (2003). The herbaceous layer as a filter determining spatial pattern in forest tree regeneration. *The herbaceous layer in forests of eastern North America*, 265-282.

Gerlach, T. (1967). Hillslope troughs for measuring sediment movement. *Revue de geomorphologie dynamique, 17*, 173.

Gerstengarbe, F. W., & Werner, P. C. (2008). Precipitation Pattern. In S. E. Jørgensen & B. D. Fath (Eds.), *Encyclopedia of Ecology* (pp. 2916-2923): Elsevier Science.

Giang, P. Q., Giang, L. T., & Toshiki, K. (2017). Spatial and temporal responses of soil erosion to climate change impacts in a transnational watershed in Southeast Asia. *Climate, 5*(1), 22.

Gill, R., & Beardall, V. (2001). The impact of deer on woodlands: the effects of browsing and seed dispersal on vegetation structure and composition. *Forestry: An International Journal of Forest Research, 74*(3), 209-218.

Gilliam, F. S. (2007). The ecological significance of the herbaceous layer in temperate forest ecosystems. *Bioscience, 57*(10), 845-858.

Goddard, G. L., & Elder, J. F. (1997). *Retention of sediments and nutrients in Jackson Creek wetland near Delavan Lake, Wisconsin, 1993-95* (Vol. 97): US Department of the Interior, US Geological Survey

Goebes, P., Seitz, S., Kühn, P., Li, Y., Niklaus, P. A., Oheimb, G. v., & Scholten, T. (2015). Throughfall kinetic energy in young subtropical forests: Investigation on tree species richness effects and spatial variability. *Agricultural and forest meteorology, 213*, 148-159. doi:10.1016/j.agrformet.2015.06.019

GSP. (2016). Global Soil Partnership endorses guidelines on sustainable soil management. Retrieved from http://www.fao.org/global-soil-partnership/resources/highlights/detail/en/c/416516/

Gumiere, S. J., Le Bissonnais, Y., Raclot, D., & Cheviron, B. (2011). Vegetated filter effects on sedimentological connectivity of agricultural catchments in erosion modelling: a review. *Earth surface processes and landforms, 36*(1), 3-19. doi:https://doi.org/10.1002/esp.2042

Hamilton, S. (2007). Just say NO to equifinality. *Hydrological processes, 21*(14), 1979-1980. doi:https://doi.org/10.1002/hyp.6800

Harrabin, R. (2019). *Climate change being fuelled by soil damage*. Retrieved from https://www.bbc.com/news/science-environment-48043134

Harvey, C. A., & Villalobos, J. A. G. (2007). Agroforestry systems conserve species-rich but modified assemblages of tropical birds and bats. *Biodiversity and conservation, 16*(8), 2257-2292.

Hewlett, J. D., & Hibbert, A. R. (1967). Factors affecting the response of small watersheds to precipitation in humid areas. *Forest hydrology, 1*, 275-290.

Highland, L. (2004). *Landslide types and processes* (2004-3072). Retrieved from http://pubs.er.usgs.gov/publication/fs20043072

Hodgson, E. (2012). Human environments: definition, scope, and the role of toxicology. In *Progress in molecular biology and translational science* (Vol. 112, pp. 1-10): Elsevier.

Horton, R. E. (1933). The role of infiltration in the hydrologic cycle. *Eos, Transactions American Geophysical Union, 14*(1), 446-460.

Houghton, R. A., Skole, D., Nobre, C. A., Hackler, J., Lawrence, K., & Chomentowski, W. H. (2000). Annual fluxes of carbon from deforestation and regrowth in the Brazilian Amazon. *Nature, 403*(6767), 301-304.

Huon, S., Evrard, O., Gourdin, E., Lefèvre, I., Bariac, T., Reyss, J.-L., . . . Ribolzi, O. (2017). Suspended sediment source and propagation during monsoon events across nested sub-catchments with contrasted land uses in Laos. *Journal of hydrology: Regional studies, 9*, 69-84. doi:https://doi.org/10.1016/j.ejrh.2016.11.018

Imron, M., Tantaryzard, M., Satria, R., Maulana, I., & Pudyatmoko, S. (2018). UNDERSTORY AVIAN COMMUNITY IN A TEAK FOREST OF CEPU, CENTRAL JAVA. *Journal of Tropical Forest Science, 30*(4), 509-518.

ITTO. (2004). Tropical Forest Update. *The prospects for plantation teak, Volume 14, Number 1*. Retrieved from https://www.itto.int/tfu/id=6660000

Jadidoleslam, N., Mantilla, R., Krajewski, W. F., & Goska, R. (2019). Investigating the role of antecedent SMAP satellite soil moisture, radar rainfall and MODIS vegetation on runoff production in an agricultural region. *Journal of hydrology, 579*, 124210. doi:https://doi.org/10.1016/j.jhydrol.2019.124210

Janeau, J. L., Bricquet, J. P., Planchon, O., & Valentin, C. (2003). Soil crusting and infiltration on steep slopes in northern Thailand. *European journal of soil science, 54*(3), 543-554. doi:10.1046/j.1365-2389.2003.00494.x

Janeau, J. L., Gillard, L. C., Grellier, S., Jouquet, P., Le, T. P. Q., Luu, T. N. M., . . . Rochelle-Newall, E. (2014). Soil erosion, dissolved organic carbon and nutrient losses under different land use systems in a small catchment in northern Vietnam. *Agricultural water management, 146*, 314-323. doi:https://doi.org/10.1016/j.agwat.2014.09.006

Janeau, J. L., Maglinao, A., & Lorenr, J. (2002). *The Off-site Effect of Soil Erosion: A Case Study of the Mae Thang Reservoir in Northern Thailand.* Paper presented at the From Soil Research to Land and.

Jayanath, A., & Gamini, H. (2003). Soil erosion in developing countries: a socio-economic appraisal. *Journal of environmental management, 68*(4), 343-353. doi:https://doi.org/10.1016/S0301-4797(03)00082-3

José, A. M.-C., Ramos, M. C., & Manel, R.-D. (2005). On-site effects of concentrated flow erosion in vineyard fields: some economic implications. *Catena, 60*(2), 129-146. doi:https://doi.org/10.1016/j.catena.2004.11.006

Jose, S. (2009). Agroforestry for ecosystem services and environmental benefits: an overview. *Agroforestry Systems, 76*(1), 1-10.

Kagabo, D., Stroosnijder, L., Visser, S., & Moore, D. (2013). Soil erosion, soil fertility and crop yield on slow-forming terraces in the highlands of Buberuka, Rwanda. *Soil and tillage research, 128*, 23-29.

Kim, M., Boithias, L., Cho, K. H., Sengtaheuanghoung, O., & Ribolzi, O. (2018). Modeling the Impact of Land Use Change on Basin-scale Transfer of Fecal Indicator Bacteria: SWAT Model Performance. *Journal of environmental quality, 47*(5), 1115-1122. doi:10.2134/jeq2017.11.0456

Kinnell, P. (1981). Rainfall Intensity-Kinetic Energy Relationships for Soil Loss Prediction. *Soil Science Society of America Journal, 45*(1), 153-155. doi:https://doi.org/10.2136/sssaj1981.03615995004500010033x

Kinnell, P. (2005). Raindrop-impact-induced erosion processes and prediction: a review. *Hydrological Processes: An International Journal, 19*(14), 2815-2844.

Kollert, W., & Cherubini, L. (2012). Forestry Department.

Kolmert, A. (2001). *Teak in northern Laos*: Swedish University of Agricultural Sciences, International Office

Koonkhunthod, N., Sakurai, K., & Tanaka, S. (2007). Composition and diversity of woody regeneration in a 37-year-old teak (Tectona grandis L.) plantation in Northern Thailand. *Forest ecology and management, 247*(1-3), 246-254.

Kosmas, C., Danalatos, N., Cammeraat, L. H., Chabart, M., Diamantopoulos, J., Farand, R., . . . Martinez-Fernandez, J. (1997). The effect of land use on runoff and soil erosion rates under Mediterranean conditions. *Catena, 29*(1), 45-59. doi:https://doi.org/10.1016/S0341-8162(96)00062-8

Kuglerová, L., Ågren, A., Jansson, R., & Laudon, H. (2014). Towards optimizing riparian buffer zones: Ecological and biogeochemical implications for forest management. *Forest ecology and management, 334*, 74-84.

Kumar, D., Bijalwan, A., Kalra, A., & Dobriyal, M. J. (2016). Effect of shade and organic manure on growth and yield of patchouli [Pogostemon cablin (blanco) benth.] under teak (Tectona grandis lf) based agroforestry system. *Indian Forester, 142*(11), 1121-1129.

Lacombe, G., Ribolzi, O., de Rouw, A., Pierret, A., Latsachak, K., Silvera, N., . . . Valentin, C. (2015). Afforestation by natural regeneration or by tree planting: examples of opposite hydrological impacts evidenced by long-term field monitoring in the humid tropics. *Hydrology and earth system sciences, 12*(12), 12615-12648. doi:10.5194/hessd-12-12615-2015

Lacombe, G., Ribolzi, O., de Rouw, A., Pierret, A., Latsachak, K., Silvera, N., . . . Valentin, C. (2016). Contradictory hydrological impacts of afforestation in the humid tropics evidenced by long-term field monitoring and simulation modelling. *Hydrology and earth system sciences, 20*(7), 2691-2704. doi:https://doi.org/10.5194/hess-20-2691-2016

Lacombe, G., Valentin, C., Sounyafong, P., de Rouw, A., Soulileuth, B., Silvera, N., . . . Ribolzi, O. (2018). Linking crop structure, throughfall, soil surface conditions, runoff and soil detachment: 10 land uses analyzed in Northern Laos. *Science of the total environment, 616-617*, 1330-1338. doi:https://doi.org/10.1016/j.scitotenv.2017.10.185

Lal, R. (1998). Soil erosion impact on agronomic productivity and environment quality. *Critical reviews in plant sciences, 17*(4), 319-464. doi:https://doi.org/10.1080/07352689891304249

Lambin, E. F., Geist, H. J., & Lepers, E. (2003). Dynamics of land-use and land-cover change in tropical regions. *Annual review of environment and resources, 28*(1), 205-241.

Le Bissonnais, Y., Lecomte, V., & Cerdan, O. (2004). Grass strip effects on runoff and soil loss. *Agronomie 24*(3), 129 - 136. doi:https://dx.doi.org/10.1051/agro:2004010

Le, H. T., Rochelle-Newall, E., Ribolzi, O., Janeau, J. L., Huon, S., Latsachack, K., & Pommier, T. (2020). Land use strongly influences soil organic carbon and bacterial community export in runoff in tropical uplands-. *Land degradation & development, 31*(1), 118-132.

Ledermann, T., Herweg, K., Liniger, H. P., Schneider, F., Hurni, H., & Prasuhn, V. (2010). Applying erosion damage mapping to assess and quantify off-site effects of soil erosion in Switzerland. *Land degradation & development, 21*(4), 353-366. doi:https://doi.org/10.1002/ldr.1008

Lestrelin, G. (2010). Land degradation in the Lao PDR: Discourses and policy. *Land use policy, 27*(2), 424-439. doi:https://doi.org/10.1016/j.landusepol.2009.06.005

Lestrelin, G., & Giordano, M. (2007). Upland development policy, livelihood change and land degradation: interactions from a Laotian village. *Land degradation & development, 18*(1), 55-76. doi:https://doi.org/10.1002/ldr.756

Li, X., Niu, J., & Xie, B. (2014). The effect of leaf litter cover on surface runoff and soil erosion in Northern China. *PloS one, 9*(9), e107789.

Loftas, T., & Ross, J. (1995). *Dimensions of need: an atlas of food and agriculture.* (T. Loftas Ed.). Rome, Italy: Food and Agriculture Organization of the United Nations. ISBN: 92-5-103737-X

Mahabaleshwara, H., & Nagabhushan, H. (2014). A study on soil erosion and its impacts on floods and sedimentation. *International Journal of Research in Engineering and Technology, 3*(03), 443-451.

Martin-Clouaire, R. (2018). Ontological Foundation of Ecosystem Services and the Human Dimension of Agroecosystems.

Martíni, A. F., Favaretto, N., De Bona, F. D., Durães, M. F., de Paula Souza, L. C., & Goularte, G. D. (2020). Impacts of soil use and management on water quality in agricultural watersheds in Southern Brazil. *Land degradation & development, 32*(2), 975-992. doi:https://doi.org/10.1002/ldr.3777

McHenry, J. R. (1974). RESERVOIR SEDIMENTATION 1. *Journal of the American Water Resources Association, 10*(2), 329-337. doi:https://doi.org/10.1111/j.1752-1688.1974.tb00572.x

McKergow, L. A., Prosser, I. P., Grayson, R. B., & Heiner, D. (2004). Performance of grass and rainforest riparian buffers in the wet tropics, Far North Queensland. 2. Water quality. *Soil Research, 42*(4), 485-498. doi:https://doi.org/10.1071/SR02156

Mekonnen, M., Keesstra, S. D., Stroosnijder, L., Baartman, J. E., & Maroulis, J. (2014). Soil conservation through sediment trapping: a review. *Land degradation & development, 26*(6), 544-556. doi:https://doi.org/10.1002/ldr.2308

Midgley, S., Blyth, M., Mounlamai, K., Midgley, D., & Brown, A. (2007). Towards improving profitability of teak in integrated smallholder farming systems in northern Laos. *Australian Centre for International Agricultural Research (ACIAR): Canberra, Australia*, 95.

Midgley, S., Somaiya, R., Stevens, P., Brown, A., Nguyen, D. K., & Laity, R. (2015). Planted teak: global production and markets, with reference to Solomon Islands. *ACIAR Technical Reports Series*(85).

Miettinen, J., Shi, C., & Liew, S. C. (2011). Deforestation rates in insular Southeast Asia between 2000 and 2010. *Global change biology, 17*(7), 2261-2270.

Miyata, S., Kosugi, K. i., Gomi, T., & Mizuyama, T. (2009). Effects of forest floor coverage on overland flow and soil erosion on hillslopes in Japanese cypress plantation forests. *Water Resources Research, 45*(6). doi:10.1029/2008wr007270

Mohamadi, M. A., & Kavian, A. (2015). Effects of rainfall patterns on runoff and soil erosion in field plots. *International Soil and Water Conservation Research, 3*(4), 273-281.

Monaghan, R., Smith, L., & Muirhead, R. (2016). Pathways of contaminant transfers to water from an artificially-drained soil under intensive grazing by dairy cows. *Agriculture, ecosystems & environment, 220*, 76-88.

Morgan, R. P. C. (2005). *Soil erosion and conservation* (3rd ed.): Blackwell Publishing. ISBN: 1-4051-1781-8

Mouelhi, S., Michel, C., Perrin, C., & Andréassian, V. (2006). Stepwise development of a two-parameter monthly water balance model. *Journal of hydrology, 318*(1-4), 200-214.

Muller, R. N. (2003). Nutrient relations of the herbaceous layer in deciduous forest ecosystems. *the herbaceous layer in forests of eastern North America. Oxford University Press, New York*, 15-37.

Myers, N. (1988). Threatened biotas:" hot spots" in tropical forests. *The Environmentalist, 8*(3), 187-208.

Nadeu, E., Quiñonero-Rubio, J. M., de Vente, J., & Boix-Fayos, C. (2015). The influence of catchment morphology, lithology and land use on soil organic carbon export in a Mediterranean mountain region. *Catena, 126*, 117-125. doi:https://doi.org/10.1016/j.catena.2014.11.006

Naiman, R. J., Décamps, H., & McClain, M. E. (2013). Riparian Landscapes. In S. A. Levin (Ed.), *Encyclopedia of Biodiversity (Second Edition)* (pp. 461-468). Waltham: Academic Press. doi:https://doi.org/10.1016/B978-0-12-384719-5.00393-2

Nakhle, P., Boithias, L., Pando-Bahuon, A., Thammahacksa, C., Gallion, N., Sounyafong, P., . . . Ribolzi, O. (2021). Decay Rate of Escherichia coli in a Mountainous Tropical Headwater Wetland. *Water, 13*(15), 2068. doi:https://doi.org/10.3390/w13152068

Nandi, A., & Luffman, I. (2012). Erosion related changes to physicochemical properties of Ultisols distributed on calcareous sedimentary rocks. *Journal of sustainable development, 5*(8), 52.

Nearing, M. A., Pruski, F., & O'neal, M. (2004). Expected climate change impacts on soil erosion rates: a review. *Journal of soil and water conservation, 59*(1), 43-50.

Nearing, M. A., Yin, S.-q., Borrelli, P., & Polyakov, V. O. (2017). Rainfall erosivity: An historical review. *Catena, 157*, 357-362.

Neave, M., & Rayburg, S. (2007). A field investigation into the effects of progressive rainfall-induced soil seal and crust development on runoff and erosion rates: The impact of surface cover. *Geomorphology, 87*(4), 378-390. doi:https://doi.org/10.1016/j.geomorph.2006.10.007

Negishi, J., Sidle, R., Ziegler, A., Noguchi, S., & Rahim, N. A. (2008). Contribution of intercepted subsurface flow to road runoff and sediment transport in a logging-disturbed tropical catchment. *Earth Surface Processes and Landforms: The Journal of the British Geomorphological Research Group, 33*(8), 1174-1191.

Newby, J. C., Cramb, R. A., Sakanphet, S., & McNamara, S. (2012). Smallholder teak and agrarian change in northern Laos. *Small-scale Forestry, 11*(1), 27-46.

Neyret, M., Robain, H., de Rouw, A., Janeau, J.-L., Durand, T., Kaewthip, J., . . . Valentin, C. (2020). Higher runoff and soil detachment in rubber tree plantations compared to annual cultivation is mitigated by ground cover in steep mountainous Thailand. *Catena, 189*, 104472. doi:https://doi.org/10.1016/j.catena.2020.104472

Nouvelot, J.-F. (1993). *Guide des pratiques hydrologiques sur les petits bassins versants ruraux en Afrique tropicale et équatoriale*. Retrieved from

Nouwakpo, S. K., Weltz, M. A., Green, C. H. M., & Arslan, A. (2018). Combining 3D data and traditional soil erosion assessment techniques to study the effect of a vegetation cover gradient on hillslope runoff and soil erosion in a semi-arid catchment. *Catena, 170*, 129-140. doi:10.1016/j.catena.2018.06.009

Nut, N., Mihara, M., Jeong, J., Ngo, B., Sigua, G., Prasad, P. V. V., & Reyes, M. R. (2021). Land Use and Land Cover Changes and Its Impact on Soil Erosion in Stung Sangkae Catchment of Cambodia. *Sustainability, 13*(16), 9276. Retrieved from https://www.mdpi.com/2071-1050/13/16/9276

Oldeman, L. (1992). Global extent of soil degradation. In *Bi-Annual Report 1991-1992/ISRIC* (pp. 19-36): ISRIC.

Oldeman, L. (1994). *The global extent of soil degradation.* Paper presented at the Soil resilience and sustainable land use. , Wallingford, Oxon, United Kingdom.

Olson, D. M., Dinerstein, E., Wikramanayake, E. D., Burgess, N. D., Powell, G. V. N., Underwood, E. C., . . . Kassem, K. R. (2001). Terrestrial Ecoregions of the World: A New Map of Life on Earth: A new global map of terrestrial ecoregions provides an innovative tool for conserving biodiversity. *Bioscience, 51*(11), 933-938. doi:10.1641/0006-3568(2001)051[0933:Teotwa]2.0.Co;2

Owens, P., Batalla, R., Collins, A., Gomez, B., Hicks, D., Horowitz, A., . . . Peacock, D. (2005). Fine-grained sediment in river systems: environmental significance and management issues. *River research and applications, 21*(7), 693-717. doi: https://doi.org/10.1002/rra.878

Pachas, A. N. A., Newby, J. C., Siphommachan, P., Sakanphet, S., & Dieters, M. J. (2020). Broom grass in Lao PDR: a market chain analysis in Luang Prabang Province. *Forests, Trees and Livelihoods*, 1-18. doi:10.1080/14728028.2020.1722259

Pachas, A. N. A., Sakanphet, S., Midgley, S., & Dieters, M. (2019). Teak (Tectona grandis) silviculture and research: applications for smallholders in Lao PDR. *Australian Forestry, 82*(sup1), 94-105.

Pan, D., Gao, X., Wang, J., Yang, M., Wu, P., Huang, J., . . . Zhao, X. (2018). Vegetative filter strips—Effect of vegetation type and shape of strip on run-off and sediment trapping. *Land degradation & development, 29*(11), 3917-3927. doi:https://doi.org/10.1002/ldr.3160

Panagos, P., Borrelli, P., Poesen, J., Ballabio, C., Lugato, E., Meusburger, K., . . . Alewell, C. (2015). The new assessment of soil loss by water erosion in Europe. *Environmental science & policy, 54*, 438-447.

Parsons, A. J., Wainwright, J., Brazier, R. E., & Powell, D. M. (2008). Is sediment delivery a fallacy? Reply. *Earth Surface Processes and Landforms: The Journal of the British Geomorphological Research Group, 33*(10), 1630-1631. doi: https://doi.org/10.1002/esp.1627

Patin, J., Mouche, E., Ribolzi, O., Chaplot, V., Sengtahevanghoung, O., Latsachak, K. O., . . . Valentin, C. (2012). Analysis of runoff production at the plot scale during a long-term survey of a small agricultural catchment in Lao PDR. *Journal of hydrology, 426-427*, 79-92. doi:https://doi.org/10.1016/j.jhydrol.2012.01.015

Patin, J., Mouche, E., Ribolzi, O., Sengtahevanghoung, O., Latsachak, K. O., Soulileuth, B., . . . Valentin, C. (2018). Effect of land use on interrill erosion in a montane catchment of Northern Laos: An analysis based on a pluri-annual runoff and soil loss database. *Journal of hydrology, 563*, 480-494. doi:https://doi.org/10.1016/j.jhydrol.2018.05.044

Perrin, C., Michel, C., & Andréassian, V. (2003). Improvement of a parsimonious model for streamflow simulation. *Journal of hydrology, 279*(1-4), 275-289.

Perrin, R. (1976). Pest management in multiple cropping systems. *Agro-ecosystems, 3*, 93-118.

Petersen, C., Jovanovic, N., & Grenfell, M. (2020). The effectiveness of riparian zones in mitigating water quality impacts in an agriculturally dominated river system in South Africa. *African Journal of Aquatic Science*, 1-14.

Phan Ha, H. A., Huon, S., Henry des Tureaux, T., Orange, D., Jouquet, P., Valentin, C., . . . Tran Duc, T. (2012). Impact of fodder cover on runoff and soil erosion at plot scale in a cultivated catchment of North Vietnam. *Geoderma, 177-178*, 8-17. doi:https://doi.org/10.1016/j.geoderma.2012.01.031

Phillips, J. D. (1989). FLUVIAL SEDIMENT STORAGE IN WETLANDS1. *JAWRA Journal of the American Water Resources Association, 25*(4), 867-873. doi:https://doi.org/10.1111/j.1752-1688.1989.tb05402.x

Pimentel, D. (2006). Soil erosion: a food and environmental threat. *Environment, development and sustainability, 8*(1), 119-137. doi:https://doi.org/10.1007/s10668-005-1262-8

Pimentel, D., & Burgess, M. (2013). Soil erosion threatens food production. *Agriculture, 3*(3), 443-463.

Pimentel, D., Harvey, C., Resosudarmo, P., Sinclair, K., Kurz, D., McNair, M., . . . Saffouri, R. (1995). Environmental and economic costs of soil erosion and conservation benefits. *Science, 267*(5201), 1117-1123.

Pimm, S. L. (2007). Deforestation. In *Encyclopedia Britannica*.

Podwojewski, P., Orange, D., Jouquet, P., Valentin, C., Janeau, J., & Tran, D. T. (2008). Land-use impacts on surface runoff and soil detachment within agricultural sloping lands in Northern Vietnam. *Catena, 74*(2), 109-118. doi:https://doi.org/10.1016/j.catena.2008.03.013

Poesen, J. (1989). *Conditions for gully formation in the Belgian loam belt and some ways to control them.* Paper presented at the Soil erosion protection measures in Europe. Proc. EC workshop. Freising, 1988.

Poesen, J. (2018). Soil erosion in the Anthropocene: Research needs. *Earth surface processes and landforms, 43*(1), 64-84.

Poesen, J. W., & Hooke, J. M. (1997). Erosion, flooding and channel management in Mediterranean environments of southern Europe. *Progress in physical geography, 21*(2), 157-199.

Polyakov, V., & Lal, R. (2008). Soil organic matter and CO2 emission as affected by water erosion on field runoff plots. *Geoderma, 143*(1-2), 216-222. doi:https://doi.org/10.1016/j.geoderma.2007.11.005

Prokop, P., & Poręba, G. (2012). Soil erosion associated with an upland farming system under population pressure in Northeast India. *Land degradation & development, 23*(4), 310-321.

Quinn, G., & Keough, M. (2002). *Experimental design and data analysis for biologists*: Cambridge University Press, Cambridge. ISBN: 0-521-00976-6

Renard, K. G., & Ferreira, V. A. (1993). RUSLE Model Description and Database Sensitivity. *Journal of environmental quality, 1993 v.22 no.3*(no. 3), pp. 458-450. doi:10.2134/jeq1993.00472425002200030009x

Rey, F., Ballais, J.-L., Marre, A., & Rovéra, G. (2004). Rôle de la végétation dans la protection contre l'érosion hydrique de surface. *Comptes Rendus Geoscience, 336*(11), 991-998. doi:https://doi.org/10.1016/j.crte.2004.03.012

Ribaudo, M. O. (1986). *Reducing Soil Erosion: Offsite Benefits* (561). Retrieved from Washington, D.C. 20005-4788: https://ageconsearch.umn.edu/record/308013

Ribolzi, O., Cuny, J., Sengsoulichanh, P., Mousques, C., Soulileuth, B., Pierret, A., . . . Sengtaheuanghoung, O. (2011a). Land use and water quality along a Mekong tributary in northern Lao P.D.R. *Environmental management, 47*(2), 291-302. doi:https://doi.org/10.1007/s00267-010-9593-0

Ribolzi, O., Evrard, O., Huon, S., de Rouw, A., Silvera, N., Latsachack, K. O., . . . Valentin, C. (2017). From shifting cultivation to teak plantation: effect on overland flow and sediment yield in a montane tropical catchment. *Scientific reports, 7*(1), 3987. doi:https://doi.org/10.1038/s41598-017-04385-2

Ribolzi, O., Evrard, O., Huon, S., Rochelle-Newall, E., Henri-des-Tureaux, T., Silvera, N., . . . Sengtaheuanghoung, O. (2016). Use of fallout radionuclides ((7)Be, (210)Pb) to estimate resuspension of Escherichia coli from streambed sediments during floods in a tropical montane catchment. *Environmental science and pollution research, 23*(4), 3427-3435. doi:https://doi.org/10.1007/s11356-015-5595-z

Ribolzi, O., Lacombe, G., Pierret, A., Robain, H., Sounyafong, P., de Rouw, A., . . . Silvera, N. (2018). Interacting land use and soil surface dynamics control groundwater outflow in a montane catchment of the lower Mekong basin. *Agriculture, ecosystems & environment, 268*, 90-102. doi:https://doi.org/10.1016/j.agee.2018.09.005

Ribolzi, O., Patin, J., Bresson, L. M., Latsachack, K. O., Mouche, E., Sengtaheuanghoung, O., . . . Valentin, C. (2011b). Impact of slope gradient on soil surface features and infiltration on steep slopes in northern Laos. *Geomorphology, 127*(1-2), 53-63. doi:https://doi.org/10.1016/j.geomorph.2010.12.004

Ribolzi, O., Silvera, N., Xayyakummanh, K., Latchachak, K., Tasaketh, S., & Vanethongkham, K. (2005). The use of pH to spot groundwater inflows along the stream of a cultivated catchment in the northern Lao PDR. *The Lao Journal of Agriculture and Forestry, 10*, 74-84.

Rieley, J., & Page, S. (2005). Wise use of tropical peatlands: focus on Southeast Asia. Alterra, Netherlands. In.

Robinson, M., & Ward, R. C. (2017). *Hydrology: principles and processes*: Iwa Publishing. ISBN: 1780407289

Robotham, J., Old, G., Rameshwaran, P., Sear, D., Gasca-Tucker, D., Bishop, J., . . . McKnight, D. (2021). Sediment and Nutrient Retention in Ponds on an Agricultural Stream: Evaluating Effectiveness for Diffuse Pollution Mitigation. *Water, 13*(12), 1640. Retrieved from https://www.mdpi.com/2073-4441/13/12/1640

Rochelle-Newall, E., Nguyen, T. M. H., Le, T. P. Q., Sengtaheuanghoung, O., & Ribolzi, O. (2015). A short review of fecal indicator bacteria in tropical aquatic ecosystems: knowledge gaps and future directions. *Frontiers in microbiology, 6*(308). doi:https://doi.org/10.3389/fmicb.2015.00308

Rochelle-Newall, E., Ribolzi, O., Viguier, M., Thammahacksa, C., Silvera, N., Latsachack, K., . . . Pierret, A. (2016). Effect of land use and hydrological processes on Escherichia coli concentrations in streams of tropical, humid headwater catchments. *Scientific reports, 6*, 32974. doi:https://doi.org/10.1038/srep32974

Roehl, J. (1962). Sediment source areas, and delivery ratios influencing morphological factors. *Int. Assoc. Hydro. Sci., 59*, 202-213. doi:https://doi.org/

Roose, E. (1996). *Land husbandry: components and strategy*. Rome: FAO. ISBN: ISBN 92-5-103451-6

Sabzevari, T., & Talebi, A. (2019). Effect of hillslope topography on soil erosion and sediment yield using USLE model. *Acta Geophysica, 67*(6), 1587-1597. doi:https://doi.org/10.1007/s11600-019-00361-8

Santamaría Leandro, F. (1992). Evaluación de la pérdida de suelo en plantaciones de teca, bajo la aplicación de sistemas de conservación de suelos en Nicoya, Guanacaste.

Santoro, A., Venturi, M., Bertani, R., & Agnoletti, M. (2020). A Review of the Role of Forests and Agroforestry Systems in the FAO Globally Important Agricultural Heritage

Systems (GIAHS) Programme. *Forests, 11*(8), 860. Retrieved from https://www.mdpi.com/1999-4907/11/8/860

Sartori, M., Philippidis, G., Ferrari, E., Borrelli, P., Lugato, E., Montanarella, L., & Panagos, P. (2019). A linkage between the biophysical and the economic: Assessing the global market impacts of soil erosion. *Land use policy, 86*, 299-312. doi:10.1016/j.landusepol.2019.05.014

Schmadel, N. M., Harvey, J. W., Schwarz, G. E., Alexander, R. B., Gomez-Velez, J. D., Scott, D., & Ator, S. W. (2019). Small Ponds in Headwater Catchments Are a Dominant Influence on Regional Nutrient and Sediment Budgets. *Geophysical research letters, 46*(16), 9669-9677. doi:https://doi.org/10.1029/2019GL083937

Schroeder, P. (1993). Agroforestry systems: integrated land use to store and conserve carbon. *Climate Research, 3*(1), 53-60.

Sharma, N., Singh, R. J., Mandal, D., Kumar, A., Alam, N., & Keesstra, S. (2017). Increasing farmer's income and reducing soil erosion using intercropping in rainfed maize-wheat rotation of Himalaya, India. *Agriculture, ecosystems & environment, 247*, 43-53. doi:https://doi.org/10.1016/j.agee.2017.06.026

Sheil, D., Casson, A., Meijaard, E., Van Noordwijk, M., Gaskell, J., Sunderland-Groves, J., . . . Kanninen, M. (2009). *The impacts and opportunities of oil palm in Southeast Asia: What do we know and what do we need to know?* (Vol. 51): Center for International Forestry Research Bogor, Indonesia

Shinohara, Y., Otani, S., Kubota, T., Otsuki, K., & Nanko, K. (2016). Effects of plant roots on the soil erosion rate under simulated rainfall with high kinetic energy. *Hydrological sciences journal, 61*(13), 2435-2442. doi:10.1080/02626667.2015.1112904

Sidle, R. C., Gomi, T., Usuga, J. C. L., & Jarihani, B. (2017). Hydrogeomorphic processes and scaling issues in the continuum from soil pedons to catchments. *Earth-science reviews*.

Sidle, R. C., Ziegler, A. D., Negishi, J. N., Nik, A. R., Siew, R., & Turkelboom, F. (2006). Erosion processes in steep terrain—truths, myths, and uncertainties related to forest management in Southeast Asia. *Forest ecology and management, 224*(1-2), 199-225. doi:https://doi.org/10.1016/j.foreco.2005.12.019

Skutsch, M., Bird, N., Trines, E., Dutschke, M., Frumhoff, P., De Jong, B. H., . . . Murdiyarso, D. (2007). Clearing the way for reducing emissions from tropical deforestation. *Environmental science & policy, 10*(4), 322-334.

Smith, H., Ling, S., & Boer, K. (2017). Teak plantation smallholders in Lao PDR: what influences compliance with plantation regulations? *Australian Forestry, 80*(3), 178-187.

Smolko, P., Veselovská, A., & Kropil, R. (2018). Seasonal dynamics of forage for red deer in temperate forests: importance of the habitat properties, stand development stage and overstorey dynamics. *Wildlife biology, 2018*(1).

Sok, T., Oeurng, C., Ich, I., Sauvage, S., & Miguel Sánchez-Pérez, J. (2020). Assessment of Hydrology and Sediment Yield in the Mekong River Basin Using SWAT Model. *Water, 12*(12), 3503. Retrieved from https://www.mdpi.com/2073-4441/12/12/3503

Song, L., Boithias, L., Sengtaheuanghoung, O., Oeurng, C., Valentin, C., Souksavath, B., . . . Ribolzi, O. (2020). Understory Limits Surface Runoff and Soil Loss in Teak Tree

Plantations of Northern Lao PDR. *Water, 12*(9), 2327. doi:https://doi.org/10.3390/w12092327

Soto-Pinto, L., Anzueto, M., Mendoza, J., Ferrer, G. J., & de Jong, B. (2009). Carbon sequestration through agroforestry in indigenous communities of Chiapas, Mexico. *Agroforestry Systems, 78*(1), 39. doi:10.1007/s10457-009-9247-5

Soto-Pinto, L., & Armijo-Florentino, C. (2014). Changes in agroecosystem structure and function along a chronosequence of Taungya system in Chiapas, Mexico. *Journal of Agricultural Science, 6*(11), 43.

Thomaz, E. L. (2009). The influence of traditional steep land agricultural practices on runoff and soil loss. *Agriculture, ecosystems & environment, 130*(1-2), 23-30. doi:10.1016/j.agee.2008.11.009

Thothong, W., Huon, S., Janeau, J.-L., Boonsaner, A., de Rouw, A., Planchon, O., . . . Parkpian, P. (2011). Impact of land use change and rainfall on sediment and carbon accumulation in a water reservoir of North Thailand. *Agriculture, ecosystems & environment, 140*(3-4), 521-533. doi:10.1016/j.agee.2011.02.006

Thrippleton, T., Bugmann, H., & Snell, R. S. (2018). Herbaceous competition and browsing may induce arrested succession in central European forests. *Journal of ecology, 106*(3), 1120-1132.

Tixier, P., Peyrard, N., Aubertot, J.-N., Gaba, S., Radoszycki, J., Caron-Lormier, G., . . . Sabbadin, R. (2013). Modelling interaction networks for enhanced ecosystem services in agroecosystems. In *Advances in ecological research* (Vol. 49, pp. 437-480): Elsevier.

Tracy Van, H., Michael, W. B., Kenneth, M. P., & Rodrigo, V. (2016). A stand of trees does not a forest make: Tree plantations and forest transitions. *Land use policy, 56*, 147-157. doi:https://doi.org/10.1016/j.landusepol.2016.04.015

Turner, J. N., Brewer, P. A., & Macklin, M. G. (2008). Fluvial-controlled metal and As mobilisation, dispersal and storage in the Rio Guadiamar, SW Spain and its implications for long-term contaminant fluxes to the Donana wetlands. *Science of the total environment, 394*(1), 144-161. doi:10.1016/j.scitotenv.2007.12.021

UNEP. (2021). *Making Peace with Nature: A scientific blueprint to tackle the climate, biodiversity and pollution emergencies*. Retrieved from Nairobi: https://www.unep.org/resources/making-peace-nature

United Nations, D. o. E. a. S. A., Population Division. (2019). *World Population Prospects 2019: Highlights* (ST/ESA/SER.A/423). Retrieved from https://population.un.org/wpp/Publications/

USGS. (2021). Surface Water. *Water Science School*. Retrieved from https://www.usgs.gov/special-topic/water-science-school/science/runoff-surface-and-overland-water-runoff?

Vaezi, A. R., Bahrami, H. A., Sadeghi, S. H. R., & Mahdian, M. H. (2010). Modeling relationship between runoff and soil properties in dry-farming lands, NW Iran. *Hydrol. Earth Syst. Sci. Discuss., 2010*, 2577-2607. doi:https://doi.org/10.5194/hessd-7-2577-2010

Valentin, C. (2018). Soil Surface Crusting of Soil and Water Harvesting. In C. Valentin (Ed.), *Soils as a Key Component of the Critical Zone 5: Degradation and Rehabilitation* (Vol. 5, pp. 21-38). doi:https://doi.org/10.1002/9781119438298.ch2

Valentin, C., Agus, F., Alamban, R., Boosaner, A., Bricquet, J.-P., Chaplot, V., . . . Orange, D. (2008). Runoff and sediment losses from 27 upland catchments in Southeast Asia: Impact of rapid land use changes and conservation practices. *Agriculture, ecosystems & environment, 128*(4), 225-238. doi:https://doi.org/10.1016/j.agee.2008.06.004

Valentin, C., & Bresson, L.-M. (1992). Morphology, genesis and classification of surface crusts in loamy and sandy soils. *Geoderma, 55*(3-4), 225-245. doi:https://doi.org/10.1016/0016-7061(92)90085-L

Valentin, C., & Casenave, A. (1992). Infiltration into sealed soils as influenced by gravel cover. *Soil Science Society of America Journal, 56*(6), 1667-1673. doi:doi:10.2136/sssaj1992.03615995005600060002x

Valentin, C., Poesen, J., & Li, Y. (2005). Gully erosion: impacts, factors and control. *Catena, 63*(2-3), 132-153. doi:https://doi.org/10.1016/j.catena.2005.06.001

Valentin, C., & Rajot, J. L. (2018). Erosion and Principles of Soil Conservation. In *Soils as a Key Component of the Critical Zone 5: Degradation and Rehabilitation* (Vol. 5, pp. 39-82). doi:https://doi.org/10.1002/9781119438298.ch3

Valentin, C., & Ruiz Figueroa, J. (1987). Effects of kinetic energy and water application rate on the development of crusts in a fine sandy loam soil using sprinkling irrigation and rainfall simulation. *Micromorphologie des Sols*, 401-408.

van der Werf, G. R., Morton, D. C., DeFries, R. S., Olivier, J. G., Kasibhatla, P. S., Jackson, R. B., . . . Randerson, J. T. (2009). CO 2 emissions from forest loss. *Nature geoscience, 2*(11), 737-738.

Van Dijk, A., & Bruijnzeel, L. (2004). Runoff and soil loss from bench terraces. 2. An event-based erosion process model. *European journal of soil science, 55*(2), 317-334. doi:https://doi.org/10.1111/j.1365-0754.2004.00605.x

Van Dijk, A., Bruijnzeel, L., & Eisma, E. (2003). A methodology to study rain splash and wash processes under natural rainfall. *Hydrological processes, 17*(1), 153-167. doi:https://doi.org/10.1002/hyp.1154

Van Dijk, A., Bruijnzeel, L., & Rosewell, C. (2002). Rainfall intensity–kinetic energy relationships: a critical literature appraisal. *Journal of hydrology, 261*(1-4), 1-23.

Van Lynden, G., & Oldeman, L. (1997). *The assessment of the status of human-induced soil degradation in South and Southeast Asia*. Retrieved from

Van Noordwijk, M., Poulsen, J. G., & Ericksen, P. J. (2004). Quantifying off-site effects of land use change: filters, flows and fallacies. *Agriculture, ecosystems & environment, 104*(1), 19-34.

Vandaele, K., & Poesen, J. (1995). Spatial and temporal patterns of soil erosion rates in an agricultural catchment, central Belgium. *Catena, 25*(1-4), 213-226. doi:https://doi.org/10.1016/0341-8162(95)00011-G

Vannoppen, W., Vanmaercke, M., De Baets, S., & Poesen, J. (2015). A review of the mechanical effects of plant roots on concentrated flow erosion rates. *Earth-science reviews, 150*, 666-678.

Verbist, B., Poesen, J., van Noordwijk, M., Suprayogo, D., Agus, F., & Deckers, J. (2010). Factors affecting soil loss at plot scale and sediment yield at catchment scale in a tropical volcanic agroforestry landscape. *Catena, 80*(1), 34-46.

Verstraeten, G., Poesen, J., Gillijns, K., & Govers, G. (2006). The use of riparian vegetated filter strips to reduce river sediment loads: an overestimated control measure? *Hydrological Processes: An International Journal, 20*(20), 4259-4267. doi:https://doi.org/10.1002/hyp.6155

Vidon, P. G., & Hill, A. R. (2004). Landscape controls on nitrate removal in stream riparian zones. *Water Resources Research, 40*(3). doi:https://doi.org/10.1029/2003WR002473

Vigiak, O., Ribolzi, O., Pierret, A., Sengtaheuanghoung, O., & Valentin, C. (2008). Trapping efficiencies of cultivated and natural riparian vegetation of northern Laos. *Journal of environmental quality, 37*(3), 889-897. doi:https://doi.org/10.2134/jeq2007.0251

Walling, D. E. (1983). The sediment delivery problem. *Journal of hydrology, 65*(1-3), 209-237. doi:https://doi.org/10.1016/0022-1694(83)90217-2

Walling, D. E., Collins, A. L., Jones, P. A., Leeks, G. J. L., & Old, G. (2006). Establishing fine-grained sediment budgets for the Pang and Lambourn LOCAR catchments, UK. *Journal of hydrology, 330*(1-2), 126-141. doi:https://doi.org/10.1016/j.jhydrol.2006.04.015

Wenger, S. (1999). A review of the scientific literature on riparian buffer width, extent and vegetation.

Weyman, D. (1970). Throughflow on hillslopes and its relation to the stream hydrograph. *Hydrological sciences journal, 15*(3), 25-33.

WMO. (2006). *Environmental Aspects of Integrated Flood Management* (Vol. WMO- No. 1009). Geneva, Switzerland: WMO/GWP. ISBN: 92-63-11009-3

Wold, S. (1995). PLS for multivariate linear modeling. In H. v. d. Waterbeemd (Ed.), *Chemometric methods in molecular design* (Vol. 17, pp. 195-218): Wiley. doi:https://doi.org/10.1002/9783527615452

Wuepper, D., Borrelli, P., & Finger, R. (2020). Countries and the global rate of soil erosion. *Nature sustainability, 3*(1), 51-55. doi:https://doi.org/10.1038/s41893-019-0438-4

Wunderle Jr, J. M. (1997). The role of animal seed dispersal in accelerating native forest regeneration on degraded tropical lands. *Forest ecology and management, 99*(1-2), 223-235. doi:https://doi.org/10.1016/S0378-1127(97)00208-9

Yin, S.-q., Xie, Y., Liu, B., & Nearing, M. (2015). Rainfall erosivity estimation based on rainfall data collected over a range of temporal resolutions. *Hydrology and earth system sciences, 12*(5). doi:https://doi.org/10.5194/hess-19-4113-2015

Yu, B., Rose, C., Coughlan, K., & Fentie, B. (1997). Plot-scale rainfall-runoff characteristics and modeling at six sites in Australia and Southeast Asia. *Transactions of the ASAE, 40*(5), 1295-1303. doi:https://doi.org/10.13031/2013.21387

Yuan, S., Tang, H., Xiao, Y., Xia, Y., Melching, C., & Li, Z. (2019). Phosphorus Contamination of the Surface Sediment at a River Confluence. *Journal of hydrology*. doi:https://doi.org/10.1016/j.jhydrol.2019.02.036

Zaldívar Santamaría, E., Molina Dagá, D., & Palacios García, A. T. (2019). Statistical Modelization of the Descriptor "Minerality" Based on the Sensory Properties and Chemical Composition of Wine. *Beverages, 5*(4), 66. doi:https://doi.org/10.3390/beverages5040066

Zarris, D., Vlastara, M., & Panagoulia, D. (2011). Sediment Delivery Assessment for a Transboundary Mediterranean Catchment: The Example of Nestos River Catchment.

Water Resources Management, 25(14), 3785. doi:https://doi.org/10.1007/s11269-011-9889-8

Zhang, J., van Meerveld, H. I., Tripoli, R., & Bruijnzeel, L. A. (2018). Runoff response and sediment yield of a landslide-affected fire-climax grassland micro-catchment (Leyte, the Philippines) before and after passage of typhoon Haiyan. *Journal of hydrology, 565*, 524-537. doi:https://doi.org/10.1016/j.jhydrol.2018.08.016

Ziegler, A. D., Giambelluca, T. W., Nullet, M. A., Sutherland, R. A., Tantasarin, C., Vogler, J. B., & Negishi, J. N. (2009). Throughfall in an evergreen-dominated forest stand in northern Thailand: Comparison of mobile and stationary methods. *Agricultural and forest meteorology, 149*(2), 373-384. doi:https://doi.org/10.1016/j.agrformet.2008.09.002

Ziegler, A. D., Giambelluca, T. W., & Sutherland, R. A. (2001). Erosion prediction on unpaved mountain roads in northern Thailand: validation of dynamic erodibility modelling using KINEROS2. *Hydrological processes, 15*(3), 337-358. doi:https://doi.org/10.1002/hyp.96

Ziegler, A. D., Giambelluca, T. W., Tran, L. T., Vana, T. T., Nullet, M. A., Fox, J., . . . Evett, S. (2004). Hydrological consequences of landscape fragmentation in mountainous northern Vietnam: evidence of accelerated overland flow generation. *Journal of hydrology, 287*(1-4), 124-146. doi:https://doi.org/10.1016/j.jhydrol.2003.09.027

Ziegler, A. D., Tran, L. T., Giambelluca, T. W., Sidle, R. C., Sutherland, R. A., Nullet, M. A., & Vien, T. D. (2006). Effective slope lengths for buffering hillslope surface runoff in fragmented landscapes in northern Vietnam. *Forest ecology and management, 224*(1-2), 104-118. doi:https://doi.org/10.1016/j.foreco.2005.12.011